

November 26, 2019

Docket: PROJ0769

U.S. Nuclear Regulatory Commission
ATTN: Document Control Desk
One White Flint North
11555 Rockville Pike
Rockville, MD 20852-2738

SUBJECT: NuScale Power, LLC Submittal of Topical Report, "Non-Loss-of-Coolant Accident Analysis Methodology," TR-0516-49416, Revision 2

REFERENCES:

1. Letter from NuScale Power, LLC to U.S. Nuclear Regulatory Commission, "Submittal of 'Non-Loss-of-Coolant Accident Methodology,' Revision 0," dated January 10, 2017 (ML17010A427)
2. Letter from NuScale Power, LLC to U.S. Nuclear Regulatory Commission, "Submittal of 'Non-Loss-of-Coolant Accident Methodology,' Revision 1," dated August 10, 2017 (ML17222A827)

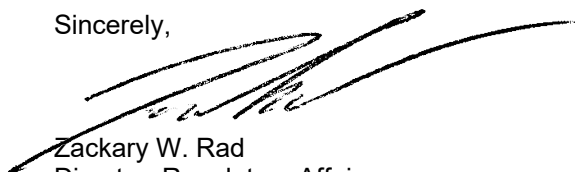
NuScale Power, LLC (NuScale) hereby submits Revision 2 of "Non-Loss-of-Coolant Accident Analysis Methodology," TR-0516-49416.

Enclosure 1 is the proprietary version of the report titled "Non-Loss-of-Coolant Accident Analysis Methodology." NuScale requests that the proprietary version be withheld from public disclosure in accordance with the requirements of 10 CFR § 2.390. The enclosed affidavit (Enclosure 3) supports this request. Enclosure 1 has also been determined to contain Export Controlled Information. This information must be protected from disclosure per the requirements of 10 CFR § 810. Enclosure 2 is the nonproprietary version of the report titled "Non-Loss-of-Coolant Accident Analysis Methodology."

This letter makes no regulatory commitments or revisions to any existing regulatory commitments.

If you have any questions, please feel free to contact Matthew Presson at (541) 452-7531 or at mpresson@nuscalspower.com. if you have any questions.

Sincerely,



Zackary W. Rad
Director, Regulatory Affairs
NuScale Power, LLC

Distribution: Samuel Lee, NRC, OWFN-8H12
Gregory Cranston, NRC, OWFN-8H12
Rani Franovich, NRC, OWFN-8H12
Michael Dudek, NRC, OWFN-8H12

Enclosure 1: "Non-Loss-of-Coolant Accident Analysis Methodology," TR-0516-49416-P, Revision 2, proprietary version
Enclosure 2: "Non-Loss-of-Coolant Accident Analysis Methodology," TR-0516-49416-NP, Revision 2, nonproprietary version
Enclosure 3: Affidavit of Zackary W. Rad, AF-1119-67901

Enclosure 1:

“Non-Loss-of-Coolant Accident Analysis Methodology,” TR-0516-49416-P, Revision 2, proprietary version

Enclosure 2:

“Non-Loss-of-Coolant Accident Analysis Methodology,” TR-0716-49416-NP, Revision 1,
nonproprietary version

Non-Loss-of-Coolant Accident Analysis Methodology

November 2019

Revision 2

Docket: PROJ0769

NuScale Power, LLC

1100 NE Circle Blvd., Suite 200

Corvallis, Oregon 97330

www.nuscalepower.com

COPYRIGHT NOTICE

This report has been prepared by NuScale Power, LLC and bears a NuScale Power, LLC, copyright notice. No right to disclose, use, or copy any of the information in this report, other than by the U.S. Nuclear Regulatory Commission (NRC), is authorized without the express, written permission of NuScale Power, LLC.

The NRC is permitted to make the number of copies of the information contained in this report that is necessary for its internal use in connection with generic and plant-specific reviews and approvals, as well as the issuance, denial, amendment, transfer, renewal, modification, suspension, revocation, or violation of a license, permit, order, or regulation subject to the requirements of 10 CFR 2.390 regarding restrictions on public disclosure to the extent such information has been identified as proprietary by NuScale Power, LLC, copyright protection notwithstanding. Regarding nonproprietary versions of these reports, the NRC is permitted to make the number of copies necessary for public viewing in appropriate docket files in public document rooms in Washington, DC, and elsewhere as may be required by NRC regulations. Copies made by the NRC must include this copyright notice and contain the proprietary marking if the original was identified as proprietary.

Department of Energy Acknowledgement and Disclaimer

This material is based upon work supported by the Department of Energy under Award Number DE-NE0008820.

This report was prepared as an account of work sponsored by an agency of the United States Government. Neither the United States Government nor any agency thereof, nor any of their employees, makes any warranty, express or implied, or assumes any legal liability or responsibility for the accuracy, completeness, or usefulness of any information, apparatus, product, or process disclosed, or represents that its use would not infringe privately owned rights. Reference herein to any specific commercial product, process, or service by trade name, trademark, manufacturer, or otherwise does not necessarily constitute or imply its endorsement, recommendation, or favoring by the United States Government or any agency thereof. The views and opinions of authors expressed herein do not necessarily state or reflect those of the United States Government or any agency thereof.

CONTENTS

Abstract	1
Executive Summary	2
1.0 Introduction	6
1.1 Purpose	6
1.2 Scope	6
1.3 Abbreviations.....	7
2.0 Background	12
2.1 Non-LOCA Evaluation Model Roadmap	12
2.2 Regulatory Requirements	17
3.0 Plant Design Overview	20
3.1 Description of NuScale Plant.....	20
3.2 Plant Operation	22
3.3 Decay Heat Removal System.....	23
3.4 Emergency Core Cooling System	23
3.5 Other Important Systems and Functions	24
4.0 Transient and Accident Analysis Overview	26
4.1 Design-Basis Events and Event Classification	26
4.2 Design Basis Event Acceptance Criteria	29
4.3 Non-LOCA Transient Analysis Process	34
4.3.1 Develop Plant Base Model NRELAP5 Input.....	34
4.3.2 Adapt Plant Base Model NRELAP5 Input for Event Transient Analysis	38
4.3.3 Perform NRELAP5 Steady State and Transient System Analysis Calculations	38
4.3.4 Evaluate Results of Transient Analysis Calculations	38
4.3.5 Identification of Cases for Subchannel Analysis and Extraction of Boundary Condition Data	39
4.3.6 Identification of Cases for Accident Radiological Analysis.....	43
5.0 NRELAP5 Applicability for Non-LOCA Transient Analysis.....	45
5.1 Non-LOCA Phenomena Identification and Ranking Table and Evaluation of High-Ranked Phenomena	45
5.1.1 Phenomena Identification and Ranking Table Process	45
5.1.2 Non-LOCA Event Scenarios and Phases	45

5.1.3	Phenomena Identification and Ranking Table Figures-of-Merit and Phenomenon Ranking	47
5.1.4	Highly Ranked Phenomena	49
5.2	Evaluation of Non-LOCA Phenomena Identification and Ranking Table High-Ranked Phenomena	110
5.3	NRELAP5 Validation and Assessments for Non-LOCA	110
5.3.1	KAIST	111
5.3.2	NIST-1 Decay Heat Removal System Separate Effects Tests	117
5.3.3	NIST-1 Non-LOCA Integral Test	169
5.3.4	Code to Code Benchmark for Integral Assessment of Reactivity Event Response	262
5.3.5	Steam Generator Modeling	284
5.4	Conclusions of NRELAP5 Applicability for Non-LOCA	292
6.0	NuScale NRELAP5 Plant Model	295
6.1	Thermal-Hydraulic Volumes and Heat Structures	295
6.1.1	Reactor Primary	299
6.1.2	Core kinetics	309
6.1.3	Fuel rod design input	309
6.1.4	Secondary System	310
6.1.5	Decay Heat Removal System	313
6.1.6	Emergency Core Cooling System	316
6.1.7	Containment Vessel	316
6.1.8	Reactor Cooling Pool	319
6.2	Material Properties	319
6.3	Control Systems	319
6.3.1	Module Control System (Nonsafety-related)	320
6.3.2	Module Protection System (Safety-related)	322
7.0	Non-LOCA Analysis Methodology	325
7.1	General	325
7.1.1	Achieving Steady State Conditions	325
7.1.2	Treatment of Plant Controls	329
7.1.3	Loss of Power Conditions	330
7.1.4	Single Failures	333
7.1.5	Bounding Reactivity Parameters	335

7.1.6	Biasing of Other Parameters	338
7.1.7	Credit for Nonsafety-related Components or Operator Actions	344
7.2	Event Specific Methodology	345
7.2.1	Decrease in Feedwater Temperature	347
7.2.2	Increase in Feedwater Flow	356
7.2.3	Increase in Steam Flow	362
7.2.4	Steam System Piping Failure Inside or Outside of Containment.....	369
7.2.5	Containment Flooding / Loss of Containment Vacuum	378
7.2.6	Turbine Trip / Loss of External Load.....	387
7.2.7	Loss of Condenser Vacuum	392
7.2.8	Main Steam Isolation Valve(s) Closure.....	397
7.2.9	Loss of Nonemergency AC Power.....	403
7.2.10	Loss of Normal Feedwater Flow.....	411
7.2.11	Inadvertent Decay Heat Removal System Actuation.....	416
7.2.12	Feedwater System Pipe Break Inside or Outside Containment	423
7.2.13	Uncontrolled Control Rod Assembly Bank Withdrawal from Subcritical or Low Power Startup Conditions	429
7.2.14	Uncontrolled Control Rod Assembly Bank Withdrawal at Power.....	436
7.2.15	Control Rod Misoperation.....	442
7.2.16	Inadvertent Decrease in Boron Concentration	453
7.2.17	Chemical and Volume Control System Malfunction that Increases Reactor Coolant System Inventory	463
7.2.18	Failure of Small Lines Outside Containment	468
7.2.19	Steam Generator Tube Failure	479
8.0	Representative Calculations	487
8.1	Cooldown and/or Depressurization of the Reactor Coolant System	487
8.1.1	Decrease in Feedwater Temperature	487
8.1.2	Increase in Steam Flow	495
8.1.3	Main Steam Line Break	504
8.2	Heatup and/or Pressurization of the Reactor Coolant System	511
8.2.1	Loss of Normal Feedwater Flow	511
8.2.2	Loss of Normal AC Power	525
8.2.3	Feedwater Line Break	530

8.3	Reactivity Anomaly	537
8.3.1	Uncontrolled Control Rod Assembly Bank Withdrawal from Subcritical or Low Power Startup Conditions	537
8.3.2	Control Rod Misoperation	544
8.4	Increase in Reactor Coolant System Inventory	551
8.4.1	Chemical and Volume Control System Malfunction that Increases Reactor Coolant System Inventory	551
8.5	Decrease in Reactor Coolant System Inventory	560
8.5.1	Small Line Break Outside of Containment	560
8.5.2	Steam Generator Tube Failure	568
9.0	Quality Assurance	577
10.0	Summary and Conclusions	578
11.0	References	580

TABLES

Table 1-1	Abbreviations	7
Table 1-2	Definitions	10
Table 2-1	Evaluation model development and assessment process steps and associated application in the non-LOCA evaluation model	14
Table 4-1	Design basis events for which the non-LOCA system transient analysis is performed, event category, and event classification	28
Table 4-2	Acceptance criteria for anticipated operational occurrences	31
Table 4-3	Acceptance criteria for infrequent events	32
Table 4-4	Acceptance criteria for postulated accidents	33
Table 5-1	Importance rankings	48
Table 5-2	Knowledge levels	48
Table 5-3	High-ranked phenomena for non-LOCA events	51
Table 5-4	Comparison between NuScale Power Module decay heat removal system and KAIST test section dimensions	114
Table 5-5	Comparison between NuScale Power Module decay heat removal system and KAIST range of operations	114
Table 5-6	Comparison between NuScale Power Module decay heat removal system and KAIST NRELAP5 model nodalization	114
Table 5-7	NIST-1 decay heat removal system separate effects tests for NRELAP5 code validation	131
Table 5-8	Comparison between NPM and NIST-1 decay heat removal NRELAP5 nodalizations	132
Table 5-9	NIST-1 HP-03 test cases	134
Table 5-10	NIST-1 HP04 test ranges	160
Table 5-11	NIST-1 integral effects tests for NRELAP5 code validation	170
Table 5-12	NLT-02a sequence of events	177

Table 5-13	NLT-02b sequence of events.....	187
Table 5-14	NLT-15p2 sequence of events.....	238
Table 5-15	Non-LOCA transients helical coil steam generator operating range vs. NRELAP5 validated range	285
Table 6-1	Reactor coolant system regions and typical NRELAP5 components	299
Table 6-2	NuScale Power Module safety logic with NRELAP5 signals in bold	323
Table 7-1	Typical list of initial conditions considered	327
Table 7-2	Example of normalized trip worth vs. time after trip.....	338
Table 7-3	Examples of analytical limits and actuation delays (reactor trip system and engineered safety features actuation system).....	344
Table 7-4	Regulatory acceptance criteria	345
Table 7-5	Acceptance criteria, single active failure, loss of power scenarios – decrease in feedwater temperature.....	348
Table 7-6	Acceptance criteria – decrease in feedwater temperature	349
Table 7-7	Initial conditions, biases, and conservatism – decrease in feedwater temperature	350
Table 7-8	Representative fuel exposure study	354
Table 7-9	Representative fuel temperature study.....	354
Table 7-10	Representative feedwater temperature transient study.....	355
Table 7-11	Representative boundary condition type / single active failure studies	355
Table 7-12	Acceptance criteria, single active failure, loss of power scenarios – increase in feedwater flow	357
Table 7-13	Acceptance criteria – increase in feedwater flow	357
Table 7-14	Initial conditions, biases, and conservatism – increase in feedwater flow	358
Table 7-15	Representative increase in feedwater flow study – high SG performance with maximum power and minimum RCS flow	362
Table 7-16	Representative increase in feedwater flow study – low SG performance with maximum power and minimum RCS flow	362
Table 7-17	Acceptance criteria, single active failure, loss of power scenarios – increase in steam flow	364
Table 7-18	Acceptance criteria – increase in steam flow	364
Table 7-19	Initial conditions, biases, and conservatism – increase in steam flow	365
Table 7-20	Representative steam flow study – nominal steam generator heat transfer.....	369
Table 7-21	Representative steam flow study – steam generator heat transfer biased low	369
Table 7-22	Acceptance criteria, single active failure, loss of power scenarios – steam line break.....	371
Table 7-23	Acceptance criteria – steam line break.....	372
Table 7-24	Initial conditions, biases, and conservatism – steam line break	372
Table 7-25	Steam line break study	377
Table 7-26	Acceptance criteria, single active failure, loss of power scenarios – containment flooding / loss of containment vacuum.....	379
Table 7-27	Acceptance criteria – containment flooding / loss of containment vacuum	380
Table 7-28	Initial conditions, biases, and conservatism – containment flooding / loss of containment vacuum	381
Table 7-29	Example sensitivity studies – containment flooding / loss of containment vacuum.....	385

Table 7-30	Acceptance criteria, single active failure, loss of power scenarios – turbine trip / loss of external load.....	387
Table 7-31	Acceptance criteria – turbine trip / loss of external load	388
Table 7-32	Initial conditions, biases, and conservatisms – turbine trip / loss of external load.....	388
Table 7-33	Representative sensitivity studies – turbine trip / loss of external load	392
Table 7-34	Acceptance criteria, single active failure, loss of power scenarios – loss of condenser vacuum	393
Table 7-35	Acceptance criteria – loss of condenser vacuum	393
Table 7-36	Initial conditions, biases, and conservatisms – loss of condenser vacuum.....	394
Table 7-37	Representative sensitivity studies – loss of condenser vacuum.....	397
Table 7-38	Acceptance criteria, single active failure, loss of power scenarios – main steam isolation valve closure	398
Table 7-39	Acceptance criteria – main steam isolation valve closure	399
Table 7-40	Initial conditions, biases, and conservatisms – main steam isolation valve closure	400
Table 7-41	Representative sensitivity studies – main steam isolation valve closure.....	403
Table 7-42	Acceptance criteria, single active failure, loss of power scenarios – loss of normal AC power.....	405
Table 7-43	Acceptance criteria – loss of normal AC power.....	406
Table 7-44	Initial conditions, biases, and conservatisms – loss of normal AC power.....	406
Table 7-45	Representative sensitivity studies – loss of normal AC power	410
Table 7-46	Acceptance criteria, single active failure, loss of power scenarios – loss of normal feedwater flow	411
Table 7-47	Acceptance criteria – loss of normal feedwater flow	412
Table 7-48	Initial conditions, biases, and conservatisms – loss of normal feedwater flow	413
Table 7-49	Sensitivity studies – loss of normal feedwater flow	415
Table 7-50	Acceptance criteria, single active failure, loss of power scenarios – inadvertent decay heat removal system actuation	417
Table 7-51	Acceptance criteria – inadvertent decay heat removal system actuation.....	418
Table 7-52	Initial conditions, biases, and conservatisms – inadvertent decay heat removal system actuation.....	419
Table 7-53	Representative sensitivity studies – inadvertent decay heat removal system actuation	422
Table 7-54	Acceptance criteria, single active failure, loss of power scenarios – feedwater line break	424
Table 7-55	Acceptance criteria – feedwater line break.....	424
Table 7-56	Initial conditions, biases, and conservatisms – feedwater line break	425
Table 7-57	Representative sensitivity studies – feedwater line break	428
Table 7-58	Acceptance criteria, single active failure, loss of power scenarios – uncontrolled control rod bank withdrawal from subcritical or low power startup conditions	430
Table 7-59	Acceptance criteria – uncontrolled control rod bank withdrawal from subcritical or low power startup conditions.....	431
Table 7-60	Initial conditions, biases, and conservatisms – uncontrolled control rod bank withdrawal from subcritical or low power startup conditions	432

Table 7-61	Representative sensitivity studies – uncontrolled control rod bank withdrawal from subcritical or low power startup conditions.....	435
Table 7-62	Acceptance criteria, single active failure, loss of power scenarios – uncontrolled control rod bank withdrawal at power	437
Table 7-63	Acceptance criteria – uncontrolled control rod bank withdrawal at power	437
Table 7-64	Initial conditions, biases, and conservatism – uncontrolled control rod bank withdrawal at power	438
Table 7-65	Representative sensitivity studies – uncontrolled control rod bank withdrawal at power	441
Table 7-66	Acceptance criteria, single active failure, loss of power scenarios – control rod misoperation.....	444
Table 7-67	Acceptance criteria – control rod misoperation	445
Table 7-68	Initial conditions, biases, and conservatism – control rod misoperation, single control rod assembly withdrawal.....	446
Table 7-69	Representative sensitivity studies – control rod misoperation, single control rod assembly withdrawal	449
Table 7-70	Initial conditions, biases, and conservatism – control rod misoperation, dropped control rod assemblies	450
Table 7-71	Representative sensitivity studies – control rod misoperation, dropped control rod assemblies	453
Table 7-72	Acceptance criteria, single active failure, loss of power scenarios – inadvertent decrease in boron concentration	457
Table 7-73	Acceptance criteria – inadvertent decrease in boron concentration.....	458
Table 7-74	Initial conditions, biases, and conservatism – inadvertent decrease in boron concentration.....	458
Table 7-75	Representative results – inadvertent decrease in boron concentration in Mode 1 at hot full power with the Perfect Mixing Model	460
Table 7-76	Representative results – inadvertent decrease in boron concentration in Mode 1 at 25 percent rated thermal power.....	461
Table 7-77	Representative results – inadvertent decrease in boron concentration in Mode 1 at hot zero power with the Wave Front Model	461
Table 7-78	Representative results – inadvertent decrease in boron concentration in Mode 2	462
Table 7-79	Representative results – inadvertent decrease in boron concentration in Mode 3	462
Table 7-80	Acceptance criteria, single active failure, loss of power scenarios – reactor coolant system inventory increase	463
Table 7-81	Acceptance criteria – reactor coolant system inventory increase.....	464
Table 7-82	Initial conditions, biases, and conservatism – reactor coolant system inventory increase	464
Table 7-83	Representative sensitivity studies – reactor coolant system inventory increase	468
Table 7-84	Acceptance criteria, single active failure, loss of power scenarios – breaks in small lines carrying primary coolant outside containment	471
Table 7-85	Acceptance criteria – breaks in small lines carrying primary coolant outside containment	472
Table 7-86	Initial conditions, biases, and conservatism – breaks in small lines carrying primary coolant outside containment.....	473

Table 7-87	Representative break, time in life, power, flow, and temperature sensitivity study for mass release - breaks in small lines carrying primary coolant outside containment	477
Table 7-88	Representative break, time in life, power, flow, and temperature sensitivity study for iodine spiking time - breaks in small lines carrying primary coolant outside containment.....	478
Table 7-89	Acceptance criteria, single active failure, loss of power scenarios – steam generator tube failure	480
Table 7-90	Acceptance criteria – steam generator tube failure	481
Table 7-91	Initial conditions, biases, and conservatisms – steam generator tube failure.....	483
Table 7-92	Representative break characteristics, initial conditions, loss of power, and single active failure sensitivity study - steam generator tube failure.....	486
Table 8-1	Decrease in feedwater temperature sequence of events	490
Table 8-2	Increase in steam flow sequence of events.....	498
Table 8-3	Main steam line break sequence of events	506
Table 8-4	Loss of normal feedwater flow sequence of events – reactor coolant system pressure case	513
Table 8-5	Loss of normal feedwater flow sequence of events – secondary pressure case	520
Table 8-6	Sequence of events for loss of AC power.....	526
Table 8-7	Sequence of events for feedwater line break outside containment	532
Table 8-8	Withdrawal of a control rod assembly bank from a low power startup condition sequence of events	539
Table 8-9	Single rod withdrawal sequence of events – MCHFR case.....	546
Table 8-10	Increase in reactor coolant system inventory sequence of events	553
Table 8-11	Sequence of events for small line breaks carrying primary coolant outside containment.....	562
Table 8-12	Sequence of events for steam generator tube failure.....	570

FIGURES

Figure 2-1	Evaluation model development and assessment process.....	13
Figure 3-1	NuScale Power Module schematic.....	21
Figure 4-1	{{ }} ^{2(a),(c)}	42
Figure 5-1	Schematic of KAIST test facility.....	113
Figure 5-2	Measured vs predicted heat transfer coefficient.....	116
Figure 5-3	Schematic of NIST-1 integral test facility	118
Figure 5-4	NIST-1 test facility configuration	119
Figure 5-5	Photograph of the NIST-1 facility.....	121
Figure 5-6	Reactor pressure vessel thermal-hydraulic regions	123
Figure 5-7	Lower core flow plate	124
Figure 5-8	Full-height decay heat removal condenser.....	127
Figure 5-9	Scaled decay heat removal heat condensers.....	128
Figure 5-10	NIST-1 nodding diagram for full-height decay heat removal system separate effect tests	133
Figure 5-11	NIST-1 HP-03-01 decay heat removal system enthalpy flow rate code-to-data comparison.....	137

Figure 5-11a	NIST-1 HP-03-01 decay heat removal system power code-to-data comparison.....	138
Figure 5-12	NIST-1 HP-03-01 decay heat removal system level code-to-data comparison.....	139
Figure 5-13	NIST-1 HP-03-01 decay heat removal system internal fluid temperature code-to-data comparison.....	140
Figure 5-14	NIST-1 HP-03-01 cooling pool vessel temperature code-to-data comparison (1 of 2)	141
Figure 5-14a	NIST-1 HP-03-01 cooling pool vessel temperature code-to-data comparison (2 of 2)	142
Figure 5-15	NIST-1 HP-03-01 cooling pool vessel level code-to-data comparison	143
Figure 5-16	NIST-1 HP-03-02c decay heat removal system enthalpy flow rate code-to-data comparison.....	145
Figure 5-16a	NIST-1 HP-03-02c decay heat removal system power code-to-data comparison.....	146
Figure 5-17	NIST-1 HP-03-02c decay heat removal system level code-to-data comparison.....	147
Figure 5-18	NIST-1 HP-03-02c decay heat removal system internal fluid temperature code-to-data comparison.....	148
Figure 5-19	NIST-1 HP-03-02c cooling pool vessel temperature code-to-data comparison (1 of 2)	149
Figure 5-19a	NIST-1 HP-03-02c cooling pool vessel temperature code-to-data comparison (2 of 2)	150
Figure 5-20	NIST-1 HP-03-02c cooling pool vessel level code-to-data comparison.....	151
Figure 5-21	NIST-1 HP-03-03-P1 decay heat removal system enthalpy flow rate code-to-data comparison.....	153
Figure 5-21a	NIST-1 HP-03-03-Part1 decay heat removal system power code-to-data comparison.....	154
Figure 5-22	NIST-1 HP-03-03-Part1 decay heat removal system level code-to-data comparison.....	155
Figure 5-23	NIST-1 HP-03-03-Part1 decay heat removal system internal fluid temperature code-to-data comparison	156
Figure 5-24	NIST-1 HP-03-03-Part1 cooling pool vessel temperature code-to-data comparison (1 of 2)	157
Figure 5-24a	NIST-1 HP-03-03-Part1 cooling pool vessel temperature code-to-data comparison (2 of 2)	158
Figure 5-25	NIST-1 HP-03-03-Part1 cooling pool vessel level code-to-data comparison.....	159
Figure 5-26	NIST-1 HP-04-02 decay heat removal system energy transfer rate.....	162
Figure 5-27	NIST-1 HP-04-02 decay heat removal system condensate temperature	163
Figure 5-28	NIST-1 HP-04-02 decay heat removal system internal collapsed level.....	163
Figure 5-29	NIST-1 HP-04-02 cooling pool vessel level	164
Figure 5-30	NIST-1 HP-04-02 mid cooling pool vessel fluid temperatures	164
Figure 5-31	NIST-1 HP-04-02 upper cooling pool vessel fluid temperatures.....	165
Figure 5-32	NIST-1 HP-04-03 decay heat removal system energy transfer rate.....	166
Figure 5-33	NIST-1 HP-04-03 decay heat removal system condensate temperature	167
Figure 5-34	NIST-1 HP-04-03 decay heat removal system internal collapsed level comparison.....	167

Figure 5-35	NIST-1 HP-04-03 cooling pool vessel level comparison.....	168
Figure 5-36	NIST-1 HP-04-03 mid cooling pool vessel axial temperatures	168
Figure 5-37	NIST-1 HP-04-03 upper cooling pool vessel axial temperatures	169
Figure 5-38	NRELAP5 noding diagram for the NIST-1 facility	173
Figure 5-39	NRELAP5 NIST-1 model secondary system nodalization layout (NLT-2b)	174
Figure 5-40	NIST-1 feedwater split headers at the steam generator tube coils connection (at the time of NLT-2b test).....	176
Figure 5-41	NLT-02a transient feedwater flow comparison	179
Figure 5-42	NLT-02a transient core heater rod power comparison	179
Figure 5-43	NLT-02a transient pressurizer pressure comparison.....	180
Figure 5-44	NLT-02a transient riser mass flow rate comparison	180
Figure 5-45	NLT-02a transient pressurizer level comparison	181
Figure 5-46	NLT-02a transient core inlet temperature	181
Figure 5-47	NLT-02a transient combined middle and outer steam generator tube coil differential pressure comparison	182
Figure 5-48	NLT-02a transient inner steam generator tube coil differential pressure comparison.....	182
Figure 5-49	NLT-02a transient core exit fluid temperature comparison	183
Figure 5-49a	NLT-02a transient riser inlet fluid temperature comparison	183
Figure 5-50	NLT-02a transient pressurizer heater rod power comparison.....	184
Figure 5-51	NLT-02a transient steam line pressure comparison	184
Figure 5-52	NLT-02a transient steam line mass flow rate comparison	185
Figure 5-53	NLT-02b phase 1 transient core power comparison	191
Figure 5-54	NLT-02b phase 1 transient pressurizer pressure comparison	191
Figure 5-55	NLT-02b phase 1 transient pressurizer level comparison.....	192
Figure 5-56	Not Used	192
Figure 5-57	NLT-02b phase 1 transient core inlet and outlet temperature comparison	192
Figure 5-58	Not Used	193
Figure 5-59	NLT-02b phase 1 transient steam generator steam pressure comparison.....	193
Figure 5-60	NLT-02b phase 1 transient steam generator thermal power comparison.....	193
Figure 5-61	NLT-02b phase 1 transient decay heat removal system heat exchanger thermal power comparison	194
Figure 5-62	NLT-02b phase 1 calculated compensation flow for steam generator and decay heat removal system heat exchanger level equalization	194
Figure 5-62a	NLT-02b phase 1 integrated compensation flow for SG and DHRS HX level equalization	195
Figure 5-63	NLT-02b phase 1 transient steam generator level comparison	195
Figure 5-64	NLT-02b phase 1 transient decay heat removal system heat exchanger level comparison	196
Figure 5-65	NLT-02b phase 1 transient decay heat removal system condensate temperature comparison	196
Figure 5-66	NLT-02b phase 1 transient decay heat removal system condensate flow comparison.....	197
Figure 5-67	NLT-02b phase 1 transient steam generator outlet temperature comparison.....	197
Figure 5-68	NLT-02b phase 1 transient cooling pool vessel level comparison	198
Figure 5-69	NLT-02b phase 1 transient cooling pool vessel region 4 temperature comparison (below decay heat removal system heat exchanger).....	198

Figure 5-69a	NLT-02b phase 1 transient cooling pool vessel region 5 temperature comparison (near bottom of decay heat removal system heat exchanger).....	199
Figure 5-69b	NLT-02b phase 1 transient cooling pool vessel region 6 temperature comparison (near mid-point of decay heat removal system heat exchanger)	199
Figure 5-70	NLT-02b phase 1 transient cooling pool vessel region 7 temperature comparison (just above the decay heat removal system heat exchanger tube region)	200
Figure 5-71	NLT-02b phase 2 transient core power comparison	202
Figure 5-72	NLT-02b phase 2 transient pressurizer pressure comparison	203
Figure 5-73	NLT-02b phase 2 transient pressurizer level comparison.....	203
Figure 5-74	Not Used	203
Figure 5-75	NLT-02b phase 2 transient core inlet and outlet temperature comparison	204
Figure 5-76	Not Used	204
Figure 5-77	NLT-02b phase 2 transient steam generator steam pressure comparison.....	204
Figure 5-78	NLT-02b phase 2 transient steam generator thermal power comparison.....	205
Figure 5-79	NLT-02b phase 2 transient decay heat removal system heat exchanger thermal power comparison	205
Figure 5-80	NLT-02b phase 2 transient steam generator level comparison	206
Figure 5-81	NLT-02b phase 2 calculated compensation flow for steam generator and decay heat removal system heat exchanger level equalization	206
Figure 5-81a	NLT-02b phase 2 integrated compensation flow for SG and DHRS HX level equalization	207
Figure 5-82	NLT-02b phase 2 transient decay heat removal system condensate temperature comparison	207
Figure 5-83	NLT-02b phase 2 transient decay heat removal system condensate flow comparison.....	208
Figure 5-84	NLT-02b phase 2 transient steam generator outlet temperature comparison.....	208
Figure 5-85	NLT-02b phase 2 transient decay heat removal system heat exchanger level comparison	209
Figure 5-86	NLT-02b phase 2 transient cooling pool vessel level comparison	209
Figure 5-87	NLT-02b phase 2 transient cooling pool vessel region 4 temperature comparison (below decay heat removal system heat exchanger).....	210
Figure 5-87a	NLT-02b phase 2 transient cooling pool vessel region 5 temperature comparison (near bottom of decay heat removal system heat exchanger).....	211
Figure 5-87b	NLT-02b phase 2 transient cooling pool vessel region 6 temperature comparison (near mid-point of decay heat removal system heat exchanger)	211
Figure 5-88	NLT-02b phase 2 transient cooling pool vessel region 7 temperature comparison (just above the decay heat removal system heat exchanger tube region)	212
Figure 5-89	NLT-02b phase 3 transient core power comparison	215
Figure 5-90	NLT-02b phase 3 transient pressurizer pressure comparison	215
Figure 5-91	NLT-02b phase 3 transient pressurizer level comparison.....	216
Figure 5-92	Not Used	216
Figure 5-93	NLT-02b phase 3 transient core inlet and outlet temperature comparison	216
Figure 5-94	Not Used	217

Figure 5-95	NLT-02b phase 3 transient steam generator steam pressure comparison	217
Figure 5-96	NLT-02b phase 3 transient steam generator thermal power comparison	217
Figure 5-97	NLT-02b phase 3 transient decay heat removal system heat exchanger thermal power comparison	218
Figure 5-98	NLT-02b phase 3 transient steam generator level comparison	218
Figure 5-99	NLT-02b phase 3 calculated compensation flow for steam generator and decay heat removal system heat exchanger level equalization	219
Figure 5-99a	NLT-02b phase 3 integrated compensation flow for SG and DHRS HX level equalization	219
Figure 5-100	NLT-02b phase 3 transient decay heat removal system condensate temperature comparison	220
Figure 5-101	NLT-02b phase 3 transient decay heat removal system condensate flow comparison	220
Figure 5-102	NLT-02b phase 3 transient steam generator outlet temperature comparison	221
Figure 5-103	NLT-02b phase 3 transient decay heat removal system heat exchanger level comparison	221
Figure 5-104	NLT-02b phase 3 transient cooling pool vessel level comparison	222
Figure 5-105	NLT-02b phase 3 transient cooling pool vessel region 4 temperature comparison (below decay heat removal system heat exchanger)	222
Figure 5-105a	NLT-02b phase 3 transient cooling pool vessel region 5 temperature comparison (near bottom of decay heat removal system heat exchanger)	223
Figure 5-105b	NLT-02b phase 3 transient cooling pool vessel region 6 temperature comparison (near mid-point of decay heat removal system heat exchanger)	223
Figure 5-106	NLT-02b phase 3 transient cooling pool vessel region 7 temperature comparison (just above the decay heat removal system heat exchanger tube region)	224
Figure 5-107	NLT-02b phase 4 transient core power comparison	226
Figure 5-108	NLT-02b phase 4 transient pressurizer pressure comparison	227
Figure 5-109	NLT-02b phase 4 transient pressurizer level comparison	227
Figure 5-110	NLT-02b phase 4 transient reactor pressure vessel level	228
Figure 5-111	NLT-02b phase 4 transient reactor pressure vessel upper plenum temperature comparison	228
Figure 5-112	NLT-02b phase 4 transient core inlet and outlet temperature comparison	229
Figure 5-113	Not Used	229
Figure 5-114	NLT-02b phase 4 transient steam generator steam pressure comparison	229
Figure 5-115	NLT-02b phase 4 transient steam generator thermal power comparison	230
Figure 5-116	NLT-02b phase 4 transient decay heat removal system heat exchanger thermal power comparison	230
Figure 5-117	NLT-02b phase 4 transient steam generator level comparison	231
Figure 5-118	NLT-02b phase 4 calculated compensation flow for steam generator and decay heat removal system heat exchanger level equalization	231
Figure 5-118a	NLT-02b phase 4 integrated compensation flow for SG and DHRS HX level equalization	232
Figure 5-119	NLT-02b phase 4 transient decay heat removal system condensate temperature comparison	232

Figure 5-120	NLT-02b phase 4 transient decay heat removal system condensate flow comparison.....	233
Figure 5-121	NLT-02b phase 4 transient steam generator outlet temperature comparison.....	233
Figure 5-122	NLT-02b phase 4 transient decay heat removal system heat exchanger level comparison	234
Figure 5-123	NLT-02b phase 4 transient cooling pool vessel level comparison	234
Figure 5-124	NLT-02b phase 4 transient cooling pool vessel region 4 temperature comparison (below decay heat removal system heat exchanger).....	235
Figure 5-124a	NLT-02b phase 4 transient cooling pool vessel region 5 temperature comparison (near bottom of decay heat removal system heat exchanger).....	235
Figure 5-124b	NLT-02b phase 4 transient cooling pool vessel region 6 temperature comparison (near mid-point of decay heat removal system heat exchanger)	236
Figure 5-125	NLT-02b phase 4 transient cooling pool vessel region 7 temperature comparison (just above the decay heat removal system heat exchanger tube region)	236
Figure 5-126	NLT-15p2, transient core power	245
Figure 5-127	NLT-15p2, transient RPV pressure short term.....	245
Figure 5-128	NLT-15p2, transient RPV pressure	246
Figure 5-129	NLT-15p2, transient pressurizer level	246
Figure 5-130	NLT-15p2, transient RPV level	247
Figure 5-131	NLT-15p2, transient riser mass flow rate.png	247
Figure 5-132	NLT-15p2, transient core inlet temperature	248
Figure 5-133	NLT-15p2, transient riser inlet temperature	248
Figure 5-134	NLT-15p2, transient upper plenum temperature	249
Figure 5-135	NLT-15p2, transient secondary side pressure - 0 to 500 seconds	249
Figure 5-136	NLT-15p2, transient DHRS loop flow - 0 to 500 seconds	250
Figure 5-137	NLT-15p2, transient measured steam line temperatures - 0 to 500 seconds	250
Figure 5-138	NLT-15p2, transient DHRS HX level - 0 to 500 seconds	251
Figure 5-139	NLT-15p2, transient secondary side pressure	251
Figure 5-140	NLT-15p2, transient DHRS HX inlet temperature	252
Figure 5-141	NLT-15p2, transient DHRS HX outlet temperature	252
Figure 5-142	NLT-15p2, transient DHRS loop flow - short term	253
Figure 5-143	NLT-15p2, transient DHRS loop flow rate - long term	253
Figure 5-144	NLT-15p2, transient DHRS HX level.....	254
Figure 5-145	NLT-15p2, transient steam generator tube coil level - long term	254
Figure 5-146	NLT-15p2, transient steam generator tube coil level - short term.....	255
Figure 5-147	NLT-15p2, transient DHRS condensate line differential pressure	255
Figure 5-148	NLT-15p2, transient DHRS steam line differential pressure	256
Figure 5-149	NLT-15p2, transient steam generator tube coil power removal	256
Figure 5-150	NLT-15p2, transient DHRS power removal	257
Figure 5-151	NLT-15p2, transient cooling pool vessel level	257
Figure 5-152	NLT-15p2, transient cooling pool vessel fluid temperature at level 3 (below decay heat removal heat exchanger)	258
Figure 5-153	NLT-15p2, transient cooling pool vessel fluid temperature at level 5 (near bottom of DHRS heat exchanger)	258

Figure 5-154	NLT-15p2, transient cooling pool vessel fluid temperature at level 6 (near midpoint of DHRS heat exchanger).....	259
Figure 5-155	NLT-15p2, transient cooling pool vessel fluid temperature at level 7 (top to just above DHRS heat exchanger region).....	259
Figure 5-156	NLT-15p2, transient cooling pool vessel fluid temperature at level 8 (above DHRS heat exchanger region)	260
Figure 5-157	NLT-15p2, transient cooling pool vessel fluid temperature at level 9 (above DHRS heat exchanger region)	260
Figure 5-158	Core power (fast uncontrolled rod withdrawal)	266
Figure 5-159	Total reactivity (fast uncontrolled rod withdrawal).....	267
Figure 5-160	Pressurizer pressure (fast uncontrolled rod withdrawal)	267
Figure 5-161	Pressurizer level (fast uncontrolled rod withdrawal)	268
Figure 5-162	Core flow (fast uncontrolled rod withdrawal)	268
Figure 5-163	Core inlet temperatures (fast uncontrolled rod withdrawal)	269
Figure 5-164	Core outlet temperatures (fast uncontrolled rod withdrawal).....	269
Figure 5-165	Core power (slow uncontrolled rod withdrawal).....	271
Figure 5-166	Total reactivity (slow uncontrolled rod withdrawal)	271
Figure 5-167	Pressurizer pressure (slow uncontrolled rod withdrawal)	272
Figure 5-168	Pressurizer level (slow uncontrolled rod withdrawal).....	272
Figure 5-169	Core flow (slow uncontrolled rod withdrawal)	273
Figure 5-170	Core inlet temperature (slow uncontrolled rod withdrawal)	273
Figure 5-171	Core outlet temperature (slow uncontrolled rod withdrawal)	274
Figure 5-172	Core power (power reduction).....	275
Figure 5-173	Total reactivity (power reduction).....	276
Figure 5-174	Pressurizer pressure (power reduction)	276
Figure 5-175	Pressurizer level (power reduction).....	277
Figure 5-176	Core flow (power reduction)	277
Figure 5-177	Core inlet temperature (power reduction).....	278
Figure 5-178	Core outlet temperature (power reduction).....	278
Figure 5-179	Core power (dropped control rod)	280
Figure 5-180	Total reactivity (dropped control rod)	280
Figure 5-181	Pressurizer pressure (dropped control rod).....	281
Figure 5-182	Pressurizer level (dropped control rod)	281
Figure 5-183	Core flow (dropped control rod).....	282
Figure 5-184	Core inlet temperature (dropped control rod)	282
Figure 5-185	Core outlet temperature (dropped control rod).....	283
Figure 5-186	Coil 1 representative pressure drop for {{ }} ^{2(a),(c)} nodes (left) and {{ }} ^{2(a),(c)} nodes (right).....	287
Figure 5-187	Coil 1 representative fluid temperature for {{ }} ^{2(a),(c)} nodes (left) and {{ }} ^{2(a),(c)} nodes (right).....	288
Figure 5-188	Coil 1 representative wall temperature for {{ }} ^{2(a),(c)} nodes (left) and {{ }} ^{2(a),(c)} nodes (right).....	288
Figure 5-189	Decrease in feedwater temperature nodalization sensitivity steam generator secondary side inlet pressure	289
Figure 5-190	Decrease in feedwater temperature nodalization sensitivity steam generator secondary side outlet pressure	289
Figure 5-191	Decrease in feedwater temperature nodalization sensitivity reactor coolant system flow rate	290

Figure 5-192	Decrease in feedwater temperature nodalization sensitivity reactor coolant system lower plenum pressure	290
Figure 5-193	Decrease in feedwater temperature nodalization sensitivity reactor coolant system core inlet temperature.....	291
Figure 5-194	Decrease in feedwater temperature nodalization sensitivity reactor power	291
Figure 6-1	NuScale Power Module (typical)	296
Figure 6-2	Typical primary and secondary side nodalization (heat structures and component cell details excluded)	297
Figure 6-3	Typical NRELAP5 plant module volume regions.....	298
Figure 6-4	Reactor pressure vessel downcomer nodalization	300
Figure 6-5	Core and lower plenum nodalization	302
Figure 6-6	Reflector / core bypass without fuel assemblies (for illustration only)	303
Figure 6-7	Lower riser region, immediately above the core (for illustration only)	304
Figure 6-8	Reactor pressure vessel core and lower riser	305
Figure 6-9	Reactor pressure vessel upper riser.....	306
Figure 6-10	Reactor pressure vessel pressurizer	308
Figure 6-11	Steam generator nodalization	311
Figure 6-12	Main steam system nodalization	313
Figure 6-13	Decay heat removal system division 1 nodalization	315
Figure 6-14	Not used.	316
Figure 6-15	Not used.	316
Figure 7-1	Example of decay heat comparisons	337
Figure 7-2	Example of setpoint relationships.....	343
Figure 8-1	Temperature of feedwater during the representative decrease in feedwater temperature event	491
Figure 8-2	Power response for the representative decrease in feedwater temperature event	491
Figure 8-3	Core outlet temperature for the representative decrease in feedwater temperature event	492
Figure 8-4	Steam generator 2 pressure response for the representative decrease in feedwater temperature event	492
Figure 8-5	Reactor pressure vessel pressure response for the representative decrease in feedwater temperature event.....	493
Figure 8-6	Pressurizer level for the representative decrease in feedwater temperature event	493
Figure 8-7	Reactor coolant system flow rate for the representative decrease in feedwater temperature event	494
Figure 8-8	Core inlet temperature for the representative decrease in feedwater temperature event	494
Figure 8-9	Net reactivity for the representative decrease in feedwater temperature event.....	495
Figure 8-10	Main steam transient flow rate during the representative increase in steam flow event	499
Figure 8-11	Steam generator 2 pressure response for the representative increase in steam flow event	499
Figure 8-12	Steam generator 2 secondary side flow for the representative increase in steam flow event	500
Figure 8-13	Core inlet temperature for the representative increase in steam flow event	500

Figure 8-14	Power response for the representative increase in steam flow event	501
Figure 8-15	Core outlet temperature for the representative increase in steam flow event.....	501
Figure 8-16	Reactor pressure vessel pressure response for the representative increase in steam flow event	502
Figure 8-17	Pressurizer level for the representative increase in steam flow event.....	502
Figure 8-18	Reactor coolant system flow rate for the representative increase in steam flow event	503
Figure 8-19	Net reactivity for the representative increase in steam flow event	503
Figure 8-20	Steam generators 1 (unaffected) and 2 (affected) secondary flow rates for the representative main steam line break event.....	507
Figure 8-21	Core inlet temperature for the representative main steam line break event.....	507
Figure 8-22	Net reactivity for the representative main steam line break event.....	508
Figure 8-23	Power response for the representative main steam line break event.....	508
Figure 8-24	Steam generators 1 (unaffected) and 2 (affected) pressure response for the representative main steam line break event.....	509
Figure 8-25	Pressurizer level for the representative main steam line break event.....	509
Figure 8-26	Reactor pressure vessel pressure response for the representative main steam line break event	510
Figure 8-27	Reactor coolant system flow rate for the representative main steam line break event.....	510
Figure 8-28	Core outlet temperature for the representative main steam line break event.....	511
Figure 8-29	Reactor pressure vessel pressure response for the representative loss of normal feedwater flow event – reactor coolant system pressure case.....	514
Figure 8-30	Pressurizer level for the representative loss of normal feedwater flow event – reactor coolant system pressure case	514
Figure 8-31	Steam generator 2 pressure response for the representative loss of normal feedwater flow event – reactor coolant system pressure case.....	515
Figure 8-32	Power response for the representative loss of normal feedwater flow event – reactor coolant system pressure case	515
Figure 8-33	Reactor coolant system flow rate for the representative loss of normal feedwater flow event – reactor coolant system pressure case.....	516
Figure 8-34	Core inlet temperature for the representative loss of normal feedwater flow event – reactor coolant system pressure case.....	516
Figure 8-35	Core outlet temperature for the representative loss of normal feedwater flow event – reactor coolant system pressure case.....	517
Figure 8-36	Net reactivity for the representative loss of normal feedwater flow event – reactor coolant system pressure case.....	517
Figure 8-37	Steam generator 2 secondary flow for the representative loss of normal feedwater flow event – reactor coolant system pressure case.....	518
Figure 8-38	Core inlet temperature for the representative loss of normal feedwater flow event – secondary pressure case	520
Figure 8-39	Core outlet temperature for the representative loss of normal feedwater flow event – secondary pressure case	521
Figure 8-40	Reactor pressure vessel pressure response for the representative loss of normal feedwater flow event – secondary pressure case	521

Figure 8-41	Pressurizer level for the representative loss of normal feedwater flow event – secondary pressure case	522
Figure 8-42	Steam generator 2 pressure response for the representative loss of normal feedwater flow event – secondary pressure case	522
Figure 8-43	Power response for the representative loss of normal feedwater flow event – secondary pressure case	523
Figure 8-44	Reactor coolant system flow rate for the representative loss of normal feedwater flow event – secondary pressure case	523
Figure 8-45	Net reactivity for the representative loss of normal feedwater flow event – secondary pressure case	524
Figure 8-46	Steam generator 2 secondary flow for the representative loss of normal feedwater flow event – secondary pressure case	524
Figure 8-47	Primary temperature response for the representative loss of AC power event.....	527
Figure 8-48	System pressure response for the representative loss of AC power event	527
Figure 8-49	Reactor pressure vessel core power response for the representative loss of AC power event	528
Figure 8-50	Decay heat removal system response for the representative loss of AC power event.....	528
Figure 8-51	RSV flow response for the representative loss of AC power event	529
Figure 8-52	Reactor coolant system flow response for the representative loss of AC power event.....	529
Figure 8-53	Pressurizer level response for the representative loss of AC power event	530
Figure 8-54	Feedwater line break flow response for the representative feedwater line break event.....	533
Figure 8-55	Primary temperature response for the representative feedwater line break event.....	534
Figure 8-56	System pressure response for the representative feedwater line break event.....	534
Figure 8-57	Reactor pressure vessel core power response for the representative feedwater line break event	535
Figure 8-58	Reactor safety valve flow response for the representative feedwater line break event.....	535
Figure 8-59	Decay heat removal system response for the representative feedwater line break event	536
Figure 8-60	Pressurizer level response for the representative feedwater line break event.....	536
Figure 8-61	Reactor coolant system flow response for the representative feedwater line break event	537
Figure 8-62	Pressurizer pressure response for the bank withdrawal from a low power startup condition	540
Figure 8-63	Reactor pressure vessel and steam generator pressure responses for the bank withdrawal from a low power startup condition	540
Figure 8-64	Power response for the bank withdrawal from a low power startup condition	541
Figure 8-65	Core inlet temperature for the bank withdrawal from a low power startup condition	541

Figure 8-66	Core inlet density for the bank withdrawal from a low power startup condition	542
Figure 8-67	Core outlet temperature for the bank withdrawal from a low power startup condition	542
Figure 8-68	Reactor coolant system flow rate for the bank withdrawal from a low power startup condition	543
Figure 8-69	Net reactivity for the bank withdrawal from a low power startup condition	543
Figure 8-70	Power response for the representative single rod withdrawal MCHFR case	546
Figure 8-71	Reactor pressure vessel pressure response for the representative single rod withdrawal MCHFR case	547
Figure 8-72	Pressurizer level for the representative single rod withdrawal MCHFR case	547
Figure 8-73	Core outlet temperature for the representative single rod withdrawal MCHFR case	548
Figure 8-74	Steam generator 2 pressure response for the representative single rod withdrawal MCHFR case	548
Figure 8-75	Reactor coolant system flow rate for the representative single rod withdrawal MCHFR case	549
Figure 8-76	Steam generator 2 secondary flow for the representative single rod withdrawal MCHFR case	549
Figure 8-77	Core inlet temperature for the representative single rod withdrawal MCHFR case	550
Figure 8-78	Net reactivity for the representative single rod withdrawal MCHFR case	550
Figure 8-79	Makeup flow for increase in reactor coolant system inventory	553
Figure 8-80	Recirculation pump flow for increase in reactor coolant system inventory	554
Figure 8-81	Letdown flow for increase in reactor coolant system inventory	554
Figure 8-82	CVCS recirculation flow rate into the reactor pressure vessel for increase in reactor coolant system inventory	555
Figure 8-83	CVCS recirculation flow rate out of the reactor pressure vessel for increase in reactor coolant system inventory	555
Figure 8-84	Pressure at the bottom of the pressurizer for increase in reactor coolant system inventory	556
Figure 8-85	Pressurizer level for increase in reactor coolant system inventory	556
Figure 8-86	Reactor power for increase in reactor coolant system inventory	557
Figure 8-87	Reactor coolant system flow for increase in reactor coolant system inventory	557
Figure 8-88	Decay heat removal system flow rate for increase in reactor coolant system inventory	558
Figure 8-89	Steam generator pressure for increase in reactor coolant system inventory	558
Figure 8-90	Core inlet and exit coolant liquid temperature for increase in reactor coolant system inventory	559
Figure 8-91	Total reactivity for increase in reactor coolant system inventory	559
Figure 8-92	Instantaneous break flow response (0 to 350 sec) for the representative small break outside containment event	563
Figure 8-93	Pressurizer level response for the representative small break outside containment event	563

Figure 8-94	Reactor pressure vessel pressure response (0 to 350 sec) for the representative small break outside containment event	564
Figure 8-95	Steam generator pressure responses for the representative small break outside containment event	564
Figure 8-96	Core power response for the representative small break outside containment event	565
Figure 8-97	Integrated break flow response (0 to 350 sec) for the representative small break outside containment event	565
Figure 8-98	Reactor coolant system flow rate response for the representative small break outside containment event	566
Figure 8-99	Core outlet temperature response for the representative small break outside containment event	566
Figure 8-100	Reactor pressure vessel pressure response (0 to 3000 sec) for the representative small break outside containment event	567
Figure 8-101	Net reactivity response for the representative small break outside containment event	567
Figure 8-102	Level above top of core response for the representative small break outside containment event	568
Figure 8-103	Pressurizer level response for the representative steam generator tube failure event	571
Figure 8-104	Reactor pressure vessel and steam generator pressure responses (0 to 500 sec) for the representative steam generator tube failure event (tube failure occurs in SG1)	571
Figure 8-105	Core power response for the representative steam generator tube failure event	572
Figure 8-106	Instantaneous break flow response for the representative steam generator tube failure event	572
Figure 8-107	Steam generator level response for the representative steam generator tube failure event	573
Figure 8-108	Integrated break mass release to steam generator before isolation (0 to 500 sec) for the representative steam generator tube failure event	573
Figure 8-109	Reactor coolant system flow rate response for the representative steam generator tube failure event	574
Figure 8-110	Core inlet and exit temperature responses for the representative steam generator tube failure event	574
Figure 8-111	Reactor pressure vessel and steam generator responses (0 to 6000 sec) for the representative steam generator tube failure event	575
Figure 8-112	Net reactivity response for the representative steam generator tube failure event	575
Figure 8-113	Level above top of core response for the representative steam generator tube failure event	576

Abstract

The purpose of this report is to present the NuScale evaluation model (EM) used to evaluate the NuScale Power Module (NPM) short-term system transient response to non-loss-of-coolant accident (non-LOCA) events. The non-LOCA evaluation model was developed following a graded approach to the guidance provided in Regulatory Guide (RG) 1.203 for the evaluation model development and assessment process (EMDAP). This report summarizes the NuScale plant design, non-LOCA initiating events, classification of the events and acceptance criteria. The scope of the non-LOCA system transient analysis is described in this report, as well as the interfaces to other safety analysis methodologies. The non-LOCA events cover several different event types based on the main effect on the reactor coolant system (RCS). A comprehensive, integrated phenomena identification and ranking table (PIRT) was developed for the range of non-LOCA event types and phases of the event progression. The high-ranked phenomena of the PIRT and how they are assessed are summarized in this report. The NRELAP5 code is the system thermal-hydraulic code used for non-LOCA system transient analysis. Applicability of NRELAP5 for non-LOCA system transient analysis is assessed based on the high ranked phenomena identified in the PIRT. This report describes the selection of appropriately conservative input when applying this EM to perform non-LOCA system transient analyses. The non-LOCA methodology ensures that system transient calculations are executed for sufficient duration to demonstrate that the initiating event is mitigated and stable cooling is established. For non-LOCA initiating events that actuate the decay heat removal system, the EM is applicable for the short-term transient progression; during this time frame the mixture level remains above the top of the riser and primary side natural circulation is maintained. Representative calculations of non-LOCA events demonstrate large margins to the primary and secondary pressure acceptance criteria. Other quantitative acceptance criteria, such as minimum critical heat flux ratio and radiological dose limits applicable for the non-LOCA events, are evaluated in downstream subchannel and accident radiological analyses which are documented in separate reports.

Executive Summary

The purpose of this report is to present the NuScale evaluation model (EM) used to evaluate the NuScale Power Module (NPM) short-term system transient response to non-loss-of-coolant accident (LOCA) events. This report summarizes the NuScale plant design, non-LOCA initiating events, classification of the events and acceptance criteria. The scope of the non-LOCA system transient analysis and interfaces to other safety analysis methodologies is described. Development of the non-LOCA phenomena identification and ranking table is described; the high-ranked phenomena and how they are assessed are summarized. The NRELAP5 code is the system thermal-hydraulic code used for non-LOCA system transient analysis. Applicability of NRELAP5 for non-LOCA system transient analysis is assessed. Parameters considered in the system transient analyses to specify appropriately conservative input in application of the EM are discussed. Representative transient calculations for different types of non-LOCA events are presented. These representative calculations demonstrate the application of the method only and are not intended for NRC approval of the NuScale plant design.

The NPM is a small, light water integral pressurized water reactor (PWR) consisting of a nuclear core, two helical coil steam generators (SGs), and a pressurizer, all contained within a single reactor vessel. The reactor vessel is located within a small, compact steel containment vessel. The NPM is designed to operate efficiently at full power conditions using natural circulation as the means of providing core coolant flow, eliminating the need for reactor coolant pumps. The helical coil SGs, which produce superheated steam, are located in the annular space between the RCS hot leg riser and the reactor vessel inside diameter wall. The relative locations of the thermal centers in the core and the SGs promote buoyancy driven natural circulation flow. Power conversion occurs via a secondary system that includes the steam turbine-generator, the main condenser, and the plant components necessary to provide feedwater. Each NPM has dedicated chemical and volume control system (CVCS), emergency core cooling system (ECCS), and decay heat removal system (DHRS). The CVCS is used to regulate the primary side inventory via makeup and letdown to maintain pressurizer level and boron concentration during normal operation. Pressurizer heaters and spray control primary side pressure. The DHRS is a normally isolated, closed-loop, two-phase natural circulation cooling system; two trains of decay heat removal equipment are provided, one connected to each SG secondary side loop.

The NuScale power plant consists of one or more NPMs, each partially immersed in its own bay of the common reactor pool. The reactor pool serves as the ultimate heat sink (UHS) and is located in a Seismic Category I building designed to withstand postulated adverse natural conditions and aircraft impact. The NuScale design instrumentation and control architecture includes the safety-related module protection system, and nonsafety-related module and plant control systems.

The non-LOCA system transient evaluation model for analysis of the NPM system transient response to non-LOCA events was developed following a graded approach to the guidance provided in Regulatory Guide (RG) 1.203 for the evaluation model development and assessment process (EMDAP). The EMDAP as defined in RG 1.203 provides a structured process to establish the adequacy of a methodology for evaluating complex events that are postulated to occur in nuclear power plant systems. Six basic principles are identified in RG 1.203 as important in the process of developing and assessing an EM. Four of the principles (using 20 steps as identified in the EMDAP process) are addressed in this report. The remaining principles related to

establishing an appropriate quality assurance program and providing comprehensive, accurate, up-to-date documentation are addressed outside of this report as part of “NuScale Topical Report: Quality Assurance Program Description for the NuScale Power Plant,” NP-TR-1010-859-NP-A (Reference 3).

As part of defining the requirements of the non-LOCA transient system analysis methodology, the events to which the methodology applies and the specific event acceptance criteria applicable to the events are identified. The NPM design was evaluated to assure that a sufficiently broad spectrum of transients, accidents, and initiating events have been included in the scope of design basis analyses presented in DCD Chapter 15. The NPM is a natural circulation integral PWR. Many of the events analyzed for operating plants and in recent design certification applications are applicable to the NuScale design. NuScale-specific events reflect unique aspects of the NuScale design such as the DHRS and normal operation of the containment at vacuum conditions. The design-basis events for which non-LOCA system transient analysis are performed are categorized into one of 5 categories:

1. Increase in heat removal from the RCS
2. Decrease in heat removal by the secondary system
3. Reactivity and power distribution anomalies
4. Increase in reactor coolant inventory
5. Decrease in reactor coolant inventory

Each event is classified as an anticipated operational occurrence (AOO), infrequent event (IE), or accident. The specific event acceptance criteria are derived from the regulatory requirements and guidance. The non-LOCA transient system analysis is part of several stages of analysis performed to confirm the plant design meets applicable acceptance criteria for a limiting set of AOOs, IEs, and accidents. The interfaces of the non-LOCA transient system analysis with downstream subchannel analysis and accident radiological analysis methodologies are identified. The subchannel analysis codes and methods, and the accident radiological source term and dose analyses are covered in separate methodologies and assessments. For non-LOCA initiating events that actuate the DHRS, the EM is applicable for the short-term transient progression; during this time frame the mixture level remains above the top of the riser and primary side natural circulation is maintained.

As part of developing the non-LOCA evaluation model, a phenomena identification and ranking table (PIRT) was developed. The non-LOCA events cover several different event types based on the main effect on the RCS. A comprehensive, integrated PIRT was performed for the range of non-LOCA event types and phases of the event progression. The PIRT panel considered the NPM design to identify systems, components, and subcomponents of the design for which phenomena were assessed. Phenomena were identified and ranked considering their level of importance relative to identified figures of merit for the different non-LOCA event types and phases of the transient progression; a knowledge ranking was established for each of the phenomena.

NRELAP5 is NuScale’s system thermal-hydraulics code used to simulate the NPM system response during both the non-LOCA and LOCA short-term transient event progression. The NRELAP5 code was derived from the Idaho National Laboratory (INL) RELAP5-3D® computer

code. RELAP5-3D, version 4.1.3 was used as the baseline development platform for the NRELAP5 code. RELAP5-3D was procured and commercial grade dedication was performed by NuScale. Subsequently, features were added and changes made to address unique aspects of the NPM design and licensing methodology. NRELAP5 is a non-homogenous, non-equilibrium two-fluid thermal hydraulic systems analysis code capable of performing non-LOCA system transient analyses for the NPM. The NRELAP5 code has a heat conduction and heat transfer package that is similar in capability to other thermal-hydraulic codes in its class (such as TRAC, RETRAN or TRACE). It includes the trips and logic control systems that enable simulation of the plant protection and control system logic for analysis of a non-LOCA event in the NPM. The NRELAP5 code is described in the NuScale LOCA Evaluation Model licensing topical report. The NRELAP5 code has been assessed against several separate effects and integral effects tests as part of the code development and development of the NuScale LOCA evaluation model to demonstrate the capability to simulate the NPM response to LOCA events.

Phenomena identified as high-ranked for the non-LOCA transients were evaluated with respect to the high-ranked phenomena identified and assessed as part of the NuScale LOCA evaluation model development. Additional validation of NRELAP5 against separate effects testing, integral effects testing, and code to code benchmarking, were performed as necessary to justify applicability of the NRELAP5 code for non-LOCA system thermal-hydraulic analysis. High-ranked phenomena for non-LOCA events that were not assessed as part of the NuScale LOCA evaluation model development were therefore addressed in different ways:

1. additional NRELAP5 code assessment performed against separate effects or integral effects test data
2. code-to-code benchmark performed between NRELAP5 and independent system thermal-hydraulics code
3. phenomena addressed as part of the downstream subchannel analysis
4. phenomena addressed by specifying appropriately conservative input to the system transient analysis

In particular, separate and integral effects testing were performed at the NIST-1 facility to support applicability of the NRELAP5 code for non-LOCA system transient analysis. Separate effects testing of the DHRS was performed. Integral effects testing of the NPM response to a decrease in secondary side heat transfer, and integral effects testing of DHRS operation were performed. A code-to-code benchmark was performed to compare the NRELAP5 and RETRAN-3D responses to a range of reactivity insertion conditions in the NPM.

The general non-LOCA transient analysis process is described in this report. The general methodology for conservatively biasing initial and boundary conditions for event analysis is presented. Each initiating event is then considered to identify the acceptance criteria that may be challenged during the event. For each non-LOCA event, a description of the event is provided including biases and conservatisms applied, sensitivity studies performed, single active failures and loss of power scenarios that challenge the event acceptance criteria. For each transient event, the acceptance criteria where margin to the limit may be challenged are identified. For these acceptance criteria, sensitivity calculations are performed as necessary to confirm that appropriately conservative inputs are specified and to determine conditions that result in minimum margin. For other acceptance criteria where margin to the limit is not challenged, representative

results from the overall scope of sensitivity calculations performed are sufficient to demonstrate that margin to the acceptance criterion is maintained. For non-LOCA initiating events that actuate the DHRS, the EM is applicable for the short-term transient progression; during this time frame the mixture level remains above the top of the riser and primary side natural circulation is maintained.

For selected non-LOCA events, representative system transient results are provided to demonstrate the application of the evaluation model for the NPM. System transient calculations are executed for sufficient duration to demonstrate that the initiating event is mitigated and stable cooling is established. Results of representative calculations show that the maximum primary and secondary pressure acceptance criteria are not significantly challenged in the NPM design. Margin to other quantitative acceptance criteria for minimum critical heat flux ratio, fuel centerline temperature, and radiological dose limits applicable for the non-LOCA events are demonstrated as part of downstream subchannel or accident radiological analyses that are described in separate reports. In addition, long-term cooling analysis methodology is presented in a separate report.

NuScale requests U.S. Nuclear Regulatory Commission (NRC) approval to use the EM described in this report for analyses of NPM design basis non-LOCA events that require system transient analysis. The specific scope of the non-LOCA events for which the EM applies is delineated in Section 1.2. NuScale is not seeking NRC approval of the representative calculations that are described in this report.

1.0 Introduction

1.1 Purpose

The purpose of this report is to present the NuScale evaluation model (EM) used to evaluate the NuScale Power Module (NPM) system transient response to non-loss-of-coolant accident (non-LOCA) events with the NRELAP5 code. This report summarizes the NuScale plant design and identifies the potential non-LOCA initiating events for the NPM analyzed by this EM. The classification of these non-LOCA events and relevant acceptance criteria that are prescribed in the NRC standard review plan (SRP) and the NuScale design specific review standard (DSRS) are discussed in this report.

The purpose of the non-LOCA evaluation model is to model the NPM response to a non-LOCA design basis event. The non-LOCA system transient evaluation model was developed following a graded approach to the guidance provided in Regulatory Guide (RG) 1.203 (Reference 1). The non-LOCA phenomena identification and ranking table (PIRT) is described, including a summary of the high-ranked phenomena and how they are assessed. The applicability of NRELAP5 for non-LOCA system transient analysis is assessed. The scope of the non-LOCA system transient analysis is described in this report, as well as interfaces to other safety analysis methodologies. This report describes the selection of appropriately conservative input when applying this EM to perform non-LOCA system transient analyses. Representative transient calculations from application of the EM for the range of non-LOCA events are presented.

1.2 Scope

NuScale requests U.S. Nuclear Regulatory Commission (NRC) approval to use the EM described in this report for analyses of NPM design basis non-LOCA events that require system transient analysis. Representative analysis results are provided in Section 8.0 of this report to illustrate results from application of the EM. These representative cases are not necessarily based on final NuScale NPM design inputs, and NRC approval of the representative results is not requested. The scope of this report includes the applicability and acceptability of this methodology to evaluate the primary and secondary system pressure acceptance criteria found in Chapter 15 of the NuScale DSRS and the SRP. This report also describes how the non-LOCA evaluation model interfaces with other analyses that will evaluate acceptance criteria that are not evaluated by the non-LOCA evaluation model.

The scope of the NuScale non-LOCA system transient analysis EM is summarized below:

- The non-LOCA evaluation model uses the NRELAP5 code to perform system transient analysis of the NPM design basis events listed in Table 4-1. The general and event-specific analysis methodologies of the EM are presented in Section 7.0. Sensitivity studies justifying the selected biasing direction are presented in Section 7.2 as part of the event-specific analysis methodology of the EM. The NRELAP5 code is described in the LOCA Evaluation Model (Reference 2).
- The non-LOCA evaluation model is applicable to a nuclear power plant that follows the general description of the NuScale plant design in Section 3.0. The applicability of

the EM is based on the non-LOCA phenomena identification and ranking table and assessment of the high-ranked phenomena that are treated as part of the system transient analysis.

- The non-LOCA evaluation model does not address the evaluation of specified acceptable fuel design limits (SAFDLs), which are evaluated in a downstream subchannel analysis. The subchannel analysis codes and methods are covered in separate methodologies and assessments (Reference 6). However, the interface of the non-LOCA system transient analysis with the downstream subchannel analysis is part of the non-LOCA evaluation model.
- The non-LOCA evaluation model does not address the evaluation of the accident radiological source term and dose. The accident radiological source term and dose analyses are covered in separate methodologies and assessments (Reference 8). However, the interface of the non-LOCA system transient analysis with downstream radiological analysis is part of the non-LOCA evaluation model.
- The EM is applicable for the short-term non-LOCA transient progression; the non-LOCA transient analysis short-term duration and analysis process are discussed further in Sections 4.2 and 4.3. During this time frame the mixture level remains above the top of the riser and primary side natural circulation is maintained. Long-term cooling analysis methodology, including events that transition from DHRS cooling to ECCS cooling, is addressed in Section 15.0.5 of the NuScale design certification application.
- Control rod ejection accident analysis is addressed by a separate methodology (Reference 21) and is not part of the non-LOCA evaluation model.
- Loss of coolant accident analysis is addressed by a separate methodology (Reference 2) and is not part of the non-LOCA evaluation model.
- Analysis of an inadvertent opening of a valve on the reactor vessel as an initiating event is addressed in Section 15.6.6 of the NuScale design certification application and is not part of the non-LOCA evaluation model.
- Analysis of the peak containment pressure and temperature response is addressed in Section 6.2 of the NuScale design certification application and is not part of the non-LOCA evaluation model.
- Evaluation of a return to power assuming the worst case stuck rod is addressed in Section 15.0.6 of the NuScale design certification application and is not part of the non-LOCA evaluation model.

1.3 Abbreviations

Table 1-1 Abbreviations

Term	Definition
AC	alternating current
ANS	American Nuclear Society
AOO	anticipated operational occurrence

Term	Definition
ASME	American Society of Mechanical Engineers
BOC	beginning of cycle
CFR	Code of Federal Regulations
CHF	critical heat flux
CHFR	critical heat flux ratio
CNV	containment vessel
CPV	cooling pool vessel
CRA	control rod assembly
CVC	chemical and volume control
CVCS	chemical and volume control system
DACS	data acquisition and control system
DC	direct current
DCA	Design Certification Application
DCD	Design Control Document
DFWT	decrease in feedwater temperature
DHRS	decay heat removal system
DNB	departure from nucleate boiling
DSRS	Design Specific Review Standard
DTC	Doppler temperature coefficient
ECCS	emergency core cooling system
EDNS	normal DC power system
EDSS	highly reliable DC power system
ELVS	low voltage (480 V and 120 V) AC electrical distribution system
EM	evaluation model
EMDAP	evaluation model development and assessment process
EMVS	medium voltage (4.16 kV) AC electrical distribution system
EOC	end of cycle
ESFAS	engineered safety features actuation system
FOM	figure of merit
FWIV	feedwater isolation valve
FWRV	feedwater regulating valve
GDC	General Design Criteria
HTP	heat transfer plate
HX	heat exchanger
ID	inside diameter
IE	infrequent event
IET	integral effects test
INL	Idaho National Laboratory
KAIST	Korea Advanced Institute of Science and Technology
L/D	length to diameter ratio
LOCA	loss-of-coolant accident
LOP	loss of power
MASLWR	multi-application small light water reactor
MCHFR	minimum critical heat flux ratio

Term	Definition
MCS	module control system
MPS	module protection system
MSIV	main steam isolation valve
MSS	main steam system
MTC	moderator temperature coefficient
NIST-1	NuScale Integral System Test Facility
NPM	NuScale Power Module
NRC	Nuclear Regulatory Commission
NRELAP5	NuScale version of RELAP5-3D®
OD	outside diameter
OSU	Oregon State University
P/L	pressure/level
PCS	plant control system
P/D	pitch to diameter ratio
PIRT	phenomena identification and ranking table
PWR	pressurized water reactor
PZR	pressurizer
QAP	Quality Assurance Program
RCS	reactor coolant system
RG	Regulatory Guide
RPV	reactor pressure vessel
RRV	reactor recirculation valve
RSV	reactor safety valve
RTP	rated thermal power
RTS	reactor trip system
RVV	reactor vent valve
SAF	single active failure
SAFDL	specified acceptable fuel design limit
SET	separate effects test
SG	steam generator
SGTF	steam generator tube failure
SMR	small modular reactor
SRP	standard review plan
SSC	structures, systems, and components
TMDPJUN	time dependent junction
TMDPVOL	time dependent volume
UCRW	uncontrolled rod withdrawal
UCRWS	uncontrolled rod withdrawal from subcritical (or low power)
UHS	ultimate heat sink
VAC	volts alternating current

Table 1-2 Definitions

Term	Definition
Analytical limit	Limit of a measured or calculated variable established by the safety analysis to ensure that a safety limit is not exceeded
Anticipated operational occurrences (AOOs)	Conditions of normal operation that are expected to occur one or more times during the life of the nuclear power unit
Design basis accidents	A postulated accident that a nuclear facility must be designed and built to withstand without loss to the systems, structures and components necessary to ensure public health and safety.
Design basis events	Postulated events used in the design to establish the acceptable performance requirements for the structures, systems and components.
Design bases	That information which identifies the specific functions to be performed by a system, structure or component of a facility, and the specific values or ranges of values chosen for controlling parameters as reference bounds for design. These values may be (1) restraints derived from generally accepted “state of the art” practices for achieving functional goals, or (2) requirements derived from analysis (based on calculation and/or experiments) of the effect of a postulated accident for which a structure, system or component must meet its functional goals.
Excellent agreement	One of the acceptance criteria defined in RG 1.203. “Excellent” agreement applies when the code exhibits no deficiencies in modeling a given behavior. Major and minor phenomena and trends are correctly predicted. The calculated results are judged to agree closely with the data. The calculation will, with few exceptions, lie within the specified or inferred uncertainty bands of the data. The code may be used with confidence in similar applications.
Infrequent events (IEs)	Events which are not classified as AOOs or as accidents, and are not expected to occur during the design life of the plant. For IEs, the acceptance criteria are specified such that some fuel damage may occur but the radiological acceptance criteria are stricter than those imposed for accidents. These include events which may be historically considered as AOOs for operating plants, but due to aspects of the NPM design, the events are not expected to occur during the design life of the NPM operation.
Insufficient agreement	One of the acceptance criteria defined in RG 1.203. “Insufficient” agreement applies when the code exhibits major deficiencies. The code provides an unacceptable prediction of the test data because major trends are not predicted correctly. Most calculated values lie outside the specified or inferred uncertainty bands of the data.
Loss-of-coolant accident	Those postulated accidents that result in a loss of reactor coolant at a rate in excess of the capability of the reactor makeup system from breaks in the reactor coolant pressure boundary, up to and including a break equivalent in size to the double-ended rupture of the largest pipe in the reactor coolant system.

Term	Definition
Minimal agreement	One of the acceptance criteria defined in RG 1.203. "Minimal" agreement applies when the code exhibits significant deficiencies. Overall, the code provides a prediction that is only conditionally acceptable. Some major trends or phenomena are not predicted correctly, and some calculated values lie considerably outside the specified or inferred uncertainty bands of the data. Incorrect conclusions about trends and phenomena may be reached if the code were used in similar applications, and an appropriate warning needs to be issued to users. Selected code models or facility model nodding need to be reviewed, modified and assessed before the code can be used with confidence in similar applications.
Non-LOCA transient	Reactor coolant system transients described in the standard review plan Sections 15.1, 15.2, 15.4, and 15.5, and other comparable transients that may be unique to the NuScale system. Other sections in the standard review plan are specific to events with reactor coolant pumps, LOCA, radiological analysis, anticipated transient without scram, or boiling water reactors, and are outside of scope.
Postulated accidents	A postulated accident that a nuclear facility must be designed and built to withstand without loss to the systems, structures and components necessary to ensure public health and safety.
"Reasonable" agreement	One of the acceptance criteria defined in RG 1.203. "Reasonable" agreement applies when the code exhibits minor deficiencies. Overall, the code provides an acceptable prediction. All major trends and phenomena are correctly predicted. Differences between calculation and data are greater than deemed necessary for excellent agreement. The calculation will frequently lie outside but near the specified or inferred uncertainty bands of the data. However, the correct conclusions about trends and phenomena would be reached if the code were used in similar applications.
Safety-related structures, system and components	Those structures, systems and components that are relied upon to remain functional during and following design-basis events to assure: (1) the integrity of the reactor coolant pressure boundary, (2) the capability to shut down the reactor and maintain it in a safe shutdown condition; or (3) the capability to prevent or mitigate the consequences of accidents which could result in potential offsite exposures comparable to the applicable guideline exposures set forth in 10 CFR 50.34(a)(1).

2.0 Background

This topical report provides a description of the NuScale non-LOCA system transient analysis EM. The non-LOCA system transient analysis EM has been developed following a graded application of the guidelines in the evaluation model development and assessment process (EMDAP) of RG 1.203.

Six basic principles are identified in RG 1.203 as important in the process of developing and assessing an EM. Four of the principles (using 20 steps as identified in the EMDAP process) are addressed in this report. The remaining principles related to establishing an appropriate quality assurance program and providing comprehensive, accurate, up-to-date documentation are addressed outside of this report as part of “NuScale Topical Report: Quality Assurance Program Description for the NuScale Power Plant,” NP-TR-1010-859-NP-A (Reference 3).

This EM utilizes the NRELAP5 code that was developed from the Idaho National Laboratory (INL) RELAP5-3D[®] computer code. The NRELAP5 code is described in Reference 2. Applicability of the NRELAP5 code for application in non-LOCA system transient analysis is discussed in this report.

2.1 Non-LOCA Evaluation Model Roadmap

Analyses are performed to demonstrate that a nuclear power plant can meet applicable NRC regulatory acceptance criteria for a limiting set of AOOs, IEs, and accidents.

The EMDAP as defined in RG 1.203 provides a structured process to establish the adequacy of a methodology for evaluating complex events that are postulated to occur in nuclear power plant systems. The EM described here has been developed for simulating the NPM system transient response to non-LOCA events.

NRELAP5 is NuScale’s system thermal-hydraulics code used to simulate the NPM system response during both the non-LOCA and LOCA short-term transient event progression. The NuScale LOCA EM (Reference 2) was developed following the EMDAP guidelines of RG 1.203. As described in Section 5.0, phenomena identified as high-ranked for the non-LOCA transients were evaluated with respect to the high-ranked phenomena identified as part of the NuScale LOCA evaluation model development. Considering the overlap in high-ranked phenomena and conservatism applied to input and boundary conditions in the non-LOCA plant transient calculations (see Section 7), a graded approach to the EMDAP is applied for development of the non-LOCA system transient EM.

Figure 2-1 shows various elements of EMDAP as defined in RG 1.203. The elements of the EMDAP and sections of this report that relate to the elements and steps of the EMDAP are summarized in Table 2-1.

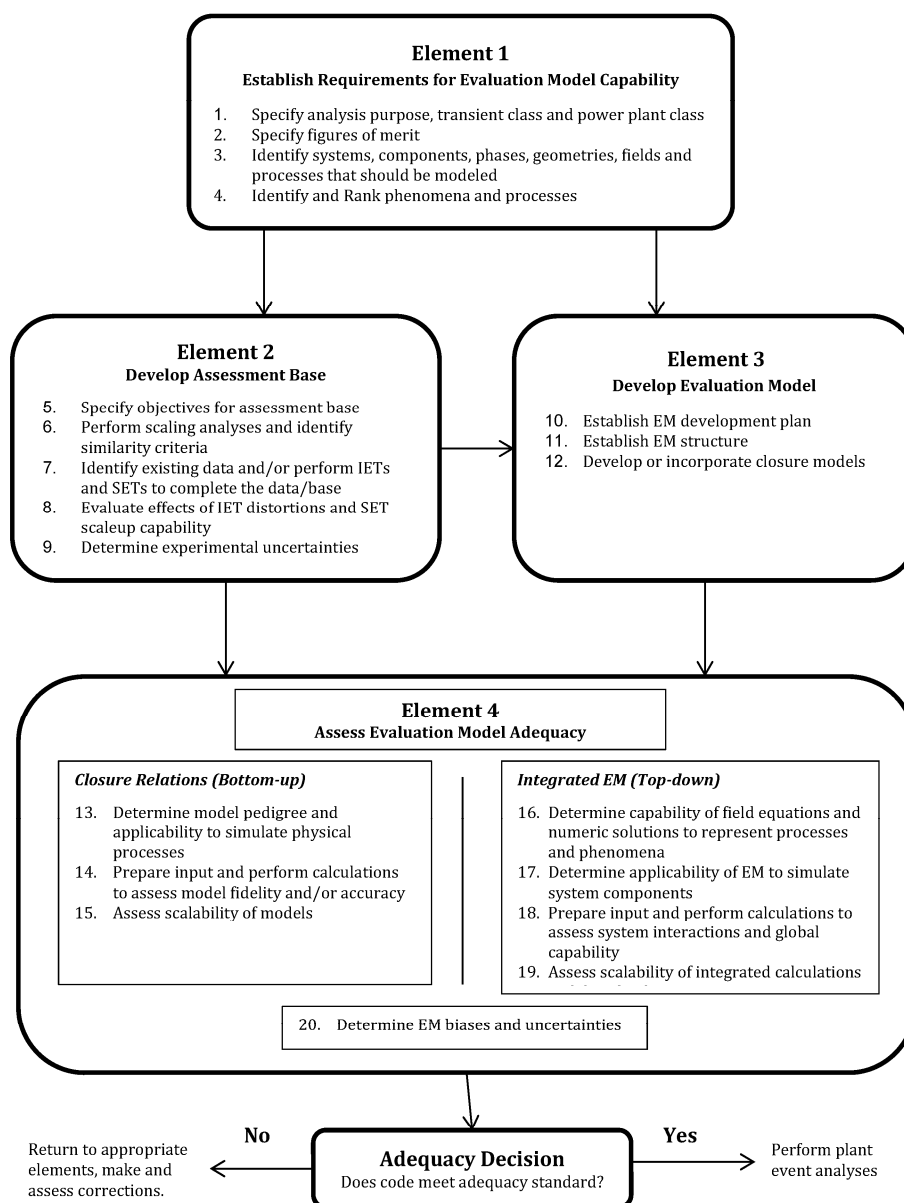


Figure 2-1 Evaluation model development and assessment process

Table 2-1 Evaluation model development and assessment process steps and associated application in the non-LOCA evaluation model

EMDAP Step	Description	EM Section
Element 1, Establish Requirements for Evaluation Model Capability		
1	Specify analysis purpose, transient class and power plant class.	<p>The purpose of the non-LOCA system transient analysis methodology is described in Section 1.1. Section 2.0 briefly describes the background of the process followed to develop the non-LOCA system transient analysis methodology and the principal software used.</p> <p>Section 3.0 provides an overview of the NPM and a description of the plant operation. This includes the safety systems, the system logic, and operational phases which could occur in the NuScale SMR design.</p> <p>The high level regulatory requirements that the methodology is designed to comply with are described in Section 2.2.</p> <p>In Section 4.1 the non-LOCA initiating events and the classification of the events for the NPM are discussed. The acceptance criteria for the events are identified in Section 4.2. As identified in Section 4.2, margin to some of these acceptance criteria are demonstrated based on the results of the non-LOCA system transient analysis; other acceptance criteria are met as part of downstream analyses such as subchannel and radiological analyses. Downstream analyses are outside the scope of this topical report as discussed in Section 1.2. The non-LOCA transient analysis process, including interfaces with other safety analysis methodologies, is described in Section 4.3.</p>
2	Specify figures of merit (FOMs).	Section 5.1 discusses the FOMs that are used for the development of the NPM non-LOCA PIRT.
3	Identify systems, components, phases, geometries, fields, and processes that should be modeled.	Systems, components, phases and processes are identified as a part of the non-LOCA PIRT discussed in Section 5.1.
4	Identify and rank phenomena and processes.	Section 5.1 describes the NPM non-LOCA PIRT.
Element 2, Develop Assessment Base		
5	Specify objectives for assessment base.	Section 5.2 describes the high ranked phenomena identified from the PIRT process and how the phenomena are addressed by NRELAP5 assessment or other approach. Many of the high ranked phenomena were assessed against experimental data as part of the LOCA evaluation model development (Reference 2); additional assessments were identified as described in Section 5.2.

EMDAP Step	Description	EM Section
6	Perform scaling analysis and identify similarity criteria.	<p>A scaling analysis of the LOCA and emergency core cooling system (ECCS) has been performed for the NPM centered on the NuScale Integral Systems Test-1 (NIST-1) facility. The results of the scaling analysis are discussed in Reference 2.</p> <p>Considering the overlap in high-ranked phenomena and conservatism applied to input and boundary conditions in the non-LOCA plant transient calculations, these assessments are considered adequate for the non-LOCA system transient EM.</p>
7	Identify existing data and perform integral effects test (IETs) and separate effects tests (SETs) to complete database.	Reference 2 and Section 5.3 of this report provide the results of the NRELAP5 validation against the SETs and IETs.
8	Evaluate effects of IET distortions and SET scaleup capability.	In Reference 2, a bottom-up assessment of NRELAP5 closure models and correlations is presented; this assessment addresses the fidelity of the models and correlations to the appropriate fundamental or SET data. In Reference 2, a top-down assessment of the NRELAP5 governing equations and numerics is presented. Considering the overlap in high-ranked phenomena and conservatism applied to input and boundary conditions in the non-LOCA plant transient calculations, these assessments are considered adequate for the non-LOCA system transient EM.
9	Determine experimental uncertainties.	Reference 2 and Section 5.3 of this report cover experimental uncertainties for NRELAP5 assessments against the SETs and IETs.
Element 3, Develop Evaluation Model		
10	Establish EM development plan.	The NRELAP5 development plan includes programming standards and procedures, quality assurance procedures, and configuration control which are summarized in Reference 2.
11	Establish EM structure.	<p>Reference 2 provides a summary of NRELAP5 models and correlations.</p> <p>The non-LOCA transient analysis process, including interfaces with other safety analysis methodologies, is described in Section 4.3. For non-LOCA system transient analysis, the plant model is described in Section 6.0. The non-LOCA analysis methodology is described in Section 7.0.</p>
12	Develop or incorporate closure models.	Reference 2 provides a summary of NRELAP5 models and correlations. A full description of the closure models and the associated equations used in the non-LOCA evaluation model is provided in the NRELAP5 theory and users manuals.

EMDAP Step	Description	EM Section
Element 4, Assess Evaluation Model Adequacy Closure Relations (Bottom-up)		
13	Determine model pedigree and applicability to simulate physical processes.	Reference 2 includes a bottom-up assessment of important NRELAP5 models and correlations essential to simulate high-ranked PIRT phenomena for LOCA events, including discussion of model pedigree and applicability. Considering the overlap in high-ranked phenomena and conservatism applied to input and boundary conditions in the non-LOCA plant transient calculations, these assessments are considered adequate for the non-LOCA system transient EM.
14	Prepare input and perform calculations to assess model fidelity and accuracy.	Reference 2 and Section 5.3 summarize the results of comparison of NRELAP5 against the selected SETs and IETs including evaluation of code fidelity and accuracy.
15	Assess scalability of models.	Reference 2 includes discussion on scalability of dominant NRELAP5 models and correlations that are essential to simulate high-ranked PIRT phenomena for LOCA events. Considering the overlap in high-ranked phenomena and conservatism applied to input and boundary conditions in the non-LOCA plant transient calculations, these assessments are considered adequate for the non-LOCA system transient EM.
Element 4, Assess Evaluation Model Adequacy Integrated EM (Top-down)		
16	Determine capability of field equations and numeric solutions to represent processes and phenomena.	NRELAP5 field equations and the numeric solution scheme are discussed in Reference 2 and evaluated for their applicability to NPM LOCA. Considering the overlap in high-ranked phenomena and conservatism applied to input and boundary conditions in the non-LOCA plant transient calculations, these assessments are considered adequate for the non-LOCA system transient EM.
17	Determine applicability of EM to simulate system components.	The applicability of the EM to simulate the NPM system and components is demonstrated by assessment of NRELAP5 against NuScale design-specific SETs and IETs.
18	Prepare input and perform calculations to assess system interactions and global capability.	Reference 2 and Section 5.3 summarize the results of an assessment of NRELAP5 against NIST-1 IET data.
19	Assess scalability of integrated calculations and data for distortions.	Reference 2 provides an evaluation of scaling distortions between the NIST-1 LOCA IET data and the NPM design. The scalability of the EM to represent NPM LOCA phenomena and processes is presented therein. Considering the overlap in high-ranked phenomena and conservatism applied to input and boundary conditions in the non-LOCA plant transient calculations, these assessments are considered adequate for the non-LOCA system transient EM.

EMDAP Step	Description	EM Section
20	Determine EM biases and uncertainties.	For the non-LOCA system transient analyses, suitably conservative input is specified in the plant calculations as described in Section 7.0, considering the effects on the appropriate acceptance criteria.

2.2 Regulatory Requirements

The following General Design Criteria (GDC) of 10 CFR Part 50 Appendix A (Reference 4) are relevant to the non-LOCA transient analyses:

- GDC 5, as it relates to demonstrating that any sharing of structures, systems, and components (SSC) does not significantly impact the ability of the SSC to perform their safety function.
- GDC 10, as it relates to demonstrating that SAFDLs are not exceeded during AOOs.
- GDC 15, as it relates to demonstrating that the reactor coolant system pressure boundary will not be breached during AOOs.
- GDC 17, as it relates to providing electric power systems to permit functioning of SSC to assure that SAFDLs and design conditions of the reactor coolant pressure boundary are not exceeded as a result of AOOs, and that the core is cooled and containment integrity and other vital functions are maintained in the event of postulated accidents. The NuScale design supports an exemption from GDC 17, as documented in the NuScale DCA, and therefore GDC 17 is not relevant to this methodology.
- GDC 20, as it relates to demonstrating that the automatic operation of systems by the reactor protection system ensures that the plant does not exceed SAFDLs during AOOs.
- GDC 25, as it relates to demonstrating that the protection system design assures that SAFDLs are not exceeded for any single malfunction of the reactivity control system, such as accidental withdrawal (not ejection or dropout) of control rods.
- GDC 26, as it relates to demonstrating that the control rods are capable of reliably controlling reactivity changes to assure that SAFDLs are not exceeded during AOOs, with appropriate margin for malfunctions such as stuck rods.
- GDC 27, as it relates to demonstrating that the reactivity control systems are capable of reliably controlling reactivity changes to assure capability to cool the core is maintained under postulated accident conditions, with appropriate margin for stuck rods. The NuScale design supports an exemption from GDC 27, and instead implements a NuScale-specific Principal Design Criterion (PDC) 27, as documented in the NuScale DCA. As relevant to this methodology, NuScale PDC 27 is equivalent to GDC 27 (i.e., differences are not within the scope of this evaluation methodology).
- GDC 28, as it relates to demonstrating that the effects of postulated reactivity accidents can neither result in damage to the reactor coolant pressure boundary greater than limited local yielding, nor impair significantly the capability to cool the core.

- GDC 31, as it relates to demonstrating that the probability of a rapidly propagating fracture of the reactor coolant pressure boundary is minimized when the pressure boundary is stressed under postulated accident conditions.
- GDC 34, as it relates to demonstrating that residual heat is removed from the reactor core at a rate such that SAFDLs and the design conditions of the reactor coolant pressure boundary are not exceeded, assuming a single failure and considering offsite power availability. The NuScale design supports an exemption from GDC 34, and instead implements a NuScale-specific Principal Design Criterion (PDC) 34, as documented in the NuScale DCA. As relevant to this methodology, NuScale PDC 34 is equivalent to GDC 34 (i.e., differences are not within the scope of this evaluation methodology).

Regulatory guidance documents relevant to the non-LOCA transient system analysis EM development include:

- Regulatory Guide 1.203, “Transient and Accident Analysis Methods,” December 2005.
- NuScale Design Specific Review Standard Sections:
 - 15.0, Revision 0, “Introduction - Transient and Accident Analyses” June 2016.
 - 15.1.1-15.1.4, Revision 0, “Decrease in Feedwater Temperature, Increase in Feedwater Flow, Increase in Steam Flow, and Inadvertent Opening of the Turbine Bypass System or Inadvertent Operation of the Decay Heat Removal System,” June 2016.
 - 15.1.5, Revision 0, “Steam System Piping Failures Inside and Outside of Containment,” June 2016.
 - 15.1.6, Revision 0, “Loss of Containment Vacuum,” June 2016.
 - 15.2.1-15.2.5, Revision 0, “Loss of External Load; Turbine Trip; Loss of Condenser Vacuum; Closure of Main Steam Isolation Valve; and Steam Pressure Regulator Failure (Closed),” June 2016.
 - 15.2.6, Revision 0, “Loss of Nonemergency AC Power to the Station Auxiliaries,” June 2016.
 - 15.2.7, Revision 0, “Loss of Normal Feedwater Flow,” June 2016.
 - 15.2.8, Revision 0, “Feedwater System Pipe Breaks Inside and Outside Containment (PWR),” June 2016.
 - 15.5.1-15.5.2, Revision 0, “Chemical and Volume Control System Malfunction that Increases Reactor Coolant Inventory,” June 2016.
- NUREG-0800 Sections:
 - 15.0.2, Revision 0, “Review of Transient and Accident Analysis Methods,” March 2007.

- 15.4.1, Revision 3, “Uncontrolled Control Rod Assembly Withdrawal from a Subcritical or Low Power Startup Condition,” March 2007.
- 15.4.2, Revision 3, “Uncontrolled Control Rod Assembly Withdrawal at Power,” March 2007.
- 15.4.3, Revision 3, “Control Rod Misoperation (System Malfunction or Operator Error),” March 2007.
- 15.4.4-15.4.5, Revision 2, “Startup of an Inactive Loop or Recirculation Loop at an Incorrect Temperature, and Flow Controller Malfunction Causing an Increase in BWR Core Flow Rate,” March 2007.
- 15.4.6, Revision 2, “Inadvertent Decrease in Boron Concentration in the Reactor Coolant System (PWR),” March 2007.

3.0 Plant Design Overview

3.1 Description of NuScale Plant

The NPM is a small, light water cooled, pressurized water reactor (PWR) consisting of a nuclear core, two helical coil SGs, and a pressurizer, all contained within a single containment vessel (CNV) (refer to Figure 3-1). Power conversion occurs via a standard secondary system that includes the steam turbine-generator, the main condenser, and the plant components necessary to provide feedwater.

Each NPM is covered by a reinforced concrete biological shield and enclosed in a Reactor Building, and has a dedicated chemical and volume control system (CVCS), ECCS, and DHRS.

The NPM is designed to operate efficiently at full power conditions using natural circulation as the means of providing core coolant flow, eliminating the need for reactor coolant pumps.

Unique features of the NPM include:

- a reduced core size relative to operating PWRs,
- natural circulation reactor coolant flow (i.e., no reactor coolant pumps),
- integrated SGs and pressurizer inside the reactor pressure vessel (RPV) (i.e., there is no piping connecting the SGs or pressurizer with the reactor),
- simplified passive safety systems that do not rely on ECCS pumps, accumulators, tanks, or connected piping,
- a high-pressure steel containment, and
- containment partially immersed in a water-filled pool providing an effective passive heat sink for emergency cooling and decay heat removal.

NuScale has achieved a substantial improvement in safety over existing plants through simplicity of design, reliance on passive safety systems, and small fuel inventory.

The NuScale Power Plant consists of one or more NPMs, each in its own bay of the common reactor pool. The entire pool is lined with stainless steel for leakage control. Each bay has a reinforced concrete cover that serves as a biological shield. The cover also serves to prevent deposition of foreign materials onto an NPM. The reactor pool is located in a Seismic Category I building designed to withstand postulated adverse natural conditions and aircraft impact.

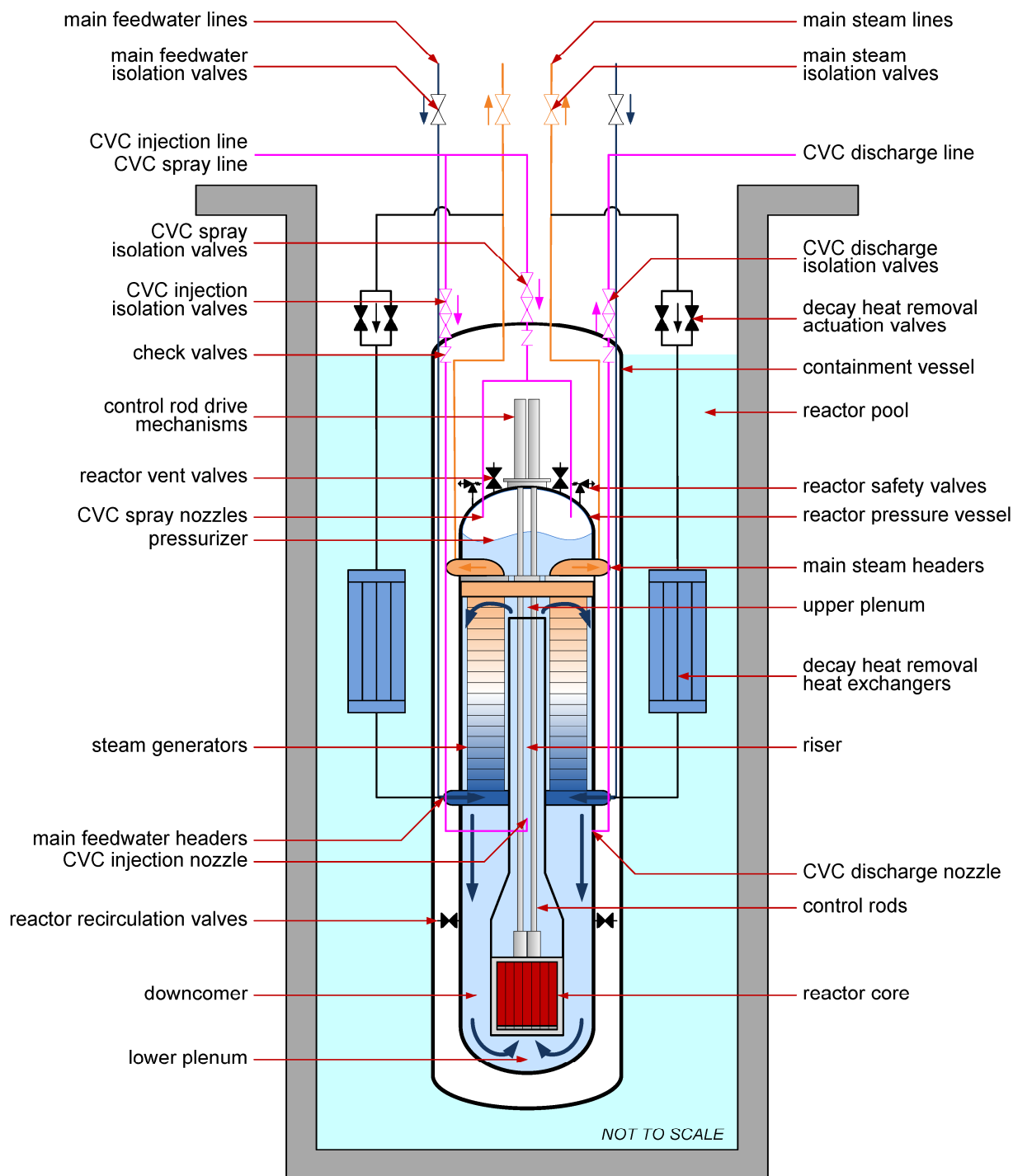


Figure 3-1 NuScale Power Module schematic

3.2 Plant Operation

During nominal full power operation, the control rods are retracted to within their insertion limits and borated water is used as the primary coolant, which is driven by natural circulation. The CVCS is used to regulate the primary side inventory via manually operated makeup and automatic letdown to maintain pressurizer level and boron concentration to maintain criticality. Pressurizer heaters and spray control primary side pressure. The helical coil SGs transfer the heat from the primary side to the feedwater. The DHRS heat exchangers are isolated during normal operation. The containment is evacuated to provide an insulated barrier between the reactor pressure vessel and containment. The NPM is partially immersed in the reactor pool within the Reactor Building, which serves as the ultimate heat sink (UHS) and is open to atmospheric pressure. The pool cooling equipment is designed to maintain an average bulk pool temperature such that plant personnel can work in the Reactor Building.

The NuScale instrumentation and control architecture primarily consists of the following systems:

- module control system (MCS)
- plant control system (PCS)
- module protection system (MPS)
- plant protection system

The MCS and PCS provide control and monitoring of the non-safety nuclear steam supply system (e.g., steam bypass to condensers, pressurizer heaters and sprays, and feedwater control), balance of plant systems (e.g., turbine control); rod control and position indication, and plant-wide, non-safety control and indication.

The MPS is composed primarily of the reactor trip system (RTS) and the engineered safety features actuation system (ESFAS). The MPS protection functions are limited to automated safety responses to off-normal conditions. The MPS functional response to an initiating event is a reactor trip, isolation (as necessary) of feedwater, MS, CVCS (including demineralized water system isolation to mitigate boron dilution), and containment, followed by an integrated safety actuation of one or more of the passive safety systems (DHRS and ECCS).

The RTS consists of four independent separation groups with independent measurement channels to monitor plant parameters that can generate a reactor trip. Each measurement channel trips when the parameter exceeds a predetermined setpoint. The RTS coincident logic is designed so that no single failure can prevent a reactor trip when required, and no failure in a single measurement channel can generate an unnecessary reactor trip.

The ESFAS consists of four independent separation groups with independent measurement channels to monitor plant parameters that can activate the operation of the engineered safety features. Each measurement channel trips when the parameter exceeds a predetermined setpoint. The ESFAS coincident logic is designed so that no

single failure can prevent a safeguards actuation when required, and no failure in a single measurement channel can generate an unnecessary safeguards actuation.

Transients requiring decay heat removal are addressed by the DHRS, which provides cooling through one or both of the SGs. For a steam generator tube failure (SGTF), main steam line break, and feedwater line break, the affected SG is isolated and the DHRS provides cooling through the intact SG (depending on the break location DHRS may be operational in both SGs). Manual operation of the nonsafety-related CVCS can also be used to offset decreases in RCS inventory. If the CVCS is inadequate to address the inventory decrease, containment isolation occurs and the DHRS is actuated. If RCS inventory loss to containment persists, ECCS is actuated.

Module-specific systems and functions that operate to mitigate the effects of postulated non-LOCA events (and credited in the safety analysis) include the ECCS, DHRS, CVCS and demineralized water system isolation, MPS, RTS, containment isolation and PZR heater isolation. The only safety system shared between modules is the UHS. The non-LOCA safety analyses consider ranges of UHS conditions and heat transfer such that non-LOCA analysis of a single module bounds possible UHS interactions between modules.

3.3 Decay Heat Removal System

The DHRS is a closed-loop, two-phase natural circulation cooling system. Two trains of decay heat removal equipment are provided, one attached to each SG loop. Each train is capable of removing 100 percent of the decay heat load and cooling the RCS. Each train has a passive condenser immersed in the reactor pool. Upon receipt of an actuation signal, the main steam isolation valves (MSIVs) and the feedwater isolation valves close, and the decay heat removal actuation valves open, allowing heat removal via the SGs. The decay heat removal actuation valves would open upon the loss of power, thus enabling reliable long term cooling. For successful operation, liquid water enters the SG through the feedwater line and is boiled by heat from the RCS. The vapor exits the SG through the steam line and is directed to the DHRS condenser where it condenses back to liquid to return to the SG. Thus, the loop transfers heat from the RCS to the DHRS fluid using the SG and then from the DHRS to the reactor pool water.

3.4 Emergency Core Cooling System

The ECCS consists of three independent reactor vent valves (RVVs) and two independent reactor recirculation valves (RRVs). The ECCS is initiated by simultaneously actuating the RVVs on the top of the RPV in the pressurizer region and the RRVs on the side of the RPV in the downcomer region. Opening the ECCS valves allows a natural circulation path to be established – water is vaporized in the core, leaves as steam through the RVVs, condenses and collects in the containment, and returns to the downcomer region inside the RPV through the RRVs. During normal operation, each ECCS valve is held closed by the hydraulic pressure across the valve main disc. Included in the ECCS valve design is an inadvertent actuation block consisting of a spring loaded arming valve in the vent port path from the main disc chamber to the vent line. If the differential pressure across this arming valve is greater than a threshold value, the arming valve closes, which prevents the main disc chamber from discharging through the vent line, blocking the ECCS valve

from opening. The ECCS valve will not open until the arming valve differential pressure decreases below the release pressure.

Provided the IAB device setpoint has been reached, the RVV and RRV components fail to the open (safe) position upon the loss of power, thus enabling reliable long-term cooling without operator actions, alternating current (AC) or direct current (DC) power, or make-up water. Successful operation of the ECCS requires isolation of the containment, such that the coolant inventory of the RCS is preserved.

3.5 Other Important Systems and Functions

Other systems and functions that are important in mitigating plant response during a postulated non-LOCA event are discussed below.

Reactor Coolant System

The reactor coolant system (RCS) consists of the RPV, reactor core, riser, upper plenum, SGs (shell side), downcomer, lower plenum, and pressurizer (PZR). The arrangement of the RCS and the relative locations of the thermal centers in the core and the SGs promote buoyancy driven natural circulation flow.

The RPV consists of a steel cylinder with an inside diameter of approximately 9 ft and an overall height of approximately 58 ft and is designed for an operating pressure of approximately 1850 psia. Nozzles on the upper head provide connections for reactor safety valves (RSVs) and RVVs.

The core configuration for the NPM consists of 37 fuel assemblies and 16 control rod assemblies (CRAs). The fuel assembly design is modeled from a standard 17x17 PWR fuel assembly with 24 guide tube locations for control rod fingers and a central instrument tube. The assembly is nominally half the height of standard plant fuel and is supported by five spacer grids. The U-235 enrichment is below the current U.S. manufacturer limit of 4.95 weight percent.

Each NPM uses two once-through helical coil SGs for steam production. The SGs, which produce superheated steam, are located in the annular space between the RCS hot leg riser and the reactor vessel inside diameter wall. Each SG is designed to remove 50 percent of the rated core thermal power.

The PZR provides the primary means for controlling RCS pressure. PZR heaters and spray maintain a constant reactor coolant pressure during operation. A steel PZR baffle plate, integral with the SG tube sheets and the RPV, acts as a thermal barrier and allows for surge flow between the PZR and the RCS.

Feedwater System

Feedwater from the condenser is pumped by condensate pumps to the condensate polishing equipment, where impurities are removed. Downstream of the polishing equipment, variable speed feedwater pumps supply flow to the feedwater heaters before

the feedwater regulating valves control feed to the SGs. In unit operation, preheated feedwater is pumped into the tube side of the SGs where it boils. Upon receipt of a DHRS actuation signal the feedwater isolation valves close.

Main Steam System

Superheated steam produced in the SGs flows to a dedicated steam turbine. A generator, driven by the turbine, generates electric power that is delivered to the utility grid through a step-up transformer. A turbine steam bypass valve is provided that will allow the reactor to remain in operation in the event of a turbine trip. Upon receipt of a DHRS actuation signal the MSIVs close (the steam system contains backup isolation valves in the event that an MSIV fails to isolate).

Chemical and Volume Control System

The primary functions of the CVCS are to purify reactor coolant, adjust the boron concentration in the reactor coolant, and supply spray flow to the pressurizer. Makeup and letdown operation can also be used to adjust the RCS inventory as needed. Equipment within the CVCS also allows for chemical addition to the reactor coolant, and heats the reactor coolant during startup. The CVCS includes demineralized water system isolation valves to mitigate boron dilution. When used for reactor coolant heating, the CVCS heats the RCS to the hot standby startup temperature, and develops natural circulation through the core sufficient to maintain the required RCS flow prior to nuclear heat addition.

Containment Vessel

The major safety functions of the CNV are to contain the release of radioactivity following postulated accidents, protect the RPV and its contents from external hazards, and to provide heat rejection to the reactor pool following ECCS actuation.

Following an actuation of the ECCS, heat removal through the CNV rapidly reduces the containment pressure and temperature and maintains them at less than design conditions for extended periods of time. Steam is condensed on the inside surface of the CNV, which is passively cooled by conduction and convection heat transfer to the reactor pool water.

Reactor Pool

The reactor pool is a large stainless steel lined pool located below the plant ground level in the Reactor Building. During normal plant operations, heat is removed from the pool through a cooling system and ultimately rejected into the atmosphere through a cooling tower or other external heat sink. In an event where AC power is lost, heat is removed from the NPM by allowing the pool to heat up and boil. Water inventory in the reactor pool is maintained at a level that is sufficient to provide at least three days of DHRS operation.

4.0 Transient and Accident Analysis Overview

As part of defining the requirements of the non-LOCA transient system analysis methodology, the events to which the methodology applies and the specific event acceptance criteria applicable to the events are identified. The specific event acceptance criteria are derived from the regulatory requirements and guidance discussed in Section 2.2. The non-LOCA transient system analysis is part of several stages of analyses performed to confirm the plant design meets applicable acceptance criteria for a limiting set of AOOs, IEs, and accidents. The methodology includes the interfaces of the non-LOCA transient system analysis with other analysis methodologies, and identifies where margin to the event acceptance criteria is demonstrated.

4.1 Design-Basis Events and Event Classification

The NuScale design-basis events for which the non-LOCA system transient analysis is performed, the event category, and the event classification are listed in Table 4-1.

A broad spectrum of transients, accidents, and initiating events are considered in the scope of design basis analyses presented in Chapter 15 of the NuScale Final Safety Analysis Report (FSAR). The design basis events are identified based on:

- review of the NuScale plant systems to identify failures that would result in a design basis initiating event
- review of initiating events considered in the NuScale probabilistic risk assessment analyses to identify design basis initiating events. The probabilistic risk assessment initiating events included consideration of:
 - the master logic diagram of failure mechanisms that may result in core damage
 - industry generic data sources reviewed to identify initiating events
 - advanced reactor probabilistic risk assessments

As described in Section 3.0, the NPM is a natural circulation PWR with SGs that are integral to the reactor vessel. Many of the events analyzed for operating plants and in recent design certification applications are applicable to the NuScale design. NuScale-specific events reflect unique aspects of the NuScale design such as the DHRS and vacuum conditions of containment during normal operation.

The design basis events are categorized by type and expected frequency of occurrence. Limiting cases in each group are quantitatively analyzed and specific acceptance criteria for each postulated initiating event are applied. The design basis events that require non-LOCA system transient analysis are categorized into one of five categories:

1. increase in heat removal from the RCS

In the NuScale design, this may be due to increased heat removal by the secondary system or due to increased heat removal to the containment.

2. decrease in heat removal by the secondary system
3. reactivity and power distribution anomalies
4. increase in reactor coolant inventory
5. decrease in reactor coolant inventory

The NPM design-basis events are classified into one of three event categories:

1. AOOs – These are events that are expected to occur one or more times in the design life of the plant, conservatively quantified as events with a frequency of occurrence of 1×10^{-2} per module year or greater. An event that is not expected to occur in the design life of the plant may also be categorized as an AOO for conservatism.
2. Infrequent event – These are events that are not expected to occur during the design life of the plant. For IEs, the acceptance criteria are specified such that some fuel damage may occur but the radiological acceptance criteria are stricter than those imposed for accidents.
3. Postulated Accidents – These are design-basis events that are not expected to occur during the design life of the NPM operation.

Historical precedent is used for event classification where the event is initiated by abnormal system conditions that are similar to those experienced in currently operating plants and certified designs. Event frequencies from the probabilistic risk assessment were considered for events that are unique to the NPM design or where the NPM design is such that the event frequency is expected to differ from currently operating plants and certified designs.

The non-LOCA EM is applicable for the initiating events listed in Table 4-1. Because the control rod ejection accident analysis, LOCA analysis, and analysis of an inadvertent opening of a valve on the reactor vessel initiating event are addressed by different methodologies, these initiating events are not included in Table 4-1.

The non-LOCA system transient analyses are performed for a single module. In the NuScale design, the only shared safety-related system relied upon for event mitigation in the design basis system transient event analysis is the reactor pool portion of the UHS. Some initiating events may affect only a single module; others may affect multiple modules. In the non-LOCA system transient analysis calculations, the initial temperature of the reactor pool is bounded as described in Section 7.0. This approach bounds various module responses that may occur due to an initiating event that affects more than one module in the plant.

Table 4-1 Design basis events for which the non-LOCA system transient analysis is performed, event category, and event classification

Initiating Event	Event Classification
<u><i>Increase in Heat Removal from the Reactor Coolant System</i></u>	
Decrease in feedwater temperature	AOO
Increase in feedwater flow	AOO
Increase in steam flow	AOO
Inadvertent opening of SG relief or safety valve	AOO
Steam system piping failure inside or outside of containment	Postulated accident
Containment flooding/loss of containment vacuum	AOO
Inadvertent DHRS actuation ⁽¹⁾	AOO
<u><i>Decrease in Heat Removal by the Secondary System</i></u>	
Loss of external load	AOO
Turbine trip	AOO
Loss of condenser vacuum	AOO
Main steam isolation valve closure	AOO
Loss of nonemergency AC power to station auxiliaries	AOO
Loss of normal feedwater flow	AOO
Inadvertent DHRS actuation ⁽¹⁾	AOO
Feedwater system pipe break inside or outside of containment	Postulated accident
<u><i>Reactivity and Power Distribution Anomalies</i></u>	
Uncontrolled control rod assembly bank withdrawal from a subcritical or low power startup condition	AOO
Uncontrolled control rod assembly bank withdrawal at power	AOO
Control rod misoperation ⁽²⁾ Single control rod assembly drop Control rod bank drop Single control rod assembly withdrawal	AOO
Inadvertent decrease in boron concentration in the reactor coolant	AOO
<u><i>Inadvertent System Operation that Increases Reactor Coolant Inventory</i></u>	
Chemical and volume control system malfunction that increases reactor coolant system inventory	AOO
<u><i>Decrease in Reactor Coolant System Inventory</i></u>	
Failure of small lines carrying primary coolant outside containment	Infrequent event
Steam generator tube failure	Postulated accident

1. Depending on the operating power at which an inadvertent DHRS actuation occurs, it may initially result in either an increase or decrease in heat removal from the RCS.
2. Control rod misoperation includes several types of events; those that require system transient analysis are identified.

4.2 Design Basis Event Acceptance Criteria

Safety analyses are performed to demonstrate that a nuclear power plant can meet applicable acceptance criteria for a limiting set of AOOs, IEs, and accidents. If the risk of an event is defined as the product of the event's frequency of occurrence and its consequences, then the design of the plant should be such that events produce about the same level of risk. The acceptance criteria indicated by the GDC for nuclear power plants (Reference 4) reflect the risk of an event. Relatively frequent events such as AOOs are prohibited from resulting in serious consequences, but relatively rare events (postulated accidents) are allowed to produce more severe consequences.

Design basis events for the NPM are categorized as AOOs, IEs, or postulated accidents. Table 4-2, Table 4-3, and Table 4-4 summarize the acceptance criteria applied for AOOs, IEs, and postulated accidents, respectively.

The applicable acceptance criteria identified for each event are based on the event classification as identified in Table 4-1. For a limited number of events, a more conservative acceptance criterion may be applied than required based on the event classification.

For many non-LOCA transient events, the specific acceptance criterion will not be challenged during the event progression. For example, events that result in an increase in heat removal from the RCS may have a maximum RCS pressure higher than the initial operating pressure, but will not challenge the margin to the maximum RCS pressure acceptance criterion. In contrast, events that result in a decrease in heat removal from the RCS may result in an RCS pressurization that could challenge the maximum RCS pressure acceptance criterion. In Section 7.2, the acceptance criteria of interest for each non-LOCA event are identified. The acceptance criteria of interest are those where margin to the limit may be challenged during the event progression.

In the event-specific transient analysis, sensitivity calculations are performed as necessary to ensure that the event meets acceptance criteria that may be challenged. These sensitivity calculations are performed to confirm that appropriately conservative inputs are specified to identify the case that results in minimum margin to the acceptance criterion of interest. For other acceptance criteria where margin to the limit is not challenged, representative results from the overall scope of sensitivity calculations performed are sufficient to demonstrate that margin to the acceptance criterion is maintained.

A prime example of an acceptance criterion where the NPM design has significant margin is the maximum secondary system pressure. Unlike in typical PWR designs, in the NuScale design, the design pressure of the SG secondary side up to the second containment isolation valves is equal to the RCS design pressure. This feature supports the design and operation of the SG and DHRS. In a non-LOCA event that results in DHRS actuation, typically the maximum secondary side pressure occurs in the first minutes of the transient progression, following DHRS actuation. After DHRS is actuated, the fluid in the DHRS flows into the SG. Heat is transferred from the RCS primary system to the SG, where the DHRS loop inventory boils in the SG tubes. The steam flow is then condensed

in the DHRS condensers and the energy is transferred to the reactor pool UHS. The maximum pressure in the SG secondary side is limited to the saturation pressure at the temperature of the RCS fluid on the SG primary side. Therefore, the maximum secondary pressure is affected by the secondary side inventory and the primary side conditions at the time of DHRS actuation, and is less sensitive to a specific initiating event. The SG design pressure is significantly higher than pressures expected during DHRS operation. The margin to the SG design pressure is physically limited, based on the primary side conditions. The representative transient results in Section 8.0 demonstrate that significant margin to the maximum SG pressure acceptance criterion is maintained for all types of events. Therefore, extensive sensitivity calculations to maximize secondary side pressure are not necessary for the non-LOCA transient analysis calculations.

Table 4-2 Acceptance criteria for anticipated operational occurrences

Parameter	Acceptance Criterion	How Acceptance Criterion is Satisfied
Maximum reactor coolant primary system pressure	$\leq 110\%$ of design pressure	Margin to this acceptance criterion is demonstrated by the non-LOCA system transient analysis results.
Maximum main steam secondary system pressure	$\leq 110\%$ of design pressure	Margin to this acceptance criterion for the steam system piping up to the second containment isolation valve is demonstrated by the non-LOCA system transient analysis results.
Minimum critical heat flux ratio	$> 95/95$ critical heat flux ratio (CHFR) Limit	Margin to this acceptance criterion is demonstrated by the subchannel analysis results. Subchannel analysis is outside scope of this topical report.
Maximum fuel centerline temperature	\leq melting temperature (adjusted for burnup effects)	Margin to this acceptance criterion is demonstrated by the subchannel analysis results. Subchannel analysis is outside scope of this topical report.
An AOO should not result in a significant loss of reactor containment barrier	Margins to containment pressure and temperature limits are maintained.	Margin to this acceptance criterion is demonstrated by the peak containment pressure/temperature analysis results performed according to a separate analysis methodology. Maximum containment pressure and temperature analysis is outside scope of this topical report.
An AOO should not generate a postulated accident without other faults occurring independently	A postulated accident is not generated by the AOO.	This acceptance criterion is satisfied by demonstrating that the other acceptance criteria are met.

Table 4-3 Acceptance criteria for infrequent events

Parameter	Acceptance Criterion	How Acceptance Criterion is Satisfied
Maximum reactor coolant primary system pressure	$\leq 120\%$ of design pressure	Margin to this acceptance criterion is demonstrated by the non-LOCA system transient analysis results.
Maximum main steam secondary system pressure	$\leq 120\%$ of design pressure	Margin to this acceptance criterion for the steam system piping up to the second containment isolation valve is demonstrated by the non-LOCA system transient analysis results.
Fuel cladding integrity	<p>If the minimum CHFR is less than or equal to the 95/95 CHFR limit, the fuel rod is assumed to be failed.</p> <p>If the maximum fuel centerline temperature exceeds the melting temperature, the fuel rod is assumed to be failed.</p>	<p>Margin to this acceptance criterion is demonstrated by the subchannel analysis results.</p> <p>Subchannel analysis is outside scope of this topical report.</p>
Containment integrity	Margins to containment pressure and temperature limits are maintained.	<p>Margin to this acceptance criterion is demonstrated by the peak containment pressure/temperature analysis results performed according to a separate analysis methodology.</p> <p>Maximum containment pressure and temperature analysis is outside scope of this topical report.</p>
Release of radioactive material	Calculated offsite doses are less than 10% of the 10 CFR 52.47(a)(2)(iv) (Reference 5) reference values.	<p>Margin to this acceptance criterion is demonstrated by the accident radiological analysis results.</p> <p>Accident radiological analysis is outside scope of this topical report.</p>

Table 4-4 Acceptance criteria for postulated accidents

Parameter	Acceptance Criterion	How Acceptance Criterion is Satisfied
Maximum reactor coolant primary system pressure	$\leq 120\%$ of design pressure	Margin to this acceptance criterion is demonstrated by the non-LOCA system transient analysis results.
Maximum main steam secondary system pressure	$\leq 120\%$ of design pressure	Margin to this acceptance criterion for the steam system piping up to the second containment isolation valve is demonstrated by the non-LOCA system transient analysis results.
Fuel cladding integrity	<p>If the minimum CHFR is less than or equal to the 95/95 CHFR limit, the fuel rod is assumed to be failed.</p> <p>If the maximum fuel centerline temperature exceeds the melting temperature, the fuel rod is assumed to be failed.</p>	<p>Margin to this acceptance criterion is demonstrated by the subchannel analysis results.</p> <p>Subchannel analysis is outside scope of this topical report.</p>
Containment integrity	Margins to containment pressure and temperature limits are maintained.	<p>Margin to this acceptance criterion is demonstrated by the peak containment pressure/temperature analysis results performed according to a separate analysis methodology.</p> <p>Maximum containment pressure and temperature analysis is outside scope of this topical report.</p>
Release of radioactive material	Release does not result in offsite doses in excess of the guidelines of 10 CFR 52.47(a)(2)(iv) (Reference 5).	<p>Margin to this acceptance criterion is demonstrated by the accident radiological analysis results.</p> <p>Accident radiological analysis is outside scope of this topical report.</p>

4.3 Non-LOCA Transient Analysis Process

The main steps of the non-LOCA system transient analysis process for a specific transient event are:

1. Develop plant base model NRELAP5 input.
2. Adapt NRELAP5 base model as necessary for specific event analysis, and desired initial conditions.
3. Perform steady state and transient system analysis calculations with NRELAP5.
4. Evaluate results of transient analysis calculations:
 - a. Confirm margin to maximum RCS pressure acceptance criterion
 - b. Confirm margin to maximum SG pressure acceptance criterion
 - c. Confirm appropriate transient run execution time
5. Identify which cases provide input for downstream subchannel analysis and extract boundary condition data.
6. Identify which cases provide input for downstream accident radiological analysis and extract boundary condition data.

The non-LOCA system transient analysis is performed and documented in accordance with NuScale's QAP (Reference 3).

The main steps of the non-LOCA system transient analysis are discussed in the following subsections.

4.3.1 Develop Plant Base Model NRELAP5 Input

NRELAP5 is NuScale's system thermal-hydraulics code used to simulate the NPM system response during non-LOCA short-term transient event progression, for events that require system transient analysis.

The NRELAP5 code was developed based on the Idaho National Laboratory (INL) RELAP5-3D[®] computer code. RELAP5-3D, version 4.1.3 was used as the baseline development platform for the NRELAP5 code. RELAP5-3D was procured and commercial grade dedication was performed by NuScale, and subsequently features were added and changes made to address unique aspects of the NPM design and licensing methodology.

The NRELAP5 code includes models for characterization of hydrodynamics, heat transfer between structures and fluids, modeling of fuel, point reactor kinetics models, and control systems. NRELAP5 utilizes a two-fluid, non-equilibrium, non-homogenous fluid model to simulate system thermal-hydraulic responses. The NRELAP5 code is described in Reference 2. As discussed in Reference 2 and in Section 9.0, the NRELAP5 code has been developed and is maintained within NuScale's QAP.

The applicability of NRELAP5 for non-LOCA transient analysis is discussed in Section 5.0.

As discussed in Section 4.2, the non-LOCA figures of merit evaluated with NRELAP5 are as follows:

- Primary side pressure
- Secondary side pressure (up to the second containment isolation valve)

In addition, the RCS level response is evaluated with NRELAP5 for non-LOCA events that result in decrease in RCS inventory (SGTF and small line breaks outside of containment) to demonstrate that the inventory decrease is isolated in a timely manner and the DHRS provides effective decay heat removal for these events.

The NRELAP5 plant base model is described in Section 6.0.

Interfaces with the core design and fuel rod performance design that provide input to the transient analyses are described in the following subsections.

4.3.1.1 Interface with Core Design (Input to the Transient Analysis)

Core design analysis performed in accordance with a methodology approved for the NuScale design provides input to the system transient analysis. The NuScale transient analysis methodology using NRELAP5 can be applied to a typical light water reactor fuel assembly design, and does not require that a specific code or suite of codes be used for the steady state core design analysis. The non-LOCA evaluation model methodology for specifying the input for the reactor kinetics model, axial power shape, and energy deposition factor are described in the following subsections.

4.3.1.1.1 Reactor Kinetics Model

The system transient analyses are performed assuming either beginning of cycle (BOC) or end of cycle (EOC) conditions based on direction of conservatism for reactivity feedback for the transient.

The total core power during a non-LOCA transient is the combination of the fission power and the decay heat. For the non-LOCA transients the fission power response is modeled using the separable point reactor kinetics model in NRELAP5. The NRELAP5 point reactor kinetics model computes both the immediate (prompt and delayed) fission power and the power from decay of fission products.

In NRELAP5, input needed for the separable point kinetics model includes:

- Effective delayed neutron precursor yield of group i (β_i)
- Effective delayed neutron decay constant of group i (λ_i)
- Prompt neutron generation time (Λ)
- Reactivity feedback
- Reactivity changes from control rod movement (normal controls), or scram

- Decay heat model input

In the non-LOCA evaluation model, the input to the point kinetics model is specified to give a conservatively high power response prior to actuation of reactor scram. The power response is biased by the input accounting for the reactivity feedback effects of moderator temperature, fuel temperature, and the normal control rod movement. After a reactor scram signal, the negative reactivity associated with insertion of the control and safety banks is conservatively modeled as described in Section 7.1.5.

The moderator temperature coefficient (MTC) is a measure of the relative change in reactivity associated with a change in moderator (coolant) temperature. The Doppler temperature coefficient (DTC) is a measure of the relative change in the reactivity as the fuel temperature changes. In the non-LOCA evaluation model, reactivity feedback effects from moderator temperature changes and fuel temperature changes are conservatively bounded as described in Section 7.1.5. Negative reactivity insertion due to void generation impacts on moderator density is conservatively neglected.

As described in Section 6.0 and Section 7.1.2, the rod control system and associated control logic are incorporated into the NRELAP5 model to allow simulation of reactivity changes (negative or positive) associated with normal control rod movement in response to postulated transients. In cooldown events, the normal rod control function will attempt to increase average temperature by withdrawing control rods and therefore adding positive reactivity. For transients where operation of the normal rod control function provides more adverse consequences of the transient, the highest integral control rod bank worth (over time in cycle) is modeled, in conjunction with the maximum control bank withdrawal speed and bounding input for MTC, to increase the power response to the modeled control rod movement.

The decay heat power contribution is conservatively bounded high or low, as appropriate for the specific transient, as described in Section 7.1.5.

Appropriate input based on the core design is used for other parameters needed as input to the point reactor kinetics model.

4.3.1.1.2 Axial Power Shape

For the system transient analysis, a single channel core model is used, as described in Section 6.0. A nominal center-peaked average axial power shape is input for the single core channel for consistency with development of the reactivity feedback coefficients determined in the core design analyses.

Uncertainties associated with the axial power shape and axial and radial power peaking factors that can affect the minimum critical heat flux ratio (MCHFR) and peak centerline fuel temperature are accounted for in the downstream subchannel analyses as described in Reference 6. The design features of the NPM preclude challenge to the primary and secondary pressure acceptance criteria as discussed in Section 7.0 and as shown in the representative results in Section 8.0. Sensitivity studies on the axial power shape confirm that the primary and secondary system pressure, flow and fluid temperature responses

are not significantly affected by the axial power shape. Therefore, use of a nominal center-peaked average axial power shape input is appropriate for the system transient analyses.

4.3.1.1.3 Energy Deposition Factor

The energy deposition factor is the portion of the energy generated in the core that is directly deposited in the fuel. A bounding high energy deposition factor that results in all energy being deposited in the fuel is used in the non-LOCA analyses. For cooldown or reactivity insertion events that cause total core power changes, increasing the core energy deposited in the fuel slows the thermal-hydraulic response of the system to changing power levels. The effect of the energy deposition factor on the primary system pressure response is generally insignificant except in very fast reactivity events such as control rod ejection where Doppler reactivity feedback is important; control rod ejection analysis is outside the scope of this EM. Sensitivity studies on this parameter confirm that its effect on the system response is not significant with respect to demonstrating margin to acceptance criteria for NPM events addressed by the non-LOCA evaluation model due to the reactor trip system design and selection of the analytical limits to actuate reactor trip.

4.3.1.2 Interface with Fuel Rod Performance Design (Input to the Transient Analysis)

Fuel rod design analysis performed using a fuel performance code approved for the NuScale design provides input to the system transient analysis. The NuScale transient analysis methodology using NRELAP5 can be applied to a typical light water reactor fuel assembly design, and does not require that a specific code or suite of codes be used for the fuel performance analysis. The fuel assembly geometry, required material properties, and the fuel performance data needed for appropriate steady state initialization of the model are specified as input to the transient system analysis.

The NuScale transient analysis requires input for the fuel rod and assembly geometry, fuel rod thermo-mechanical properties, and fuel rod performance information to assure adequate modeling of the initial fuel rod stored energy and transient response.

4.3.1.2.1 Fuel Rod and Fuel Assembly Geometry

Nominal fuel rod and fuel assembly geometry information forms the basis for the NRELAP5 inputs required to describe the core heat structures, core coolant channels, and bypass channels. Pressure losses due to fuel assembly grid spacers and wall friction are accounted for. The NRELAP5 model is described in Section 6.0.

4.3.1.2.2 Fuel Rod Material Properties

Fuel rod material properties appropriate for the fuel assembly design are specified by user input in the NRELAP5 model. Fuel rod material properties needed include:

- fuel pellet thermal conductivity
- fuel pellet specific heat
- fuel pellet density

- cladding thermal conductivity
- cladding specific heat
- cladding density

Nominal fuel rod material properties as a function of temperature are specified.

For the fuel pellet properties, UO_2 properties are used to reflect the core average response. Since the fuel pellet thermal conductivity is a function of burnup and fuel temperature, and the fuel pellet thermal conductivity degrades with burnup, a representative time-in-cycle core average burnup is used to calculate the fuel thermal conductivity as a function of temperature.

4.3.1.2.3 Fuel Rod Performance Data

The fuel rod gap conductance, specific heat and density in the NRELAP5 fuel rod heat structure are used to set the initial core average fuel temperature. Bounding values for fuel rod gap conductance are selected to provide conservatively high or low core average fuel temperature for the time-in-life of interest for the calculation.

The conservative core average fuel temperatures are confirmed on a cycle-specific basis.

4.3.2 Adapt Plant Base Model NRELAP5 Input for Event Transient Analysis

The NRELAP5 plant base model is described in Section 6.0. The NRELAP5 plant base model is adapted as necessary to perform the specific event analysis. Section 7.0 describes the non-LOCA analysis methodology, including conservative biasing of initial and boundary conditions, single failures, and loss of power scenarios for the event analyses.

4.3.3 Perform NRELAP5 Steady State and Transient System Analysis Calculations

For each analysis, one or more steady state initialization calculations are developed. After acceptable steady state conditions are obtained, the transient calculations are performed. Section 7.0 describes the non-LOCA analysis methodology including the steady state initialization and performance of null transients prior to the transient calculation.

4.3.4 Evaluate Results of Transient Analysis Calculations

The results of the transient analysis calculations are assessed to confirm that the system transient response is acceptable.

4.3.4.1 Maximum Pressure Acceptance Criteria

Based on the results of the transient analysis calculations performed for an event, margin to the maximum RCS pressure acceptance criterion and margin to the maximum SG secondary pressure acceptance criterion are confirmed.

4.3.4.2 Short-Term Transient Duration

For each transient calculation, the following parameters are reviewed to assure that the transient calculation was executed for an appropriate duration to confirm that design basis event acceptance criteria are met.

- MPS actuations expected in direct response to the initiating event, for mitigation of the design basis event, have occurred
- if reactor trip occurs during the transient, the nuclear heat source is reduced to decay heat levels and decreases with time
- core average temperature is stable, or decreasing following reactor trip
- RCS pressure is stable or decreasing
- RCS fluid inventory is stable
- containment pressure is stable or decreasing

These conditions are demonstrated for a reasonable time, typically a few hundred seconds, following the last safety system actuation expected to occur in the short term transient progression, to demonstrate that core cooling is established and conditions that result in minimum margin to the acceptance criteria have occurred.

4.3.5 Identification of Cases for Subchannel Analysis and Extraction of Boundary Condition Data

For the NPM non-LOCA events, VIPRE-01 is used for performance of subchannel analysis calculations. Reference 6 describes the subchannel analysis methodology.

In the transient subchannel analysis, the following acceptance criteria are assessed:

- MCHFR
- maximum fuel centerline temperature

For non-LOCA events that require subchannel analysis, the NRELAP5 transient analyses provide the following input from the system transient calculation to the downstream subchannel analysis:

- reactor power as a function of time
- core exit pressure as a function of time
- core inlet temperature as a function of time
- total system flow rate as a function of time

In the NRELAP5 system transient analysis, cases for downstream subchannel analysis are identified based on the conservative bias directions for the boundary condition input and considering the NPM natural circulation design. The conservative bias directions are

discussed below, followed by a description of the methodology for identifying cases for downstream subchannel analysis.

As identified in Reference 6, for the system transient parameters provided by NRELAP5, the conservative bias directions to minimize the CHF are as follows:

- maximum reactor power (higher power increases the actual heat flux)
- maximum core exit pressure (see additional discussion below)
- maximum core inlet temperature (higher temperature reduces energy addition needed to raise coolant to saturated conditions).
- minimum system flow rate (minimum flow is conservative as there is less coolant flow in the reactor core available for heat transfer)

The effect of pressure on critical heat flux (CHF) involves the physical properties of the water coolant and the subcooling effect. If subcooling is removed as a contributing factor (i.e. inlet subcooling is held constant with varying pressure) then changes in water properties with varying pressure lead to a negative trend of CHF versus pressure. The latent heat of vaporization of water has a negative trend with pressure. This is the primary driver of the negative trend in CHF versus pressure, because liquid-to-vapor phase conversion requires more enthalpy as pressure decreases. The specific vapor volume has an exponential relationship with pressure that is relatively flat above 3.0 to 4.0 MPa (approximately 435-580 psia), but increases rapidly below this point. This increase in vapor volume at low pressures leads to increased vapor crowding on the surface of the heated rods and a subsequent decrease in heat transfer capability. These two competing effects are responsible for the change from a negative trend in CHF versus pressure to a positive one below 3.0 to 4.0 MPa (approximately 435-580 psia). This is demonstrated by numerous CHF tests of various designs at multiple testing facilities.

When the subcooling effect is included, which is more appropriate for non-LOCA transient event calculations with VIPRE-01, the trends discussed above do not necessarily hold true. In traditional PWRs, pressure uncertainties are negatively applied (i.e. uncertainty is subtracted from best estimate value). This practice is based on the sensitivity of CHF to pressure seen historically in PWRs. The NPM operates in a different manner than traditional PWRs in that it does not rely on forced circulation via reactor coolant pumps to cool the core, but instead relies upon natural circulation. This results in a much lower mass flux (coolant flow) than is experienced in traditional PWR designs. The subcooling effect is influenced by coolant flow in a reactor for a given amount of power; as mass flux increases the subcooling effect grows stronger, due to decreasing enthalpy rise, leading to decreasing thermodynamic quality values. At high flows the subcooling effect is dominant and allows for a greater power capacity as pressure increases. {{

}}^{2(a),(c)}

In the NuScale design, for a given reactor module operating condition, reactor power, core inlet temperature and system flow rate are tightly coupled. As described in Section 7.1, ranges in these parameters are considered as part of biasing the system transient analysis steady state initial conditions. The NRELAP5 system analysis methodology for determining the limiting CHF cases for downstream subchannel analysis is primarily dependent on the limiting initialization. The CHF cases are evaluated at the minimum flow initialization. Other initial conditions are forced to the limiting initialization for a given transient progression to ensure the maximum power, primary pressure and core inlet fluid temperature are simultaneously reached prior to reactor trip system actuation. For example, in the case of a heatup event, the RCS will increase in temperature, causing a pressurizer insurge and subsequent increase in pressure. The limiting CHF scenario is the transient progression that results in the highest core outlet temperature at the time of reactor trip on high pressure, which is generally the faster heatups where the pressurizer initialization is biased to delay the high pressure trip.

For some transients, a spectrum of cases is analyzed from the limiting initialization. {{

}}^{2(a),(c)}

After the system transient analysis calculations are performed and assessed, for events that require subchannel analysis, one or more cases are identified as limiting for MCHFR. For the limiting case(s) selected, the required system transient parameters are tabulated as a function of time for input to the downstream subchannel analysis calculations, to confirm margin to CHF.

The system transient parameters are provided for subchannel analysis for sufficient time for the subchannel analyses to demonstrate that the MCHFR has occurred, typically at least 10-15 seconds following reactor trip.

{{

Figure 4-1 {{

}}^{2(a),(c)}

}}^{2(a),(b),(c)}

4.3.6 Identification of Cases for Accident Radiological Analysis

Radiological acceptance criteria are assessed in the accident radiological analyses. Reference 8 describes the NuScale accident radiological source term analysis methodology. This section only describes radiological analyses cases that involve nuclear steam supply system transients (i.e. primary and secondary coolant system transients) and does not encompass any radiological analyses involving spent fuel movement or postulated failures in the radioactive waste system.

The transient analyses provides input to the accident radiological analyses for events that result in RCS fluid loss outside of containment such as a break of small RCS piping outside of containment or SGTF. For these events, one or more transient analysis cases are identified to provide conservative input to the accident radiological analysis. The conservative bias directions for the transient analysis input to the accident radiological analysis are:

- Maximum integrated mass release outside of containment prior to isolation of the RCS mass release.

Basis: For a constant radionuclide concentration in the RCS, the greater the mass released outside of containment, the more severe the radiological consequences.

- Maximum integrated mass release between time of reactor trip and time of isolation of the RCS mass release.

Basis: Reference 8 describes how iodine spiking is accounted for in the accident radiological analyses. During a transient progression, changes in reactor power, RCS average temperature, or RCS pressure could result in iodine spiking, changing the radionuclide concentration in the RCS. Consistent with Standard Review Plan Section 15.6.2 (Reference 9), for accident radiological calculations assuming a coincident iodine spike (iodine spike occurring during the event), the iodine spiking is assumed to begin at the time of reactor trip as the result of the reactor shutdown or depressurization of the primary system. In some cases, particularly for smaller breaks in RCS piping, the time between reactor trip and isolation of the break flow could be extended compared to larger break sizes. The increased time between reactor trip and isolation increases the time of mass release when the RCS radionuclide inventory reflects iodine spiking. If there is sufficient time after reactor trip before the MPS would respond, plant operators may isolate the release.

For each transient analysis case identified, the input provided for accident radiological analysis includes:

- Time of reactor trip if it is calculated to occur
- Isolation time, at which point release of RCS fluid outside of containment is stopped. The isolation may be due to MPS response or due to operator action (as identified in Section 7.1.7, operator actions may be taken to prevent abnormal operating events from resulting in more severe events).

- RCS fluid mass release outside of containment as a function of time
- System transient response parameters such as
 - Reactor power as a function of time
 - RCS average temperature as a function of time
 - RCS pressure as a function of time
 - Secondary side feedwater and steam flow rates as a function of time

5.0 NRELAP5 Applicability for Non-LOCA Transient Analysis

5.1 Non-LOCA Phenomena Identification and Ranking Table and Evaluation of High-Ranked Phenomena

5.1.1 Phenomena Identification and Ranking Table Process

The PIRT process is a systematic way of gathering information from experts on a specific subject and ranking the importance of the information to meet some decision-making objective. It has been applied to many nuclear technology issues to help guide research and develop activities to satisfy regulatory requirements.

The purpose of the NuScale non-LOCA PIRT was to provide an assessment of the relative importance of phenomena and processes that may occur in the NuScale Power Module (NPM) during non-LOCA events in relation to specified figures of merit (FOMs). This assessment is part of the process prescribed by Regulatory Guide 1.203 (Reference 1).

The current non-LOCA PIRT was developed by a panel of experts for the NPM and was built upon the state-of-knowledge at the time of its development. Non-LOCA events can be divided into several different event types based on the main effect on the reactor coolant system, as described in Section 5.1.2. A comprehensive, integrated PIRT was performed for the range of non-LOCA event types and phases of the event progression. The PIRT panel considered the NPM design to identify systems, components, and subcomponents of the design for which phenomena were assessed. The panel then followed the PIRT process to identify and rank phenomena considering the level of importance for each phenomena relative to identified FOMs for the different non-LOCA event types and phases of the transient progression. The panel also established a knowledge ranking for each of the phenomena.

Following the development of the PIRT, additional insights from testing, code validation, plant calculations and analysis were established. The following discussions of the PIRT phenomena, importance, knowledge rankings, and how the phenomena are addressed reflect these developments as appropriate.

5.1.2 Non-LOCA Event Scenarios and Phases

As described in Section 4.1, the non-LOCA events for the NPM are divided into five event categories based on the type of effect on the RCS. These categories are summarized below.

1. increase in heat removal from the reactor coolant system
2. decrease in heat removal by the secondary system
3. reactivity and power distribution anomalies
4. increase in reactor coolant inventory
5. decrease in reactor coolant inventory

For the non-LOCA PIRT, the panel evaluated five design-basis non-LOCA events, one representative of each category:

- Main steam line break inside containment: Representative of events that result in an increase in heat removal from the RCS (cooldown/depressurization events)
- Feedwater line break inside containment: Representative of events that result in a decrease in heat removal from the RCS (heatup/pressurization events)
- CRA withdrawal: Representative of events that result in a reactivity increase
- CVCS malfunction: Representative of events that result in an increase in RCS inventory
- SGTF: Representative of events that result in a decrease in RCS inventory

The PIRT panel divided the short-term, non-LOCA event progression into three phases, generic for each transient type:

Phase 1 – Pre-trip transient

Phase 1 begins with the event initiation. The RCS power, pressure and flow rates increase or decrease from the normal power conditions, depending on the event type. The DHRS is inactive. This phase ends with actuation of the MPS response to the off-normal NPM conditions.

Phase 2 – Post-trip transition

Phase 2 begins with MPS actuation of reactor trip and, for most non-LOCA events, actuation of the DHRS in response to faulted secondary heat removal conditions. In cases where DHRS is actuated, the DHRS actuation valves open and the normal secondary side flow paths from the feedwater system and to the main steam system (MSS) are isolated. The secondary side DHRS loop pressurizes as decay and residual heat are transferred from the primary, causing the DHRS loop inventory to boil off in the steam generator and condense in the DHRS condenser. The reactor coolant system power and flow rates transition towards decay heat levels.

Phase 3 – Stable natural circulation

During phase 3, stable primary side natural circulation conditions exist with reactor coolant system power and flow rates reflecting decay power levels. In cases where DHRS is actuated, stable natural circulation in the DHRS loop is established. Secondary side flow rates and pressures in the DHRS loop decrease as the primary side pressure and temperature decrease.

Section 4.3 describes criteria for the short-term non-LOCA transient end conditions.

5.1.3 Phenomena Identification and Ranking Table Figures-of-Merit and Phenomenon Ranking

The PIRT panel identified figures-of-merit for each phase of the non-LOCA transient. The FOMs reflect the non-LOCA event acceptance criteria (see Section 4.2) and important factors relative to the NPM design.

Phase 1 – Pre-trip transient

- CHF – Demonstrating that margin to CHF is maintained for AOOs, or identifying the number of fuel rods that exceed CHF for IEs or postulated accidents is a primary non-LOCA acceptance criterion. The non-LOCA event analyses confirm that the plant system design is such that margin to CHF is maintained until the module protection system actuates to mitigate the event.

In the NPM design, margin to CHF may be challenged during cooldown events or reactivity insertion events.

- Primary pressure – The maximum primary system pressure is one of the non-LOCA acceptance criteria to demonstrate acceptable RCS performance. The non-LOCA event analyses confirm that the plant system design is such that margin to the maximum primary system pressure limits is maintained until the module protection system actuates to mitigate the event.

In the NPM design, margin to the maximum primary system pressure limits may be challenged during heatup events or events that increase RCS inventory.

Phase 2 – Post-trip transition

- CHF – See above.
- Primary pressure – See above.
- Secondary pressure – The maximum secondary system pressure is one of the non-LOCA acceptance criteria to demonstrate acceptable RCS performance.

In the NPM design, as the DHRS is actuated in Phase 2, the maximum secondary side pressure in the SG can occur.

- Containment pressure – The maximum containment pressure is an indicator of containment integrity.

In the NPM design, vapor released into containment is condensed on the containment wall and heat is transferred through the containment wall directly to the reactor pool portion of the UHS. Non-LOCA events could result in mass and energy release into containment. The containment design is intended to effectively transfer heat to the UHS so that containment integrity is maintained.

Phase 3 – Stable natural circulation

- CHF – See above.

- **Coolant mixture level** – The RCS primary mixture level represents the boundary between a two-phase or single-phase liquid region below the level and a single-phase vapor region above the level. This level indicates whether the primary side natural circulation flow path is maintained.

In the NPM design, depending on the initial and boundary condition assumptions such as initial RCS level and temperature, decay heat, and number of DHRS trains operating, the DHRS heat removal may provide sufficient cooling of the RCS that the increased primary side liquid density results in coolant volume shrinkage sufficient to decrease the RCS water level to below the top of the riser, resulting in interrupted natural circulation. If interruption of natural circulation occurs, it is the end of Phase 3, and it occurs well after reactor trip and engineered safety features have responded to the initiating event.

- **Subcriticality** – Maintaining subcriticality following reactor trip limits the nuclear fuel heat source to decay heat levels. If the soluble boron concentration in the core is significantly reduced following reactor trip and the MPS response to the initiating event, then maintaining subcriticality could be adversely affected. While RCS cooldown following reactor trip also affects the net reactivity, the non-LOCA analysis methodology is applicable to DHRS cooling shutdown evaluations only when the mixture level is above the top of the riser and primary side natural circulation flow is maintained.

In the NPM design, the boron in the primary system is limited to the soluble boron at the RCS critical boron concentration from normal operating conditions. During Phase 3 of the non-LOCA event progression, primary side natural circulation flow is maintained.

Each phenomenon identified in the PIRT was assigned an importance ranking and knowledge level ranking. Table 5-1 and Table 5-2 describe the importance rankings and the knowledge level rankings considered by the PIRT panel.

Table 5-1 Importance rankings

Importance Ranking	Definition
High (H)	Significant influence on FOM
Medium (M)	Moderate influence on FOM
Low (L)	Small influence on FOM
Inactive (I)	Phenomenon not present or negligible

Table 5-2 Knowledge levels

Knowledge Level	Definition
4	Well-known/small uncertainty
3	Known/moderate uncertainty
2	Partially known/large uncertainty
1	Very limited knowledge/uncertainty cannot be characterized

5.1.4 Highly Ranked Phenomena

The following subsections summarize the phenomena listed in Table 5-3 that were ranked high importance by the PIRT panel in at least one of the three phases of the non-LOCA short-term transient response scenarios. The knowledge level assigned by the PIRT panel, and the systems and components where the phenomenon was ranked as high importance are also included.

The non-LOCA PIRT was a comprehensive, integrated PIRT covering the range of non-LOCA event types and the phases of event progression. The NPM systems, components, and relevant phenomena were considered in detail.

As discussed in Section 1.1, NRELAP5 is the system thermal-hydraulics code used to simulate the NPM system response during the non-LOCA short-term transient event progression. The NRELAP5 assessments performed as part of the development of Reference 2 demonstrate the capability of the code to simulate the NPM response to LOCA events.

The high-ranked phenomena identified by the PIRT process for the NPM non-LOCA transients were evaluated with respect to the high-ranked phenomena identified by the PIRT process for the NPM LOCA scenarios, and the code assessments performed as part of the development of Reference 2. A gap analysis was performed to identify high-ranked phenomena for non-LOCA transients that were not assessed as part of the development of Reference 2.

High-ranked phenomena for non-LOCA events which were not assessed as part of the development of Reference 2 were addressed in a variety of ways that included:

1. Additional NRELAP5 code assessments performed against separate effects or integral effects test data.
2. Code-to-code benchmark performed between NRELAP5 and an independent system thermal-hydraulics code.
3. The phenomenon was addressed as part of the downstream subchannel analysis.
4. The phenomenon was addressed by specifying appropriately conservative input to the system transient analysis.

The following subsections also describe the means by which each high-ranked phenomenon for non-LOCA events was assessed. In this instance, the NRELAP5 assessments performed as part of the development of Reference 2 were combined with one or more of the means described above to qualify NRELAP5 for the high rank non-LOCA PIRT phenomena. Specific details related to the qualification of NRELAP5 include:

1. The NRELAP5 assessment against Korea Advanced Institute of Science and Technology (KAIST) high pressure condensation data, as presented in Reference 2, is described in Section 5.3.1 for convenience.

2. Separate effects testing of the full-length DHRS was performed at the NIST-1 facility and the NRELAP5 assessment is summarized in Section 5.3.2.
3. An integral effects test of the NPM response to a decrease in heat transfer from the secondary side, and integral effects test of DHRS operation was performed at the NIST-1 facility, and is summarized in Section 5.3.3.
4. A code-to-code benchmark was performed to assess the NRELAP5 prediction of the NPM response to reactivity insertion events as described in Section 5.3.4.
5. The NRELAP5 assessments against the SIET data (TF-1 and TF-2) and other legacy experiments are summarized in Reference 2. Due to the importance of heat transfer through the SG as part of the DHRS loop for non-LOCA transients, further review of these assessments is documented in Section 5.3.5.

Table 5-3 High-ranked phenomena for non-LOCA events

Phenomenon		Subsection
{		
		} ^{2(a),(c)}

5.1.4.1 {{

$$\}}^{2(a),(c)}$$

5.1.4.2 {{

}}^{2(a),(c)}

5.1.4.3 {{

}}^{2(a),(c)}

5.1.4.4 {{

}}^{2(a),(c)}

5.1.4.5 {{

}}^{2(a),(c)}

{{

}}^{2(a),(c)}

5.1.4.6 {{

}}^{2(a),(c)}

5.1.4.7 {{

}}^{2(a),(c)}

5.1.4.8 {{

}}^{2(a),(c)}

5.1.4.9 {{

}}^{2(a),(c)}

5.1.4.10 {{

}}^{2(a),(c)}

5.1.4.11 {{

}}^{2(a),(c)}

5.1.4.12 {{

}}^{2(a),(c)}

5.1.4.13 {{

}}^{2(a),(c)}

5.1.4.14 {{

}}^{2(a),(c)}

5.1.4.15 {{

}}^{2(a),(c)}

5.1.4.16 {{

}}^{2(a),(c)}

5.1.4.17 {{

}}^{2(a),(c)}

5.1.4.18 {{

}}^{2(a),(c)}

5.1.4.19 {{

}}^{2(a),(c)}

5.1.4.20 {{

}}^{2(a),(c)}

5.1.4.21 {{

}}^{2(a),(c)}

5.1.4.22 {{

}}^{2(a),(c)}

5.1.4.23 {{

}}^{2(a),(d)}

5.1.4.24 {{

}}^{2(a),(c)}

5.1.4.25 {{

}}^{2(a),(c)}

5.1.4.26 {{

}}^{2(a),(c)}

5.1.4.27 {{

}}^{2(a),(c)}

5.1.4.28 {{

}}^{2(a),(c)}

5.1.4.29 {{

}}^{2(a),(c)}

5.1.4.30 {{

}}^{2(a),(c)}

5.1.4.31 {{

}}^{2(a),(c)}

5.1.4.32 {{

}}^{2(a),(c)}

5.1.4.33 {{

}}^{2(a),(c)}

5.1.4.34 {{

}}^{2(a),(c)}

5.1.4.35 {{

}}^{2(a),(c)}

5.1.4.36 {{

}}^{2(a),(c)}

5.1.4.37 {{

}}^{2(a),(c)}

5.1.4.38 {{

}}^{2(a),(c)}

5.1.4.39 {{

}}^{2(a),(c)}

5.1.4.40 {{

}}^{2(a),(c)}

5.1.4.41 {{

}}^{2(a),(c)}

5.1.4.42 {{

}}^{2(a),(c)}

5.1.4.43 {{

}}^{2(a),(c)}

5.1.4.44 {{

}}^{2(a),(c)}

5.1.4.45 {{

}}^{2(a),(c)}

5.1.4.46 {{

}}^{2(a),(c)}

5.1.4.47 {{

}}^{2(a),(c)}

5.1.4.48 {{

}}^{2(a),(c)}

5.1.4.49 {{

}}^{2(a),(c)}

5.1.4.50 {{

}}^{2(a),(c)}

5.1.4.51 {{

}}^{2(a),(c)}

5.1.4.52 {{

}}^{2(a),(c)}

5.1.4.53 {{

}}^{2(a),(c)}

5.1.4.54 {{

}}^{2(a),(c)}

5.1.4.55 {{

}}^{2(a),(c)}

5.1.4.56 {{

}}^{2(a),(c)}

5.1.4.57 {{

}}^{2(a),(c)}

5.2 Evaluation of Non-LOCA Phenomena Identification and Ranking Table High-Ranked Phenomena

The information in this section was moved to Section 5.1.4. Evaluation results of high ranked phenomena and text discussing how they were addressed were incorporated into the discussion of each of the phenomenon listed in Section 5.1.4. This section was not deleted to maintain accuracy in other documents which may have referenced material from this document in sections located after this section.

5.3 NRELAP5 Validation and Assessments for Non-LOCA

In Section 5.1 and Section 5.2, the high-ranked phenomena from the non-LOCA PIRT are summarized and how they are assessed in the non-LOCA evaluation model is identified. As identified in Table 5.3, additional assessments were performed to support the qualification of the NRELAP5 code for some of the non-LOCA high-ranked phenomena. This section summarizes the additional assessments performed. This section also discusses a limited number of assessments performed as part of the LOCA evaluation model development that demonstrate qualification of NRELAP5 for prediction of heat transfer from the RCS to the SG to the DHRS.

Heat transfer from the RCS to reactor pool via the SG and the DHRS is important for prediction of non-LOCA transient progression after DHRS actuation, to demonstrate heat removal from the core. The NRELAP5 prediction of heat transfer in the DHRS is assessed with the KAIST high-pressure condensation experiments (Section 5.3.1), and with separate effects testing of the full-length DHRS at the NIST-1 facility (Section 5.3.2). The KAIST data was assessed as part of the LOCA evaluation model development (Reference 2) and key results are summarized in this report. The NRELAP5 code validation for the helical coil SG was assessed as part of the LOCA evaluation model (Reference 2), with testing performed at the SIET facility and other legacy experiments. The operating ranges expected during the non-LOCA transients are assessed to demonstrate the adequacy of the validation for the range of conditions expected in the non-LOCA transients (Section 5.3.5).

Integral effects testing was performed at the NIST-1 test facility to support the NRELAP5 validation for non-LOCA events (Section 5.3.3). The testing assessed primary side pressurization and heat-up due to a decrease in heat transfer from the secondary side, and primary and secondary side conditions during operation of the scaled integral DHRS.

In addition to the validation against test data, a code-to-code benchmark against the RETRAN-3D code (Reference 12) was performed to assess the NRELAP5 prediction of the NPM power and integral primary system response to reactivity insertion events (Section 5.3.4).

Agreement between code predictions and data or for the code to code comparison is assessed according to the criteria described in RG 1.203 (Reference 1):

Validation Requirements:

“Excellent Agreement” applies when the code exhibits no deficiencies in modeling a given behavior. Major and minor phenomena and trends are correctly predicted. The calculated results are judged to agree closely with data.

“Reasonable Agreement” applies when the code exhibits minor deficiencies. Overall, the code provides an acceptable prediction. All major trends and phenomena are predicted correctly. Differences between calculated values and data are greater than are deemed necessary for excellent agreement.

“Minimal Agreement” applies when the code exhibits significant deficiencies. Overall, the code provides a prediction that is not acceptable. Some major trends or phenomena are not predicted correctly, and some calculated values lie considerably outside the specified or inferred uncertainty bands of the data.

“Insufficient Agreement” applies when the code exhibits major deficiencies. The code provides an unacceptable prediction of the test data because major trends are not predicted correctly. Most calculated values lie outside the specified or inferred uncertainty bands of the data.

5.3.1 KAIST

The NRELAP5 prediction of high pressure condensation experimental data produced at the KAIST experimental facility was assessed as part of the LOCA EM development (Reference 2). The phenomenon addressed with the KAIST experimental cases provides test data for condensation inside tubes and heat transfer across tubes for the DHRS. As part of demonstrating qualification of NRELAP5 for calculation of DHRS heat transfer rates, the assessment of NRELAP5 against the KAIST tests is summarized. The data from the KAIST experiment are qualified for use by applying non-mandatory guidance provided by NQA-1 2008/2009 Addendum (Reference 20).

5.3.1.1 Facility Description and Range of Experimental Data Assessed

A schematic of the KAIST experimental facility is shown in Figure 5-1. The maximum design pressure and temperature of the test facility were 7.5 MPa (1088 psia) and 300 degrees C (572 degrees F), respectively.

The major components of the test facility include: SG, which supplied steam (maximum power 200 kW, test section tube, the cooling pool (cools the test section), steam line (transports steam from SG to the test section inlet), condensate drain line, lower plenum (or condensate collection tank) and air supply system. The test section was immersed in the cooling pool and was cooled by boiling and single-phase convective heat transfer on the outside surface of the test section (Reference 24).

The test section was a vertical tube with an inside diameter of 4.62 cm and an effective heat transfer length of 1.8 m. The thickness of the tube wall was 2.3 mm. To reduce the entrance effect, the top 0.5 m length of the test section was insulated. The test section was submerged in the cooling pool (1.2 m × 1.2 m × 2.5 m). A steam line with an inside diameter 2.34 cm was connected from the top of the SG to the top of the test section. The condensate from the test section was drained to the lower plenum (or condensate collection tank) by gravity and then pumped back to the SG.

Table 5-4 summarizes the KAIST and NPM decay heat removal system tube geometry. Table 5-5 summarizes the operational range covered by the KAIST experiment and in the NPM decay heat removal system. Table 5-6 shows a comparison between the NRELAP5 discretization between the KAIST and NPM decay heat removal system condenser tubes. Based on Table 5-4, Table 5-5, and Table 5-6 it is concluded that the geometry and operating range comparisons are acceptable for validation. {{

}}^{2(a),(c)}

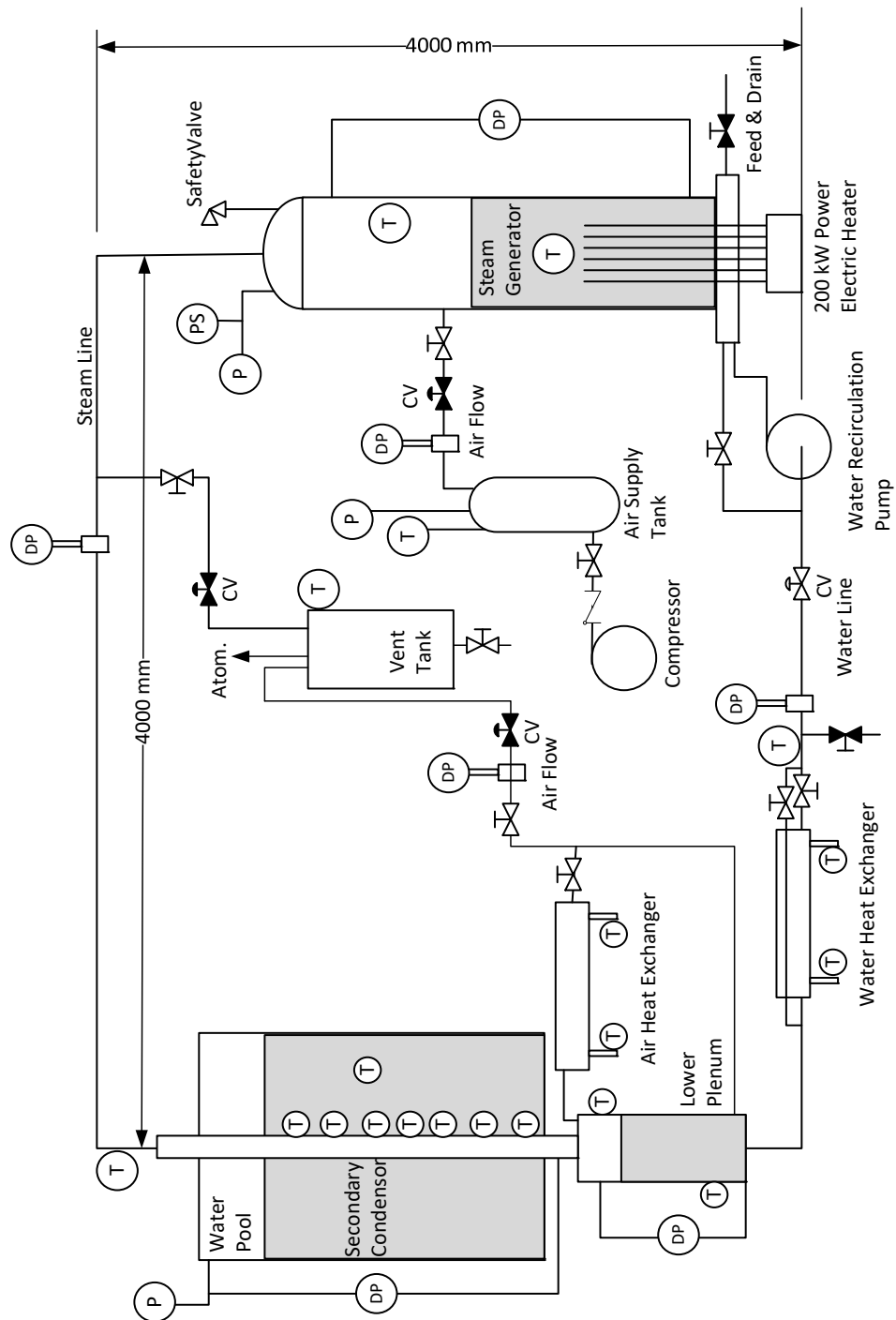


Figure 5-1 Schematic of KAIST test facility

Table 5-4 Comparison between NuScale Power Module decay heat removal system and KAIST test section dimensions

Parameter	KAIST Test Section	NPM DHRS
Geometry	Single circular cross-section tube	For a single DHRS condenser tube (80 tubes per DHRS condenser)
ID, cm (in)	4.62 (1.818)	2.79 (1.097)
OD, cm (in)	5.08 (1.91)	3.34 (1.315)
Active length, m (ft)	1.8 (5.9)	2.874 (9.43)
Wall thickness, mm (in)	2.3 (0.091)	2.8 (0.109)
Material	Stainless steel	Stainless steel

Table 5-5 Comparison between NuScale Power Module decay heat removal system and KAIST range of operations

Parameter	KAIST	NPM DHRS ⁽¹⁾
SG pressure, psia (MPa)	155.3 to 1059.5 (1.071 to 7.305)	{{ }} ^{2(a),(c)}
Steam flow rates lbm/hr (kg/s)	79.37 to 793.7 (0.01 to 0.1)	{{ }} ^{2(a),(c)}
SG steam temperature F (C)	362.12 to 552.2 (183.4 to 289)	{{ }} ^{2(a),(c)}

1. Approximate range expected for DHRS operation during the non-LOCA short-term response
2. Flow rate per tube for one of the 80 DHRS condenser tubes

Table 5-6 Comparison between NuScale Power Module decay heat removal system and KAIST NRELAP5 model nodalization

Parameter	KAIST Condenser Tube NRELAP5 Nodalization	NPM DHRS Condenser Tube NRELAP5 Nodalization
L/D	3.788 to 6.494	{{ }} ^{2(a),(c)}
Total number of nodes	8	{{ }} ^{2(a),(c)}

5.3.1.2 Experimental Procedure

Conditions into the condenser tubes and pool were specified. The experiments were started by purging all non-condensable gas (i.e., air) from the test loop. This was done by supplying steam to the test loop and venting it to the atmosphere through the vent valve located below the test section. After all non-condensable gas was purged, the vent valve was closed and the test section was allowed to fill with the condensate by keeping the condensate drain valve closed. After the test section was completely filled, the SG pressure was increased to the test pressure. As soon as the test pressure was reached, the condensate drain valve was opened and the condensate recirculation pump was started. A constant water level in the lower plenum was maintained by control of the recirculation pump flow rate. Data acquisition was started after the process had reached a steady state.

5.3.1.3 Assessment Results

The comparison results of condensed liquid flows, heat transfer coefficients, and inner wall temperatures show reasonable to excellent agreement between the calculated NRELAP5 and the KAIST measured experimental data. This is a result of implementation of the 2009 extended Shah correlation in NRELAP5, which is intended to improve the predicted high pressure condensation response.

Figure 5-2 presents a summary of the measured versus calculated assessments of the KAIST steam condensation experiments. The overall majority of the assessments lie within the experimental uncertainty (28 percent for heat transfer coefficient).

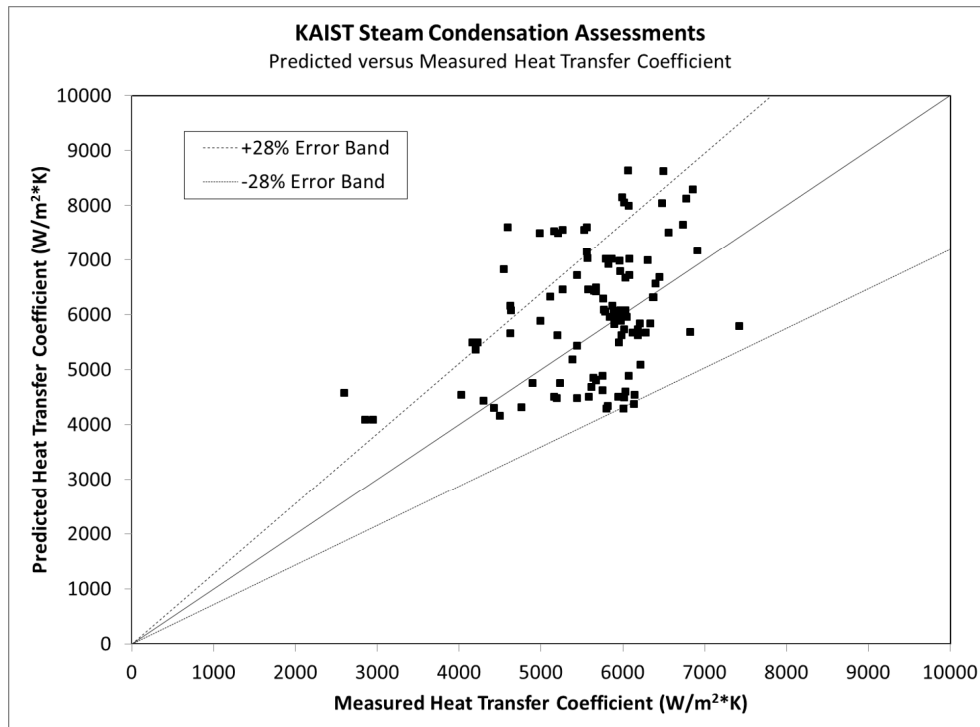


Figure 5-2 Measured vs predicted heat transfer coefficient

5.3.2 NIST-1 Decay Heat Removal System Separate Effects Tests

5.3.2.1 NIST-1 Facility

The NPM design relies on natural circulation flow to remove energy produced in the core. Energy is transferred to the secondary side as the primary coolant flows down over the SG tube coils. During off-normal transients, the design relies on natural circulation driven by steam condensation within the CNV or the DHRS to cool the RPV. Energy within the CNV is transferred through the CNV walls into the surrounding UHS, represented by the reactor cooling pool. The NPM containment vessel is designed to accept and promote steam condensation at pressures varying from vacuum to maximum design pressures.

Due to the unique nature of the NPM design the number of IET facilities is limited. A scaled facility of the NPM was constructed at Oregon State University (OSU), referred to as the NuScale Integral System Test-1 (NIST-1) facility, to assist in validation of the NRELAP5 system thermal-hydraulic code. The NIST-1 facility is a scaled facility of the NPM and consists of the major components in the NPM. These components include: an RPV, a helical coil SG system with a DHRS, a CNV, and a cooling pool vessel (CPV).

What is now the NIST-1 facility was originally conceived at OSU in 2000 as a proof-of-concept testing platform for development of small modular reactor (SMR) technology. During this period it was referred to as the multi-application small light water reactor (MASLWR) facility (see Reference 11).

Although the NuScale design was based on MASLWR, the concept has evolved considerably since NuScale's inception in 2008. At the time that NuScale was formed, the facility was renamed the NIST facility. The NIST facility is a scaled, non-nuclear reactor that uses electric heater rods to analogously represent the heat produced from fission. It is designed to produce experimental data in support of verification and validation of thermal-hydraulic codes.

In 2014 and 2015, the original NIST facility was modified by NuScale to necessitate accurate simulation and to bring the facility in-line with the current NuScale plant design configuration. A scaling analysis was employed for design of the NIST test facility to ensure that the facility design is capable of capturing important plant phenomena with minimal distortions. Following the upgrade, the NIST facility became the NIST-1 facility.

Updates to the NIST facility included in NIST-1 are:

- installation of a DHRS
- scaling of the RVVs and RRVs to the plant design
- replacement of the existing CNV heat transfer plate (HTP), ECCS, and CPV; increased containment pressure rating from about 300 psi to approximately 1,000 psi
- replacement and installation of new instrumentation

- upgrade of the data acquisition and control system (DACS) and rewiring the instrumentation with DACS
- modification of portions of integral reactor vessel

The updated NIST-1 facility provides a well-scaled representation of NuScale's current reactor design that minimizes distortions and provides the measurements necessary for safety code and reactor design validation. A schematic of the NIST-1 facility is shown in Figure 5-3.

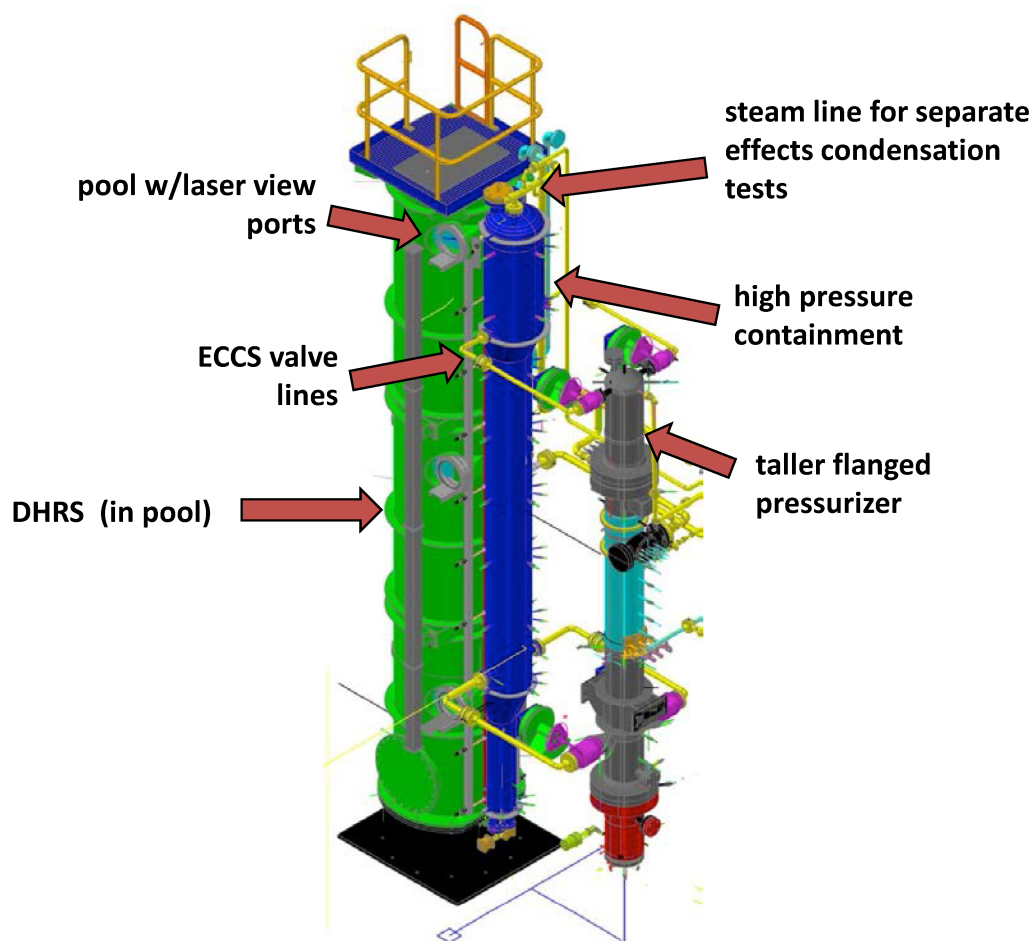


Figure 5-3 Schematic of NIST-1 integral test facility

The configuration of the NIST-1 facility is shown in Figure 5-4.

{{

}}^{2(a),(c),ECI}

Figure 5-4 NIST-1 test facility configuration

The NIST-1 facility models the NPM at 1:3.3 length scale, 1:227.5 volume scale, and 1:1 time scale. There are three vessels in the NIST-1 facility: the RPV, CNV, and CPV as shown in Figure 5-3. A photograph of the NIST-1 facility is shown in Figure 5-5. Unlike the plant, the RPV and CNV are not concentric and the CNV is not immersed in the cooling pool. Rather the RPV and CNV are connected by piping that contains valves that perform the functions of the RRVs, RVVs and breaks as shown in Figure 5-3. The CNV is connected to the CPV through an HTP that is scaled to allow energy transfer to the pool in the same proportion as in the NPM.

Natural circulation flow in the primary circuit is driven by heat input in the core region and heat removal to the SG tubes. Fluid heated in the core region flows upward through the RCS hot leg riser, and then downward around the outside of the SG tubes, the cold leg and the downcomer. The flow then returns to the core through the lower plenum. The core is comprised of a $\{\{ \}^{2(a),(c),ECI}$ electric heater rod bundle with a maximum power of $\{\{ \}^{2(a),(c),ECI}$ a power level scaled to simulate decay heat. System pressure is controlled by the pressurizer component which contains heater rods to bring the pressurizer fluid up to saturation temperature.

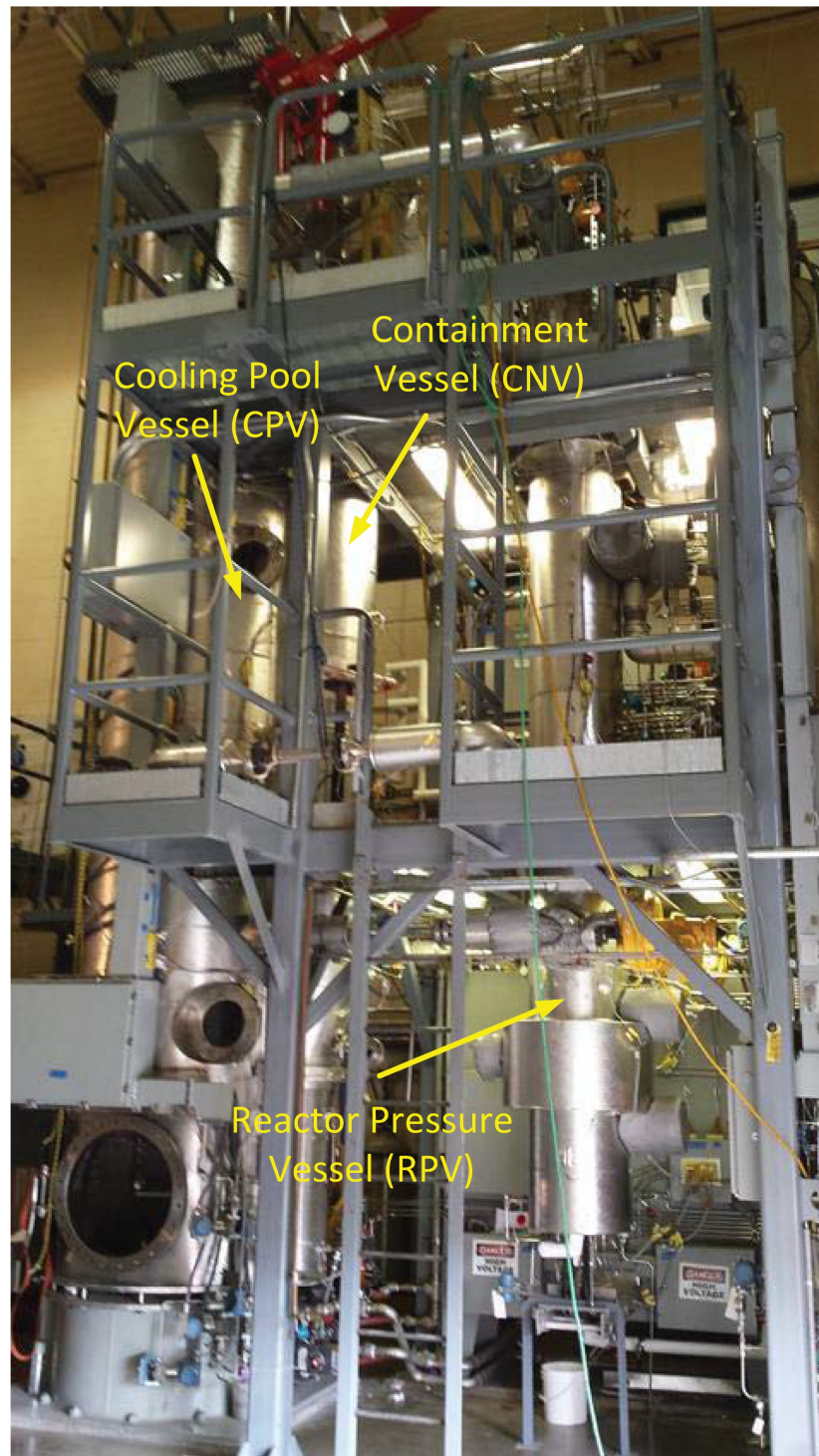


Figure 5-5 Photograph of the NIST-1 facility

Reactor Pressure Vessel

Major internal components in the RPV are the core, RCS hot leg riser, pressurizer, and SG bundle.

Figure 5-6 shows a view of the RPV thermal-hydraulic regions with the pressurizer at the top, separated from the lower part of the RPV by a perforated pressurizer baffle plate. The upper plenum occupies the region below the pressurizer baffle plate and above the RCS hot leg riser that extends down to the top of the core. The upper annulus between the RCS hot leg riser and the RPV shell contains the helical coil SG tubes and is labeled as the SG region. The lower part of the annulus immediately below the SG tubes is the cold leg. The lower annulus at the core elevation is the downcomer, which is separated from the core by the core shell. The lower plenum occupies the bottom of the RPV and hydraulically connects the downcomer and the core. The RPV shells and flanges are covered by {{
}}^{2(a),(c),ECI}

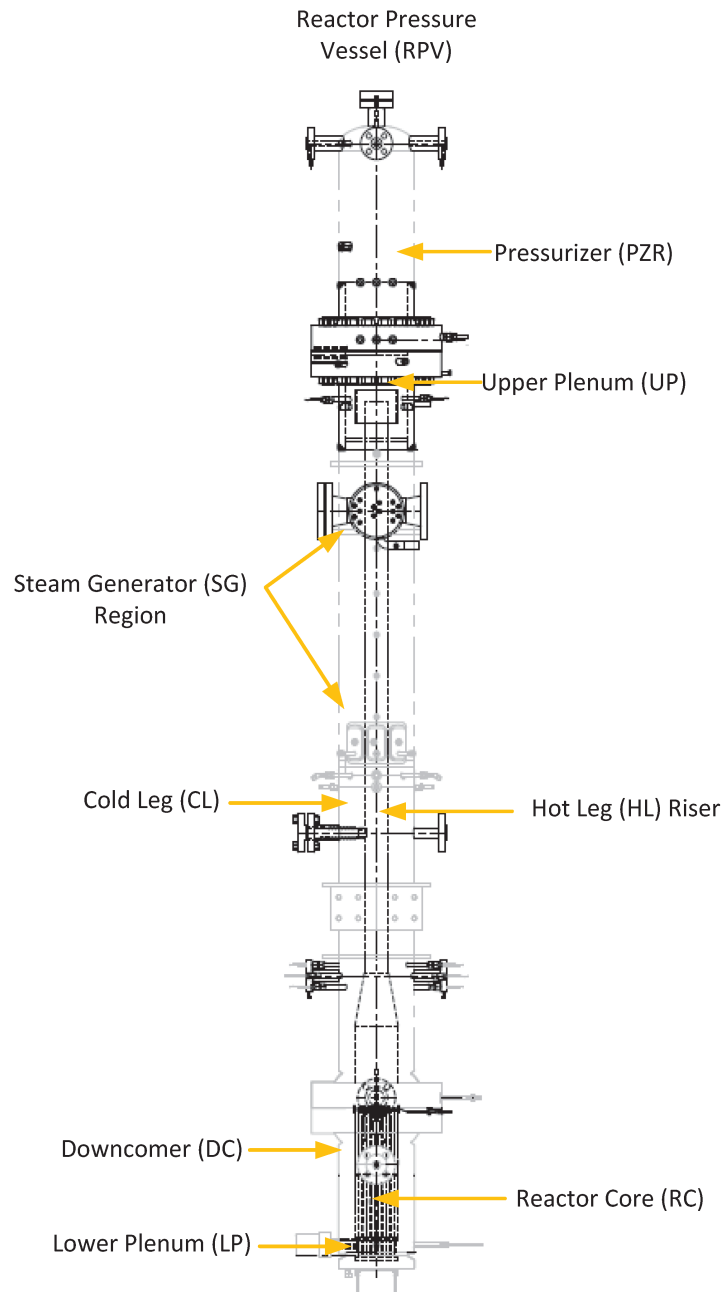


Figure 5-6 Reactor pressure vessel thermal-hydraulic regions

The RPV houses the core, which is modeled by a {{

}}^{2(a),(c),ECI}



Figure 5-7 Lower core flow plate

Reactor Coolant System Hot Leg Riser

After leaving the core, the flow enters the chimney of the RCS hot leg riser. The RCS hot leg riser extends from above the core shroud to the upper plenum, creating a riser and downcomer configuration to enable natural circulation. As shown in

Figure 5-6, the RCS hot leg riser consists of a lower shell, a conical transition, a middle shell containing the flowmeter for the primary circuit, and an upper shell. Flow exits the riser into the upper plenum, which is the space between the RCS hot leg riser outlet and the bottom of the pressurizer baffle plate.

Upper Plenum

After leaving the top of the RCS hot leg riser, the flow enters the upper plenum and is directed radially outward to flow down in the annulus between the riser and the RPV shell. The pressurizer baffle plate separates the upper plenum from the pressurizer. Hydraulic communication between the pressurizer and the RPV occurs via $\{ \{ \}^{2(a),(c)}$ holes in the pressurizer baffle plate that are grouped in eight clusters of three circles radially located $\{ \{ \}^{2(a),(c),ECI}$ from the center of the plate.

Pressurizer

The pressurizer is located above the upper plenum and is in thermal hydraulic communication with the upper plenum via the pressurizer baffle plate holes. The pressurizer maintains primary system static pressure during normal steady-state and transient conditions through the use of three heater elements. Each element has $\{ \{ \}^{2(a),(c),ECI}$ of power and is modulated by the facility control system to maintain system static pressure.

Cold Leg Downcomer

After leaving the upper plenum, the flow continues downward through the SG section and into the cold leg downcomer region. The cold leg downcomer is the annular space bounded by the RPV shell inner diameter and the RCS hot leg riser outer diameter. When fluid reaches the RCS hot leg riser conical transition shell, the flow area is reduced. Flow exits the cold leg downcomer into the lower plenum before it recirculates back into the core.

Steam Generators

The SG is a helical coil, once-through HX consisting of three vertical, parallel banks of tubes (an inner, middle, and outer coil) that wrap counter to each other in the annular space between the RCS hot leg riser and the RPV shell inner surface. In the NIST-1 facility, the primary coolant is circulated around the outside of the SG tubes. Feedwater supplied from the feedwater storage tank is pumped through the SG coils by a regenerative turbine pump. This pump utilizes a variable speed controller, which allows for precise control of the feedwater mass flow rate. Pressure in the secondary side is regulated by a

pneumatically operated variable position valve located in the steam line portion of the flow loop.

In the feed line, feedwater is pre-heated in an in-line heater before going into the different inlet headers. Feedwater enters the coil bundle at the bottom of the SG and is fully boiled in the tubes, resulting in steam that is superheated at the SG outlet. The boil off length is a function of core power, core exit temperature, main feed pump flow rate, and secondary side pressure. Every coil exhausts the superheated steam into a common steam bustle (header), at which point, depending on the test, piping either directs the steam to atmosphere (i.e. the stack), the CNV, or the DHRS inlet header.

Lower Plenum

The lower plenum is the region bounded between the tubesheet and the lower core flow plate. The lower plenum provides the connection between the downcomer and the core, thus completing the RPV flow loop.

Decay Heat Removal System

The NIST-1 facility has three possible configurations with the DHRS. A full-height DHRS is used for separate effects testing. The full-height DHRS has a total of eight tubes, distributed between three rows. Figure 5-8 shows the full-height DHRS. Two decay heat removal HXs are scaled for testing integral DHRS effects in the NIST-1 facility. Because the NPM has two decay heat removal trains available for use, one scaled DHR HX has one tube for simulating one NPM decay heat removal train and the second scaled HDR HX has two tubes representing two NPM decay heat removal trains. Figure 5-9 shows the scaled decay heat removal HXs.

{{

}}^{2(a),(c),ECI}

Figure 5-8 Full-height decay heat removal condenser

{

}}^{2(a),(c),ECI}

Figure 5-9 Scaled decay heat removal heat condensers

Containment and Cooling Pool Vessel

The CNV, representing the cavity volume between the RPV outer surface and the containment inside surface, is conjoined to the CPV and thermally separated by a scaled HTP. For the NPM, the RPV is located inside containment. However, with the NIST-1 facility, to maintain both volume and surface area scaling similitude, as well as allow proper instrumentation, the RPV is thermal hydraulically separated from the CNV. The heat transfer plate (HTP) models the scaled condensation heat transfer surface between the CNV and CPV. Fluid in the CPV, which is at ambient pressures, models the scaled volume in which an NPM containment vessel is partially immersed.

The CPV has a set of four ports allowing for the installation of one of three decay heat removal HXs. The baseline configuration is with a full height decay heat removal, which is used for SETs. Two decay heat removal HXs are scaled for testing integral DHRS effects in the NIST-1 facility. Because the NPM has two decay heat removal trains available for use, to simulate either one or both trains, one scaled decay heat removal has one tube for simulating one NPM decay heat removal train and the second scaled decay heat removal has two tubes representing two NPM decay heat removal trains.

Emergency Core Cooling System and Chemical and Volume Control System Lines

Eight lines connect the RPV to the CNV. Five of these lines belong to the facility ECCS, whereas the other three are part of the CVCS. As part of the ECCS, there are two independent reactor vent lines near the top of the pressurizer section, and two reactor recirculation lines in the lower downcomer of the RPV. The fifth ECCS line is a SET line that also models reactor recirculation. For the CVCS, two lines penetrate the vessel near the bottom of the SG. One of these lines penetrates both the vessel wall and the hot leg riser, simulating the make-up line into the hot leg. The other CVCS line connects to the cold leg and thus penetrates only the RPV wall. This line represents the facility CVCS discharge break line. A third CVCS line between the RPV and CNV is located at the very top of the pressurizer and functions as an analogy for the pressurizer spray line. Each line that is installed has a pneumatic isolation valve that is actuated through the test facility control system. Any lines that are not installed use a blank flange for isolation.

The facility baseline configuration consists {{

}}^{2(a),(c),ECI}

NIST-1 Facility Instrumentation and Control

Instrumentation is used throughout the facility to measure the thermal hydraulic behavior during steady-state and transient operations. The following information is obtained and recorded by the DACS:

- {{

}}^{2(a),(c),ECI}

The ECCS, CVCS and SET lines are heavily instrumented to obtain data on break flow and ECCS blowdown and recirculation flows. The components and instruments include:

- an isolation valve.
- {{

}}2(a),(c),ECI

The facility control system generates signals per the system logic, including valve and relay control signals, heater and pump control signals, etc. The following systems can be regulated by the test facility control system:

- core heaters (including decay power modeling)
- pressurizer heaters
- feedwater pump
- coolant charging pump
- containment heaters (used to maintain an adiabatic boundary condition on all walls of containment except for the prescribed condensation surface of the HTP)
- strip heat power in the ECCS, CVCS, DHRS, and steam lines (used to minimize heat loss in the lines connecting the RPV and CNV)
- CNV vacuum pump
- various pneumatic and solenoid valves for flow regulation or transient initiation

The NIST-1 facility is used to assess the operation of the NPM under normal operating conditions and to assess the passive safety system responses during transient conditions. The data generated and collected by the facility DACS is used to assist in validation of the NRELAP5 system thermal-hydraulic code for NPM analysis.

5.3.2.2 Decay Heat Removal System Separate Effects Test Matrix

The NIST-1 facility was used to perform separate effects testing with the full-height DHRS. Table 5-7 describes DHRS separate effects testing performed at the NIST-1 facility; these test assessments are presented in the following subsections.

Table 5-7 NIST-1 decay heat removal system separate effects tests for NRELAP5 code validation

{{

}}^{2(a),(c),ECI}

5.3.2.3 NRELAP5 Model Description

For the NIST-HP-03 and NIST-HP-04 test assessments, a separate effects model of the NIST-1 facility is used. This model contains hydrodynamic components and heat structures for:

- {{

}}^{2(a),(c)}

- {{

}}^{2(a),(c)}

Table 5-8 Comparison between NPM and NIST-1 decay heat removal NRELAP5 nodalizations

{{

}}^{2(a),(c)}

{{

}}^{2(a),(c)}

Figure 5-10 NIST-1 noding diagram for full-height decay heat removal system separate effect tests

5.3.2.4 HP-03 Test Description

The NIST-1 HP-03 test (HP-03) was used to assess the capability of NRELAP5 to predict convective condensation within the DHRS and heat transfer to the reactor pool across the DHRS tubes.

For HP-03, the heated NIST-1 primary system was used to produce steam within the SG tubes. The steam from the SG tubes was transferred to the steam line and routed to the full-height DHRS steam header, which was located in the upper CPV. Steam was condensed in the condenser tubes, entered the DHRS condensate header, and flowed through the condensate line. The condensate control valve in the condensate line maintained DHRS pressure by controlling the rate at which condensate discharged to the atmosphere.

During HP-03, superheated steam was delivered to the DHRS steam header at a range of flow rates and pressures. The incoming steam was allowed to condense within the condenser tubes and a pseudo steady state liquid level (DHRS level) was established.

Table 5-9 summarizes the initial conditions of the HP-03 cases.

Table 5-9 NIST-1 HP-03 test cases

{{

}}2(a)(c),ECI

5.3.2.5 HP-03 Results

The HP-03 data trends were well predicted by NRELAP5 with reasonable to excellent agreement {{ }}^{2(a),(c),ECI}. Detailed results are presented herein for three HP-03 cases, specifically HP-03-01, HP-03-02c, and HP-03-03-Part1.

For the higher DHRS inlet mass flow rate cases (i.e. HP-03-01c-Part1, Part2, and Part3), NRELAP5 code-to-data comparisons show [A.] reasonable-to-excellent or excellent agreement for DHRS power, [B.] reasonable, reasonable-to-excellent, or excellent agreement for other parameters of interest, and [C.] reasonable agreement for DHRS level. {{

}}^{2(a),(c)}

5.3.2.5.1 HP-03-01 Run

This section compares the NRELAP5 simulation results with the measured data for HP-03-01, which was run at a DHRS pressure of {{ }}^{2(a),(c),ECI}.

Figure 5-11 presents the flow enthalpy into the inlet and outlet headers of the DHRS heat exchanger (an alternate view of DHRS heat removal rate, or DHRS power). The mass flow rate, pressure, and temperature at the inlet are specified as boundary conditions. As there is a very large difference in magnitude between the inlet and outlet enthalpy flow rates, the NRELAP5 outlet enthalpy flow rate and data outlet enthalpy flow rate do not need to be perfectly matched in order for NRELAP5 DHRS power to show excellent code-to-data agreement.

Figure 5-11a presents the DHRS power. Code-to-data agreement is excellent. This indicates that NRELAP5 appropriately calculates the DHRS-to-CPV heat transfer.

Figure 5-12 presents the NRELAP5 calculated DHRS heat exchanger level. Code-to-data agreement is reasonable. {{

}}^{2(a),(b),(c)}

{{

}}^{2(a),(b),(c)}

Figure 5-13 presents the DHRS condenser tube internal fluid temperature. {{
}}^{2(a),(b),(c)} Code-to-
data agreement is reasonable.

Figure 5-14 and Figure 5-14a present the CPV temperature. Code-to-data agreement is excellent. While the NRELAP5 simulation is not run for an extended period of time, the CPV temperature is well-matched at the end of the comparison period. The high temperatures in the upper CPV indicate that boiling was occurring.

Figure 5-15 presents the CPV level. {{

}}^{2(a),(c)} code-to-data
agreement is excellent. The CPV level is observed to drop during testing, which indicates that boiling was occurring.

{{

}}^{2(a),(c)}

{{

}}^{2(a),(b),(c),ECI}

Figure 5-11 NIST-1 HP-03-01 decay heat removal system enthalpy flow rate code-to-data comparison

{{

⋮

}}^{2(a),(b),(c),ECI}

Figure 5-11a NIST-1 HP-03-01 decay heat removal system power code-to-data comparison

{{

}}2(a),(b),(c),ECI

Figure 5-12 NIST-1 HP-03-01 decay heat removal system level code-to-data comparison

{{

}}^{2(a),(b),(c),ECI}

Figure 5-13 NIST-1 HP-03-01 decay heat removal system internal fluid temperature code-to-data comparison

{{

}}2(a),(b),(c),ECI

Figure 5-14 NIST-1 HP-03-01 cooling pool vessel temperature code-to-data comparison (1 of 2)

{{

}}^{2(a),(b),(c),ECI}

Figure 5-14a NIST-1 HP-03-01 cooling pool vessel temperature code-to-data comparison
(2 of 2)

{{

}}^{2(a),(b),(c),ECI}

Figure 5-15 NIST-1 HP-03-01 cooling pool vessel level code-to-data comparison

5.3.2.5.2 HP-03-02c Run

This section compares the NRELAP5 simulation results with the measured data HP-03-02c which was run at a DHRS pressure of {{

}}^{2(a),(c),ECI}.

Figure 5-16 presents the DHRS inlet and outlet enthalpy flow rate. {{

}}^{2(a),(b),(c)}

As there is a very large difference in magnitude between the inlet and outlet enthalpy flow rates, the NRELAP5 outlet enthalpy flow rate and data outlet enthalpy flow rate do not need to be perfectly matched in order for NRELAP5 DHRS power to show excellent code-to-data agreement.

Figure 5-16a presents the DHRS power. Code-to-data agreement is excellent. This indicates that NRELAP5 appropriately calculates the DHRS-to-CPV heat transfer.

Figure 5-17 presents the DHRS level. Code-to-data agreement is reasonable.

Figure 5-18 presents the DHRS condenser tube internal fluid temperature. {{
}}^{2(a),(b),(c)} Code-to-data agreement is reasonable.

Figure 5-19 and Figure 5-19a present the CPV temperature. Overall code-to-data agreement is judged to be reasonable, as most trends are captured {{

}}^{2(a),(b),(c)}

Figure 5-20 presents the CPV level. {{

}}^{2(a),(c)} code-to-data agreement is excellent. The CPV level is observed to drop during testing, which indicates that boiling was occurring.

{{

}}^{2(a),(b),(c),ECI}

Figure 5-16 NIST-1 HP-03-02c decay heat removal system enthalpy flow rate code-to-data comparison

{{

}}^{2(a),(b),(c),ECI}

Figure 5-16a NIST-1 HP-03-02c decay heat removal system power code-to-data comparison

{{

}}^{2(a),(b),(c),ECI}

Figure 5-17 NIST-1 HP-03-02c decay heat removal system level code-to-data comparison

{{

}}^{2(a),(b),(c),ECI}

Figure 5-18 NIST-1 HP-03-02c decay heat removal system internal fluid temperature code-to-data comparison

{{

}}^{2(a),(b),(c),ECI}

Figure 5-19 NIST-1 HP-03-02c cooling pool vessel temperature code-to-data comparison
(1 of 2)

{{

}}^{2(a),(b),(c),ECI}

Figure 5-19a NIST-1 HP-03-02c cooling pool vessel temperature code-to-data comparison
(2 of 2)

{{

}}^{2(a),(b),(c),ECI}

Figure 5-20 NIST-1 HP-03-02c cooling pool vessel level code-to-data comparison

5.3.2.5.3 HP-03-03 Part 1 Run

This section compares the NRELAP5 simulation results with the measured data for the HP-03-03-Part 1 test, which was run at a DHRS pressure of {{
}}^{2(a),(c),ECI}.

Figure 5-21 presents the DHRS inlet and outlet enthalpy flow rate. Note that the inlet temperature, pressure, and mass flow rate are specified as boundary conditions. {{

}}^{2(a),(b),(c)} As there is a very large difference in magnitude between the inlet and outlet enthalpy flow rates, the NRELAP5 outlet enthalpy flow rate and data outlet enthalpy flow rate do not need to be perfectly matched in order for NRELAP5 DHRS power to show excellent code-to-data agreement.

Figure 5-21a presents the DHRS power. Code-to-data agreement is reasonable-to-excellent. This indicates that NRELAP5 appropriately calculates the DHRS-to-CPV heat transfer. {{

}}^{2(a),(c)}

Figure 5-22 presents the DHRS level. Code-to-data agreement is reasonable-to-excellent.

Figure 5-23 presents the DHRS condenser tube internal fluid temperature. {{
}}^{2(a),(b),(c)} Code-to-data agreement is reasonable.

Figure 5-24 and Figure 5-24a present the CPV temperature. Overall code-to-data agreement is reasonable-to-excellent. Most trends which appear in the test data are captured by NRELAP5.

Figure 5-25 presents the CPV level. {{

}}^{2(a),(b),(c)}

{{

}}2(a),(b),(c),ECI

Figure 5-21 NIST-1 HP-03-03-P1 decay heat removal system enthalpy flow rate code-to-data comparison

{{

}}^{2(a),(b),(c),ECI}

Figure 5-21a NIST-1 HP-03-03-Part1 decay heat removal system power code-to-data comparison

{{

}}^{2(a),(b),(c),ECI}

Figure 5-22 NIST-1 HP-03-03-Part1 decay heat removal system level code-to-data comparison

{{

}}2(a),(b),(c),ECI

Figure 5-23 NIST-1 HP-03-03-Part1 decay heat removal system internal fluid temperature code-to-data comparison

{{

}}^{2(a),(b),(c),ECI}

Figure 5-24 NIST-1 HP-03-03-Part1 cooling pool vessel temperature code-to-data comparison (1 of 2)

{{

}}^{2(a),(b),(c),ECI}

Figure 5-24a NIST-1 HP-03-03-Part1 cooling pool vessel temperature code-to-data comparison (2 of 2)

{{

}}^{2(a),(b),(c),ECI}

Figure 5-25 NIST-1 HP-03-03-Part1 cooling pool vessel level code-to-data comparison

5.3.2.5.4 HP-03 Summary

The comparisons between the HP-03 data and HP-03 NRELAP5 simulations show that NRELAP5 has the capability to accurately predict the DHRS-to-CPV heat transfer.

For DHRS power, code-to-data comparisons show reasonable-to-excellent or excellent agreement.

For the identified additional parameters of interest, including DHRS level and CPV level, code-to-data comparisons show reasonable, reasonable-to-excellent, or excellent agreement.

5.3.2.6 HP-04 Test Description

HP-04 was used to assess NRELAP5 capability to predict {{

}}^{2(a),(c)}

For the HP-04 test, the heated primary system was used to provide transfer heat to the SG and create steam. The steam from the SG tubes was transferred to the steam line and routed to the full-height DHRS steam header, located in the CPV. Steam is condensed in the condenser tubes and enters the DHRS condensate plenum and condensate line. For this test the condensate line directed the DHRS discharge to the environment.

{{

}}^{2(a),(c)} With the current facility this was achieved at two pressure conditions. Table 5-10 presents the test conditions considered for the assessment of NRELAP5.

Table 5-10 NIST-1 HP04 test ranges

{{

}}^{2(a),(c),ECI}

5.3.2.7 HP-04 Test Results

The NIST-1 HP-04 test data was compared to NRELAP5 predictions designed to simulate the test conditions and test procedures in effect during the experiment. HP-04 test data trends were well predicted by NRELAP5 with reasonable to excellent agreement for DHRS heat exchanger {{

}}^{2(a),(c),ECI} based on an enthalpy balance across the tubes.

The comparison of the calculated DHRS and cooling pool water levels show reasonable to excellent agreement with the data. The NIST-1 CPV heat-up response was not fully captured in the code to data comparison.

The comparisons between the experimental data and the code calculated values show that NRELAP5 has the capability to accurately predict the energy transfer across the DHRS heat exchanger tubes to the CPV fluid, although the CPV heat-up response is not fully captured. The heat transfer across the tubes is influenced by the condensate level inside the tubes and the cooling pool level.

These results are discussed in more detail in the following subsections for NIST-1 generated data at DHRS pressures of $\{\{ \}^{2(a),(c),ECI}$

5.3.2.7.1 HP-04-02 Run

This section compares the NRELAP5 simulation results with the measured data for the HP-04-02 run $\{\{ \}^{2(a),(c),ECI}$. In figures, the data measurement uncertainty is shown in dotted lines.

Code-to-data comparisons of the DHRS heat removal rate produced reasonable agreement, as shown by the prediction of the enthalpy change over the DHRS in Figure 5-26. $\{\{ \}^{2(a),(c)}$

The NIST-1 profiles for the DHRS condensate outlet temperature are not fully captured in the code-to-data comparisons. $\{\{ \}^{2(a),(c)}$

Code-to-data comparisons of DHRS heat exchange tube level produced reasonable agreement, as shown in Figure 5-28. $\{\{ \}^{2(a),(c)}$

Although the code-to-data comparisons of CPV level produced reasonable-to-excellent agreement, $\{\{ \}^{2(a),(b),(c),ECI}$

{{

}}^{2(a),(b),(c),ECI}

Figure 5-26 NIST-1 HP-04-02 decay heat removal system energy transfer rate

{{

}}^{2(a),(b),(c),ECI}

Figure 5-27 NIST-1 HP-04-02 decay heat removal system condensate temperature

{{

}}^{2(a),(b),(c),ECI}

Figure 5-28 NIST-1 HP-04-02 decay heat removal system internal collapsed level

{{

}}^{2(a),(b),(c),ECI}

Figure 5-29 NIST-1 HP-04-02 cooling pool vessel level

{{

}}^{2(a),(b),(c),ECI}

Figure 5-30 NIST-1 HP-04-02 mid cooling pool vessel fluid temperatures

{{

}}^{2(a),(b),(c),ECI}

Figure 5-31 NIST-1 HP-04-02 upper cooling pool vessel fluid temperatures

5.3.2.7.2 HP-04-03 Run

This section compares the NRELAP5 simulation results with the measured data for the HP-04-03 run {{ }}^{2(a),(c),ECI} In figures, the data measurement uncertainty is shown in dotted lines.

Code-to-data comparison of the DHRS heat removal rate produced reasonable to excellent agreement, as shown by the prediction of the enthalpy change over the DHRS in Figure 5-32. {{

}}^{2(a),(c)}

The NIST-1 profiles for DHRS condensate outlet temperatures are not fully captured in the code-to-data comparisons. {{

}}^{2(a),(c)}

Code-to-data comparison of DHRS heat exchanger tube level shows reasonable agreement, as shown in Figure 5-34. {{

}}^{2(a),(c)}

{{
}}^{2(a),(c)}

Although the code-to-data comparisons of CPV level produced reasonable-to-excellent agreement, {{

}}^{2(a),(b),(c),ECI}

{{

}}^{2(a),(b),(c),ECI}

Figure 5-32 NIST-1 HP-04-03 decay heat removal system energy transfer rate

{{

}}^{2(a),(b),(c),ECI}

Figure 5-33 NIST-1 HP-04-03 decay heat removal system condensate temperature

{{

}}^{2(a),(b),(c),ECI}

Figure 5-34 NIST-1 HP-04-03 decay heat removal system internal collapsed level comparison

{{

}}^{2(a),(b),(c),ECI}

Figure 5-35 NIST-1 HP-04-03 cooling pool vessel level comparison

{{

}}^{2(a),(b),(c),ECI}

Figure 5-36 NIST-1 HP-04-03 mid cooling pool vessel axial temperatures

{

}}^{2(a),(b),(c),ECI}

Figure 5-37 NIST-1 HP-04-03 upper cooling pool vessel axial temperatures

5.3.2.7.3 HP-04 Summary

Although the CPV fluid heat-up profiles for the NIST-1 HP-04 test data were not fully captured in the NRELAP5 simulations of HP-04, the code-to-data comparisons of DHRS heat removal rate were well-matched.

This assessment concludes that NRELAP5 simulations of the NPM decay heat removal system should be expected to adequately predict the DHRS heat removal rates related to a large envelope of reactor pool liquid conditions.

5.3.3 NIST-1 Non-LOCA Integral Test

5.3.3.1 NIST-1 Facility

The NIST-1 facility is described in Section 5.3.2.1. The NLT-2 tests were conducted in two sessions; first NLT-2a was conducted and a few weeks later NLT-2b was conducted. Test NLT-02a was a loss of feed water transient with a subsequent pressurization and depressurization of the RPV. In Test NLT-02b the DHRS was activated from a low reactor power level to demonstrate long term cooling capability over several hours.

5.3.3.2 Non-LOCA Integral Effects Test Matrix

The NIST-1 facility was used to perform integral effects testing with the scaled two-tube DHRS heat exchanger. Table 5-11 describes DHRS integral effects testing performed at the NIST-1 facility; these test assessments are presented in the following subsections.

Table 5-11 NIST-1 integral effects tests for NRELAP5 code validation

{{

}}^{2(a),(c),ECI}

5.3.3.3 NRELAP5 Model Description

The NRELAP5 model of the NIST-1 facility is constructed to include all of the major flow paths in the facility, including the major systems; the RPV primary and secondary, the CNV, and the CPV, as well as the ECCS. {{

diagram is shown in Figure 5-38.

{{

}}^{2(a),(c)} A nodalization

}}^{2(a),(c)}

{

}^{2(a),(c)}

{{

}}^{2(a),(c),ECI}

Figure 5-38 NRELAP5 noding diagram for the NIST-1 facility

{{

}}^{2(a),(c),ECI}

Figure 5-39 NRELAP5 NIST-1 model secondary system nodalization layout (NLT-2b)

{{

}}^{2(a),(c),ECI}

Figure 5-39a NRELAP5 NIST-1 model secondary system nodalization layout (NLT-15p2)

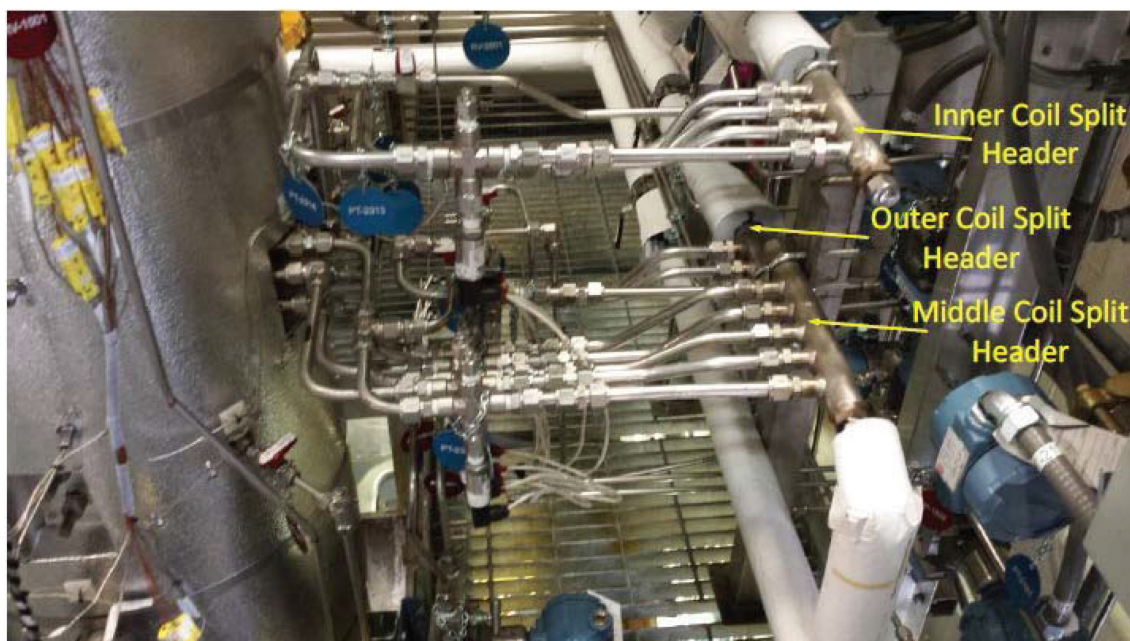


Figure 5-40 NIST-1 feedwater split headers at the steam generator tube coils connection (at the time of NLT-2b test)

5.3.3.4 NLT-2a Test Description

The objective of the NLT-02 test was to measure the scaled integral system response to a decrease in heat removal from the secondary side following a loss of feedwater event, to the point of reactor trip. In the plant design, response to a decrease in heat removal includes a reactor trip based on PZR pressure, core outlet temperature, or PZR level, as well as the activation of the DHRS heat exchanger, which permits circulation between the DHRS and the SG coils. {{

}}^{2(a),(c)}

The NIST-1 facility had the following configuration and initial conditions at the start of the NLT-02a test:

1. {{

}}^{2(a),(b),(c),ECI}

The sequence of events for the NLT-02a test is shown in Table 5-12.

Table 5-12 NLT-02a sequence of events

{{

}}^{2(a),(b),(c),ECI}

5.3.3.5 NLT-2a Test Results

The transient was initiated with the termination of feedwater flow. Feedwater flow was a boundary condition in the NRELAP5 simulation. Figure 5-41 compares the calculated feedwater flow with the data. Note that in figures, the data measurement uncertainty is shown in dotted lines.

The core heater rod power was another boundary condition applied to the simulation. Figure 5-42 compares core heater rod power used in the simulation with the measured core heater rod power that is supplied to the core heater rods.

Figure 5-43 compares the PZR pressure. The calculated pressure shows reasonable to excellent agreement with the measured data. {{

}}^{2(a),(c)}

Figure 5-44 compares the calculated riser flow rate with the measured data. The predicted response shows reasonable agreement with the data. {{

}}^{2(a),(c)}

The comparison of the measured and calculated PZR level is shown in Figure 5-45. The predicted level is considered in excellent agreement with the data; the calculation is within the uncertainty bands of the data.

The predicted core inlet temperature is compared to data in Figure 5-46. {{

}}^{2(a),(c)}

The core exit temperature comparison is shown in Figure 5-49. The initial temperature is underpredicted in the steady state but is within the uncertainty band when the core power is shut off. The trend of the predicted temperature is slightly different than the measured value between 50-125 seconds, but it remains within the uncertainty bands of the data. The predicted riser inlet fluid temperature, shown in Figure 5-49a, is in reasonable agreement with the measured temperature.

A comparison of the calculated and measured PZR heater rod power is shown in Figure 5-50. The PZR heater rods are used to keep the RPV primary side at a target pressure. If the pressure declines, the PZR heater rod power increases. Conversely, if the PZR pressure increases, the PZR heater rod power declines. {{

}}^{2(a),(c)}

The code-to-data comparison of the steam line pressure is provided in Figure 5-51. {{

}}^{2(a),(c)}

A comparison of the steam line mass flow rate is shown in Figure 5-52. The predicted steam line mass flow rate shows reasonable agreement with the data, considering {{

}}^{2(a),(c)}

In conclusion, it has been demonstrated that NRELAP5 is capable of predicting the data trends of non-LOCA events, such as a loss of feedwater, with a high degree of confidence.

{{

}}^{2(a),(b),(c),ECI}

Figure 5-41 NLT-02a transient feedwater flow comparison

{{

}}^{2(a),(b),(c),ECI}

Figure 5-42 NLT-02a transient core heater rod power comparison

{{

}}^{2(a),(b),(c),ECI}

Figure 5-43 NLT-02a transient pressurizer pressure comparison

{{

}}^{2(a),(b),(c),ECI}

Figure 5-44 NLT-02a transient riser mass flow rate comparison

{{

}}^{2(a),(b),(c),ECI}

Figure 5-45 NLT-02a transient pressurizer level comparison

{{

}}^{2(a),(b),(c),ECI}

Figure 5-46 NLT-02a transient core inlet temperature

{{

}}^{2(a),(b),(c),ECI}

Figure 5-47 NLT-02a transient combined middle and outer steam generator tube coil differential pressure comparison

{{

}}^{2(a),(b),(c),ECI}

Figure 5-48 NLT-02a transient inner steam generator tube coil differential pressure comparison

{{

}}^{2(a),(b),(c),ECI}

Figure 5-49 NLT-02a transient core exit fluid temperature comparison

{{

}}^{2(a),(b),(c),ECI}

Figure 5-49a NLT-02a transient riser inlet fluid temperature comparison

{{

}}^{2(a),(b),(c),ECI}

Figure 5-50 NLT-02a transient pressurizer heater rod power comparison

{{

}}^{2(a),(b),(c),ECI}

Figure 5-51 NLT-02a transient steam line pressure comparison

{{

}}^{2(a),(b),(c),ECI}

Figure 5-52 NLT-02a transient steam line mass flow rate comparison

5.3.3.6 NLT-2b Test Description

The objectives of the NLT-02b test were to observe the integral response of the DHRS and RPV after initial DHRS activation, under quasi-steady conditions as the cooling pool was allowed to heat-up, and finally in a period of DHRS-driven cooling and depressurization after the core power transitioned to decay heat mode. The principal parameters of interest during initial DHRS activation are DHRS condensate mass flow rate, DHRS pressure, and temperatures throughout the SG secondary and DHRS loop. After the initial pressure peak due to DHRS activation has subsided, additional parameters of interest are the primary flow rate, primary level, primary pressure and temperatures, and CPV temperatures adjacent to the DHRS heat exchanger.

{{

}}^{2(a),(c)}

The NIST-1 facility had the following configuration and initial conditions at the start of the NLT-02b test:

1. {{

}}^{2(a),(c)}

The sequence of events for the NLT-02b test is shown in Table 5-13.

{{

}}^{2(a),(c)}

Table 5-13 NLT-02b sequence of events

{{

}}^{2(a),(b),(c)}

5.3.3.7 NLT-2b Phase 1 Test Results

Code-to-data comparisons of key parameters for the first phase of the NLT-2b test are shown in Figure 5-53 through Figure 5-70. Note that in figures, the data measurement uncertainty is shown in dotted lines. This phase consisted of termination of the feedwater flow and turning off the core heater rod power prior to the opening of the DHRS steam line and condensate line valves to begin the transition to DHRS cooling. {{

}}^{2(a),(b),(c)}

In general, the NRELAP5 simulation showed reasonable agreement with the measured data for this time period.

The measured core heater rod power is used as a boundary condition in the simulation. A comparison of the core heater rod power is shown in Figure 5-53. {{

}}^{2(a),(c)}

Comparison of the PZR pressure response is provided in Figure 5-54. {{

}}^{2(a),(b),(c),ECI}

{{

}}^{2(a),(b),(c),ECI}

Code-to-data comparisons for the core inlet and exit temperatures are shown in Figure 5-57. {{

}}^{2(a),(b),(c)}

Comparison of the measured and calculated steam line pressure is shown in Figure 5-59. {{

}}^{2(a),(b),(c)}

The initial liquid mass inventory indicated by the steady state SG tube level and DHRS HX tube level showed reasonable agreement with the data in the simulation. {{

}}^{2(a),(b),(c)}

The feedwater mass flow rate was terminated prior to the opening of the DHRS loop steam and condensate valves.

Figure 5-63 and Figure 5-64 show code-to-data comparisons of the SG and DHRS heat exchanger tube liquid level, respectively. {{

}}^{2(a),(c)}

Figure 5-65 provides a comparison of the measured and calculated DHRS condensate fluid temperature. Although the trends of the data are calculated, the comparison is considered minimal, {{

}}^{2(a),(c)}

{{

}}^{2(a),(c)}

Figure 5-66 shows that DHRS condensate flow is slightly underpredicted. The predicted flow rate starts out slightly higher than the data, but the trend is correct, and the magnitude is reasonable compared to the data during the quasi steady state phase. The flow plot in combination with the DHRS heat exchanger level (Figure 5-64) and SG level (Figure 5-63), with inspection of the pressure drops in the steam lines and condensate lines, provides confidence that the total DHRS loop resistance is appropriately accounted for.

Figure 5-67 shows {{

}}^{2(a),(b),(c)}

Figure 5-68 compares predicted CPV level during phase 1 of the transient. {{

}}^{2(a),(b),(c)}

{{

Figure 5-53 NLT-02b phase 1 transient core power comparison

}}^{2(a),(b),(c),ECI}

{{

Figure 5-54 NLT-02b phase 1 transient pressurizer pressure comparison

}}^{2(a),(b),(c),ECI}

{{

}}^{2(a),(b),(c),ECI}

Figure 5-55 NLT-02b phase 1 transient pressurizer level comparison

Figure 5-56 Not Used

{{

}}^{2(a),(b),(c),ECI}

Figure 5-57 NLT-02b phase 1 transient core inlet and outlet temperature comparison

Figure 5-58 Not Used

{{

}}^{2(a),(b),(c),ECI}

Figure 5-59 NLT-02b phase 1 transient steam generator steam pressure comparison

{{

}}^{2(a),(b),(c),ECI}

Figure 5-60 NLT-02b phase 1 transient steam generator thermal power comparison

{{

}}^{2(a),(b),(c),ECI}

Figure 5-61 NLT-02b phase 1 transient decay heat removal system heat exchanger thermal power comparison

{{

}}^{2(a),(b),(c),ECI}

Figure 5-62 NLT-02b phase 1 calculated compensation flow for steam generator and decay heat removal system heat exchanger level equalization

{{

}}^{2(a),(b),(c),ECI}

Figure 5-62a NLT-02b phase 1 integrated compensation flow for SG and DHRS HX level equalization

{{

}}^{2(a),(b),(c),ECI}

Figure 5-63 NLT-02b phase 1 transient steam generator level comparison

{{

}}2(a),(b),(c),ECI

Figure 5-64 NLT-02b phase 1 transient decay heat removal system heat exchanger level comparison

{{

}}2(a),(b),(c),ECI

Figure 5-65 NLT-02b phase 1 transient decay heat removal system condensate temperature comparison

{{

}}^{2(a),(b),(c),ECI}

Figure 5-66 NLT-02b phase 1 transient decay heat removal system condensate flow comparison

{{

}}^{2(a),(b),(c),ECI}

Figure 5-67 NLT-02b phase 1 transient steam generator outlet temperature comparison

{{

}}^{2(a),(b),(c),ECI}

Figure 5-68 NLT-02b phase 1 transient cooling pool vessel level comparison

{{

}}^{2(a),(b),(c),ECI}

Figure 5-69 NLT-02b phase 1 transient cooling pool vessel region 4 temperature comparison (below decay heat removal system heat exchanger)

{{

}}^{2(a),(b),(c),ECI}

Figure 5-69a NLT-02b phase 1 transient cooling pool vessel region 5 temperature comparison
(near bottom of decay heat removal system heat exchanger)

{{

}}^{2(a),(b),(c),ECI}

Figure 5-69b NLT-02b phase 1 transient cooling pool vessel region 6 temperature comparison
(near mid-point of decay heat removal system heat exchanger)

{{

}}^{2(a),(b),(c),ECI}

Figure 5-70 NLT-02b phase 1 transient cooling pool vessel region 7 temperature comparison (just above the decay heat removal system heat exchanger tube region)

5.3.3.8 NLT-2b Phase 2 Test Results

Code-to-data comparisons of key parameters for the second phase of the NLT-2b test are shown in Figure 5-71 through Figure 5-88. Note that in figures, the data measurement uncertainty is shown in dotted lines. {{

}}^{2(a),(c)}

In general, the NRELAP5 simulation showed reasonable to excellent agreement with the measured data for this time period, except for the CPV temperatures adjacent to and above the DHRS heat exchanger. {{

}}^{2(a),(c)}

It is noted that in the simulation, the fluid temperatures at and above the DHRS heat exchanger in the CPV warm up to saturation. {{

}}^{2(a),(c)}

Figure 5-71 shows the core power comparison. The core power from the test was input directly into NRELAP5.

Figure 5-72 shows that the PZR pressure {{

}}^{2(a),(c)}

Figure 5-73 shows that the PZR level {{

}}^{2(a),(c)}

Figure 5-75 shows the core inlet and outlet temperature comparisons for phase 2. The agreement is reasonable to excellent. This indicates that the total energy added to the RPV fluid is reasonably calculated by the model. The reasonably predicted temperature indicates the RPV fluid volume change due to density change should also be reasonably predicted.

As discussed in Section 5.3.3.7 for Phase 1, the RPV loop flow rate is not compared.

Figure 5-77 compares the SG pressure data to the NRELAP5 prediction. The SG pressure {{

}}^{2(a),(c)}

Comparisons of the SG power and the DHRS HX thermal power are shown on Figure 5-78 and Figure 5-79, respectively. The thermal powers for both SG and DHRS track the data reasonably well {{

}}^{2(a),(c)}

The SG level (Figure 5-80) and DHRS heat exchanger level (Figure 5-85) compare reasonably well to the data. {{

}}^{2(a),(c)}

The DHRS condensate temperature (Figure 5-82) follows the same trends as the data, but similar to phase 1 the code prediction is about 50°F higher than the data.

Figure 5-83 compares the DHRS condensate flow. The DHRS flow {{

}}^{2(a),(c)}

The SG tube exit temperatures are compared in Figure 5-84. Similar to phase 1, {{
}}^{2(a),(c)} For reference, the fluid temperature in the steam bustle is also shown in the figure. The steam temperature increases with core power

{{
}}^{2(a),(c)}

Figure 5-86 compares the measured and calculated CPV liquid level. The comparison shows reasonable agreement when recognizing that the NRELAP5 level increase is due to thermal expansion, where the NRELAP5 liquid temperatures in the upper CPV reach saturation temperature, well above the data temperature (Figure 5-88). The CPV fluid temperatures were reset at the start of the restart run to match the data after stirring the CPV, hence the good level match at the start of phase 2 (Figure 5-87, Figure 5-87a, Figure 5-87b, and Figure 5-88). {{

{{
}}^{2(a),(c)}

}}^{2(a),(b),(c),ECI}

Figure 5-71 NLT-02b phase 2 transient core power comparison

{{

}}^{2(a),(b),(c),ECI}

Figure 5-72 NLT-02b phase 2 transient pressurizer pressure comparison

{{

}}^{2(a),(b),(c),ECI}

Figure 5-73 NLT-02b phase 2 transient pressurizer level comparison

Figure 5-74 Not Used

{{

}}^{2(a),(b),(c),ECI}

Figure 5-75 NLT-02b phase 2 transient core inlet and outlet temperature comparison

Figure 5-76 Not Used

{{

}}^{2(a),(b),(c),ECI}

Figure 5-77 NLT-02b phase 2 transient steam generator steam pressure comparison

{{

}}^{2(a),(b),(c),ECI}

Figure 5-78 NLT-02b phase 2 transient steam generator thermal power comparison

{{

}}^{2(a),(b),(c),ECI}

Figure 5-79 NLT-02b phase 2 transient decay heat removal system heat exchanger thermal power comparison

{{

}}^{2(a),(b),(c),ECI}

Figure 5-80 NLT-02b phase 2 transient steam generator level comparison

{{

}}^{2(a),(b),(c),ECI}

Figure 5-81 NLT-02b phase 2 calculated compensation flow for steam generator and decay heat removal system heat exchanger level equalization

{{

}}^{2(a),(b),(c),ECI}

Figure 5-81a NLT-02b phase 2 integrated compensation flow for SG and DHRS HX level equalization

{{

}}^{2(a),(b),(c),ECI}

Figure 5-82 NLT-02b phase 2 transient decay heat removal system condensate temperature comparison

{{

}}^{2(a),(b),(c),ECI}

Figure 5-83 NLT-02b phase 2 transient decay heat removal system condensate flow comparison

{{

}}^{2(a),(b),(c),ECI}

Figure 5-84 NLT-02b phase 2 transient steam generator outlet temperature comparison

{{

}}^{2(a),(b),(c),ECI}

Figure 5-85 NLT-02b phase 2 transient decay heat removal system heat exchanger level comparison

{{

}}^{2(a),(b),(c),ECI}

Figure 5-86 NLT-02b phase 2 transient cooling pool vessel level comparison

{{

}}^{2(a),(b),(c),ECI}

Figure 5-87 NLT-02b phase 2 transient cooling pool vessel region 4 temperature comparison (below decay heat removal system heat exchanger)

{{

}}^{2(a),(b),(c),ECI}

Figure 5-87a NLT-02b phase 2 transient cooling pool vessel region 5 temperature comparison
(near bottom of decay heat removal system heat exchanger)

{{

}}^{2(a),(b),(c),ECI}

Figure 5-87b NLT-02b phase 2 transient cooling pool vessel region 6 temperature comparison
(near mid-point of decay heat removal system heat exchanger)

{{

}}^{2(a),(b),(c),ECI}

Figure 5-88 NLT-02b phase 2 transient cooling pool vessel region 7 temperature comparison (just above the decay heat removal system heat exchanger tube region)

5.3.3.9 NLT-2b Phase 3 Test Results

Code-to-data comparisons of key parameters for the third phase of the NLT-2b test are shown in Figure 5-89 through Figure 5-106. Note that in figures, the data measurement uncertainty is shown in dotted lines.

{{

}}^{2(a),(c)}

{{

}}^{2(a),(c)}

In general, the NRELAP5 simulation showed reasonable to excellent agreement with the measured data for this time period.

A comparison of the SG and DHRS heat exchanger tube levels are shown in Figure 5-98 and Figure 5-103, respectively. The SG level calculated response exhibits excellent agreement with the measured data, and the calculated DHRS HX tube level shows reasonable agreement. During this phase, as seen in Figure 5-99, {{

}}^{2(a),(c)} Figure 5-99a shows that there is {{

}}^{2(a),(c)}

Figure 5-96 and Figure 5-97 compare the heat removal in the SG and DHRS heat exchanger tubes, respectively. {{

}}^{2(a),(c)} Figure 5-95 shows that the SG pressure is reasonably predicted in this phase.

The PZR pressure is compared in Figure 5-90. {{

}}^{2(a),(c)}

The calculated PZR level is compared to data in Figure 5-91. {{

}}^{2(a),(c)}

The core inlet and outlet temperatures are compared in Figure 5-93. Reasonable agreement is observed in these figures, {{

}}^{2(a),(c)}

As discussed in Section 5.3.3.7 for Phase 1, the RPV loop flow rate is not compared.

Figure 5-101 compares the measured and calculated DHRS condensate flow. {{

}}^{2(a),(c)}

SG tube exit temperatures are compared in Figure 5-102. The predicted temperature is {{

}}^{2(a),(c)}

The condensate fluid temperature is compared in Figure 5-100. {{

}}^{2(a),(c)}

Figure 5-104 compares the measured and calculated CPV liquid level. The comparison shows reasonable agreement with the data out to the time of the drain and refill of the CPV {{

}}^{2(a),(c)}

{{

}}^{2(a),(b),(c),ECI}

Figure 5-89 NLT-02b phase 3 transient core power comparison

{{

}}^{2(a),(b),(c),ECI}

Figure 5-90 NLT-02b phase 3 transient pressurizer pressure comparison

{{

}}^{2(a),(b),(c),ECI}

Figure 5-91 NLT-02b phase 3 transient pressurizer level comparison

Figure 5-92 Not Used

{{

}}^{2(a),(b),(c),ECI}

Figure 5-93 NLT-02b phase 3 transient core inlet and outlet temperature comparison

Figure 5-94 Not Used

{{

}}^{2(a),(b),(c),ECI}

Figure 5-95 NLT-02b phase 3 transient steam generator steam pressure comparison

{{

}}^{2(a),(b),(c),ECI}

Figure 5-96 NLT-02b phase 3 transient steam generator thermal power comparison

{{

}}^{2(a),(b),(c),ECI}

Figure 5-97 NLT-02b phase 3 transient decay heat removal system heat exchanger thermal power comparison

{{

}}^{2(a),(b),(c),ECI}

Figure 5-98 NLT-02b phase 3 transient steam generator level comparison

{{

}}^{2(a),(b),(c),ECI}

Figure 5-99 NLT-02b phase 3 calculated compensation flow for steam generator and decay heat removal system heat exchanger level equalization

{{

}}^{2(a),(b),(c),ECI}

Figure 5-99a NLT-02b phase 3 integrated compensation flow for SG and DHRS HX level equalization

{{

}}^{2(a),(b),(c),ECI}

Figure 5-100 NLT-02b phase 3 transient decay heat removal system condensate temperature comparison

{{

}}^{2(a),(b),(c),ECI}

Figure 5-101 NLT-02b phase 3 transient decay heat removal system condensate flow comparison

{{

}}^{2(a),(b),(c),ECI}

Figure 5-102 NLT-02b phase 3 transient steam generator outlet temperature comparison

{{

}}^{2(a),(b),(c),ECI}

Figure 5-103 NLT-02b phase 3 transient decay heat removal system heat exchanger level comparison

{{

}}^{2(a),(b),(c),ECI}

Figure 5-104 NLT-02b phase 3 transient cooling pool vessel level comparison

{{

}}^{2(a),(b),(c),ECI}

Figure 5-105 NLT-02b phase 3 transient cooling pool vessel region 4 temperature comparison
(below decay heat removal system heat exchanger)

{{

}}^{2(a),(b),(c),ECI}

Figure 5-105a NLT-02b phase 3 transient cooling pool vessel region 5 temperature comparison
(near bottom of decay heat removal system heat exchanger)

{{

}}^{2(a),(b),(c),ECI}

Figure 5-105b NLT-02b phase 3 transient cooling pool vessel region 6 temperature comparison
(near mid-point of decay heat removal system heat exchanger)

{{

}}^{2(a),(b),(c),ECI}

Figure 5-106 NLT-02b phase 3 transient cooling pool vessel region 7 temperature comparison (just above the decay heat removal system heat exchanger tube region)

5.3.3.10 NLT-2b Phase 4 Test Results

Code-to-data comparisons of key parameters for the fourth phase of the NLT-2b test are shown in Figure 5-107 through Figure 5-125. Note that in figures, the data measurement uncertainty is shown in dotted lines.

{{

}}^{2(a),(c)} the fluid volume had shrunk sufficiently to uncover the top of the riser pipe (located at the bottom of the upper plenum). Consistent with the scope of the short-term non-LOCA transient EM, the results presented here focus on the time after the decay heat mode was actuated until top of the riser uncovered.

The simulation gave reasonable results for this phase out to the point of riser uncover.

Measured and calculated core heater rod power is compared in Figure 5-107. The core heater rod power is a boundary condition in the simulation.

Energy continued to be removed through the SG tube coil {{
 }}^{2(a),(c)} The energy removal resulted in a cooldown of
 the primary system. The cooldown caused a shrinkage of the RPV fluid volume and
 corresponding decrease in RPV pressure (Figure 5-108). The level in the PZR declined
 due to the system cooldown as shown in Figure 5-109. The rate of PZR level decline in
 the calculation is in reasonable agreement with the measured data. {{

}}^{2(a),(c)}

As discussed in Section 5.3.3.7 for Phase 1, the RPV loop flow rate is not compared.

A comparison of the measured and calculated upper plenum fluid temperature and the
 core inlet and outlet temperatures are provided in Figure 5-111 and Figure 5-112,
 respectively. {{

}}^{2(a),(c)}

The SG pressure is compared in Figure 5-114. {{

}}^{2(a),(c)}

Figure 5-115 and Figure 5-116 show that both the SG and DHRS power {{

}}^{2(a),(c)}

Figure 5-118 and Figure 5-118a show {{

}}^{2(a),(c)}

Figure 5-117 and Figure 5-122 show comparisons on the SG tube level and DHRS HX
 tube level, respectively. {{

}}^{2(a),(c)}

Figure 5-119 compares the measured and calculated DHRS condensate temperature.
 {{

}}^{2(a),(c)}

A comparison of the SG outlet temperature is provided in Figure 5-121. The calculated
 outlet temperature shows {{

}}^{2(a),(c)}

The measured and calculated CPV level comparison is shown in Figure 5-123. After the drain and fill process, {{ }}^{2(a),(c)}, the calculated level shows reasonable agreement with the data.

Measured and calculated CPV fluid temperatures within the elevation of the DHRS heat exchanger are shown in Figure 5-124, Figure 5-124a, Figure 5-124b, and Figure 5-125. {{

}}^{2(a),(c)}

{{

}}^{2(a),(b),(c),ECI}

Figure 5-107 NLT-02b phase 4 transient core power comparison

{{

}}^{2(a),(b),(c),ECI}

Figure 5-108 NLT-02b phase 4 transient pressurizer pressure comparison

{{

}}^{2(a),(b),(c),ECI}

Figure 5-109 NLT-02b phase 4 transient pressurizer level comparison

{{

}}^{2(a),(b),(c),ECI}

Figure 5-110 NLT-02b phase 4 transient reactor pressure vessel level

{{

}}^{2(a),(b),(c),ECI}

Figure 5-111 NLT-02b phase 4 transient reactor pressure vessel upper plenum temperature comparison

{{

}}^{2(a),(b),(c),ECI}

Figure 5-112 NLT-02b phase 4 transient core inlet and outlet temperature comparison

Figure 5-113 Not Used

{{

}}^{2(a),(b),(c),ECI}

Figure 5-114 NLT-02b phase 4 transient steam generator steam pressure comparison

{{

}}^{2(a),(b),(c),ECI}

Figure 5-115 NLT-02b phase 4 transient steam generator thermal power comparison

{{

}}^{2(a),(b),(c),ECI}

Figure 5-116 NLT-02b phase 4 transient decay heat removal system heat exchanger thermal power comparison

{{

}}^{2(a),(b),(c),ECI}

Figure 5-117 NLT-02b phase 4 transient steam generator level comparison
{{

}}^{2(a),(b),(c),ECI}

Figure 5-118 NLT-02b phase 4 calculated compensation flow for steam generator and decay
heat removal system heat exchanger level equalization

{{

}}^{2(a),(b),(c),ECI}

Figure 5-118a NLT-02b phase 4 integrated compensation flow for SG and DHRS HX level equalization

{{

}}^{2(a),(b),(c),ECI}

Figure 5-119 NLT-02b phase 4 transient decay heat removal system condensate temperature comparison

{{

}}^{2(a),(b),(c),ECI}

Figure 5-120 NLT-02b phase 4 transient decay heat removal system condensate flow comparison

{{

}}^{2(a),(b),(c),ECI}

Figure 5-121 NLT-02b phase 4 transient steam generator outlet temperature comparison

{{

}}^{2(a),(b),(c),ECI}

Figure 5-122 NLT-02b phase 4 transient decay heat removal system heat exchanger level comparison

{{

}}^{2(a),(b),(c),ECI}

Figure 5-123 NLT-02b phase 4 transient cooling pool vessel level comparison

{{

}}^{2(a),(b),(c),ECI}

Figure 5-124 NLT-02b phase 4 transient cooling pool vessel region 4 temperature comparison
(below decay heat removal system heat exchanger)

{{

}}^{2(a),(b),(c),ECI}

Figure 5-124a NLT-02b phase 4 transient cooling pool vessel region 5 temperature comparison
(near bottom of decay heat removal system heat exchanger)

{{

}}^{2(a),(b),(c),ECI}

Figure 5-124b NLT-02b phase 4 transient cooling pool vessel region 6 temperature comparison
(near mid-point of decay heat removal system heat exchanger)

{{

}}^{2(a),(b),(c),ECI}

Figure 5-125 NLT-02b phase 4 transient cooling pool vessel region 7 temperature comparison
(just above the decay heat removal system heat exchanger tube region)

5.3.3.11 NLT-2 Summary

The comparisons between the NIST-1 NLT-2a integral experimental data and the code calculated values showed that NRELAP5 has the capability to accurately predict primary heat up and pressurization due to a loss of feedwater.

NLT-02b is a transient test with quasi-steady core heater rod power during an extended DHRS recirculation mode and with core heater rod decay power during a DHRS-driven decay power mode. During the DHRS recirculation mode, the transient response of pressure, level, and temperature in both the RPV and the DHRS were predicted by NRELAP5 with reasonable agreement.

NRELAP5 assessment of the NLT-2b phases 1 through 4 demonstrates the ability of the code to predict the heat transfer from primary side to the SG and from the DHRS to CPV. After completion of core power maneuvering and after full start of the DHRS loop, NRELAP5 calculated pressurizer pressure, core inlet and outlet temperature, primary flow rate, SG pressure, energy transfer from the primary to secondary, energy transfer from DHRS to CPV, SG level, DHRS level, and CPV level results are all within reasonable to excellent agreement.

The pressurizer level for NLT-2b phase 1 was {{

}}^{2(a),(b),(c)} However, even with these discrepancies, the results show that the important parameters of total energy transfer from the primary side to the SG and from the DHRS to CPV are well predicted.

For NLT-2b phases 1 through 4, the calculated condensate line temperature is in minimal agreement with data, with the temperature being over predicted by NRELAP5. However, even with the discrepancy, the important parameter of heat transfer from primary side to the SG and from the DHRS to CPV are well predicted.

For NLT-2b phases 1 through 4, the CPV fluid heat-up profiles were not fully captured in the NRELAP5 simulations. {{

}}^{2(a),(c)}

For NLT-2b phases 1 through 4, code-to-data comparisons show converged reasonable agreement of DHRS heat removal rate, which is considered to be the most important parameter in this assessment, demonstrating that NRELAP5 is capable of capturing total energy removal rate of the DHRS to the cooling pool.

5.3.3.12 NLT-15-p2 Test Description

The objective of the NLT-15-p2 test was to measure the scaled integral system response to a decrease in heat removal from the secondary side following a loss of feedwater event,

followed by core decay heat removal via the DRHS. During the test, {{

}}^{2(a),(c)}

The sequence of events for the NLT-15p2 test is shown in Table 5-14

Table 5-14 NLT-15p2 sequence of events

{{

}}^{2(a),(c)}

5.3.3.13 NLT-15 p2 Test Results

{{

}}^{2(a),(c)}

Comparison of NRELAP5 calculated parameters to the measured data are presented below. Note that in the figures, the data uncertainty is shown in dot-dashed lines. A comparison of the primary side behavior is discussed first. This is followed by a discussion of the startup of the DHRS (first 500 seconds). A comparison of the secondary side is then presented, and finally, a discussion of the CPV behavior concludes this section.

Primary side response

Figure 5-126 shows the core heater rod power. As expected, the predicted power is an overlay of the measured power since core power is a boundary condition for the simulation.

Pressurizer pressure for short term is shown in Figure 5-127. {{

}}^{2(a),(c)} The calculated pressure in the short term, compared to the measured data, is considered reasonable.

The long term pressurizer pressure comparison is shown in Figure 5-128. {{

}}^{2(a),(c)}

{{

}}^{2(a),(c)} Long term, the pressurizer level response shows excellent agreement with the measured data.

Once DHRS loop flow is established, heat removal through the steam generator tube coil cools the RPV fluid. The liquid volume in the primary loop shrinks as the RPV system cools. After the pressurizer empties, a decline in the RPV level below the pressurizer baffle plate continues as shown in Figure 5-130. This figure compares the calculated and measured RPV level. As observed, the NRELAP5 comparison of the RPV level shows excellent agreement with the measured data, and thus gives credence that NRELAP5 correctly calculates the change in volume due to fluid cooldown. {{

}}^{2(a),(c)}

The RPV riser flow rate {{

}}^{2(a),(c)}

Figure 5-132 through Figure 5-134 compare calculated RPV loop temperatures to the measured data for the core inlet, the riser inlet, and the upper plenum. Reasonable to excellent agreement is observed in the fluid temperatures. {{

}}^{2(a),(c)}

DHRS Startup

The sequence of events shows {{

}}^{2(a),(c)}

{{

}}^{2(a),(c)}

The measured DHRS HX level is shown in Figure 5-138. {{

}}^{2(a),(c)}

{{

NRELAP5 is judged to be reasonable. $\}}^{2(a),(c)}$ the response of

DHRS and Steam Generator Long Term Behavior

A comparison of the short term and long term steam line pressure response is given in Figure 5-135 and in Figure 5-139, respectively. {{

$\}}^{2(a),(c)}$

The comparison of the DHRS HX inlet and outlet temperatures are shown in Figure 5-140 and Figure 5-141, respectively. {{

$\}}^{2(a),(c)}$ The overall response of the predicted inlet temperature is deemed reasonable.

The DHRS HX outlet temperature shown in Figure 5-141 {{

$\}}^{2(a),(c)}$

Figure 5-142 and Figure 5-143 compares the short term and long term DHRS loop mass flow rate, respectively. {{

$\}}^{2(a),(c)}$

{{ }}^{2(a),(c)} Overall, the predicted DHRS flow rate follows the trends of the data and is deemed reasonable.

Comparisons of the level in the DHRS HX and in the steam generator tube coil are shown in Figure 5-144 and Figure 5-145. In general, the predicted DHRS HX level compares reasonably with the measured data. {{

{{ }}^{2(a),(c)} NRELAP5 shows reasonable agreement with the data trends.

Differential pressure comparisons across the condensate line and across the DHRS steam line are given in Figure 5-147 and Figure 5-148. {{

{{ }}^{2(a),(c)}

{{

{{ }}^{2(a),(c)}

{{

}}^{2(a),(c)} The calculation of the heat removal through the steam generator tube coil is deemed reasonable.

Figure 5-150 compares the measured heat removal rate through the DHRS HX tubes with the predicted results. {{

}}^{2(a),(c)} Again, overall, the trend of the data is represented and is deemed reasonable.

CPV Behavior

A comparison of the CPV liquid level and the liquid temperatures are provided here.

Figure 5-151 compares the measured CPV level with the calculated level. {{

}}^{2(a),(c)} The prediction of the CPV level is deemed reasonable.

Figure 5-152 through Figure 5-157 compares the measured and calculated CPV fluid temperature throughout the CPV. {{

}}^{2(a),(c)}

{{

}}^{2(a),(b),(c),ECI}

Figure 5-126 NLT-15p2, transient core power

{{

}}^{2(a),(b),(c),ECI}

Figure 5-127 NLT-15p2, transient RPV pressure short term

{{

}}^{2(a),(b),(c),ECI}

Figure 5-128 NLT-15p2, transient RPV pressure

{{

}}^{2(a),(b),(c),ECI}

Figure 5-129 NLT-15p2, transient pressurizer level

{{

}}^{2(a),(b),(c),ECI}

Figure 5-130 NLT-15p2, transient RPV level

{{

}}^{2(a),(b),(c),ECI}

Figure 5-131 NLT-15p2, transient riser mass flow rate.png

{{

}}^{2(a),(b),(c),ECI}

Figure 5-132 NLT-15p2, transient core inlet temperature

{{

}}^{2(a),(b),(c),ECI}

Figure 5-133 NLT-15p2, transient riser inlet temperature

{{

}}^{2(a),(b),(c),ECI}

Figure 5-134 NLT-15p2, transient upper plenum temperature

{{

}}^{2(a),(b),(c),ECI}

Figure 5-135 NLT-15p2, transient secondary side pressure - 0 to 500 seconds

{{

}}^{2(a),(b),(c),ECI}

Figure 5-136 NLT-15p2, transient DHRS loop flow - 0 to 500 seconds

{{

}}^{2(a),(b),(c),ECI}

Figure 5-137 NLT-15p2, transient measured steam line temperatures - 0 to 500 seconds

{{

}}^{2(a),(b),(c),ECI}

Figure 5-138 NLT-15p2, transient DHRS HX level - 0 to 500 seconds

{{

}}^{2(a),(b),(c),ECI}

Figure 5-139 NLT-15p2, transient secondary side pressure

{{

}}^{2(a),(b),(c),ECI}

Figure 5-140 NLT-15p2, transient DHRS HX inlet temperature

{{

}}^{2(a),(b),(c),ECI}

Figure 5-141 NLT-15p2, transient DHRS HX outlet temperature

{{

}}^{2(a),(b),(c),ECI}

Figure 5-142 NLT-15p2, transient DHRS loop flow - short term

{{

}}^{2(a),(b),(c),ECI}

Figure 5-143 NLT-15p2, transient DHRS loop flow rate - long term

{{

}}^{2(a),(b),(c),ECI}

Figure 5-144 NLT-15p2, transient DHRS HX level

{{

}}^{2(a),(b),(c),ECI}

Figure 5-145 NLT-15p2, transient steam generator tube coil level - long term

{{

}}^{2(a),(b),(c),ECI}

Figure 5-146 NLT-15p2, transient steam generator tube coil level - short term

{{

}}^{2(a),(b),(c),ECI}

Figure 5-147 NLT-15p2, transient DHRS condensate line differential pressure

{{

}}^{2(a),(b),(c),ECI}

Figure 5-148 NLT-15p2, transient DHRS steam line differential pressure

{{

}}^{2(a),(b),(c),ECI}

Figure 5-149 NLT-15p2, transient steam generator tube coil power removal

{{

}}^{2(a),(b),(c),ECI}

Figure 5-150 NLT-15p2, transient DHRS power removal

{{

}}^{2(a),(b),(c),ECI}

Figure 5-151 NLT-15p2, transient cooling pool vessel level

{{

}}^{2(a),(b),(c),ECI}

Figure 5-152 NLT-15p2, transient cooling pool vessel fluid temperature at level 3 (below decay heat removal heat exchanger)

{{

}}^{2(a),(b),(c),ECI}

Figure 5-153 NLT-15p2, transient cooling pool vessel fluid temperature at level 5 (near bottom of DHRS heat exchanger)

{{

}}^{2(a),(b),(c),ECI}

Figure 5-154 NLT-15p2, transient cooling pool vessel fluid temperature at level 6 (near midpoint of DHRS heat exchanger)

{{

}}^{2(a),(b),(c),ECI}

Figure 5-155 NLT-15p2, transient cooling pool vessel fluid temperature at level 7 (top to just above DHRS heat exchanger region)

{{

}}^{2(a),(b),(c),ECI}

Figure 5-156 NLT-15p2, transient cooling pool vessel fluid temperature at level 8 (above DHRS heat exchanger region)

{{

}}^{2(a),(b),(c),ECI}

Figure 5-157 NLT-15p2, transient cooling pool vessel fluid temperature at level 9 (above DHRS heat exchanger region)

5.3.3.14 NLT-15p2 Summary

Test NLT-15p2 is a loss of feedwater scenario followed by core decay heat removal via the DHRS system. {{

}}^{2(a),(c)}

The NRELAP5 simulation of this test showed reasonable to excellent agreement with the initial pressure and loop temperature response in the RPV. After isolation of the secondary side and during the initial stages of DHRS heat removal operation, the RPV pressure rose due to heat addition from the core decay power and lack of complete removal through the steam generator tube coil. A rise in the pressurizer liquid level was also observed. Both the rise in the RPV pressure and the rise in the pressurizer level were well predicted by NRELAP5.

After DHRS heat removal flow was established, the RPV pressure turned over and declined throughout the remainder of the test. NRELAP5 also predicted this pressure behavior in general.

Both the pressurizer level response and the RPV level response showed excellent agreement with the measured response, thus showing that NRELAP5 can accurately predict change in fluid volume due to cooldown.

The predicted RPV loop temperatures showed reasonable to excellent agreement with the measured data demonstrating that heat removal through the steam generator tube coil was reasonably predicted.

Prediction of the secondary side behavior showed reasonable agreement with the measured data. All major trends of the data were modeled correctly by NRELAP5. {{

}}^{2(a),(c)} However,

NRELAP5 reasonably calculated the trends of the data.

{{

}}^{2(a),(c)}

The calculated fluid temperature inside the DHRS heat exchanger tubes generally predicted the trends of the measured data. {{

}}^{2(a),(c)}

The calculated differential pressure in the DHRS condensate line and steam line {{

}}^{2(a),(c)}

Overall, NRELAP5 is capable of producing reasonable results in simulating events such as those observed in the NLT-15p2 test.

5.3.4 Code to Code Benchmark for Integral Assessment of Reactivity Event Response

5.3.4.1 Background

The NRELAP5 code is used in the non-LOCA evaluation model to perform non-LOCA system transient analysis for the NPM. A series of code-to-code benchmarking comparison calculations was performed with the RETRAN-3D code to validate the performance of NRELAP5's point kinetics model during the reactivity transient events and to supplement the validation of the integral primary system thermal-hydraulic response to reactivity transients.

RETRAN-3D was developed to perform transient thermal-hydraulic analysis of light water reactors. RETRAN-3D was developed as an evolution to the RETRAN codes that have been sponsored by EPRI since 1975 and used for licensing basis analyses of commercial light water reactors in the U.S.

The RETRAN-3D code is based on the one-dimensional homogeneous equilibrium model, in comparison to the two-fluid, non-equilibrium non-homogeneous fluid model utilized in the NRELAP5 code.

The NRC has reviewed RETRAN-3D and issued a Safety Evaluation Report indicating that RETRAN-3D is an acceptable tool for performing PWR licensing analyses for a series of categories of anticipated transients, infrequent incidents and accident analyses for PWRs, including the reactivity transient events (Reference 12). Compared to operating PWRs, the NPM natural circulation primary system flow and helical coil SG design are unique features. For NRELAP5, a new helical coil SG component was added to the NRELAP5 code as described in Reference 2; primary and secondary side fluid flow and heat transfer over the SG were validated against testing performed at the SIET-TF1 and SIET-TF2 facilities, as described in Section 5.3.5. RETRAN-3D does not include specific models for helical coil SG heat transfer and wall friction; as described in Section 5.3.4.2,

for the purposes of the benchmark calculations, a modeling simplification was made such that the RETRAN-3D and NRELAP5 primary side heat transfer coefficients were consistent under steady state conditions. Therefore, the scope of the benchmark calculation is focused on the reactivity response and the integral primary side response during a reactivity transient.

The scope of the code-to-code benchmarking includes comparisons of reactor power, reactivity, primary side flow, pressure and temperatures for a set of benchmarking reactivity transients. These stylized benchmark cases are designed so as to be representative of the NuScale reactivity transients, but simplified to minimize impact of model differences in the secondary side or control system responses that are not the focus of the benchmark comparisons.

5.3.4.2 Approach for RETRAN-3D Benchmark

To perform the code-to-code benchmark calculations, the NPM was modeled using both NRELAP5 and RETRAN-3D. The NRELAP5 base model used for code-to-code benchmarking is the same as for the non-LOCA transient analysis, as described in Section 6.0 of this report.

The RETRAN-3D base model was developed based on the NRELAP5 base model. The NRELAP5 model provided the geometric information, trips, control systems and reactor kinetics to convert to RETRAN-3D input cards.

The NRELAP5 model volume, junction and heat conductor (heat structure) input were used as the initial basis for the RETRAN-3D model input and nodalization. {{

}}^{2(a),(c)}

For NRELAP5, a new helical coil SG component was added to the NRELAP5 code as described in Reference 2 to model the helical coil SG heat transfer and wall friction in the NPM design. In RETRAN-3D there is no helical coil model, {{

}}^{2(a),(c)}

Differences in the predicted pressurizer pressure and level were observed in the benchmark calculation results due to differences between the pressurizer modeling in the NRELAP5 and RETRAN-3D calculations. {{
}}^{2(a),(c)}

{{

}}^{2(a),(c)} The RETRAN-3D thermal-hydraulics computer code used in this study, the version with a safety evaluation report (SER) from the NRC, uses a basic three-equation homogeneous equilibrium model. When two-phase, the constraint on this representation is equilibrium (saturation) between the phases of water. When fluid surges into or out of the pressurizer, steam can be compressed or water can flash, which is why RETRAN-3D has a two-region non-equilibrium pressurizer model that allows non-equilibrium between the phases of water.

RETRAN-3D also includes a volume change term in the phasic energy equations for the two-region component. The RETRAN-3D two region model allows the user limited control at the interface. Additional interfacial modeling is available in RETRAN-3D when using the sub-node option in the code. Comparisons between the NRELAP5 code and two region models (Reference 13, for example) can show larger pressures in a two-region component than in NRELAP5 for in-surge transients. This is due to some degree because of work terms for volume change and using enthalpy in the formulation. RETRAN-3D uses enthalpy at the junctions for the energy equations whereas NRELAP5 uses internal energy. Enthalpy contains internal energy in addition to the flow work term, which NRELAP5 does not include in its formulation, except for special application models for blow down.

There are also differences in pressurizer spray, the letdown and charging models, along with insurge for the two codes. Contrary to the NRELAP5 model that uses a standard junction to model spray, the RETRAN-3D model uses a special spray junction in the pressurizer spray system that condenses sufficient steam from the vapor region to bring the spray flow to saturation. This involves removal of mass and energy from the vapor region of the pressurizer and depositing the mass of the spray and condensed vapor directly into the liquid region of the pressurizer without a time delay, which leads to higher pressurizer pressure.

After the RETRAN-3D base deck was developed, a steady-state calculation was performed where adequately consistent results between the two code calculations were obtained. Then, four transient calculations were performed. These stylized transients were selected to cover a range of reactivity insertion rates and RCS response that are observed in the NPM reactivity event calculations. The calculations performed were:

1. Uncontrolled rod withdrawal from full power steady-state, using a higher reactivity insertion rate to result in a high power MPS actuation signal (fast uncontrolled rod withdrawal [UCRW]).
2. Uncontrolled rod withdrawal from full power steady-state, using a lower reactivity insertion rate to result in a high pressurizer pressure MPS actuation signal (slow UCRW).
3. Power reduction from full power to 50 percent of rated power.
4. Dropped control rod assembly from 50 percent rated power steady state conditions, using a dropped rod worth that is relatively large, but insufficient to cause reactor trip.

{{

}}^{2(a),(c)}

For the reactivity transients, the focus of the benchmark comparison is on the primary side response before scram, driven by the reactivity insertion and power change, and the short term responses after scram, driven by the scram worth. The longer term and secondary side response is not examined in detail due to the simplified modeling of the helical coil SG in the RETRAN-3D model, and the high pressure condensation conditions after DHRS actuation that are not typical of operating pressurized water reactors. Therefore the key parameters of interest for the reactivity benchmarking transients are reactor power, reactivity, pressurizer pressure and level, core flow, and core temperatures. These parameters are plotted and compared for each transient.

When performing code-to-code comparisons, agreement must be assessed in some manner. The method used herein is based on RG 1.203 (Reference 1) as described in Section 5.3. The acceptance criterion applied herein for the benchmarking calculations is that at least “reasonable agreement” must be observed.

5.3.4.3 Fast Uncontrolled Rod Withdrawal from Full Power

In this case, the uncontrolled rod withdrawal occurs at time zero from the full power steady state condition and a high reactivity insertion rate (13.36 pcm/sec) is assumed. This reactivity insertion rate causes a reactor scram on high power. The DHRS is not actuated on high power and therefore normal secondary side cooling continues. The automatic turbine trip following reactor trip is not credited. The steam flow will vary depending on the SG pressure. {{
}}^{2(a),(c)}

Figure 5-158 through Figure 5-164 show excellent agreement between the two models. At the end of the full power steady state initialization, the core flow, inlet temperatures and outlet temperatures are slightly different between the two models. These differences are carried over to the transient, which can be observed at time zero on Figure 5-162 through Figure 5-164. Due to these steady-state differences and their effects to the reactivity feedback, the core power increase rates are slightly different when the UCRW reactivity insertion is modeled. The RETRAN-3D model predicts a slightly earlier time to reach the high core power trip analytical limit (Figure 5-158 and Figure 5-159). The core power and reactivity curves are very close to each other between the two models during the transient. The pressurizer pressure and level match well during the short time after scram, and then the NRELAP5 model predicts a slightly higher pressurizer pressure and level (Figure 5-160 and Figure 5-161).

The core flow and outlet temperature match fairly well between the RETRAN-3D model and the NRELAP5 model, after considering the differences from the steady state condition at the transient initiation (Figure 5-162 and Figure 5-164). The timing of the core inlet

temperature drop is slightly off (Figure 5-163), indicating the heat transfer to the secondary side is slightly different between the two models.

{{

}}^{2(a),(b),(c)}

Figure 5-158 Core power (fast uncontrolled rod withdrawal)

{{

}}^{2(a),(b),(c)}

Figure 5-159 Total reactivity (fast uncontrolled rod withdrawal)

{{

}}^{2(a),(b),(c)}

Figure 5-160 Pressurizer pressure (fast uncontrolled rod withdrawal)

{{

}}^{2(a),(b),(c)}

Figure 5-161 Pressurizer level (fast uncontrolled rod withdrawal)

{{

}}^{2(a),(b),(c)}

Figure 5-162 Core flow (fast uncontrolled rod withdrawal)

{{

}}^{2(a),(b),(c)}

Figure 5-163 Core inlet temperatures (fast uncontrolled rod withdrawal)

{{

}}^{2(a),(b),(c)}

Figure 5-164 Core outlet temperatures (fast uncontrolled rod withdrawal)

5.3.4.4 Slow Uncontrolled Rod Withdrawal from Full Power

In this case, the uncontrolled rod withdrawal occurs at time zero from the full power steady state condition, and a lower reactivity insertion rate (5.344 pcm/sec) is assumed. This reactivity insertion results in RCS heatup and reactor scram from a high RCS pressure rather than a high power condition. During the slow UCRW transient, upon reactor trip on high RCS pressure, DHRS is actuated and therefore normal steam flow and feedwater flow are isolated.

In addition to the reduced reactivity insertion rate, pressurizer spray and CVCS were isolated on transient initiation to maximize the pressurization rate. The UCRW reactivity insertion is initiated at time zero.

Figure 5-165 through Figure 5-171 show reasonable to excellent agreement between the two codes. As explained in Section 5.3.4.3, at the end of the full power steady state initialization, the core flow, inlet and outlet temperatures are slightly different between the two models. These differences are carried over to the transient, which can be observed at time zero on Figure 5-169 through Figure 5-171. Due to these steady-state differences and their effects to the reactivity feedback, the rates of core power increase are slightly different when the UCRW reactivity insertion is modeled. The RETRAN-3D model predicts a slightly faster power increase rate than NRELAP5 (Figure 5-165). Due to the faster power increase and different pressurizer models (see discussion in Section 5.3.4.2), RETRAN-3D predicts higher increase rates on the pressurizer pressure and level after transient initiation (Figure 5-167 and Figure 5-168), and therefore a slightly earlier timing of the reactor trip on high pressurizer pressure.

Following the reactor scram, the core power and reactivity curves are very close to each other between the two models during the transient (Figure 5-165 and Figure 5-166). Pressurizer pressure and level continue to increase and reach their peak values before decreasing. NRELAP5 predicts a slightly higher peak pressurizer pressure and level (Figure 5-167 and Figure 5-168). As the pressure and level decrease, RETRAN-3D has a faster initial depressurization resulting in a lower pressurizer pressure. Then the relative rate of decrease changes and the RETRAN-3D pressure is higher than the NRELAP5 pressure. {{

}}^{2(a),(b),(c)} The pressurizer levels predicted by the two codes show similar behavior. The discrepancy is attributed to different heat removal rates from the pressurizer between the NRELAP5 and RETRAN-3D pressurizer models, due to differences in the pressurizer modeling as discussed in Section 5.3.4.2.

The core flow and outlet temperature match fairly well between the RETRAN-3D model and the NRELAP5 model, after considering the differences from the steady state condition at the transient initiation (Figure 5-169 and Figure 5-171). The core inlet temperatures shown the same trend and the biggest difference is approximately 2 percent (Figure 5-170). The core inlet temperature difference could be attributed to the core flow differences.

{{

}}^{2(a),(b),(c)}

Figure 5-165 Core power (slow uncontrolled rod withdrawal)

{{

}}^{2(a),(b),(c)}

Figure 5-166 Total reactivity (slow uncontrolled rod withdrawal)

{{

Figure 5-167 Pressurizer pressure (slow uncontrolled rod withdrawal) ^{2(a),(b),(c)}

{{

^{2(a),(b),(c)}

Figure 5-168 Pressurizer level (slow uncontrolled rod withdrawal)

{{

Figure 5-169 Core flow (slow uncontrolled rod withdrawal)

}}^{2(a),(b),(c)}

{{

Figure 5-170 Core inlet temperature (slow uncontrolled rod withdrawal)

}}^{2(a),(b),(c)}

{{

}}^{2(a),(b),(c)}

Figure 5-171 Core outlet temperature (slow uncontrolled rod withdrawal)

5.3.4.5 Power Reduction

In this case, the benchmark calculations start at full power conditions, followed by a reduction to 50 percent power {{

}}^{2(a),(c)} It is noted that the dropped rod transient benchmark calculation (Section 5.3.4.6) is then performed as a continuation from the 50 percent power steady state condition.

{{

}}^{2(a),(b)}

Figure 5-172 through Figure 5-178 show reasonable to excellent agreement between the two codes. The core power and reactivity curves are almost identical (Figure 5-172 and Figure 5-173).

At the time of the power reduction, the RETRAN-3D pressurizer level drops below the pressurizer level of NRELAP5. {{

}}^{2(a),(c),(b)}
During the power reduction, the RETRAN-3D predicted pressurizer pressure is higher than NRELAP5. The biggest difference of approximately 3.5 percent is attributed to different heat removal rates from the pressurizer between the NRELAP5 and RETRAN-3D pressurizer models, due to differences in the pressurizer modeling as discussed in Section 5.3.4.2.

As explained in Section 5.3.4.3, at the end of the full power steady state initialization, the core flow, core inlet and core outlet temperatures are slightly different between the two models. These differences are carried over to the transient calculation, which can be observed at time zero on Figure 5-176 through Figure 5-178. During the transient power reduction, the core flow, core inlet and core outlet temperatures have a consistent small difference between the RETRAN-3D and NRELAP5 predictions.

{{

}}^{2(a),(b),(c)}

Figure 5-172 Core power (power reduction)

{{

{{

Figure 5-173 Total reactivity (power reduction)

}}^{2(a),(b),(c)}

Figure 5-174 Pressurizer pressure (power reduction)

}}^{2(a),(b),(c)}

{{

}}^{2(a),(b),(c)}

Figure 5-175 Pressurizer level (power reduction)

{{

}}^{2(a),(b),(c)}

Figure 5-176 Core flow (power reduction)

{{

}}^{2(a),(b),(c)}

Figure 5-177 Core inlet temperature (power reduction)

{{

}}^{2(a),(b),(c)}

Figure 5-178 Core outlet temperature (power reduction)

5.3.4.6 Dropped Control Rod

The dropped control rod case is initiated from the 50 percent power steady state condition at time zero. {{

}}^{2(a),(c)}

Figure 5-179 through Figure 5-185 show reasonable to excellent agreement between the two codes. The core power drops from 80 MWth to {{
}}^{2(a),(b),(c)} due to reactivity feedback effects (Figure 5-179 and Figure 5-180). The core power and reactivity curves are very close.

The pressurizer pressure and pressurizer level are close when they decrease following the dropped rod negative reactivity insertion. When the pressurizer pressure and level start to increase following the power recovery, NRELAP5 predicts slightly higher pressure and level compared to RETRAN-3D. {{

}}^{2(a),(b),(c)}

As explained in Section 5.3.4.5, when the transient reaches steady state at the end of the power reduction, the core flow, core inlet and core outlet temperatures are slightly different between the two models. These differences are carried over to the transient calculation, which can be observed at time zero on Figure 5-183 through Figure 5-185. During the transient, the core flow, core inlet and core outlet temperatures have a consistent small difference between the RETRAN-3D and NRELAP5 predictions.

{{

}}^{2(a),(b),(c)}

Figure 5-179 Core power (dropped control rod)

{{

}}^{2(a),(b),(c)}

Figure 5-180 Total reactivity (dropped control rod)

{{

}}^{2(a),(b),(c)}

Figure 5-181 Pressurizer pressure (dropped control rod)

{{

}}^{2(a),(b),(c)}

Figure 5-182 Pressurizer level (dropped control rod)

{{

}}^{2(a),(b),(c)}

Figure 5-183 Core flow (dropped control rod)

{{

}}^{2(a),(b),(c)}

Figure 5-184 Core inlet temperature (dropped control rod)

{

}}^{2(a),(b),(c)}

Figure 5-185 Core outlet temperature (dropped control rod)

5.3.4.7 Conclusions from Benchmark

Four different transients were performed for code-to-code benchmarking between NRELAP5 and RETRAN-3D: Reactivity insertion reflecting a fast UCRW from full power conditions, reactivity insertion reflecting a slow UCRW from full power conditions, negative reactivity insertion to reduce power from 100 percent to 50 percent power, and negative reactivity insertion simulating a dropped rod from 50 percent power. The results from all four of the transients showed that the comparison between the power and the total reactivity were consistently excellent, in that the calculation results of the two codes lined up nearly identically with one another. This is important because the main purpose of the benchmark is to compare the point kinetics model response between NRELAP5 and RETRAN-3D.

There was also an overall pattern in the core inlet and outlet temperatures of a small temperature difference from the steady state conditions that continued throughout the calculation; however, the overall phenomena matched well.

The pressurizer pressure and the pressurizer level were the two characteristics of the system that did not provide as close of a comparison as the other four characteristics, but still reasonably close. The discrepancy is attributed to differences between the NRELAP5 and RETRAN-3D pressurizer models, as discussed in Section 5.3.4.2.

Overall, NRELAP5 and RETRAN-3D have reasonable to excellent agreement on the parameters of interest in the reactivity feedback and primary system response in the benchmark calculations. The power and reactivity responses predicted by the NRELAP5

point kinetics model during the transients show excellent agreement with the RETRAN-3D prediction.

5.3.5 Steam Generator Modeling

5.3.5.1 Background

NuScale's LOCA Topical Report (Reference 2) Section 7.4 discusses the validation of NRELAP5 for helical coil SG (HCSG) modeling. The validation was mainly against SIET TF-1 and TF-2 test data. It was concluded that NRELAP5 showed reasonable to excellent agreement with test data.

The validation is further investigated in this report to ensure the unique characteristics of the non-LOCA transients (comparing to LOCA) are identified and evaluated. Specifically, this investigation ensures the operating ranges expected during the non-LOCA transients are covered by the validated ranges.

5.3.5.2 Helical Coil Steam Generator Modeling

In the LOCA topical report (Reference 2), NRELAP5 shows reasonable to excellent agreement with test data on the HCSG primary and secondary side, based on comparisons against the SIET TF-2 and SIET TF-1 test data.

5.3.5.3 Helical Coil Steam Generator Operating Ranges vs. Validated Ranges

In the LOCA topical report (Reference 2), NRELAP5 shows reasonable to excellent agreement with test data on the helical coil SG secondary side. {{

}}^{2(a),(c)} Further evaluation is provided
herein to ensure NRELAP5 is validated for DHRS operation.

Based on the typical helical coil SG secondary pressure, temperature and flow rate during DHRS operation, {{

}}^{2(a),(b),(c)}

Table 5-15 summarizes the helical coil SG operating range for non-LOCA transients vs. the validated range in NRELAP5. The majority of the helical coil SG secondary side operating range is covered by the validated range of NRELAP5. {{
}}^{2(a),(c)}

{{

}}^{2(a),(c)} Therefore, the operating range of the helical coil SG primary side is sufficiently covered by the validated range of NRELAP5.

Table 5-15 Non-LOCA transients helical coil steam generator operating range vs. NRELAP5 validated range

{{

|
|
|
|
|
|
|
|

}}^{2(a),(b),(c)}

|

5.3.5.4 Helical Coil Steam Generator Nodalization Sensitivity

{{

}}^{2(a),(c)}

Based on these studies, modeling the helical coil SG with {{ }}^{2(a),(c)} nodes is expected to produce reasonably accurate results for the non-LOCA transients. Considering these studies, steam generator modeling requirements are summarized in Sections 6.1.1 and 6.1.4.2 for the primary and the secondary, respectively.

{{

Figure 5-186 Coil 1 representative pressure drop for {{ }}^{2(a),(c)} nodes (left) and {{ }}^{2(a),(b),(c),ECI} nodes (right)

{{

}}^{2(a),(b),(c),ECI}

Figure 5-187 Coil 1 representative fluid temperature for {{
}}^{2(a),(c)} nodes (right)

}}^{2(a),(c)} nodes (left) and {{

{{

}}^{2(a),(b),(c),ECI}

Figure 5-188 Coil 1 representative wall temperature for {{
}}^{2(a),(c)} nodes (right)

}}^{2(a),(c)} nodes (left) and {{

{{

}}^{2(a),(b),(c)}

Figure 5-189 Decrease in feedwater temperature nodalization sensitivity steam generator secondary side inlet pressure

{{

}}^{2(a),(b),(c)}

Figure 5-190 Decrease in feedwater temperature nodalization sensitivity steam generator secondary side outlet pressure

{{

}}^{2(a),(b),(c)}

Figure 5-191 Decrease in feedwater temperature nodalization sensitivity reactor coolant system flow rate

{{

}}^{2(a),(b),(c)}

Figure 5-192 Decrease in feedwater temperature nodalization sensitivity reactor coolant system lower plenum pressure

{{

}}^{2(a),(b),(c)}

Figure 5-193 Decrease in feedwater temperature nodalization sensitivity reactor coolant system core inlet temperature

{{

}}^{2(a),(b),(c)}

Figure 5-194 Decrease in feedwater temperature nodalization sensitivity reactor power

5.4 Conclusions of NRELAP5 Applicability for Non-LOCA

The high-ranked phenomena identified by the PIRT process for the NPM non-LOCA transients were evaluated with respect to the high-ranked phenomena identified by the PIRT process for the NPM LOCA scenarios, as well as the NRELAP5 assessments performed as part of the NuScale LOCA evaluation model development. A gap analysis was performed to identify high-ranked phenomena for non-LOCA transients that are not assessed as part of the NuScale LOCA evaluation model development.

High-ranked phenomena for non-LOCA events that are not assessed as part of the NuScale LOCA evaluation model development were addressed in different ways:

1. Additional NRELAP5 code assessment performed against separate effects or integral effects test data
2. Code-to-code benchmark performed between NRELAP5 and independent system thermal-hydraulics code
3. Phenomenon is addressed as part of the downstream subchannel analysis
4. Phenomenon is addressed by specifying appropriately conservative input to the system transient analysis

As identified in Table 5 3, in addition to the NRELAP5 assessments performed as part of the LOCA evaluation model development, further assessments were performed to demonstrate NRELAP5 qualification for high rank non-LOCA PIRT phenomena.

Assessment of NRELAP5 against KAIST data demonstrates the code's ability to model heat transfer within tubes and appropriately model the key thermal-hydraulic phenomena associated with condensation within the DHRS heat exchanger tubes.

The comparisons between the NIST-1 HP-03 experimental data and the code calculated values showed that NRELAP5 has the capability to accurately predict the energy transfer across the DHRS heat exchanger tubes to the CPV fluid resulting in reasonable to excellent agreement in capturing cooling pool heat up during these tests in which the cooling pool remains subcooled.

The comparisons between the NIST-1 HP-04 experimental data and the code calculated values showed that NRELAP5 has the capability to accurately predict the energy transfer across the DHRS heat exchanger tubes to the CPV fluid. The HP-04 test duration was longer than that of HP-03. In HP-04, saturated conditions in the pool were reached and thermal stratification developed. Although the CPV fluid heat-up profiles for the HP-04 test data were not fully reproduced in the NRELAP5 simulations of HP-04, the code-to-data comparisons of DHRS heat removal rate were well-matched demonstrating that NRELAP5 is capable of predicting the total energy removal rate of the DHRS to the cooling pool.

The comparisons between the NIST-1 NLT-2a integral experimental data and the code calculated values showed that NRELAP5 has the capability to accurately predict primary coolant system heat up and pressurization due to a loss of feedwater flow.

NRELAP5 assessment of the NIST-1 NLT-2b phases 1 through 4 demonstrates the ability of the code to predict the heat transfer from primary side to the SG and from the DHRS to CPV. After completion of core power maneuvering and after full start of the DHRS loop, NRELAP5 calculated pressurizer pressure, core inlet and outlet temperature, SG pressure, energy transfer from the primary to secondary, energy transfer from DHRS to CPV, SG level, DHRS level, and CPV level results are all within reasonable to excellent agreement with NLT-2b test data.

The pressurizer level for NLT-2b phase 1 was {{

}}^{2(a),(b),(c)} However, even with these discrepancies, the results show that the important parameter of total energy transfer from the primary side to the SG and from the DHRS to CPV are well predicted.

For NLT-2b phases 1 through 4, the calculated condensate temperature is in minimal agreement with data, with the temperature being over predicted by NRELAP5. However, even with this discrepancy, the important parameter of heat transfer from primary side to the SG and from the DHRS to CPV are well predicted.

For NLT-2b phases 1 through 4, although the CPV fluid heat-up profiles were not fully captured in the NRELAP5 simulations, the code-to-data comparisons of DHRS heat removal rate were well-matched demonstrating that NRELAP5 is capable of capturing the important parameter of total energy removal rate of the DHRS to the cooling pool and that the integral response is insensitive to the CPV temperature profile. {{

}}^{2(a),(c)}

NRELAP5 assessment of the NIST-1 NLT-15p2 test demonstrates the ability of the code to predict the heat transfer from primary side to the SG and from the DHRS to CPV. The NRELAP5 calculated pressurizer and RPV level, core inlet and outlet temperature, primary flow rate, steam generator pressure, energy transfer from the primary to secondary, energy transfer from DHRS to CPV, SG level, DHS level, and CPV level results are predicted reasonably compared to the NLT-15p2 test data. The NRELAP5 calculation of the initial pressurizer pressure response to decrease in secondary side heat transfer due to loss of feedwater, and the RPV pressure turn over after core power decreased to decay heat levels and DHRS heat removal flow was established, was well-predicted.

{{

}}^{2(a),(c)}

The calculated fluid temperature inside the DHRS heat exchanger tubes predicted the trends of the measured data. {{

}}^{2(a),(c)}

The calculated differential pressure across the DHRS steam line {{

}}^{2(a),(c)}

Four different transients were performed for code-to-code benchmarking between NRELAP5 and RETRAN-3D: Reactivity insertion representative of a fast UCRW from full power conditions, reactivity insertion representative of a slow UCRW from full power conditions, negative reactivity insertion to reduce power from 100 percent to 50 percent power, and negative reactivity insertion simulating a dropped rod from 50 percent power. The results from all four of the transients showed that the comparison between the power and the total reactivity were consistently excellent, in that the calculation results of the two codes were nearly identically with one another.

NuScale's LOCA Topical Report (Reference 2) Section 7.4 discusses the validation of NRELAP5 for helical coil SG modeling. The validation was mainly against SIET TF-1 and TF-2 test data. The operating range of the helical coil SG primary and secondary side is demonstrated to be sufficiently covered by the validated range of NRELAP5. It was concluded that NRELAP5 showed reasonable to excellent agreement with test data for all phenomena at conditions important for the non-LOCA analysis.

A nodalization sensitivity of the steam generator for a main steam line break scenario was performed comparing the effect of modeling the SG {{

}}^{2(a),(c)}

Considering the high-ranked phenomena identified from the PIRT process, the NRELAP5 code along with the NPM system model is applicable for calculation of the NPM system response for the non-LOCA short-term transient event progression as part of this EM based on separate effects and integral effects testing, code-to-code benchmarking, and appropriate conservative input for initial and boundary conditions.

6.0 NuScale NRELAP5 Plant Model

This section discusses the NuScale NRELAP5 non-LOCA plant transient model. A summary overview of the plant components and features simulated by the NRELAP5 model is provided, including the reactor primary and secondary (SG) systems, core fuel rods and kinetics, ECCS and DHRS, containment and reactor pool, and trips and controls.

The NRELAP5 plant model is developed to support the non-LOCA analysis methodology described in Section 7.0. The model was developed following the NRELAP5 code manual user guidelines, supplemented by NuScale-specific modeling guidelines. The guidelines describe how to model a NuScale Plant Module using the NRELAP5 code, and include directions on how to select code options, nodalizing the system, and selecting heat transfer correlations.

6.1 Thermal-Hydraulic Volumes and Heat Structures

The NRELAP5 plant model contains multiple hydraulic components, heat structures and junctions. The model simulates the majority of a typical NPM (Figure 6-1) including the RPV and internals, the containment, and the reactor cooling pool. {{

}}^{2(a),(c)} Both DHRS trains are included in the model, along with the ECCS consisting of the RVVs and RRVs. Control system components include variable and logical trips, control blocks and general tables. Figure 6-2 shows a typical nodalization diagram for the primary and secondary systems and is meant to convey the overall model structure rather than show nodalization details of any particular component.

Figure 6-3 shows a cut-away of the typical NPM reactor coolant system and CNV with the key nodalization regions included in the NRELAP5 model. The circled numbers in the figure represent RCS fluid regions and the numbers in squares represent containment regions. Table 6-1 lists the RCS regions and the associated NRELAP5 components.

This NRELAP5 model of the NPM serves as the standalone baseline model for non-LOCA safety analysis, as well as various aspects of plant design support. The information presented herein describes the base model as it is configured for non-LOCA analysis.

{{

}}^{2(a),(c)}

{

}}^{2(a),(c)}

Where precise noding is described in Section 6.1, the specified level of detail is considered the minimum level of detail required for the component of interest. Should additional detail be needed in the future, the relevant benchmarks, sensitivity studies, and transient analyses will be reviewed for continued applicability. If necessary, the relevant benchmarks, sensitivity studies, and transient analyses will be revised to demonstrate the higher level of detail for the component of interest is applicable to the NPM.

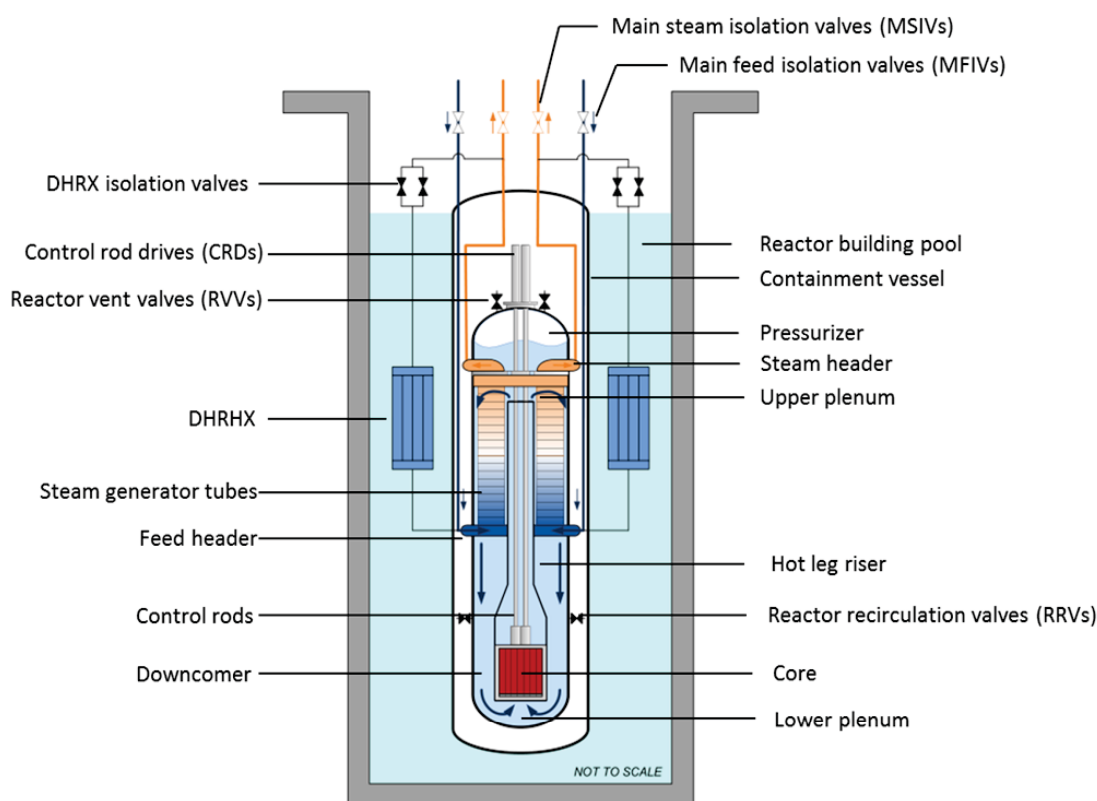


Figure 6-1 NuScale Power Module (typical)

{{

}}^{2(a),(c)}

Figure 6-2 Typical primary and secondary side nodalization (heat structures and component cell details excluded)

{{

}}^{2(a),(c)}

Figure 6-3 Typical NRELAP5 plant module volume regions

Table 6-1 Reactor coolant system regions and typical NRELAP5 components

{{

}}^{2(a),(c)}

6.1.1 Reactor Primary

Reactor Pressure Vessel Downcomer

{{

|

}}^{2(a),(c)}

|

{{

}}^{2(a),(c)}

Figure 6-4 Reactor pressure vessel downcomer nodalization

Steam Generator Primary

The SG is a helical coiled, once-through HX, with the primary system on the shell side and the secondary system on the tube side. The primary system water is cooled as it flows over the outer surfaces of the SG tubes before passing over the feedwater plena that are located above the elevation of the conical transition riser fairing in the RPV. On the secondary side, feedwater enters the bottom of the SG tubes via the feedwater plena and is heated as it flows upward, with superheated steam exiting the tops of the tubes. Two independent sets of interwoven SG tube banks occupy the SG region, each having independent feedwater and steam plena. If the tube banks experience different secondary side conditions, the primary coolant does not experience any corresponding asymmetries because of the interwoven design of the helical coiled tubes.

The heat transfer to the SG tubes occurs in the upper downcomer. The heat transfer and pressure drop resulting from the presence of the SG tubes was assessed with data from SIET TF-2 (See Section 5.3.5). This assessment used special heat transfer model options and determined the methodology for accurately predicting the pressure drop in the region.

{{

}}^{2(a),(c)}

Core and Lower Plenum

{{

}}^{2(a),(c)}

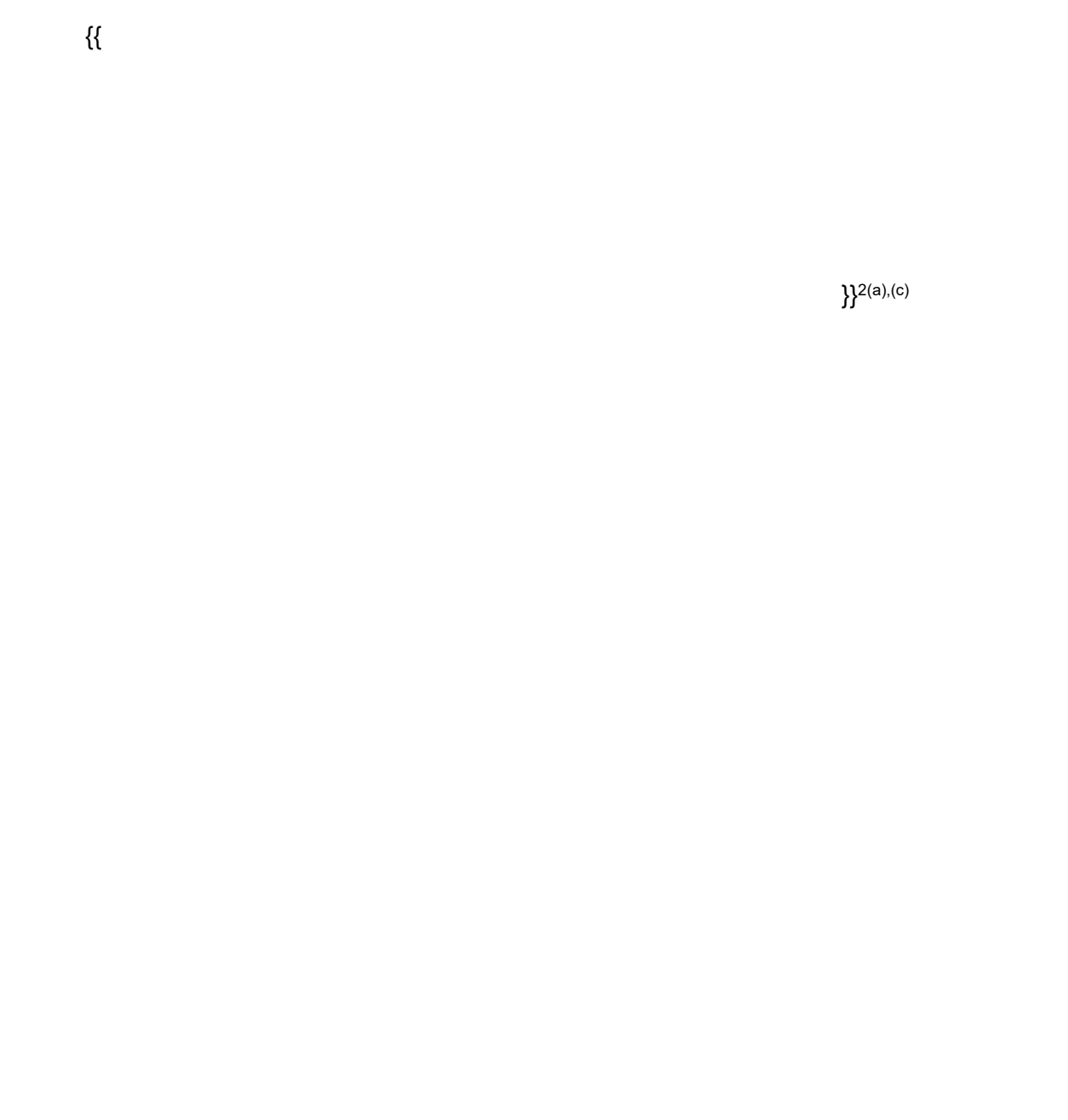
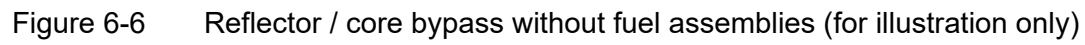


Figure 6-5 Core and lower plenum nodalization

 $\{\{$
$$\}}^{2(a),(c)}$$

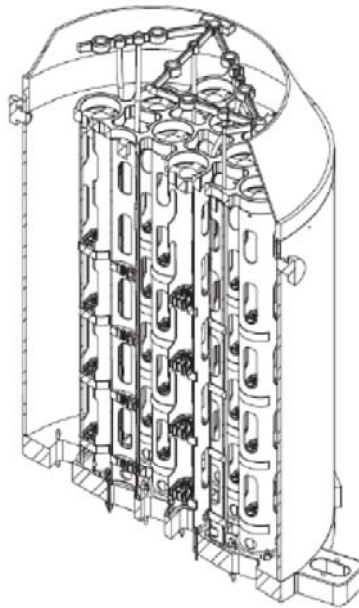


Figure 6-7 Lower riser region, immediately above the core (for illustration only)



Figure 6-8 Reactor pressure vessel core and lower riser

Upper Riser

Normal flow in the riser is single-phase subcooled water. Transients that involve RPV depressurization or inventory loss can result in flashing and two-phase flow in the riser region.



Figure 6-9 Reactor pressure vessel upper riser

Pressurizer

{{

}}^{2(a),(c)}

{{

|

}}^{2(a),(c)}

Figure 6-10 Reactor pressure vessel pressurizer

|

6.1.2 Core kinetics

The separable point kinetics model is used to calculate reactivity feedback to the core power from the moderator, the fuel, and decay heat. The various point kinetic parameters are input based on the fuel burnup (for example, new core, BOC, or EOC) and control rod insertion amounts assumed for the analysis. NRELAP5 assumes an infinite core operating time at the initialized power when determining the decay heat power. The fission product decay type is specified as 'gamma-ac' with the 'ans73' model, which calculates decay heat in accordance with the 1973 ANS standard while adding the contribution from actinides. A fission product yield factor of 1.0 is specified in the base model, which can be changed to suit the scenario being analyzed.

Control variable inputs to the core kinetics model are used to simulate control rod movement and reactivity feedback from a variety of parameters including, but not limited to fuel temperature, moderator temperature, and moderator density. Trips are used to enable or disable each reactivity feedback mechanism as needed. The fuel and moderator feedback controllers utilize volume weighting of the fuel and moderator temperatures to specify bounding reactivity feedback input; volume weighting is used for consistency with how the reactivity feedback design limits are confirmed in the core design.

A scram table is used to simulate control rod insertion following reactor trip. Appropriately conservative scram curves are developed based on the core time-in-life, the initial power level, the location of the control bank, and other relevant factors to preserve the minimum shutdown margin.

6.1.3 Fuel rod design input

{{

}}^{2(a),(c)} Fuel performance data (Section 4.3.1.2) is incorporated into the NRELAP5 non-LOCA model via material thermal property tables for the UO₂ fuel region, the gas gap, and the cladding. Because the density of UO₂ changes with burnup, the thermal property tables can be revised as needed to match time in cycle.

As discussed in Section 4.3.1.1, the core power distribution is based on a nominal average axial power shape with power distributed solely in the fuel pellet. {{

}}^{2(a),(c)} The gap thermal conductivity is selected as a function of burnup to ensure that the fuel volume average temperature is appropriately bounded compared to fuel performance design data. This adjustment also accounts for gap closure over the fuel cycle.

6.1.4 Secondary System

6.1.4.1 Feedwater System

In the NPM design two feedwater lines penetrate the CNV immediately downstream of the FWIVs. Each feedwater line splits into two lines before connecting to the SGs. {{

}}^{2(a),(c)}

6.1.4.2 Steam Generator Secondary

The NRELAP5 specific helical coil SG component ('hlcoil') is used to simulate the helical coil SG that is characteristic of the NPM (Reference 2 describes the helical coil component). The steam generator nodalization is shown in Figure 6-11. The primary coolant flows through the SG shell side while the feedwater and steam flow through the tube side. The tube and shell side of the SG elevation nodalization schemes are one-to-one. The SG nodes are uniform, or may be finer towards inlet and coarser towards the exit if necessary to capture the phase change process in the lower region of the tubes. For non-LOCA transient calculations, finer nodalization is not needed near the tube exits due to the state of the fluid being single phase vapor. Section 5.3.5.4 summarizes SG nodalization sensitivity calculations. Based on these studies, modeling the helical coil SG with {{

}}^{2(a),(c)}

nodes is expected to produce reasonably accurate results

for the non-LOCA transients. Should additional detail be needed in the future, the relevant benchmarks, sensitivity studies, and transient analyses will be reviewed for continued applicability and updated as necessary to demonstrate the higher level of detail for the component is applicable to the NPM.

{{

}}^{2(a),(c)}

{{

}}^{2(a),(c)}

Figure 6-11 Steam generator nodalization

6.1.4.3 Main Steam System

{{

shown in Figure 6-12. {{
}}^{2(a),(c)} The MSS nodalization is
}}^{2(a),(c)} DHRS modeling is discussed in Section 6.1.5.

{{

}}^{2(a),(c)}

{{

}}^{2(a),(c)}

Figure 6-12 Main steam system nodalization

6.1.5 Decay Heat Removal System

The NPM incorporates two separate DHRSs that are treated individually in the NRELAP5 model. {{

}}^{2(a),(c)} Figure 6-13 shows the nodalization for DHRS loop 1. Loop 2 is modeled similarly. While each DHRS line in the NPM features two parallel actuation valves, {{
}}^{2(a),(c)}

The number of hydrodynamic volumes in the DHRS piping and HX regions are based on results from NRELAP5 assessments using data from the NIST-1 facility (See Section 5.3.2). {{

}}^{2(a),(c)}

{{
}}^{2(a),(c)}

In the actual NPM the DHRS heat exchanger is located in the reactor cooling pool. {{

}}^{2(a),(c)}

{{

}}^{2(a),(c)}

Figure 6-13 Decay heat removal system division 1 nodalization

Figure 6-14 Not used.

6.1.6 Emergency Core Cooling System

The ECCS hydrodynamic components consist of two reactor recirculation valves (RRVs) and three reactor vent valves (RVVs). {{

}}^{2(a),(c)}

Figure 6-15 Not used.

6.1.7 Containment Vessel

{{

}}^{2(a),(c)}

{

}^{2(a),(c)}

{{

}}^{2(a),(c)}

Figure 6-16 Containment and reactor pool nodalization

6.1.8 Reactor Cooling Pool

{{

}}^{2(a),(c)}

6.2 Material Properties

Thermal properties (thermal conductivity and volumetric heat capacity) are specified by user input in the NRELAP5 non-LOCA base model for the following materials used in the heat structures. These material properties may be amended or revised as the NPM design evolves:

1. fuel cladding (AREVA's M5® cladding)
2. inconel 690 (SG tubes)
3. uranium dioxide (UO₂)
4. stainless steel (SA-240 304L)
5. fuel-to-cladding gas gap (initially pressurized helium at BOC; mixture of fission product gases and helium after irradiation)
6. carbon steel (SA-508)
7. {{

}}^{2(a),(c)}

6.3 Control Systems

With its combination of trips, control functions, and user-defined tables, NRELAP5 provides flexibility to accurately simulate plant control and protection system responses during both steady-state and transient operation. The NRELAP5 non-LOCA base model contains logic for "normal controls" that simulate normal operational plant response, as well as user-convenience controls that make it easier to initialize the model for particular transients and easier to interpret the transient results. It also contains trip and control logic that accurately simulates the MPS, i.e., the safety-related trips that protect the reactor core and fission product boundaries.

6.3.1 Module Control System (Nonsafety-related)

The MCS as implemented in the NRELAP5 non-LOCA model provides control systems that may be used for model initialization and for simulating normal operating transients. These control systems can be used to initialize the model at new steady state conditions or to evaluate the nominal MCS response to a transient initiator. The MCS model allows the simulation of a variety of prototypic control scheme responses to transient conditions to provide nominal responses of these control schemes. The model also includes the capability to disable these control schemes to allow for conservative modeling applications as necessary.

6.3.1.1 Pressurizer Pressure Control (Nonsafety-related)

The RPV pressure is controlled via the use of pressurizer heaters and spray to maintain the pressurizer steam pressure at a target value. When the pressure drops, the power to the PZR heaters increases, and if pressure increases, a portion of the CVCS recirculation flow is diverted to the pressurizer spray nozzles to collapse the steam space via condensation and reduce pressure.

6.3.1.2 Chemical Volume Control System Control (Nonsafety-related)

The control systems implemented in the NRELAP5 non-LOCA model include simplified mechanisms for controlling CVCS recirculation flow, injection temperature and RCS inventory control (makeup and letdown). {{

}}^{2(a),(c)} The water level in the pressurizer is controlled to a programmed setpoint by operation of the CVCS makeup pumps and the letdown control valve. While operation of CVCS letdown is automatically initiated by the MCS, control of the CVCS makeup is not. Instead, operator permission is required for CVCS makeup to be initiated.

For non-LOCA transient analyses where loss of inventory or inventory shrinkage is expected to indicate makeup is needed, the process by which the operator approves makeup is considered. Since approval to initiate makeup is a manual action by the operator, the non-LOCA transient analyses do not credit this action. For spurious inventory addition events where automatic letdown could reduce the event consequences, credit for this action is not taken for the non-LOCA transient analyses.

6.3.1.3 Reactor Coolant System Temperature Control (Nonsafety-related)

The MCS model controls RCS average temperature by changing reactivity in the core to increase or decrease core power. This is accomplished with a control rod controller and a boron controller. The control rod controller uses design data to model a calculated rate of reactivity insertion due to maximum or nominal rod movement rates. {{

}}^{2(a),(c)}

{{ }}^{2(a),(c)} Neither controller accounts for all the actual core physics including the effect of xenon or other decay products or poisons that could be expected with control rod repositioning.

The average coolant temperature is controlled by adjusting core power, which is accomplished by moving the control rods or changing the boron concentration of the reactor coolant. The choice of which method is based on the desired rate of change for core power. The control rods are moved to achieve faster power changes to meet the target average coolant temperature; slower power changes are accomplished by changing the boron concentration of the reactor coolant. At full power, the rod control system is set to 'insert only' mode to prevent automatic withdrawal of the control rods during a transient.

6.3.1.4 Steam Pressure Control (Nonsafety-related)

In the NPM design the turbine throttle and bypass valves are used to control steam pressure at the programmed values, {{

{{ }}^{2(a),(c)}

6.3.1.5 Feedwater and Turbine Load Control (Nonsafety-related)

The NPM prototypic control scheme design for the feedwater system is based on turbine load demand. The NPM feedwater pumps are variable speed and can provide variable flow for module operations over a wide range of power without adjustments to the feedwater regulating valve. {{

{{ }}^{2(a),(c)}

6.3.1.6 Containment Pressure Control (Nonsafety-related)

The containment pressure is established at sub-atmospheric conditions via operation of the containment evacuation system. The impact of this system continuing to operate is considered for the non-LOCA transient analyses.

6.3.2 Module Protection System (Safety-related)

6.3.2.1 Analytical Limits and Delays

The MPS implemented in the NRELAP5 base model is intended for the purposes of performing safety analysis transient simulations. As such, the logic and actuation points are based on the NPM safety analysis analytical limits. Fixed delay times are specified considering different sensor response times. {{

}}^{2(a),(c)} In addition to the sensor delays, a given safety signal is subject to instrumentation string delays, an MPS processing delay, and an actuation delay. The NRELAP5 non-LOCA model incorporates the methodology assumption that a bounding total for these additional delays is applied as a signal delay in addition to the individual sensor delay.

Table 6-2 shows the type of safety signals for the NuScale NPM design. Signals in bold are included in the NRELAP5 non-LOCA model. The control logic for other MPS signals may be added if needed for a particular event analysis or as necessary to maintain consistency with the MPS design.

Table 6-2 NuScale Power Module safety logic with NRELAP5 signals in bold

{{

}}^{2(a),(c)}

6.3.2.2 NRELAP5 Modeling

The NRELAP5 components used to model the MPS include variable and logical trips that are used to sense the MPS trip limits, apply signal delays and generate actuation signals. The MPS instrumentation and sensors are typically modelled by comparing the volume or junction parameter at the location of the sensor and comparing it to the associated analytical limit, rather than explicitly modeling the sensor.

The reactor trip system (RTS) logic is fairly simple, as each RTS signal is computed and compared against the trip setpoint on each timestep. The trips are organized together in a series of “or” logical trips. Should one trip limit be reached, the cascade of logical trips will immediately reach the final RTS logical trip, which then causes the RPS actuation signal to become true after a fixed delay that conservatively accounts for signal processing

and rod latch mechanism delays. Other subsystems such as containment isolation, DHRS actuation, ECCS actuation, etc. are modeled similarly.

{{

}}^{2(a),(c)}

The pressurizer level signal is generated by modeling the collapsed liquid level, {{

}}^{2(a),(c)}

The ECCS actuation logic includes the ability for the user to set additional electrical or mechanical conditions that are external to the NRELAP5 hydrodynamic model. {{

}}^{2(a),(c)} The effects of external conditions can be added to any of the control system models as needed for a given transient scenario.

7.0 Non-LOCA Analysis Methodology

7.1 General

The discussion in the following sub-sections is applicable for all transients unless the event-specific methodology states otherwise in Section 7.2.

7.1.1 Achieving Steady State Conditions

This section identifies the initial and boundary conditions considered for biasing in non-LOCA analyses, including prioritization during the initialization process. While the majority of parameters identified herein are initial conditions relevant to the steady state, other parameters are considered as bounding input for the plant response during the transient progression.

7.1.1.1 Background

Establishing the appropriate initial conditions is paramount to obtaining an appropriate plant response for the transient of interest. To this end, it is important to ensure the NRELAP5 model achieves a valid steady state prior to initiating the transient.

The effect of various initial conditions on the response to a specific acceptance criterion is assessed for each non-LOCA transient. Several means are available to perform the assessment. For example, the assessment may consist of a combination of:

- Qualitative engineering assessment in the calculation to identify why an initial condition bias is limiting or non-limiting
- Quantitative assessment by execution of appropriate sensitivity calculations in the calculation
- Reference to applicable regulatory precedent that identifies why a particular initial condition bias is not limiting for a particular transient or type of transient, or why a nominal condition is appropriate

7.1.1.2 Identification of Relevant Parameters

A list of initial conditions to be considered for biasing was developed for the non-LOCA analyses, including the target value for the initial plant condition and acceptable tolerance to the target value.

Other parameters needed to obtain a steady state include: certain fuel-related and core-related inputs; measurement uncertainties for various safety-related processes; the plant operational limits assumed in the safety analyses; and the DHRS initial conditions.

Table 7-1 identifies a typical list of initial conditions considered for non-LOCA analyses. This list of initial conditions includes both direct inputs and calculated results. Most of these parameters are directly input to NRELAP5. The calculated results are identified as a

“target” because the analyst uses this parameter as a target during the initialization process.

Under best-estimate primary flow conditions and various reactor powers, it has been shown that there is relatively little variation in liquid inventory in the steam generator. The inventory does not change appreciably when considering variations in primary coolant temperature and primary flow rates. Consequently, steam generator inventory is not a target during the initialization process. {{

}}^{2(a),(c)}

For reactor powers greater than or equal to 20 percent full power (FP) and best-estimate primary flow conditions, the steam superheat increases with power for the defined main feedwater conditions. {{

}}^{2(a),(c)}

The removal of any restrictions regarding steam generator inventory and steam superheat allows use of the parameters in Table 7-1 for initialization without over-specifying or under-specifying the problem.

Table 7-1 Typical list of initial conditions considered

Region	Parameter
Core	Power
	Calorimetric power uncertainty
	Volume-weighted core average fuel temperature (target)
	Moderator temperature coefficient
	Doppler temperature coefficient
	Effective delayed neutron fraction
	Ratio of effective delayed neutron fraction to prompt neutron lifetime
	^{238}U neutron capture to fission ratio
	Energy deposition factor
	Average core axial power shape
	Scram reactivity (shutdown margin)
	Control rod bank differential worth
	Decay heat and decay heat uncertainty
	Boron concentration
RCS	Primary system mass flow rate (target)
	RCS average fluid temperature (target)
	Pressurizer pressure
	Pressurizer level
	Total core bypass flow rate
	Pressurizer spray bypass flow rate
	Pressurizer heater power
	Heat losses to containment from the RPV and from piping inside containment
Steam generator secondary, feedwater system, and MSS	Feedwater mass flow rate
	Feedwater temperature
	Steam chest pressure (turbine header pressure)
	Steam generator tube plugging, fouling factor
Containment	Pressure
	Heat losses from containment to reactor pool and reactor building
	Temperature
Reactor pool	Temperature
	Level
DHRS	Liquid volume

7.1.1.3 Prioritization of Initial Conditions

An important design feature of the NPM is the natural circulation of primary reactor coolant. This design feature may also limit the ability of the NRELAP5 non-LOCA transient model to achieve a given set of initial conditions. In particular, changes in core power or parameters that affect the SG secondary side heat removal rate will alter the reactor

coolant flow rate and density distribution in the primary coolant. The initial conditions are prioritized based on the greatest impact to the transient of interest.

Initial conditions may be treated in the NRELAP5 non-LOCA transient model in different ways. For instance, the initial conditions can be specified directly as input or calculated by the code. Parameters identified as important initial conditions for a particular transient (whether directly input or indirectly determined by the code) are checked as part of the steady state balance to confirm that either: 1) the parameter is within the allowable tolerance to the target value based on design references; or, 2) the parameter conservatively bounds the target design value and is adequately steady (within acceptable tolerances). If the initial condition is calculated by the code but not identified as important for a transient, the parameter may or may not be directly checked as part of the steady state initialization process against design values.

7.1.1.4 Typical Initialization Process

Prior to the initialization process, certain parameters critical to establishing the correct steady state for the event of interest are identified. Once the parameters of interest achieve steady state target values within acceptable tolerances, on the basis of engineering judgement, {{

}}^{2(a),(c)} A steady state solution has been achieved when the change in the target value during the loop transits is within the variance band described for each parameter.

A typical list of critical parameters for initializing the primary and secondary systems is provided below.

- reactor power: tolerance (or bounded) and variance
- fuel temperature: tolerance (or bounded) and variance
- RCS temperature: tolerance (or bounded) and variance
- PZR pressure: tolerance (or bounded) and variance
- PZR level: tolerance (or bounded) and variance
- RCS flow: tolerance (or bounded) and variance
- steam pressure: tolerance (or bounded) and variance
- feedwater flow rate: variance
- feedwater temperature: tolerance (or bounded) and variance

Null transients are used to ensure the re-initialization cases achieve the desired steady state conditions. {{

}}^{2(a),(c)} In addition, feedback from the point kinetics model is active for the null transients.

7.1.2 Treatment of Plant Controls

Control systems are necessary to maneuver the NPM within the power range in accordance with normal operating transients. However, not all of these control systems are relevant to the non-LOCA transient analyses because the action of the control system does not alter the event consequences. This section identifies the normal, nonsafety-related plant controls considered in non-LOCA transient analyses.

The effect of various plant controls on the response to a specific acceptance criterion is assessed for each non-LOCA transient. Several means are available to perform the assessment. For example, the assessment may consist of a combination of:

- Providing a qualitative engineering assessment that identifies why operation of a PCS is limiting or non-limiting.
- Performing a quantitative assessment via appropriate sensitivity cases.
- Referencing to applicable regulatory precedent that identifies why a particular normal plant control is not limiting for a specific transient or type of transient.

When considering operation of the various plant controls, the approach is based on the event consequences for a given acceptance criterion. Specifically, if operation of the control system leads to a less severe plant response, then the actions of the control system are not simulated for the transient of interest. Conversely, if operation of the control system causes the event consequences to be more severe, the PCS is assumed to operate as designed. {{

}}^{2(a),(c)}

The normal PCSs to be considered in design basis event analysis are:

Pressurizer Pressure Control

Pressurizer pressure is controlled via operation of the pressurizer spray and the pressurizer heaters.

Pressurizer Water Level Control

The water level in the pressurizer is controlled to a programmed setpoint by operation of the CVCS makeup pumps and the letdown control valve. While operation of CVCS letdown is automatically initiated by the MCS, control of the CVCS makeup is not. Instead, operator permission is required for CVCS makeup to be initiated.

For non-LOCA transient analyses where loss of inventory or inventory shrinkage is expected to indicate makeup is needed, the process by which the operator approves makeup is considered. Since approval to initiate makeup is a manual action by the operator, the non-LOCA transient analyses do not credit this action. For spurious inventory addition events where automatic letdown could reduce the event consequences, credit for this action is not taken for the non-LOCA transient analyses.

Core Average Coolant Temperature Control

The average coolant temperature is controlled by moving the control rods or changing the boron concentration of the reactor coolant. This selection is based on the desired rate of change for core power. Hence, the control rods are moved to achieve faster power changes to meet the target average coolant temperature; slower power changes are accommodated by changing the boron concentration of the reactor coolant. At full power, the rod control system is set to 'insert only' mode to prevent automatic withdrawal of the control rods during a transient.

Steam Pressure Control

Steam pressure is controlled to the desired value using the turbine throttle valves or the turbine bypass valves. The effect of these valves to a change in steam pressure is considered for the non-LOCA transient analyses.

Turbine Load Control

The mass flow rate and pressure provided by the feedwater pump is used to meet the desired turbine load, which reflects the power generation rate. The impact of the feedwater pumps continuing to operate until the feedwater line is isolated is considered for the non-LOCA transient analyses when DHRS is actuated.

Containment pressure control

The containment pressure is established at sub-atmospheric conditions via operation of the containment evacuation system. The impact of this system continuing to operate is considered for the non-LOCA transient analyses.

7.1.3 Loss of Power Conditions

This section defines the term "loss of normal power" as applied to the NPM; describes the various power supplies (AC and DC); and, explains how the loss of these power supplies is treated by the non-LOCA transient analyses.

7.1.3.1 Background

Chapter 15 of the SRP (Reference 15) does not ordinarily consider a loss of offsite power for events that require a malfunction of an active system for which power must be available; however, exceptions are made for some reactivity initiated events. The role of offsite power is less defined for the NPM plant than for traditional plants for several reasons, but the use of natural circulation for normal operation and safety systems is the fundamental reason. Consequently, these design features limit the impact of a power loss to the NPM plant compared to a traditional plant design that relies on forced circulation.

The term 'loss of normal power' is used herein for the NPM because the normal power source for the plant is not the offsite grid, and there are no onsite safety-related power generating sources (AC or DC). Although the NPM plant design does not include a safety-

related electrical power generation source, the highly reliable DC power system (EDSS) includes a battery backup as part of the design. This battery backup allows the EDSS to provide uninterrupted DC power for 72 hours of MPS operation. Because the MPS also provides power to keep the ECCS valves closed, if a loss of normal AC power to the EDSS buses occurs, the MPS will shed the load to the ECCS valves after 24 hours. This action allows the ECCS valves to open if the pressure difference between the RPV and the containment is low enough.

The effect of various power availability scenarios on the response to a specific acceptance criterion is assessed for each non-LOCA transient. This assessment can be performed using several methods. For example, the assessment may consist of a combination of:

- providing a qualitative engineering assessment that identifies why operation of a power availability scenario is limiting or non-limiting
- performing a quantitative assessment via appropriate sensitivity cases
- referencing to applicable regulatory precedent that identifies why a particular power availability scenario is not limiting for a specific transient or type of transient

When considering various power availability scenarios, the approach is based on the event consequences for a given acceptance criterion. Because nonsafety-related AC power sources are not credited for the non-LOCA event analyses, in all scenarios where AC power is lost, the ECCS valves open at some point during the transient. For non-LOCA transients that do not demand ECCS actuation during the short-term event progression, i.e., during the time frame in which the peak pressures, MCHFR, or peak fuel centerline temperature occur, the time at which the ECCS valves open is beyond the scope of this methodology document.

7.1.3.2 Consideration of Loss of Power to All Transients

The subsections of SRP Chapter 15 (Reference 15) applicable to the NPM, and the Chapter 15 DSRS sections, were reviewed to identify which subsections explicitly address a loss of power or GDC 17 (Reference 4). This review concluded that given the differences between the design of the NPM and typical PWRs, particularly with respect to the safety system design and response, the effect of loss of power on each non-LOCA transient should be considered.

7.1.3.3 Electrical Systems with Important Loads

A review of the electrical systems applicable to the NPM design was undertaken to identify which electrical systems have loads important to the non-LOCA transient analyses. Consideration was given to both direct and indirect impact to the transient analyses. A direct impact to the transient analyses is one that will alter the primary or secondary side conditions if the electrical system is lost. An indirect impact to the transient analyses is one that affects the ability to monitor the system or affects a connecting system. The following electrical systems have loads important to the non-LOCA transient analyses.

- EHVS – High voltage (13.8 kV) AC electrical system and switchyard
- EMVS – Medium voltage (4.16 kV) AC electrical distribution system
- ELVS – Low voltage (480 V and 120 V) AC electrical distribution system
- EDNS – Normal DC power system
- EDSS – Highly reliable DC power system

The EDNS and the EDSS power systems are both designed with battery backups to allow a continuous power supply in the event the power supply to the chargers is not available. The duration of the battery backup is based on the relative importance of the loads. Because the loads supplied by the EDNS are of lower importance, i.e., all loads are non-essential, the batteries are sized to supply these loads for 40 minutes. In contrast, for the higher importance (essential) loads supplied by the EDSS, with the exception of the ECCS valves, the batteries are sized to supply these loads for greater than 24 hours. The ECCS valves are unique because the MPS acts to shed the load for these valves at 24 hours after the loss of AC power to the EDSS battery chargers. The loss of normal AC power to the EDSS chargers also causes the MPS to initiate a reactor trip, actuate DHRS, and close the containment isolation valves.

Based on the electrical system design for the NPM, a loss of normal AC power means a loss of power from the ELVS. Such a condition could be due to: 1) a failure within the ELVS; or, 2) a loss of power from the 13.8 kV and switchyard system or EMVS. Since a failure of the 13.8 kV and switchyard system or EMVS results in the same response from the plant electrical systems for non-LOCA transient analyses, these failures are not considered separately. With respect to the battery backups for the DC power supply systems, the availability of the battery backups is considered because the EDNS and EDSS are not safety-related systems.

7.1.3.4 Timing for Loss of Power

The review of the subsections of SRP or DSRS Chapter 15 discussed in Section 7.1.3.2 indicates the SRP/DSRS is not prescriptive regarding when the loss of power occurs. An example is provided in DSRS Subsection 15.1.5, which states:

Assumptions as to the loss of offsite power (LOOP) and the time of loss should be made to study their effects on the consequences of the accident. A LOOP could occur simultaneously with the pipe break or during the accident, or offsite power may not be lost.

For the non-LOCA transient analyses applicable to the NPM, the loss of normal AC power is considered at two different times during the event progression:

- coincident with event initiation; or,
- coincident with turbine trip.

The basis for considering a loss of power coincident with event initiation is the loss of normal AC power could be caused by the event initiator or as a result of the event. For example, the mass and energy exiting a ruptured steam pipe could damage equipment that results in a loss of normal AC power to the plant.

The basis for considering loss of power coincident with turbine trip is because the loss of power is a consequence of the event. Specifically, the loss of AC power occurs as a result of a disruption to the electrical grid following a turbine trip. Because the electrical output for the NPM is much smaller (approximately 60 MWe) than the electrical output for a typical large plant (approximately 1000 MWe), the loss of an NPM is not anticipated to significantly disrupt the electrical grid. Regardless, the possibility of causing such a disruption is assessed as part of the non-LOCA transient analyses.

The random loss of a nonsafety-related system during an event is not typically required as part of the evaluation, and is not being postulated for the NPM. Instead, the interaction of the EDNS and EDSS electrical systems is linked to the normal AC power supply or the initiating event. Thus, combining the timing of when power is available with the electrical systems described in Section 7.1.3.3, yields the loss of power scenarios considered for the non-LOCA transient analyses.

7.1.4 Single Failures

This section discusses active single failures in fluid systems and single failures in electrical systems for consideration in non-LOCA transient analyses, as well as the relevance of fluid system passive single failures.

7.1.4.1 Background

The effect of various single active failures on the response to a specific acceptance criterion is assessed for each non-LOCA transient. Several means are available to perform the assessment. For example, the assessment may consist of a combination of:

- Providing a qualitative engineering assessment that identifies why a single failure is limiting or non-limiting.
- Performing a quantitative assessment via appropriate sensitivity cases.
- Referencing to applicable regulatory precedent that identifies why a particular single failure is not limiting for a specific transient or type of transient.

When considering various single active failures, the approach is based on the event consequences for a given acceptance criterion. Only safety-related components are considered for possible single active failures.

A nonsafety-related component whose action benefits the transient consequences is typically assumed inactive, unless the component is demonstrated to not be affected by the initiating event or the component is acting as backup protection. This treatment of

nonsafety-related components is consistent with RG 1.206 (Reference 14 Section C.I.15.6.2), which states:

Only safety-related systems or components should be used to mitigate transient or accident conditions. However, analyses may assume that nonsafety-related systems or components are operable for the following cases:

- (1) when a detectable and nonconsequential random and independent failure must occur in order to disable the system*
- (2) when nonsafety-related components are used as backup protection*

...

For any nonsafety-related systems or components credited in the design-basis analyses for mitigating the event consequences, the applicant must provide proper justification. The application must take into account nonsafety-related systems or components that may adversely affect transient or accident analyses.

Safety-related SSCs are defined in 10 CFR 50.2 (Reference 16), as:

SSCs that are relied upon to remain functional during and following design basis events to assure:

- 1) The integrity of the reactor coolant pressure boundary;*
- 2) The capability to shut down the reactor and maintain it in a safe shutdown condition; or*
- 3) The capability to prevent or mitigate the consequences of accidents which could result in potential offsite exposures comparable to the applicable guideline exposures set forth in 10 CFR 50.34(a)(1) or 10 CFR 100.11, as applicable.*

A limited number of safety-related SSCs interact with the reactor coolant system, secondary system, or containment. In most instances these safety-related SSCs were considered using the definition presented in ANSI/ANS-58.9-2002 R2015 (Reference 17), i.e., an active failure is a malfunction of a component that relies on mechanical movement to complete its intended function upon demand. Passive failures of fluid systems are not considered for the non-LOCA transient analyses during the short term (up to 24 hours).

7.1.4.2 Consideration of Single Failures

The NPM considers single active failures of fluid systems or single failures of electrical systems that could affect the non-LOCA transient analyses. Various means were used to identify these failures, including: 1) the application of design criteria and industry standards to the design of the equipment; 2) the arrangement and type of valves incorporated into the design; and, 3) the level of redundancy in equipment functionality incorporated into the design.

7.1.4.3 Consideration of Passive Single Failures

The NPM does not consider passive single failures of fluid systems during the short term (up to 24 hours) non-LOCA transient analyses; however, passive single failures of electrical systems are considered. This approach is consistent with the regulatory position in SECY-94-084 (Reference 18) and SRP Chapter 15 (Reference 15).

7.1.4.4 Single Failures to Evaluate

The NPM considers the worst active single failure in conjunction with the initiating event and with loss of power for the short term non-LOCA transient analyses. During the short term, passive single failures of fluid systems are not considered; however, passive single failures of electrical systems are considered.

The following active single failures are considered for non-LOCA transient analyses.

- safety-related main steam isolation valve – failure to close when demanded
- safety-related feedwater isolation valve – failure to close when demanded
- safety-related feedwater check valve – failure to close when demanded
- MPS – failure of a single channel to trip when demanded
- ECCS reactor recirculation valve – failure to open when demanded
- ECCS reactor vent valve – failure to open when demanded

The following passive electrical single failure is considered for non-LOCA transient analyses.

- MPS – failure to signal one ECCS reactor recirculation valve and one RVV to open when demanded

7.1.5 Bounding Reactivity Parameters

This section describes the bounding reactivity parameters used for the non-LOCA transient analyses. A brief discussion of each parameter is provided in the following sections.

- Moderator Temperature Coefficient (Section 7.1.5.1)
- Doppler Temperature Coefficient (Section 7.1.5.2)
- Decay heat contribution (Section 7.1.5.3)
- Scram worth (Section 7.1.5.4)
- Reactivity versus time for scram insertion (Section 7.1.5.5)

7.1.5.1 Moderator Temperature Coefficient

Bounding values for MTC are generally selected to represent the most positive value at BOC and the most negative value at EOC. For most non-LOCA transient analyses, the coefficient is conservatively applied as a constant value for the full range of expected moderator temperatures. If the MTC at zero power is positive, this value could be used to bound all power levels. Alternately, the positive MTC could be applied over a limited range of power levels with a different, yet bounding, MTC value for the remaining power levels.

The following MTC values are examples for the NPM. A review of the applicable core physics parameters is performed each cycle to confirm the bounding nature of the values utilized for the non-LOCA transient analyses.

- Most Positive at power > 25 percent RTP = 0 pcm / degrees F
- Most Positive at power ≤ 25 percent RTP = +6 pcm / degrees F
- Most Negative at hot full power = - 43.0 pcm / degrees F
- Most Negative at hot zero power = - 15.0 pcm / degrees F

7.1.5.2 Doppler Temperature Coefficient

Bounding values for DTC are generally selected to represent the least negative value at BOC and the most negative value at EOC. For most non-LOCA transient analyses, the coefficient is conservatively applied as a constant value for the full range of expected fuel temperatures.

The following DTC values are examples for the NPM. A review of the applicable core physics parameters is performed each cycle to confirm the bounding nature of the values utilized for the non-LOCA transient analyses.

- Minimum (least negative) = - 1.40 pcm/°F
- Maximum (most negative) = - 2.25 pcm/°F

7.1.5.3 Decay Heat Contribution

Energy production in the core comes from fission and fission product decay. This latter component is the decay heat contribution. During the initialization process the specified kinetics inputs are used to determine the balance between fission power and fission product decay. Changing the decay heat contribution, therefore, changes the fission power because the total core power is not altered.

Bounding values for decay heat are designated to represent the high contribution and the low contribution. Once specified, the decay heat contribution is utilized for the duration of the event of interest. For the non-LOCA transient analyses the decay heat contribution is based on the 1973 ANS decay heat standard, which is varied by utilizing different decay heat multipliers and specifying whether or not to include the actinide contribution.

The following decay heat contribution values are examples for the NPM. Figure 7-1 provides an example of the decay heat as a function of time for an equilibrium cycle. A review of the applicable core physics parameters is performed each cycle to confirm the bounding nature of the values utilized for the non-LOCA transient analyses.

- Low = use multiplier of 0.8 while excluding the actinide contribution
- High = use multiplier of 1.0 while including the actinide contribution

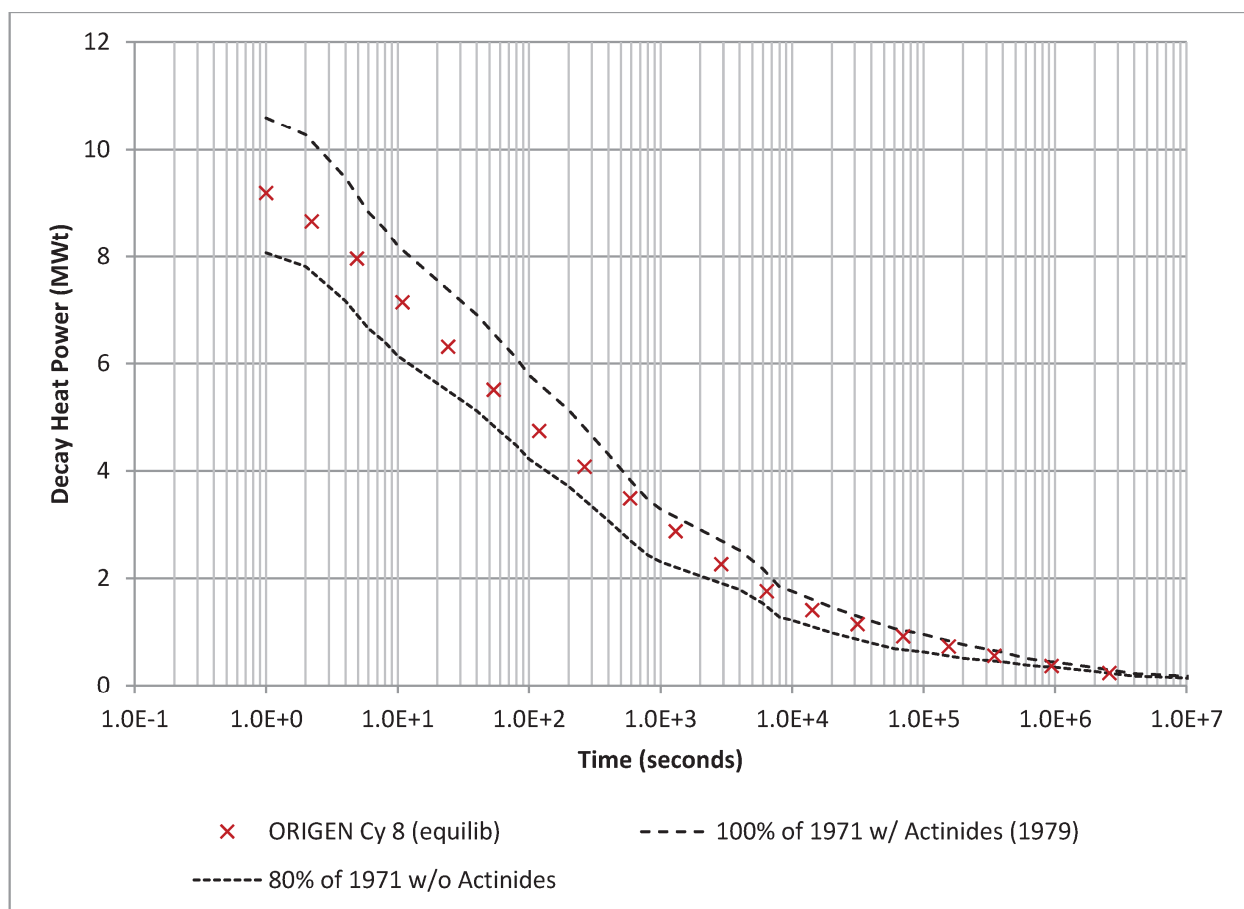


Figure 7-1 Example of decay heat comparisons

7.1.5.4 Scram Worth

After a reactor trip, the insertion of the control and safety banks imposes negative reactivity on the core. The reactivity available for insertion varies based on the time-in-life and the location of the control bank prior to trip. The inserted reactivity is sufficient to not exceed

SAFDLs under conditions of normal operation, including AOOs; and, to limit fuel damage during accidents to assure the capability to cool the core is maintained.

As applied to the non-LOCA transient analyses, the scram worth is the magnitude of the reactivity needed to take the plant from the initial core power to the desired shutdown conditions at zero power (for example, 420 degrees F) while, at a minimum, accounting for the moderator defect, the Doppler defect, the maximum worth stuck rod, and the minimum shutdown margin.

7.1.5.5 Reactivity Versus Time for Scram Insertion

The manner in which the scram worth is inserted into the core is derived as a bounding depiction of the reactivity insertion characteristics associated with a reactor trip from hot full power. An example of a normalized trip worth as a function of time, for which the control rods are fully inserted 2.278 seconds after being released by the control rod drive mechanisms, is presented in Table 7-2.

Table 7-2 Example of normalized trip worth vs. time after trip

Time After Trip (sec)	Normalized Trip Worth
0.0	0.0
0.428	0.011
0.616	0.044
0.766	0.099
0.900	0.176
1.022	0.276
1.138	0.397
1.220	0.502
1.250	0.540
1.458	0.706
1.952	0.893
2.278	1.0

7.1.6 Biasing of Other Parameters

This section describes the biasing of non-reactivity parameters used for the non-LOCA transient analyses. A brief discussion of each parameter is provided in the following sections.

- Initial Conditions (Section 7.1.6.1)
- Valve Characteristics (Section 7.1.6.2)
- Analytical Limits and Response Times (Section 7.1.6.3)

7.1.6.1 Initial Conditions

The initial conditions assumed for the non-LOCA transient analyses are the most adverse with respect to the acceptance criterion of interest. These conditions are normally consistent with steady state operation, allowing for calibration and instrument errors and steady state fluctuations. Recognizing that the initial conditions do not contribute equally to the severity of the event consequences, alternate approaches may be used to set these conditions. For instance, bounding values may be used for certain parameters to provide a more restrictive response for a specific acceptance criterion. Alternately, nominal conditions may be used if the event consequences are insensitive to a specific initial condition. A general description of the biasing of initial conditions, as applied to the non-LOCA transient analyses for the NPM, is provided below.

Initial Core Power

The initial core power is biased high by an amount equal to the heat balance uncertainty. As an example, consider full power operation with a heat balance uncertainty of ± 2 percent RTP. For this situation, the indicated core power is less than the actual core power by 2 percent RTP, i.e., the actual core power is 102 percent RTP while the indicated power is 100 percent RTP.

Initial Reactor Coolant System Average Temperature

At operating conditions the initial RCS average temperature is biased to either end of the range centered at the nominal value after consideration for any control system deadband and system/sensor measurement uncertainty.

As an example, consider a control system deadband and system/sensor measurement uncertainty of ± 10 degrees F for RCS average temperature. For this situation, the initial RCS average temperature is set to either -10 degrees F or +10 degrees F relative to the nominal temperature for the core power level of interest.

Initial Pressurizer Pressure

The initial pressurizer pressure is biased to either end of the range centered at the nominal value after consideration for any control system deadband and system/sensor measurement uncertainty.

As an example, consider a control system deadband and system/sensor measurement uncertainty of ± 70 psi for pressurizer pressure. For this situation, the initial pressurizer pressure is set to either -70 psi or +70 psi relative to the nominal pressure for the core power level of interest.

Initial Pressurizer Level

The initial pressurizer level is biased to either end of the range centered at the nominal value after consideration for any control system deadband and system/sensor measurement uncertainty.

As an example, consider a control system deadband and system/sensor measurement uncertainty of ± 8 percent for pressurizer level. For this situation, the initial pressurizer level is set to either -8 percent or +8 percent relative to the nominal level for the core power level of interest.

Initial Containment Pressure

The initial containment pressure is biased to either end of the range expected for normal operation.

As an example, consider a normal operational range of 0.037 psia to 2.0 psia for containment pressure. For this situation, the initial containment pressure is set to either 0.037 psia or 2.0 psia.

Initial Steam Generator Pressure

The initial SG pressure is biased to either end of the range centered at the nominal value after consideration for any control system deadband and system/sensor measurement uncertainty.

As an example, consider a control system deadband and system/sensor measurement uncertainty of ± 35 psi for SG pressure. For this situation, the initial SG pressure is set to either -35 psi or +35 psi relative to the nominal pressure for the core power level of interest.

Initial Feedwater Temperature

The initial feedwater temperature is biased to either end of the range centered at the nominal value after consideration for any control system deadband and system/sensor measurement uncertainty.

As an example, consider a control system deadband and system/sensor measurement uncertainty of ± 10 degrees F for feedwater temperature. For this situation, the initial feedwater temperature is set to either -10 degrees F or +10 degrees F relative to the nominal temperature for the core power level of interest.

Initial Reactor Coolant System Flow Rate

The initial RCS flow rate is biased to either end of the range expected for normal operation.

As an example, consider a normal operational range of 535 kg/s to 690 kg/s for RCS flow rate at 100 percent RTP. For this situation, the initial RCS flow rate is set to either 535 kg/s or 690 kg/s.

Initial Volume Weighted Core Average Fuel Temperature

The initial volume weighted core average fuel temperature is biased to either end of the range expected assuming limiting power histories, power shapes, and core burnups.

As an example, consider a BOC range of 960 degrees F to 1065 degrees F for volume weighted core average fuel temperature. For this situation, the initial fuel temperature is set to either 960 degrees F or 1065 degrees F.

Initial Reactor Pool Temperature

The initial reactor pool temperature is biased to either end of the range expected for normal operation.

As an example, consider a normal operational range of 40 degrees F to 200 degrees F for reactor pool temperature. For this situation, the initial reactor pool temperature is set to either 40 degrees F or 200 degrees F.

7.1.6.2 Valve Characteristics

The valve characteristics assumed for the non-LOCA transient analyses may differ depending on the type of valve. These differences are based on providing the most conservative characteristics for the acceptance criterion of interest.

A general description of the biasing of valve characteristics, as applied to the non-LOCA transient analyses for the NPM, is provided below.

Pressure Relief Valves

The characteristics applied to the pressure relief valves for the non-LOCA transient analyses include: 1) the nominal lift setpoint; 2) the lift tolerance; 3) the set pressure drift; 4) the accumulation; 5) the blowdown; 6) the blowdown tolerance; and, 7) the stroke time. In general, the characteristics are applied to delay opening a specific valve for as long as possible and to minimize the time the valve is open.

Isolation Valves

As an example, the following characteristics are applied to the isolation valves for the non-LOCA transient analyses. In general, the characteristics are applied to delay closing a specific valve for as long as possible.

- primary MSIV closing stroke time = 5 seconds
- secondary MSIV closing stroke time = 30 seconds
- FWIV closing stroke time = 5 seconds
- feedwater regulating valve closing stroke time = 30 seconds
- CVCS containment isolation valves closing stroke time = 5.0 seconds

Other Valves

As an example, the following characteristics are applied to the DHRS valves for the non-LOCA transient analyses. In general, the characteristics are applied to delay opening for as long as possible.

- DHRS open stroke time = 30 seconds

As an example, the following characteristics are applied to the feedwater check valves for the non-LOCA transient analyses. In general, the characteristics are applied to provide the most adverse characteristics for the acceptance criterion of interest.

- feedwater safety-related check valve closing stroke time = 1.0 second when reverse flow is more limiting; otherwise, a high reverse loss coefficient is employed
- feedwater nonsafety-related check valve closing stroke time = 1.0 second when used to stop flow following a single failure of the feedwater safety-related check valve

As an example, the following characteristics are applied to the turbine valves for the non-LOCA transient analyses. In general, the characteristics are applied to close as fast as possible.

- turbine stop valve closing stroke time = 0.1 second
- turbine control valve closing stroke time = 0.15 second

7.1.6.3 Analytical Limits and Response Times

The analytical limits are the limits of measured or calculated variables (such as pressures, temperatures, and levels) established by the safety analysis to assure that a safety limit is not exceeded. In the non-LOCA transient analysis, when an analytical limit is calculated to be reached, a reactor trip or engineered safeguards actuation is signaled, and then an appropriate response time is accounted for. The analytical limits (Table 6-2) and response times assumed for the non-LOCA transient analyses are selected to provide sufficient operating margin to prevent spurious actuation, yet still provide adequate protection for the acceptance criterion of interest. In general, the response times are applied to delay action while bounding the expected instrumentation delays. As an example, a diagram of the different types of limits and setpoints created to account for margin, allowances, and uncertainties is provided in Figure 7-2.

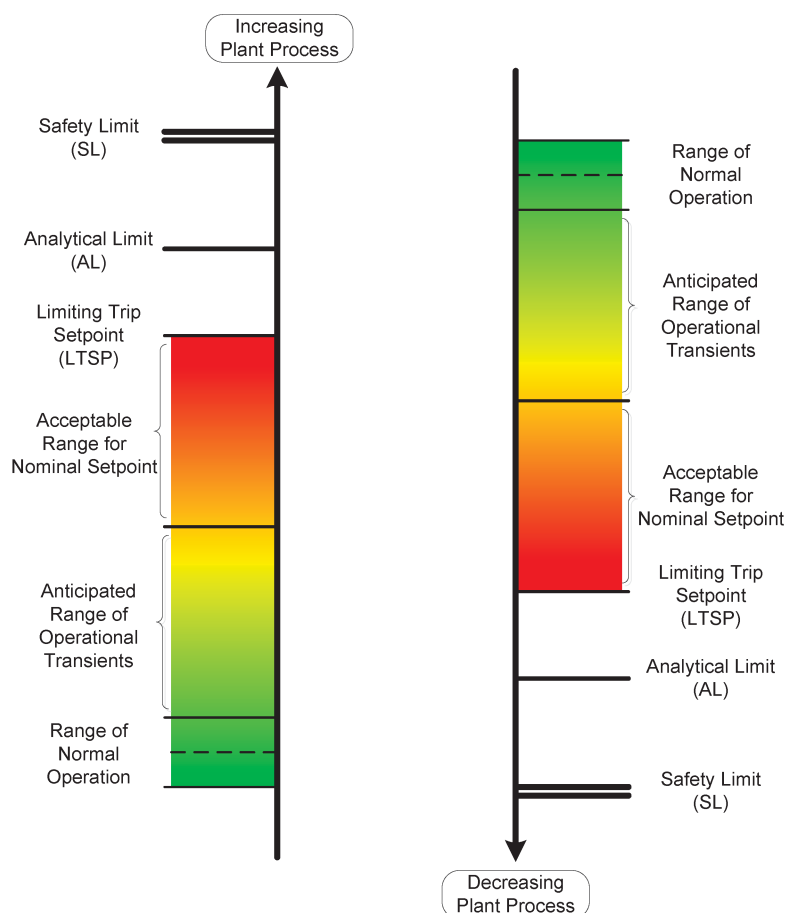


Figure 7-2 Example of setpoint relationships

The RTS response time is defined as the elapsed time from when the process reaches the analytical limit until the control rods are free to fall. Thus, the response time includes the control rod drive mechanism delatch time.

The ESFAS response time definition is similar, but does not include the control rod drive mechanism delatch time. Specifically, the ESFAS response time is defined as the elapsed time from when the process reaches the analytical limit until the actuation signal is received at the component (e.g. valve solenoid).

Examples of the analytical limits and actuation delays are summarized in Table 7-3.

Table 7-3 Examples of analytical limits and actuation delays (reactor trip system and engineered safety features actuation system)

Signal	Analytical Limit	Actuation Delay
High power	25% RTP (power < 15% RTP)	2.0 seconds
	120% RTP (power ≥ 15% RTP)	2.0 seconds
High count rate	5.0E+5 counts/second	2.0 seconds
Startup rate	3 decades/minute	31 seconds (source range)
	3 decades/minute	2 seconds (intermediate range)
High power rate	±15% RTP/minute	2.0 seconds
High RCS riser temperature	610°F	8.0 seconds
High containment pressure	9.5 psia	2.0 seconds
High pressurizer pressure	2000 psia	2.0 seconds
High pressurizer level	80%	3.0 seconds
Low pressurizer pressure	1720 psia	2.0 seconds
Low low pressurizer pressure	1600 psia	2.0 seconds
Low pressurizer level	35%	3.0 seconds
Low low pressurizer level	20%	3.0 seconds
Low steam pressure	300 psia	2.0 seconds
Low low steam pressure	100 psia	2.0 seconds
High steam pressure	800 psia	2.0 seconds
High steam superheat	150°F	8.0 seconds
Low steam superheat	0°F	8.0 seconds
Low RCS flow	1.7 ft ³ /second	6.0 seconds
Low low RCS flow	0.0 ft ³ /second	6.0 seconds
Low RCS level	350-390 inches	3.0 seconds
High CNV water level	220-260 inches	3.0 seconds
Low AC voltage	0 VAC	60.0 seconds

7.1.7 Credit for Nonsafety-related Components or Operator Actions

There are three occasions where nonsafety-related equipment is credited for event mitigation by the non-LOCA transient analyses. Listed below is the equipment associated with these occurrences.

1. The nonsafety-related secondary MSIV serves as the backup isolation device to the safety-related primary MSIV for isolation of the MSS piping penetrating the containment. (Section 7.1.4)
2. The nonsafety-related feedwater regulating valve serves as the backup isolation device to the safety related FWIV for isolation of the feedwater system piping penetrating the containment. (Section 7.1.4)
3. The nonsafety-related feedwater check valve serves as the backup isolation device to the safety-related feedwater check valve for isolation of the DHRS when reverse flow is experienced during a break in the feedwater system piping. (Section 7.1.4)

Operator actions credited for the non-LOCA transient analyses are typically justified and consistent with plant operating procedures. For the NPM, there are no occasions where operator action is credited for event mitigation by the non-LOCA transient analyses. Operator actions taken to prevent abnormal operating events from resulting in more severe events are excluded from consideration. For example, very small leaks of reactor coolant from the CVCS that do not result in automatic reactor trip for more than 30 minutes are considered an abnormal operating event where operators are expected to identify and isolate the leak before it results in a more severe event.

7.2 Event Specific Methodology

The non-LOCA event simulations are performed using conservative methodologies. Pertinent event-specific methodologies, as well as representative inputs and results for non-LOCA event simulations are presented herein, and compared with the regulatory acceptance criteria listed in Table 7-4. See Section 4.1 for additional discussion of Chapter 15 design basis events and acceptance criteria.

All criteria are considered for each event, and the criteria with the potential for being challenged are identified and evaluated in further detail (i.e., overcooling events will not challenge the acceptance criterion for primary side pressure, but may challenge the CHF acceptance criteria). An event-specific parameter that is relevant to the acceptance criterion may be described as “challenging” in the event-specific summary, however, it is recognized that the parameter may not present the highest challenge for any event.

Table 7-4 Regulatory acceptance criteria

Description	AOO Criteria	IE Criteria	Accident Criteria
RCS pressure ($P_{\text{design}} = 2100$ psia)	$\leq 110\%$ of design (2310 psia)	$\leq 120\%$ of design (2520 psia)	$\leq 120\%$ of design (2520 psia)
SG pressure ($P_{\text{design}} = 2100$ psia)	$\leq 110\%$ of design (2310 psia)	$\leq 120\%$ of design (2520 psia)	$\leq 120\%$ of design (2520 psia)
CHFR ⁽¹⁾	> Limit	Note (3)	Note (3)
Maximum fuel centerline temperature ⁽¹⁾	\leq Limit	Note (3)	Note (3)
Containment integrity ⁽²⁾	< Limits	< Limits	< Limits
Escalation of an AOO to an accident (AOO) or consequential loss of system functionality (IE or accident)?	No	No	No
Dose ⁽¹⁾	Normal operations	< Limit	< Limit

1. This criterion is confirmed as part of a separate follow-on analysis.
2. Containment integrity is evaluated by a separate analysis methodology.
3. If the minimum CHFR is less than or equal to the 95/95 CHFR limit, or if the maximum fuel centerline temperature exceeds the melting temperature, the fuel rod is assumed to be failed. If fuel failure is calculated, this is accounted for in the downstream radiological dose analysis.

For each event analyzed following the non-LOCA evaluation model, a description of the event progression, significant inputs and results, and representative results of sensitivity studies are presented in the following sections. Sensitivity studies are performed to identify plant conditions that result in bounding transient analyses. Studies that identify acceptance criteria challenges or bounding transient forcing functions are discussed as well. Other sensitivity studies that determine bounding inputs for RCS flow, fuel parameters, etc. may not necessarily be discussed for every event. The selection of parameters to be studied is focused on the acceptance criteria challenged by the event.

Unless otherwise noted, initial RCS flow is biased to the low condition in all event simulations because this is bounding for MCHF. {{

}}^{2(a),(c)}

Steam generator tube plugging is considered for each event in Section 7.2.1.3 in the "Initial conditions, biases, and conservatism" tables. The term, "Biased to the low condition" indicates no tube plugging is assumed. "Biased to the high condition" indicates {{ }}^{2(a),(c)} steam generator tube plugging.

In the NPM design, the rod control system is set to "insert only" mode at full power to prevent automatic withdrawal of the control bank at full power. Although this plant feature exists, the feature is not credited during events where control rod withdrawal results in a bounding result.

The NPM utilizes a nonsafety-related turbine bypass system sized to handle full steam flow rate at 100 percent RTP. As such, the turbine bypass valves open following a turbine trip to control the RCS temperature without steam relief to the atmosphere. Since the turbine bypass system enhances heat removal by the secondary system, these actions are not credited for the non-LOCA transient analyses. {{

}}^{2(a),(c)}

Separate analyses for subchannel CHF, fuel centerline temperature, and containment pressure calculations are performed using the appropriate licensed NuScale methodologies. Extended cooldown via the DHRS is considered as part of the system design.

7.2.1 Decrease in Feedwater Temperature

The methodology used to simulate a postulated decrease in feedwater temperature for the NPM, and an evaluation of the resulting representative plant response against the acceptance criteria for an AOO listed in Table 7-4, are presented below.

A description of the event including biases and conservatisms, sensitivity studies, single active failure (SAF) and loss of power (LOP) scenarios, challenging case, and acceptance criteria evaluation are presented in the following sections.

7.2.1.1 General Event Description and Analysis Methodology

The event is initiated by a feedwater system malfunction that causes a decrease in feedwater temperature, resulting in an unplanned overcooling of the RCS. The subsequent decrease in RCS temperature increases core reactivity due to moderator feedback, which raises reactor power. Decreasing average RCS temperature also prompts the control rod controller to withdraw the regulating bank from the core if automatic control is enabled. Rising reactor power causes RTS actuation on a high power signal (if reactor power increases at a high enough rate) or RTS and DHRS actuation on a high RCS riser temperature signal. If reactor trip is actuated by a high power signal, sustained overcooling of the RCS post-reactor trip results in continued decreasing temperature and pressure, eventually leading to DHRS actuation on the low PZR pressure signal.

Closure of the FWIVs following DHRS actuation isolates the SGs from the colder feedwater, ending the overcooling event. Core decay heat drives natural circulation, which transfers thermal energy from the RCS to the reactor pool via the DHRS. Passive DHRS cooling is established and the transient terminates with the NPM in a safe, stable condition. Table 7-5 lists the relevant acceptance criteria, SAF, and LOP scenarios.

The limiting MCHFR occurs when the event is initiated from full power conditions, the change in feedwater temperature is maximized, {{

}}^{2(a),(c)} For overcooling events, the high power analytical limit is increased, for example from 120 percent to 125 percent RTP. This is to account for the decalibration of the excore neutron detectors as downcomer density increases in response to a cooldown event. {{

}}^{2(a),(c)}

To maximize the overall feedwater temperature change, the feedwater temperature transient starts at the initial (full power) feedwater temperature biased to the high condition, and terminates at the coldest temperature in the secondary, which is saturation temperature at condenser vacuum conditions. A sensitivity study on feedwater temperature cooldown rate is performed to identify the rate that results in reactor trip on core power and high RCS riser temperature signals at approximately the same time.

{{

}}^{2(a),(c)}

Additional sensitivity studies are performed on other parameters, as necessary, to identify the case(s) with a potentially limiting MCHFR. The NRELAP5 MCHFR pre-screening process is employed to identify the cases sent for a detailed subchannel evaluation, covered by a separate methodology.

Table 7-5 Acceptance criteria, single active failure, loss of power scenarios – decrease in feedwater temperature

Acceptance Criteria / Single Active Failure / Loss of Power Scenarios of Interest	Discussion
MCHFR	CHF is the challenged acceptance criterion for this overcooling event. (Reactivity insertion rates from the overcooling event are insufficient to challenge fuel centerline temperature.)
No single failure	The challenging cases occur when all equipment operates as designed.
No loss of power	All loss of power scenarios terminate feedwater and/or trip the reactor, thus mitigating the overcooling event.

7.2.1.2 Acceptance Criteria

Evaluation of the most challenging case relative to the acceptance criteria is presented in Table 7-6.

Table 7-6 Acceptance criteria – decrease in feedwater temperature

Acceptance Criteria	Discussion
Primary pressure	Due to the depressurizing nature of the event, sensitivities that maximize primary pressure are not analyzed. Peak primary pressure resulting from a decrease in feedwater temperature is bounded by other AOO events.
Secondary pressure	Pressure in the portion of the secondary system between the FWIVs and MSIVs increases rapidly post-DHRS actuation. However, due to the depressurizing nature of this cooldown event, sensitivities that maximize peak secondary pressure are not analyzed. Peak secondary pressure resulting from a decrease in feedwater temperature is bounded by other AOO events.
CHFR	Due to the increase in reactor power and subsequent reduction of MCHFR, this acceptance criterion is challenged for the decrease in feedwater temperature event. Consequently, sensitivity cases are performed to support the follow-on MCHFR evaluation.
Maximum fuel centerline temperature	This criterion is evaluated by downstream subchannel analysis, however the reactivity insertion rate from the cooldown event is insufficient to challenge the temperature limit.
Containment integrity	Containment integrity is evaluated by a separate analysis methodology.
Escalation of an AOO to an accident	This criterion is satisfied by demonstrating stable RCS flow rates and constant or downward trending RCS and DHRS pressures and temperatures exist at the end of the transient, all acceptance criteria evaluated in the transient analysis are met, and shutdown margin is maintained at the end of the transient. RCS conditions during extended DHRS cooling are addressed in a separate analysis.

7.2.1.3 Biases, Conservatisms, and Sensitivity Studies

The biases and conservatisms indicated in Table 7-7 are considered in identifying a bounding transient simulation for MCHFR.

Table 7-7 Initial conditions, biases, and conservatisms – decrease in feedwater temperature

Parameter	Bias / Conservatism	Basis
Initial reactor power	RTP biased upwards to account for measurement uncertainty.	{{ }} ^{2(a),(c)}
Initial RCS average temperature	Biased to the high condition.	{{ }} ^{2(a),(c)}
Initial RCS flow rate	Biased to the low condition.	{{ }} ^{2(a),(c)}
Initial PZR pressure	Biased to the high condition	{{ }} ^{2(a),(c)}
Initial PZR level	Biased to the high condition.	{{ }} ^{2(a),(c)}
Initial feedwater temperature	Varied.	{{ }} ^{2(a),(c)}
Initial fuel temperature	Nominal.	{{ }} ^{2(a),(c)}
Moderator Temperature Coefficient (MTC)	Biased to EOC conditions.	{{ }} ^{2(a),(c)}
Kinetics	Biased to the EOC condition.	{{ }} ^{2(a),(c)}
Decay heat	Biased to the low condition.	{{ }} ^{2(a),(c)}
Initial SG pressure ⁽¹⁾	Varied.	{{ }} ^{2(a),(c)}
SG heat transfer	Nominal	{{ }} ^{2(a),(c)}

Parameter	Bias / Conservatism	Basis
RSV lift setpoint	Nominal	{{ }} ^{2(a),(c)}
SG tube plugging	Biased to the low condition.	{{ }} ^{2(a),(c)}
Minimum feedwater temperature	Biased to the low condition.	{{ }} ^{2(a),(c)}
Feedwater temperature cooldown rate	Varied	{{ }} ^{2(a),(c)}
RCS Temperature Control Automatic rod control	Enabled.	{{
Boron concentration	Not credited.	{{ }} ^{2(a),(c)}

Parameter	Bias / Conservatism	Basis
PZR Pressure Control PZR spray (normal)	Disabled.	{
(bypass)	Nominal.	
PZR heaters (non-prop.)	Nominal.	
(prop.)	Nominal.	
PZR Level Control Charging	Not credited.	{
Letdown	Disabled.	}} ^{2(a),(c)}
Steam Pressure Control Turbine throttle valves	Varied.	
Turbine bypass valves	Disabled.	}} ^{2(a),(c)}

1. $\{\{ \dots \}^{2(a),(c)}$

Representative results for two studies, which evaluate the effects of fuel exposure and initial fuel temperature over a range of feedwater temperature transients, are presented in Table 7-8 and Table 7-9. {{

$$\}}^{2(a),(c)}$$

The next sensitivity study identifies the feedwater temperature transient time at which the transition from the high power trip to the high RCS riser temperature trip occurs. This is the point at which the challenging MCHFR occurs because faster cooldown rates will trip on high power before the limiting RCS thermal condition can develop, and slower cooldown rates will trip on high RCS riser temperature before reactor power has increased to its maximum possible value. Representative results of this study, which are presented in Table 7-10, indicate that an NRELAP5 MCHFR of 2.591 occurs when the feedwater is allowed to decrease from 307.5 degrees F to 100 degrees F over a time period of 176 seconds, producing the most challenging conditions for this event.

Table 7-10 Representative feedwater temperature transient study

{{

}}^{2(a),(c)}

Two additional sensitivity studies are performed to evaluate the effects of steam system boundary condition type on MCHFR, and to assess the effects of a single active failure of an MSIV to isolate. Representative results for these studies are presented in Table 7-11.

The boundary condition sensitivity study evaluates the effects of a constant flow at the exit of the MSS, which allows the steam pressure to move in response to the transient. (Previous studies model a constant pressure boundary condition, which allows flow to vary while maintaining pressure.) {{

}}^{2(a),(c)}

The single active failure sensitivity study repeats the boundary condition study, adding the failure of an MSIV to isolate. Because the isolation signal occurs in conjunction with DHRS actuation post reactor trip, neither isolation, nor a failure to isolate, has any effect on the most challenging aspect of the transient for MCHFR which results in reactor trip on high RCS riser temperature and high power signals simultaneously. Once the heat flux begins to decrease subsequent to RTS actuation, the challenge to MCHFR has concluded.

Table 7-11 Representative boundary condition type / single active failure studies

{{

}}^{2(a),(c)}

7.2.2 Increase in Feedwater Flow

The methodology used to simulate a postulated increase in feedwater flow for the NPM, and an evaluation of the resulting representative plant response against the acceptance criteria for an AOO listed in Table 7-4, are presented below.

A description of the event including biases and conservatisms, sensitivity studies, single active failure, and loss of power scenarios, challenging case, and acceptance criteria evaluation are presented in the following sections.

7.2.2.1 General Event Description

A feedwater system malfunction that causes an increase in feedwater flow results in an unplanned overcooling of the RCS. The subsequent decrease in RCS temperature increases core reactivity due to moderator feedback which raises reactor power. Decreasing average RCS temperature will also prompt the control rod controller to withdraw the regulating bank from the core if automatic control is enabled. Rising reactor power will cause RTS actuation on the high power signal. The feedwater flow increase can also cause RTS actuation on low steam line superheat or high steam line pressure. DHRS actuates on the low steam line superheat or high steam line pressure signals.

Closure of the FWIVs following DHRS actuation isolates the SGs from the feedwater source, ending the overcooling event. Core decay heat drives natural circulation which transfers thermal energy from the RCS to the reactor pool via the DHRS. Passive DHRS cooling is established and the transient calculation is terminated with the NPM in a safe, stable condition. Table 7-12 lists the relevant acceptance criteria, SAF, and LOP scenarios.

A rapid (step) increase in feedwater flow is simulated. The limiting MCHFR occurs when the event is initiated from full power conditions, {{

}}^{2(a),(c)} For

overcooling events, the high power analytical limit is increased, for example from 120 percent to 125 percent RTP. This is to account for the decalibration of the excore neutron detectors as downcomer density increases in response to a cooldown event. The increase is based on an appropriate decalibration factor (change-in-power-per-change-in-temperature) and considering the downcomer temperature decrease during the overcooling events.

{{

}}^{2(a),(c)}. Additional sensitivity studies are performed on other parameters, as necessary, to identify the case(s) with a potentially limiting MCHFR.

The NRELAP5 MCHFR pre-screening process is employed to identify the cases sent for a detailed subchannel evaluation.

Table 7-12 Acceptance criteria, single active failure, loss of power scenarios – increase in feedwater flow

Acceptance Criteria / Single Active Failure / Loss of Power Scenarios of Interest	Discussion
MCHFR	CHF is challenged for this overcooling event. (Reactivity insertion rates from the overcooling event are insufficient to challenge fuel centerline temperature.)
No single failure	The challenging cases occur when all equipment operates as designed.
No loss of power	All loss of power scenarios terminate feedwater and/or trip the reactor, thus mitigating the overcooling event.

7.2.2.2 Acceptance Criteria

Evaluation of the most challenging case relative to the acceptance criteria is presented in Table 7-13.

Table 7-13 Acceptance criteria – increase in feedwater flow

Acceptance Criteria	Discussion
Primary pressure	Due to the depressurizing nature of the event, sensitivities that maximize primary pressure are not analyzed. Peak primary pressure resulting from an increase in feedwater flow is bounded by other AOO events.
Secondary pressure	A rapid initial secondary pressure increase occurs prior to RTS actuation. Pressure in the secondary side continues to increase to the peak following DHRS actuation. This second pressure increase is expected behavior following DHRS actuation and is not a direct consequence of the increase in feedwater flow event itself.
CHFR	Due to the increase in reactor power and subsequent reduction of MCHFR, this acceptance criterion is challenged for the increase in feedwater flow event. Consequently, sensitivity cases are performed to support the follow-on MCHFR evaluation.

Acceptance Criteria	Discussion
Maximum fuel centerline temperature	This criterion is evaluated by downstream subchannel analysis, however the reactivity insertion rate from the cooldown event is insufficient to challenge the temperature limit.
Containment integrity	Containment integrity is evaluated by a separate analysis methodology.
Escalation of an AOO to an accident	This criterion is satisfied by demonstrating stable RCS flow rates and constant or downward trending RCS and DHRS pressures and temperatures exist at the end of the transient, all acceptance criteria evaluated in the transient analysis are met, and shutdown margin is maintained at the end of the transient. RCS conditions during extended DHRS cooling are addressed in a separate analysis.

7.2.2.3 Biases, Conservatisms, and Sensitivity Studies

The biases and conservatisms indicated in Table 7-14 are considered in identifying a bounding transient simulation.

Table 7-14 Initial conditions, biases, and conservatisms – increase in feedwater flow

Parameter	Bias / Conservatism	Basis
Initial reactor power	RTP biased upwards to account for measurement uncertainty.	{{ }} ^{2(a),(c)}
Initial RCS average temperature	Biased to the high condition.	{{ }} ^{2(a),(c)}
Initial RCS flow rate	Biased to the low condition.	{{ }} ^{2(a),(c)}
Initial PZR pressure	Biased to the high condition.	{{ }} ^{2(a),(c)}
Initial PZR level	Biased to the high condition.	{{ }} ^{2(a),(c)}

© Copyright 2019 by NuScale Power, LLC

Parameter	Bias / Conservatism	Basis
RCS Temperature Control Automatic rod control	Enabled.	{
Boron concentration	Not credited.	
		{
PZR Pressure Control PZR spray (normal)	Disabled.	{
(bypass)	Nominal.	
PZR heaters (non-prop.)	Nominal.	
(prop.)	Nominal.	
		{
PZR Level Control Charging	Not credited.	{
Letdown	Disabled.	
		{

1. $\{\{ \dots \}^{2(a),(c)}$

}}^{2(a),(c)} Representative results for these studies are presented in Table 7-15 and Table 7-16.

Table 7-15 Representative increase in feedwater flow study – high SG performance with maximum power and minimum RCS flow

{{

}}^{2(a),(c)}

Table 7-16 Representative increase in feedwater flow study – low SG performance with maximum power and minimum RCS flow

{{

}}^{2(a),(c)}

7.2.3 Increase in Steam Flow

The methodology used to simulate a postulated increase in steam flow for the NPM, and an evaluation of the resulting representative plant response against the acceptance criteria for an AOO listed in Table 7-4, are presented below.

A description of the event including biases and conservatisms, sensitivity studies, single active failure (SAF) and loss of power (LOP) scenarios, challenging case, and acceptance criteria evaluation are presented in the following sections.

7.2.3.1 General Event Description

In the NPM design, two main steam lines exit the CNV, and combine to form a common main steam line that connects to the high pressure turbine. The turbine bypass and main steam safety valves are located in the common main steam line, which is downstream of the MSIVs. A spurious opening of the turbine bypass valve or a main steam safety valve would cause an increase in steam flow which results in an unplanned overcooling of the RCS. The subsequent decrease in RCS temperature increases core reactivity due to moderator feedback which raises reactor power. Decreasing average RCS temperature will also prompt the control rod controller to withdraw the regulating bank from the core if automatic control is enabled (rod withdrawal at 100 percent power is inhibited, however, it is conservatively allowed in the analysis). Rising reactor power will cause RTS actuation on a high power signal (if reactor power increases at a high enough rate) or RTS and DHRS actuation on a high RCS riser temperature signal. Additionally, a sufficiently large increase in steam flow would rapidly depressurize the secondary system and cause RTS and DHRS actuation on the low steam pressure signal.

If reactor trip is actuated by a high power signal, sustained overcooling of the RCS post-reactor trip will continue decreasing RCS temperature and pressure, eventually leading to DHRS actuation on the low PZR level signal. Closure of the FWIVs and MSIVs following DHRS actuation isolates the steam generators which ends the overcooling event. Core decay heat drives natural circulation which transfers thermal energy from the RCS to the reactor pool via the DHRS. Passive DHRS cooling is established and the transient calculation is terminated with the NPM in a safe, stable condition. Table 7-17 lists the relevant acceptance criteria, SAF, and LOP scenarios.

The limiting MCHFR occurs when the event is initiated from full power conditions, and the increase in steam flow is such that the attendant increase in power remains just below the high power analytical limit, and actuates the RTS sometime later (after the minimum CHFR conditions develop) on high RCS riser temperature or low steam pressure. For overcooling events, the high power analytical limit is increased, for example from 120 percent to 125 percent RTP. This is to account for the decalibration of the excore neutron detectors as downcomer density increases in response to a cooldown event. The increase is based on an appropriate decalibration factor (change-in-power-per-change-in-temperature) and considering the downcomer temperature decrease during the overcooling events.

The increase in steam flow event starts at the initial (full power) steam flow. Sensitivity studies are performed on the degree of steam flow increase and steam generator heat transfer to identify the case(s) with a potentially limiting MCHFR. The NRELAP5 MCHFR pre-screening process is employed to identify the cases sent for a detailed subchannel evaluation.

Table 7-17 Acceptance criteria, single active failure, loss of power scenarios – increase in steam flow

Acceptance Criteria / Single Active Failure / Loss of Power Scenarios of Interest	Discussion
MCHFR	CHF is challenged for this overcooling event. (Reactivity insertion rates from the overcooling event are insufficient to challenge fuel centerline temperature.)
No single failure	Note that a single active failure of a FWIV to close would occur after RTS and DHRS actuation, subsequent to when the MCHFR occurs. Consequently, the MCHFR occurs before the single active failure of an FWIV to close could affect the transient. Otherwise, the challenging cases occur when all equipment operates as designed.
No loss of power	All loss of power scenarios terminate feedwater and/or trip the reactor, thus mitigating the overcooling event.

7.2.3.2 Acceptance Criteria

Evaluation of the most challenging case relative to the acceptance criteria is presented in Table 7-18.

Table 7-18 Acceptance criteria – increase in steam flow

Acceptance Criteria	Discussion
Primary pressure	Primary pressure initially drops as inventory shrinks due to increased heat removal. As reactor power increases and as the PZR heaters respond, an increase (typically less than 100 psi) in primary pressure is observed.
Secondary pressure	Peak secondary pressure does not change significantly during the initial phase of the transient due to the relatively small increase in steam flow rate analyzed in the challenging case. It is only after DHRS actuation, accompanied by the closure of the FWIVs and MSIVs, that secondary pressure begins to increase rapidly. Steam generator pressure increase resulting from MS isolation is expected and is not a direct consequence of the increase in steam flow event itself.

CHFR	Due to the increase in reactor power and subsequent reduction of MCHFR, this acceptance criterion is challenged for the increase in steam flow event. Consequently, sensitivity cases are performed to support the follow-on MCHFR evaluation.
Maximum fuel centerline temperature	This criterion is evaluated by downstream subchannel analysis, however the reactivity insertion rate from the cooldown event is insufficient to challenge the temperature limit.
Containment integrity	Containment integrity is evaluated by a separate analysis methodology.
Escalation of an AOO to an accident	This criterion is satisfied by demonstrating stable RCS flow rates and constant or downward trending RCS and DHRS pressures and temperatures exist at the end of the transient, all acceptance criteria evaluated in the transient analysis are met, and shutdown margin is maintained at the end of the transient. RCS conditions during extended DHRS cooling are addressed in a separate analysis.

7.2.3.3 Biases, Conservatisms, and Sensitivity Studies

The biases and conservatisms indicated in Table 7-19 are considered in identifying a bounding transient simulation for MCHFR.

Table 7-19 Initial conditions, biases, and conservatisms – increase in steam flow

Parameter	Bias / Conservatism	Basis
Initial reactor power	RTP biased upwards to account for measurement uncertainty.	{{ }} ^{2(a),(c)}
Initial RCS average temperature	Biased to the high condition.	{{ }} ^{2(a),(c)}
Initial RCS flow rate	Biased to the low condition.	{{ }} ^{2(a),(c)}
Initial PZR pressure	Biased to the high condition.	{{ }} ^{2(a),(c)}
Initial PZR level	Biased to the high condition.	{{ }} ^{2(a),(c)}
Initial feedwater temperature	Nominal.	{{ }} ^{2(a),(c)}
Initial fuel temperature	Nominal.	{{ }} ^{2(a),(c)}

Parameter	Bias / Conservatism	Basis
MTC	Biased to EOC conditions.	{{ }} ^{2(a),(c)}
Kinetics	Biased to the EOC condition.	{{ }} ^{2(a),(c)}
Decay heat	Biased to the low condition.	{{ }} ^{2(a),(c)}
Initial SG pressure ⁽¹⁾	Biased to the high condition.	{{ }} ^{2(a),(c)}
SG heat transfer	Nominal	{{ }} ^{2(a),(c)}
RSV lift setpoint	Nominal	{{ }} ^{2(a),(c)}
SG tube plugging	Biased to the low condition.	{{ }} ^{2(a),(c)}
Steam flow increase	Varied	{{ }} ^{2(a),(c)}

Parameter	Bias / Conservatism	Basis
RCS Temperature Control Automatic rod control	Enabled.	{
Boron concentration	Not credited.	
		}} ^{2(a),(c)}
PZR Pressure Control PZR spray (normal)	Disabled.	{
(bypass)	Nominal.	
PZR heaters (non-prop.)	Nominal.	
(prop.)	Nominal.	
		}} ^{2(a),(c)}
PZR Level Control Charging	Not credited.	{
Letdown	Disabled.	
		}} ^{2(a),(c)}
Steam Pressure Control Turbine throttle valves	N/A.	Not applicable to this event.
Turbine bypass valves	N/A.	Not applicable to this event.

1. $\{\{ \dots \} \}^{2(a), (c)}$
2. $\{\{ \dots \} \}$

Sensitivity studies are performed as needed to identify the limiting response(s) for the acceptance criteria parameter(s) challenged by the event (i.e., system pressures for overheating events, MCHFR for overcooling events). Consequently, sensitivity studies are performed to identify cases with the lowest CHFR response for this overcooling event. For example, two sensitivity studies are performed to identify the most challenging increase in steam flow for MCHFR. {}

© Copyright 2019 by NuScale Power, LLC

Table 7-20 Representative steam flow study – nominal steam generator heat transfer

{{

}}^{2(a),(c)}

Table 7-21 Representative steam flow study – steam generator heat transfer biased low

{{

}}^{2(a),(c)}

7.2.4 Steam System Piping Failure Inside or Outside of Containment

The methodology used to simulate a postulated steam system piping failure for the NPM, and an evaluation of the resulting representative plant response against the acceptance criteria listed in Table 7-4, are presented below. Since both split breaks (relatively higher event frequency) and double-ended guillotine breaks (relatively lower event frequency) are analyzed, the more restrictive AOO criteria for system pressures, critical heat flux ratio, and fuel centerline melt applicable to breaks with higher event frequency are used in the evaluation. Radiological dose consequences are assessed as part of the downstream accident radiological dose analysis, documented in a separate report, and compared against the appropriate acceptance criteria.

A description of the event including biases and conservatisms, sensitivity studies, single active failure (SAF) and loss of power (LOP) scenarios, challenging case, and acceptance criteria evaluation are presented in the following sections.

7.2.4.1 General Event Description

The steam line break event ranges from small breaks to double ended ruptures of a main steam line causing an increase in steam flow and an over cooling of the RCS. This event can occur inside or outside the containment vessel (CNV). A break inside CNV will cause a rapid pressurization of the CNV resulting in a reactor trip and CNV isolation with a DHRS actuation. This break location is non-limiting for pressure and MCHFR but challenging to the DHRS as one loop is disabled with the break inside the CNV. A steam line break outside of the CNV will cause an increase in steam flow event that will cause either a low SG pressure trip or a high core power trip due to the reactor power response from the decreased RCS temperature. The break flow will be stopped by the MSIVs closing and depressurization of the steam system piping. Smaller breaks will cause a slower loss of secondary pressure due to the increased steam demand which could cause a high core power trip. These smaller breaks can result in a significant delay in detection time, making the small break cases challenging for MCHFR. Reactor trip and transition to stable DHRS flow eventually terminate the transients and bring the NPM to a safe, stable condition.

For this overcooling event, the high power analytical limit is increased, for example from 120 percent to 125 percent RTP. This is to account for the decalibration of the excore neutron detectors as downcomer density increases in response to a cooldown event. The increase is based on an appropriate decalibration factor (change-in-power-per-change-in-temperature) and considering the downcomer temperature decrease during the overcooling events.

{{

}}^{2(a),(c)}

The relevant acceptance criteria, SAF, and LOP scenarios are listed in Table 7-22.

Table 7-22 Acceptance criteria, single active failure, loss of power scenarios – steam line break

Acceptance Criteria / Single Active Failure / Loss of Power Scenarios of Interest	Discussion
MCHFR	Critical heat flux is potentially challenged for this overcooling event. (Reactivity insertion rates from the overcooling event are insufficient to challenge fuel centerline temperature.)
radiological consequences	A postulated break in the main steam line is evaluated for radiological consequences.
Failure of one MSIV to close on the train with break	MSIV single failure has no effect to MCHFR since DHRS actuation is not before the time when MCHFR occurs. MSIV single failure is bounding for mass releases for break locations outside the CNV, which will be used in the downstream radiological analysis.
Failure of one FWIV to close on the train with the break	FWIV single failure has no effect to MCHFR since DHRS actuation is not before the time when MCHFR occurs. FWIV single failure is bounding for mass releases for break locations inside the CNV, which will be used in the downstream radiological analysis.
No loss of power	Loss of power scenarios terminate feedwater and/or trip the reactor, thus mitigating the overcooling event.

7.2.4.2 Acceptance Criteria

Evaluation of the most challenging case relative to the acceptance criteria is presented in Table 7-23.

Table 7-23 Acceptance criteria – steam line break

Acceptance Criteria	Discussion
Primary pressure	Due to the depressurizing nature of this cooldown event, primary pressure remains below the acceptance criterion for peak primary pressure.
Secondary pressure	Due to the depressurizing nature of this cooldown event, secondary pressure remains below the acceptance criterion for peak secondary pressure.
Critical heat flux ratio	This criterion is evaluated by downstream subchannel analysis. Sensitivity cases are performed to support the follow-on MCHFR evaluation.
Maximum fuel centerline temperature	This criterion is evaluated by downstream subchannel analysis, however the reactivity insertion rate from the cooldown event is insufficient to challenge the temperature limit.
Containment integrity	Containment integrity is evaluated by a separate analysis methodology.
Escalation to a more serious accident or consequential loss of functionality	This criterion is satisfied by demonstrating stable RCS flow rates and constant or downward trending RCS and DHRS pressures and temperatures exist at the end of the transient, all acceptance criteria evaluated in the transient analysis are met, and shutdown margin is maintained at the end of the transient. RCS conditions during extended DHRS cooling are addressed in a separate analysis.

7.2.4.3 Biases, Conservatisms, and Sensitivity Studies

The biases and conservatisms indicated in Table 7-24 are considered in identifying a bounding transient simulation for MCHFR and mass release.

Table 7-24 Initial conditions, biases, and conservatisms – steam line break

Parameter	Bias / Conservatism	Basis
Initial reactor power	Biased upwards to account for measurement uncertainty.	{{ }} ^{2(a),(c)}
Initial RCS average temperature	Varied.	{{ }} ^{2(a),(c)}
Initial RCS flow rate	Biased to the low condition.	{{ }} ^{2(a),(c)}

Parameter	Bias / Conservatism	Basis
Initial PZR pressure	Varied	{{ }} ^{2(a),(c)}
Initial PZR level	Varied	{{ }} ^{2(a),(c)}
Initial feedwater temperature	Varied.	{{ }} ^{2(a),(c)}
Initial fuel temperature	Biased to the low condition.	{{ }} ^{2(a),(c)}
MTC	Both EOC and BOC conditions.	{{ }} ^{2(a),(c)}
Kinetics	Both EOC and BOC conditions.	{{ }} ^{2(a),(c)}
Decay heat	Both high and low conditions	{{ }} ^{2(a),(c)}
Initial SG pressure ⁽¹⁾	Varied.	{{ }} ^{2(a),(c)}
SG heat transfer	Nominal.	{{ }} ^{2(a),(c)}
RSV lift setpoint	Biased to the high condition.	{{ }} ^{2(a),(c)}
SG tube plugging	Varied to consider both the low and high ends of the allowable range.	{{ }} ^{2(a),(c)}

Parameter	Bias / Conservatism	Basis
RCS Temperature Control Automatic rod control	Enabled. (MCHFR)	{
	Varied. (dose)	
Boron concentration	Not credited.	
		} ^{2(a),(c)}
PZR Pressure Control PZR spray (normal)	Disabled.	{
(bypass)	Nominal.	
PZR heaters (non-prop.)	Enabled.	
(prop.)	Nominal.	
		} ^{2(a),(c)}

Parameter	Bias / Conservatism	Basis
PZR Level Control Charging	Not credited.	{
Letdown	Disabled.	
		} ^{2(a),(c)}
Steam Pressure Control Turbine throttle valves	Enabled.	{
Turbine bypass valves	Disabled.	
		} ^{2(a),(c)}
Feedwater and Turbine Load Control feedwater pump speed	Disabled.	{
		} ^{2(a),(c)}
CNV Pressure Control CNV evacuation system	Enabled.	{
		} ^{2(a),(c)}

1. { }^{2(a),(c)}

Sensitivity studies are performed as needed to identify the limiting response(s) for the acceptance criteria parameter(s) challenged by the event. Consequently, sensitivity studies are performed to identify cases with the lowest CHFR response and challenging mass releases for this overcooling event. Representative results for this study are presented in Table 7-25. In the cases modeling breaks outside of containment, the MSIV

on the train with the break is assumed to fail to close, resulting in the complete emptying of the affected SG.

In cases modeling breaks inside of containment, the FWIV on the train with the break is assumed to fail to close, which maximizes the event consequences. Break size is the fraction (percent) of the pipe cross section area.

{{

}}^{2(a),(c)}

Table 7-25 Steam line break study

{{

}}^{2(a),(c)}

7.2.5 Containment Flooding / Loss of Containment Vacuum

The methodology used to simulate a postulated containment flooding / loss of containment vacuum for the NPM, and an evaluation of the resulting representative plant response in comparison to the acceptance criteria for an AOO listed in Table 7-4, are presented below.

A description of the event including biases and conservatisms, sensitivity studies, SAF and LOP scenarios, challenging case, and acceptance criteria evaluation are presented in the following sections. This AOO is unique to the NPM design.

7.2.5.1 General Event Description and Methodology

The “loss of containment vacuum” terminology refers specifically to vapor / air or minimal water leakage into the containment vessel (CNV) that does not result in any water build-up inside the CNV. The containment evacuation (CE) system is used to maintain a vacuum in the CNV during normal operation. If the leakage rate exceeds the CE system’s capacity, a high containment pressure (> 9.5 psia) signal can occur, which will trip the reactor and isolate all containment penetrations.

The “containment flooding” terminology refers to liquid build-up in the CNV that can potentially cause loss of CNV vacuum and result in containment isolation and reactor trip.

The potential CNV flooding sources considered are pipe ruptures inside the CNV. Depending on the CNV operating pressure, some of these lines inside the CNV carry fluid at a lower temperature than the CNV saturation temperature. If one of these low temperature lines ruptures, flashing inside the CNV will not occur instantly, so the high containment pressure analytical limit will not be immediately reached. Therefore these low temperature line breaks can potentially create different challenges than the breaks in other lines carrying higher temperature fluid such as main steam and feedwater lines.

The CNV flooding sources due to a pipe rupture inside containment include a feedwater (FW) line break, main steam (MS) line break, chemical and volume control system (CVCS) line break, high point vent (HPV) pipe break, and reactor component cooling water (RCCW) line break. Only a RCCW line break inside the CNV is considered as a flooding source for the CNV flooding / loss of CNV vacuum event. Other break analyses are evaluated as separate initiating events.

During this event, heat removal from the RCS increases due to loss of CNV vacuum or CNV flooding from RCCW. As a result, the CNV flooding/loss of CNV vacuum event does not introduce more challenging conditions for RCS pressure and secondary side pressure compared to other AOOs such as the overheating events.

Due to the overcooling effect of the event, an increase in reactor power and subsequent reduction of MCHFR may occur. A series of CNV flooding sensitivities are conducted to assess the effects on MCHFR from break flow, temperature, containment pressure, primary pressure, and pool temperature.

{{

}}^{2(a),(c)} The purpose is to show that there is little observable difference between the two cases with the change in reactor power and the additional heat loss is minimal. Any loss of CNV vacuum cases that cause high CNV pressure trip should be bounded by the results obtained from the CNV flooding cases that result in reactor trip.

The relevant acceptance criteria, single active failure, and loss of power scenarios are listed in Table 7-26.

Table 7-26 Acceptance criteria, single active failure, loss of power scenarios – containment flooding / loss of containment vacuum

Acceptance Criteria / Single Active Failure / Loss of Power Scenarios of Interest	Discussion
MCHFR	MCHFR is potentially challenged during this overcooling event. (Reactivity insertion rates from the overcooling event are insufficient to challenge fuel centerline temperature.)
No single failure	The challenging cases occur when all equipment operates as designed.
No loss of power	A loss of AC power at event initiation is non-limiting because reactor trip and containment isolation mitigate the event, while a loss of AC power coincident with turbine trip does not alter the MCHFR because the time of reactor trip is not changed.

7.2.5.2 Acceptance Criteria

Evaluation of the most challenging case(s) relative to the acceptance criteria is presented in Table 7-27.

Table 7-27 Acceptance criteria – containment flooding / loss of containment vacuum

Acceptance Criteria	Discussion
Primary pressure	Due to the depressurizing nature of the event, sensitivities that maximize primary pressure are not analyzed. Peak primary pressure resulting from CNV flooding/loss of CNV vacuum is bounded by other AOO events.
Secondary pressure	Due to the depressurizing nature of this cooldown event, secondary pressure remains below the acceptance criterion for peak secondary pressure.
Critical heat flux ratio	This criterion is evaluated by downstream subchannel analysis.
Maximum fuel centerline temperature	This criterion is evaluated by downstream subchannel analysis, however the reactivity insertion rate from the cooldown event is insufficient to challenge the temperature limit.
Containment integrity	Containment integrity is evaluated by a separate analysis methodology.
Escalation of an AOO to an accident	This criterion is satisfied by demonstrating stable RCS flow rates and constant or downward trending RCS and DHRS pressures and temperatures exist at the end of the transient, all acceptance criteria evaluated in the transient analysis are met, and shutdown margin is maintained at the end of the transient. RCS conditions during extended DHRS cooling are addressed in a separate analysis.

7.2.5.3 Biases, Conservatisms, and Sensitivity Studies

The biases and conservatisms presented in Table 7-28 are considered in order to identify the bounding transient simulation for MCHFR for the CNV flooding/loss of CNV vacuum event.

Table 7-28 Initial conditions, biases, and conservatisms – containment flooding / loss of containment vacuum

Parameter	Bias / Conservatism	Basis
Initial reactor power	RTP biased upwards to account for measurement uncertainty.	{{ }} ^{2(a),(c)}
Initial RCS average temperature	Biased to the high condition.	{{ }} ^{2(a),(c)}
Initial RCS flow rate	Biased to the low condition.	{{ }} ^{2(a),(c)}
Initial PZR pressure	Varied	{{ }} ^{2(a),(c)}
Initial PZR level	Nominal	{{ }} ^{2(a),(c)}
Initial feedwater temperature	Nominal	{{ }} ^{2(a),(c)}
Initial fuel temperature	Nominal	{{ }} ^{2(a),(c)}
MTC	Biased to the EOC condition.	{{ }} ^{2(a),(c)}
Kinetics	Biased to the EOC condition.	{{ }} ^{2(a),(c)}
Decay heat	Biased to the high condition.	{{ }} ^{2(a),(c)}
Initial SG pressure ⁽¹⁾	Nominal	{{ }} ^{2(a),(c)}
SG heat transfer	Nominal	{{ }} ^{2(a),(c)}
RSV lift setpoint	Nominal	{{ }} ^{2(a),(c)}
SG tube plugging	Biased to the low condition.	{{ }} ^{2(a),(c)}
Initial containment pressure	Varied	{{ }} ^{2(a),(c)}

$$\}}^{2(a),(c)}$$

Parameter	Bias / Conservatism	Basis
PZR Level Control Charging	Not credited.	{}
Letdown	Enabled.	
		$\}}^{2(a),(c)}$
Steam Pressure Control Turbine throttle valves	Enabled.	{}
Turbine bypass valves	Disabled.	
		$\}}^{2(a),(c)}$
Feedwater and Turbine Load Control feedwater pump speed	Enabled.	{}
		$\}}^{2(a),(c)}$
CNV Pressure Control CNV evacuation system	Enabled. (CNV flooding)	{}
		$\}}^{2(a),(c)}$
	N/A. (CNV vacuum loss)	Not applicable to this event.

1. {} $\}}^{2(a),(c)}$

Sensitivity studies are performed as needed to identify the limiting response(s) for the acceptance criteria parameter(s) challenged by the event (i.e., system pressures for overheating events, MCHFR for overcooling events). Consequently, sensitivity studies are performed to identify cases with the lowest CHFR response for this overcooling event. As an example, the initial reactor power, pressurizer pressure, RCS average coolant temperature, RCS flow rate, containment pressure, pool temperature, RCCW leak flow

rate, RCCW temperature are varied to achieve the results presented in Table 7-29 for the CNV flooding/loss of CNV vacuum event.

The sensitivity studies indicate that the CNV flooding cases are more challenging to MCHFR than loss of CNV vacuum. However, considering Figure 4-1, the sensitivity study results indicate that for a variety of initial RCS conditions, reactor pool conditions, and condition of liquid or air ingress to containment, loss of containment vacuum or containment flooding results in a slow overcooling transient that is non-limiting with respect to MCHFR compared to other AOOs.

Table 7-29 Example sensitivity studies – containment flooding / loss of containment vacuum

{{

}}2(a),(c)

{{

}}^{2(a),(c)}

7.2.6 Turbine Trip / Loss of External Load

The methodology used to simulate a postulated turbine trip/loss of external load (LOEL) for the NPM, and an evaluation of the resulting representative plant response against the acceptance criteria for an AOO listed in Table 7-4, are presented below.

A description of the event including biases and conservatisms, sensitivity studies, single active failure (SAF) and loss of power (LOP) scenarios, challenging case, and acceptance criteria evaluation are presented in the following sections.

7.2.6.1 General Event Description

Turbine trip initiates with a turbine stop valve closure while loss of external load initiates with a turbine control valve closure. Otherwise, these transients are essentially equivalent and result in the sudden removal of the secondary side heat sink, overpressurization of the secondary system, and overheating of the RCS. Rising system pressures result in RTS actuation on the high PZR or steam pressure signal. Reactor trip and transition to stable DHRS flow terminates the transient with the NPM in a safe, stable condition. Table 7-30 lists the relevant acceptance criteria, SAF, and LOP scenarios.

The limiting pressure responses occur when the event is initiated from full power conditions, and the initial conditions are biased in the conservative directions. Sensitivity studies on initial primary temperature and primary/secondary pressures are performed to identify the conditions that maximize peak primary and secondary pressures. Additional sensitivity studies are performed on other parameters, as necessary, to identify the case(s) with the potentially limiting peak primary and secondary pressures.

Table 7-30 Acceptance criteria, single active failure, loss of power scenarios – turbine trip / loss of external load

Acceptance Criteria / Single Active Failure / Loss of Power Scenarios of Interest	Discussion
Primary pressure, secondary pressure	Primary and secondary pressures are challenged during this overheating event.
Failure of one FWIV to close	Challenging for secondary side pressurization cases (negligible effect for primary side pressurization cases, which assume loss of AC power at event initiation and therefore feedwater is lost).
Loss of AC power at transient initiation	Maximizes primary pressure (feedwater is lost).
No loss of power	Maximizes secondary pressure.

7.2.6.2 Acceptance Criteria

Evaluation of the most challenging case(s) relative to the acceptance criteria is presented in Table 7-31.

Table 7-31 Acceptance criteria – turbine trip / loss of external load

Acceptance Criteria	Discussion
Primary pressure	Primary pressure quickly rises to the peak value, then drops as the lowest setpoint RSV lifts to reduce pressure.
Secondary pressure	Peak secondary pressurization is largely a function of DHRS actuation, in addition to the actual turbine trip or loss of external load. The DHRS heat removal is limited by the DHR condenser so some pressurization is expected for every actuation of this system.
Critical heat flux ratio	This criterion is evaluated by downstream subchannel analysis.
Maximum fuel centerline temperature	This criterion is evaluated by downstream subchannel analysis.
Containment integrity	Containment integrity is evaluated by a separate analysis methodology.
Escalation of an AOO to an accident	This criterion is satisfied by demonstrating stable RCS flow rates and constant or downward trending RCS and DHRS pressures and temperatures exist at the end of the transient, all acceptance criteria evaluated in the transient analysis are met, and shutdown margin is maintained at the end of the transient. RCS conditions during extended DHRS cooling are addressed in a separate analysis.

7.2.6.3 Biases, Conservatisms, and Sensitivity Studies

The biases and conservatisms presented in Table 7-32 are considered in identifying the bounding transient simulation for primary and steam generator pressure.

Table 7-32 Initial conditions, biases, and conservatisms – turbine trip / loss of external load

Parameter	Bias / Conservatism	Basis
Initial reactor power	RTP biased to the high condition to account for measurement uncertainty.	{{ }} ^{2(a),(c)}
Initial RCS average temperature	Varied.	{{ }} ^{2(a),(c)}

© Copyright 2019 by NuScale Power, LLC

© Copyright 2019 by NuScale Power, LLC

1. $\{\{ \dots \} \}^{2(a),(c)}$

Representative results of this sensitivity study are presented in Table 7-33. The results of the sensitivity studies indicate that maximum RPV pressure occurs when PZR pressure is biased to the high condition, average temperature is biased to the low condition, and a loss of power leads to a loss of the secondary side heat sink (since feedwater is lost, the failure of an FWIV to close would have no effect on the event). With respect to secondary side SG pressure, maximum SG pressure occurs when average temperature and SG pressure are biased to the high condition, and all power sources are available - the failure of an FWIV to close increases the peak SG pressure by a very small amount and remains well below the design pressure of 2100 psia.

Table 7-33 Representative sensitivity studies – turbine trip / loss of external load

{

}}^{2(a),(c)}

7.2.7 Loss of Condenser Vacuum

The methodology used to simulate a postulated loss of condenser vacuum for the NPM, and an evaluation of the resulting representative plant response against the acceptance criteria for an AOO listed in Table 7-4 are presented below.

A description of the event including biases and conservatisms, sensitivity studies, single active failure (SAF) and loss of power (LOP) scenarios, challenging case, and acceptance criteria evaluation are presented in the following sections.

7.2.7.1 General Event Description

Loss of condenser vacuum initiates with a turbine stop valve closure. Also, a loss of condenser vacuum is postulated to lead to a loss of feedwater flow. Turbine trip and loss of feedwater result in the sudden removal of the secondary side heat sink, pressurization of the secondary system, and overheating of the RCS. Rising system pressures result in a rapid RTS actuation on either high PZR or steam pressure. Reactor trip and transition to stable DHRS flow terminates the transient with the NPM in a safe, stable condition. The relevant acceptance criteria, SAF, and LOP scenarios are listed in Table 7-34.

The limiting pressure response occurs when the event is initiated from full power conditions, and the initial conditions are biased in the conservative directions. Sensitivity studies on initial primary temperature and primary/secondary pressures are performed to identify the conditions that maximize peak primary and secondary pressures. Additional sensitivity studies are performed on other parameters, as necessary, to identify the case(s) with the potentially limiting peak primary and secondary pressures.

Table 7-34 Acceptance criteria, single active failure, loss of power scenarios – loss of condenser vacuum

Acceptance Criteria / Single Active Failure / Loss of Power Scenarios of Interest	Discussion
Primary pressure, secondary pressure	Primary and secondary pressures are challenged during this overheating event.
No single failure	The challenging cases for primary pressure occur when all equipment is operational. Since feedwater is lost at transient initiation, peak pressures are insensitive to the single failure of an FWIV to isolate.
No loss of power	Since feedwater is lost at transient initiation, peak pressures are insensitive to a loss of AC power.

7.2.7.2 Acceptance Criteria

Evaluation of the most challenging case(s) relative to the acceptance criteria is presented in Table 7-35.

Table 7-35 Acceptance criteria – loss of condenser vacuum

Acceptance Criteria	Discussion
Primary pressure	Primary pressure quickly rises to the peak value, then drops as the lowest-setpoint RSV lifts to reduce pressure.
Secondary pressure	Peak secondary pressurization is largely a function of DHRS actuation, in addition to the actual loss of condenser vacuum. The DHRS heat removal is limited by the DHR condenser so some pressurization is expected for every actuation of this system.
Critical heat flux ratio	This criterion is evaluated by downstream subchannel analysis.
Maximum fuel centerline temperature	This criterion is evaluated by downstream subchannel analysis.
Containment integrity	Containment integrity is evaluated by a separate analysis methodology.
Escalation of an AOO to an accident	This criterion is satisfied by demonstrating stable RCS flow rates and constant or downward trending RCS and DHRS pressures and temperatures exist at the end of the transient, all acceptance criteria evaluated in the transient analysis are met, and shutdown margin is maintained at the end of the transient. RCS conditions during extended DHRS cooling are addressed in a separate analysis.

The biases and conservatisms presented in Table 7-36 are considered in identifying the bounding transient simulation for primary and steam generator pressure.

[illegible]

© Copyright 2019 by NuScale Power, LLC

1. $\{\{ \dots \}^{2(a),(c)} \}$

Representative results of this sensitivity study are presented in Table 7-37. Several cases with consistent biases and various combinations of an FWIV failure and a loss of AC power are considered. The peak RPV pressures for all of these cases are within a few tenths of a psi, demonstrating that since feedwater is lost at transient initiation, the results are insensitive to failure of an FWIV to isolate and loss of AC power, all other things being equal. Additionally, the results of the sensitivity studies indicate that maximum RPV pressure occurs when PZR pressure is biased to the high condition, and average

temperature is biased to the low condition. With respect to secondary side SG pressure, maximum SG pressure occurs when average temperature and SG pressure are biased to the high condition, and all power sources are available (since feedwater is lost, the failure of an FWIV to close would have no effect on the event).

Table 7-37 Representative sensitivity studies – loss of condenser vacuum

{{

}}^{2(a),(c)}

7.2.8 Main Steam Isolation Valve(s) Closure

The methodology used to simulate a postulated main steam isolation valve closure for the NPM, and an evaluation of the resulting representative plant response against the acceptance criteria for an AOO listed in Table 7-4 are presented below.

A description of the event including biases and conservatisms, sensitivity studies, single active failure (SAF) and loss of power (LOP) scenarios, challenging case, and acceptance criteria evaluation are presented in the following sections.

7.2.8.1 General Event Description

A closure of one or both main steam isolation valves results in a pressurization of the secondary system and overheating of the RCS. Rising secondary side pressure results in a rapid RTS actuation on the high steam pressure signal. Reactor trip and transition to stable DHRS flow terminates the transient with the NPM in a safe, stable condition. The relevant acceptance criteria, single active failure, and loss of power scenarios are listed in Table 7-38.

The MSIV closure event can occur when one or both MSIVs close unexpectedly. The limiting pressure responses occur when the event is initiated from full power conditions, and the initial conditions are biased in the conservative directions.

Sensitivity studies on number of MSIVs closing, initial primary temperature and primary/secondary pressures are performed to identify the conditions that maximize peak primary and secondary pressures. Additional sensitivity studies are performed on other parameters, as necessary, to identify the case(s) with the potentially limiting peak primary and secondary pressures.

Table 7-38 Acceptance criteria, single active failure, loss of power scenarios – main steam isolation valve closure

Acceptance Criteria / Single Active Failure / Loss of Power Scenarios of Interest	Discussion
Primary pressure, secondary pressure	Primary and secondary pressures are challenged during this overheating event.
No single failure	Challenging for primary pressure.
Failure of one FWIV to close	Challenging for steam generator pressure. Failure of a FWIV to close is considered; however, since secondary side pressurization resulting from the initiating event (i.e., an MSIV closure) prevents significant additional feedwater from entering the steam generator, secondary side pressure response during an MSIV closure event is not highly sensitive to the failure of an FWIV to close.
Loss of AC Power at transient initiation	Maximizes primary pressure.
No loss of power	Maximizes secondary pressure.

7.2.8.2 Acceptance Criteria

Evaluation of the most challenging case(s) relative to the acceptance criteria is presented in Table 7-39.

Table 7-39 Acceptance criteria – main steam isolation valve closure

Acceptance Criteria	Discussion
Primary pressure	Primary pressure quickly rises to the peak value, then drops as the lowest setpoint RSV lifts to reduce pressure.
Secondary pressure	Peak secondary pressurization is largely a function of DHRS actuation, in addition to the actual main steam isolation valve closure. The DHRS heat removal is limited by the DHR condenser so some pressurization is expected for every actuation of this system.
Critical heat flux ratio	This criterion is evaluated by downstream subchannel analysis.
Maximum fuel centerline temperature	This criterion is evaluated by downstream subchannel analysis.
Containment integrity	Containment integrity is evaluated by a separate analysis methodology.
Escalation of an AOO to an accident	This criterion is satisfied by demonstrating stable RCS flow rates and constant or downward trending RCS and DHRS pressures and temperatures exist at the end of the transient, all acceptance criteria evaluated in the transient analysis are met, and shutdown margin is maintained at the end of the transient. RCS conditions during extended DHRS cooling are addressed in a separate analysis.

7.2.8.3 Biases, Conservatisms, and Sensitivity Studies

The biases and conservatisms presented in Table 7-40 are considered in identifying the bounding transient simulation for primary and steam generator pressure.

Table 7-40 Initial conditions, biases, and conservatisms – main steam isolation valve closure

Parameter	Bias / Conservatism	Basis
Initial reactor power	RTP biased upwards to account for measurement uncertainty.	{{ }} ^{2(a),(c)}
Initial RCS average temperature	Varied.	{{ }} ^{2(a),(c)}
Initial RCS flow rate	Varied.	{{ }} ^{2(a),(c)}
Initial PZR pressure	Varied.	{{ }} ^{2(a),(c)}
Initial PZR level	Varied.	{{ }} ^{2(a),(c)}
Initial feedwater temperature	Nominal.	{{ }} ^{2(a),(c)}
Initial fuel temperature	Biased to the high condition	{{ }} ^{2(a),(c)}
MTC	Consistent with BOC kinetics.	{{ }} ^{2(a),(c)}
Kinetics	Biased to BOC conditions.	{{ }} ^{2(a),(c)}
Decay heat	Biased to the high condition.	{{ }} ^{2(a),(c)}
Initial SG pressure ⁽¹⁾	Varied.	{{ }} ^{2(a),(c)}
Steam generator heat transfer	Nominal.	{{ }} ^{2(a),(c)}
RSV lift setpoint	Biased to the high condition.	{{ }} ^{2(a),(c)}
SG tube plugging	Biased to the low condition.	{{ }} ^{2(a),(c)}

© Copyright 2019 by NuScale Power, LLC

[illegible]

1. $\{\{ \dots \}^{2(a),(c)}$

Representative results of this sensitivity study are presented in Table 7-41. All results presented consider the closure of two MSIVs, which isolates both steam generators, and no single active failure. Maximum pressures are similar for cases in which the RSV actuation limits the RPV pressurization. For example, the maximum calculated pressure for the peak RPV pressure study is equal (to one decimal place) to the peak RPV pressures for two additional cases, namely, decreased steam generator heat transfer and decreased feedwater temperature. Additionally, the results of the sensitivity studies indicate that maximum RPV pressure occurs when PZR pressure is biased to the high condition, RCS flow is at the nominal value (if maximum RCS pressure is below the RSV lift pressure), and a loss of AC power leads to a loss of the secondary side heat sink (loss of AC power occurs coincident with reactor trip). With respect to secondary side SG pressure, maximum SG pressure occurs when average temperature is biased to the high condition, RCS flow is biased to the low condition, and all power sources are available.

Table 7-41 Representative sensitivity studies – main steam isolation valve closure

{

}}^{2(a),(c)}

7.2.9 Loss of Nonemergency AC Power

The methodology used to simulate a postulated loss of nonemergency (normal) AC power for the NPM, and an evaluation of the resulting representative plant response against the acceptance criteria for an AOO listed in Table 7-4, are presented below.

A description of the event including biases and conservatisms, sensitivity studies, single active failure (SAF) and loss of power (LOP) scenarios, challenging case, and acceptance criteria evaluation are presented in the following sections.

7.2.9.1 General Event Description

The low voltage AC electrical distribution system (ELVS) supplies AC power to plant motors, heaters, packaged equipment, and battery chargers. Loss of normal AC power to the station auxiliaries can result from electrical grid-related failures, failures in plant or switchyard equipment, or external weather events. The nonsafety-related EDNS and EDSS may remain available via battery operation; the primary loads for these systems include the CRDMs and the MPS. Loss of the EDNS and/or EDSS batteries with the loss of normal AC power is considered. A loss of AC power results in a pressurization of the secondary system and overheating of the RCS. Reactor trip and transition to stable DHRS flow terminates the transient with the NPM in a safe, stable condition. Table 7-42 lists the relevant acceptance criteria, SAF, and LOP scenarios.

There are a variety of possible loss of power combinations that could occur, including the loss of one, two, or all of the power supplies, either at event initiation or turbine trip. Since this event is initiated with a loss of normal AC power, several combinations are eliminated from further consideration. The remaining combinations are discussed below.

During the failure of the ELVS at event initiation, with EDNS and EDSS available:

- turbine trip occurs at event initiation,
- the feedwater pumps and CVCS pumps stop at event initiation,
- the PZR heaters turn off at event initiation, and
- the MPS actuates reactor trip, DHRS actuation and containment isolation within 60 s after event initiation (if not already actuated during that time), due to loss of AC power to the EDSS battery chargers.

During the failure of the ELVS and EDNS at event initiation, with EDSS available:

- turbine trip occurs at event initiation,
- the feedwater pumps and CVCS pumps stop at event initiation,
- the PZR heaters turn off at event initiation,
- the MPS actuates reactor trip, DHRS actuation and containment isolation within 60 s after event initiation (if not already actuated during that time), due to loss of AC power to the EDSS battery chargers, and
- control rods begin to drop at event initiation due loss of EDNS power to control rod drive mechanisms (CRDMs).

During the failure of the ELVS and EDSS at event initiation, with EDNS available:

- turbine trip occurs at event initiation,
- the feedwater pumps and CVCS pumps stop at event initiation,
- the CVCS isolates at event initiation (due to loss of EDSS),
- the PZR heaters turn off at event initiation, and
- the loss of AC power and EDSS causes immediate reactor trip, DHRS actuation, and containment isolation.

The equipment available during the failure of the ELVS, EDNS, and EDSS at event initiation is the same as for the failure of the ELVS and EDSS at event initiation, with EDNS available.

Of these scenarios, the only one which does not include an immediate reactor trip or full control rod insertion at event initiation is the loss of the ELVS at event initiation, with EDNS and EDSS available. Cases considering the loss of EDSS battery backup coincident with

the initiating event are considered to determine if this loss of power scenario is more challenging to the plant. It is concluded that cases where EDSS remains available are more limiting. Consequently, the limiting pressure responses occur when the event is initiated from full power conditions, reactor trip is delayed until MPS actuation, and the initial conditions are biased in the conservative directions. Sensitivity studies on initial primary temperature and primary/secondary pressures are performed to identify the conditions that maximize peak primary and secondary pressures. Additional sensitivity studies are performed on other parameters, as necessary, to identify the case(s) with the potentially limiting peak primary and secondary pressures.

Table 7-42 Acceptance criteria, single active failure, loss of power scenarios – loss of normal AC power

Acceptance Criteria / Single Active Failure / Loss of Power Scenarios of Interest	Discussion
Primary pressure, secondary pressure	Primary and secondary pressures are challenged during this overheating event.
No single failure	The challenging cases for primary pressure occur when all equipment is operational. Since feedwater is lost at transient initiation, peak secondary pressures are insensitive to the single failure of an FWIV to isolate.
Loss of AC power at transient initiation	Initiating event.

7.2.9.2 Acceptance Criteria

Evaluation of the most challenging case(s) relative to the acceptance criteria is presented in Table 7-43.

Table 7-43 Acceptance criteria – loss of normal AC power

Acceptance Criteria	Discussion
Primary pressure	Primary pressure quickly rises to the peak value, then drops as the lowest setpoint RSV lifts to reduce pressure.
Secondary pressure	Peak secondary pressurization is largely a function of DHRS actuation, in addition to the actual loss of normal AC power. The DHRS heat removal is limited by the DHR condenser so some pressurization is expected for every actuation of this system.
Critical heat flux ratio	This criterion is evaluated by downstream subchannel analysis.
Maximum fuel centerline temperature	This criterion is evaluated by downstream subchannel analysis.
Containment integrity	Containment integrity is evaluated by a separate analysis methodology.
Escalation of an AOO to an accident	This criterion is satisfied by demonstrating stable RCS flow rates and constant or downward trending RCS and DHRS pressures and temperatures exist at the end of the transient, all acceptance criteria evaluated in the transient analysis are met, and shutdown margin is maintained at the end of the transient. RCS conditions during extended DHRS cooling are addressed in a separate analysis.

7.2.9.3 Biases, Conservatisms, and Sensitivity Studies

The biases and conservatisms presented in Table 7-44 are considered in identifying the bounding transient simulation for primary and secondary pressure.

Table 7-44 Initial conditions, biases, and conservatisms – loss of normal AC power

Parameter	Bias / Conservatism	Basis
Initial reactor power	RTP biased upwards to account for measurement uncertainty.	{{ }} ^{2(a),(c)}
Initial RCS average temperature	Varied.	{{ }} ^{2(a),(c)}

© Copyright 2019 by NuScale Power, LLC

© Copyright 2019 by NuScale Power, LLC

1. $\{\{ \dots \} \}^{2(a),(c)}$
2. Loss of normal AC power initiating event results in a loss of system function by loss of power to the system thereby making the system control not relevant to the event.

Representative results of this sensitivity study are presented in Table 7-45. The results of the sensitivity studies indicate that the lowest-setpoint RSV operates to mitigate peak primary side pressurization {{

 $\}^{2(a),(c)}$

Table 7-45 Representative sensitivity studies – loss of normal AC power

{{

}}^{2(a),(c)}

7.2.10 Loss of Normal Feedwater Flow

The methodology used to simulate a postulated loss of normal feedwater flow for the NPM, and an evaluation of the resulting representative plant response against the acceptance criteria for an AOO listed in Table 7-4, are presented below.

A description of the event including biases and conservatisms, sensitivity studies, single active failure (SAF) and loss of power (LOP) scenarios, challenging case, and acceptance criteria evaluation are presented in the following sections.

7.2.10.1 General Event Description

A postulated fault results in a partial or complete loss of feedwater flow, and the water in the steam generators boils off. The loss of steam generators as a heat sink leads to a rise in the RCS temperature and pressure until the reactor trips due to high RCS temperature or high PZR pressure. Reactor trip and transition to stable DHRS flow terminates the transient with the NPM in a safe, stable condition.

The relevant acceptance criteria, SAF, and LOP scenarios are listed in Table 7-46.

Table 7-46 Acceptance criteria, single active failure, loss of power scenarios – loss of normal feedwater flow

Acceptance Criteria / Single Active Failure / Loss of Power Scenarios of Interest	Discussion
Primary pressure, secondary pressure	System pressures are challenged during this overheating event.
No single failure	The challenging cases occur when all equipment is operational.
Loss of AC power at turbine trip	Maximizes system pressures.

7.2.10.2 Acceptance Criteria

Evaluation of the most challenging case(s) relative to the acceptance criteria is presented in Table 7-47.

Table 7-47 Acceptance criteria – loss of normal feedwater flow

Acceptance Criteria	Discussion
Primary pressure	Primary pressure quickly rises to the peak value, then drops as the lowest setpoint RSV lifts to reduce pressure.
Secondary pressure	Peak secondary pressurization is largely a function of DHRS actuation, in addition to the actual loss of feedwater. The DHRS heat removal is limited by the DHR condenser so some pressurization is expected for every actuation of this system.
Critical heat flux ratio	This criterion is evaluated by downstream subchannel analysis.
Maximum fuel centerline temperature	This criterion is evaluated by downstream subchannel analysis.
Containment integrity	Containment integrity is evaluated by a separate analysis methodology.
Escalation of an AOO to an accident	This criterion is satisfied by demonstrating stable RCS flow rates and constant or downward trending RCS and DHRS pressures and temperatures exist at the end of the transient, all acceptance criteria evaluated in the transient analysis are met, and shutdown margin is maintained at the end of the transient. RCS conditions during extended DHRS cooling are addressed in a separate analysis.

7.2.10.3 Biases, Conservatisms, and Sensitivity Studies

The biases and conservatisms indicated in Table 7-48 are considered in identifying a bounding transient simulation for primary and steam generator pressure.

Table 7-48 Initial conditions, biases, and conservatisms – loss of normal feedwater flow

Parameter	Bias / Conservatism	Basis
Initial reactor power	RTP biased upwards to account for measurement uncertainty.	{{ }} ^{2(a),(c)}
Initial RCS average temperature	Varied.	{{ }} ^{2(a),(c)}
Initial RCS flow rate	Varied.	{{ }} ^{2(a),(c)}
Initial PZR pressure	Varied.	{{ }} ^{2(a),(c)}
Initial PZR level	Varied.	{{ }} ^{2(a),(c)}
Initial feedwater temperature	Varied.	{{ }} ^{2(a),(c)}
Initial fuel temperature	Biased to the high condition.	{{ }} ^{2(a),(c)}
MTC	Consistent with BOC kinetics.	{{ }} ^{2(a),(c)}
Kinetics	Biased to BOC conditions.	{{ }} ^{2(a),(c)}
Decay heat	Biased to the high condition.	{{ }} ^{2(a),(c)}
Initial SG pressure ⁽¹⁾	Varied.	{{ }} ^{2(a),(c)}
SG heat transfer	Nominal.	{{ }} ^{2(a),(c)}
RSV lift setpoint	Biased to the high condition.	{{ }} ^{2(a),(c)}
SG tube plugging	Biased to the low condition.	{{ }} ^{2(a),(c)}
Feedwater flow decrease	Varied	{{ }} ^{2(a),(c)}

© Copyright 2019 by NuScale Power, LLC

[illegible]

1. $\{\{ \dots \}^{2(a),(c)}$

Representative results of this sensitivity study are presented in Table 7-49. The results of the sensitivity studies indicate that peak primary pressure occurs during a total loss of feedwater—since this is sufficient to actuate the lowest-setpoint RSV, {{

}}2(a),(c) With respect to maximum secondary side SG pressure, maximum SG pressure occurs during a partial loss of feedwater, as the mismatch between primary heat production and secondary heat sink causes the RCS temperature to increase, and eventually actuate the RTS on high RCS riser temperature.

Table 7-49 Sensitivity studies – loss of normal feedwater flow

 $\{\{$ $\}^{2(a),(c)}$

7.2.11 Inadvertent Decay Heat Removal System Actuation

The methodology used to simulate a postulated inadvertent DHRS actuation for the NPM, and an evaluation of the resulting representative plant response against the acceptance criteria for an AOO listed in Table 7-4, are presented below.

A description of the event including biases and conservatisms, sensitivity studies, single active failure (SAF) and loss of power (LOP) scenarios, challenging case, and acceptance criteria evaluation are presented in the following sections. This event is unique to the NPM design.

7.2.11.1 General Event Description

Inadvertent actuation of the DHRS may result from either an unexpected DHR valve actuation or a spurious DHRS actuation signal. If a single valve opens unexpectedly at full power conditions (Scenario 1), and the plant does not trip on low turbine inlet temperature or low steam superheat (the safety related main steam line temperatures are measured just upstream of the junctions between the main steam lines and the DHRS steam lines), some of the feedwater is diverted through the DHRS, and a gradual heatup of the RCS occurs until it reaches the maximum analytical temperature limit and signals the MPS. This condition is the most limiting for peak secondary system pressures. If a signal malfunction results in the unexpected actuation of one (Scenario 2) or both (Scenario 3) DHRS trains, feedwater and steam systems associated with the affected DHR train(s) are isolated. This rapid loss of heat removal from the RCS results in the most challenging scenario for primary pressure. Reactor trip and transition to stable DHRS flow terminates the transients with the NPM in a safe, stable condition. The relevant acceptance criteria, SAF, and LOP scenarios are listed in Table 7-50.

Scenario 1: The unexpected opening of a single DHR valve can occur at full power or reduced power conditions. At low power conditions, a portion of the DHR liquid inventory drains into the feedwater line, which momentarily increases feedwater flow, overcooling the plant. This overcooling event is not considered further because it is bounded by other, more limiting overcooling events (i.e., increase in feedwater flow). The most challenging conditions for this heatup scenario occur at full power with initial conditions biased in the conservative directions. Since feedwater flow will tend to increase in response to the reduced steam enthalpy and turbine load, limiting the feedwater response maximizes the heatup.

Scenario 2: An inadvertent actuation signal isolates one steam generator, and opens one DHRS train. This scenario is bounded by Scenario 3.

Scenario 3: An inadvertent actuation signal isolates both steam generators, and opens both DHRS trains. This scenario represents a complete loss of normal heat removal from the RCS. The limiting conditions for this heatup scenario occur at full power with initial conditions biased in the conservative directions.

Sensitivity studies on initial primary and secondary conditions are performed as needed to identify the conditions that maximize peak system pressures.

Table 7-50 Acceptance criteria, single active failure, loss of power scenarios – inadvertent decay heat removal system actuation

Acceptance Criteria / Single Active Failure / Loss of Power Scenarios of Interest	Discussion
Primary pressure	Challenged during spurious actuation signal that closes two FWIVs and two MSIVs.
Secondary pressure	Challenged during the unexpected opening of a single DHR valve.
No single failure	The challenging primary pressurization cases occur when all equipment is operational
Failure of one FWIV to close	Challenging for secondary pressure.
No loss of power	Maximizes system pressures.

7.2.11.2 Acceptance Criteria

Evaluation of the most challenging case(s) relative to the acceptance criteria is presented in Table 7-51.

Table 7-51 Acceptance criteria – inadvertent decay heat removal system actuation

Acceptance Criteria	Discussion
Primary pressure	Primary pressure quickly rises to the peak value, then drops as the lowest setpoint RSV lifts to reduce pressure.
Secondary pressure	Peak secondary pressurization is largely a function of DHRS actuation. The DHRS heat removal is limited by the DHR condenser so some pressurization is expected for every actuation of this system.
Critical heat flux ratio	This criterion is evaluated by downstream subchannel analysis.
Maximum fuel centerline temperature	This criterion is evaluated by downstream subchannel analysis.
Containment integrity	Containment integrity is evaluated by a separate analysis methodology.
Escalation of an AOO to an accident	This criterion is satisfied by demonstrating stable RCS flow rates and constant or downward trending RCS and DHRS pressures and temperatures exist at the end of the transient, all acceptance criteria evaluated in the transient analysis are met, and shutdown margin is maintained at the end of the transient. RCS conditions during extended DHRS cooling are addressed in a separate analysis.

7.2.11.3 Biases, Conservatisms, and Sensitivity Studies

The biases and conservatisms presented in Table 7-52 are considered in identifying the bounding transient simulation for primary and steam generator pressure.

Table 7-52 Initial conditions, biases, and conservatisms – inadvertent decay heat removal system actuation

Parameter	Bias / Conservatism	Basis
Initial reactor power	Varied—most challenging cases are RTP biased upwards to account for measurement uncertainty.	{{ }} ^{2(a),(c)}
Initial RCS average temperature	Varied.	{{ }} ^{2(a),(c)}
Initial RCS flow rate	Varied.	{{ }} ^{2(a),(c)}
Initial PZR pressure	Varied.	{{ }} ^{2(a),(c)}
Initial PZR level	Varied.	{{ }} ^{2(a),(c)}
Initial feedwater temperature	Nominal.	{{ }} ^{2(a),(c)}
Initial fuel temperature	Biased to the high condition	{{ }} ^{2(a),(c)}
MTC	Consistent with BOC kinetics.	{{ }} ^{2(a),(c)}
Kinetics	Varied—most challenging cases biased to BOC conditions.	{{ }} ^{2(a),(c)}
Decay heat	Biased to the high condition.	{{ }} ^{2(a),(c)}
Initial SG pressure ⁽¹⁾	Varied.	{{ }} ^{2(a),(c)}

© Copyright 2019 by NuScale Power, LLC

1. $\{\{ \dots \} \}^{2(a),(c)}$
2. NPM RSV relieving capacities are sized to be significantly greater than transient induced NPM pressurization rates, thus minimizing pressure overshoot. $\{\{ \dots \} \}^{2(a),(c)}$

Representative results of this sensitivity study are presented in Table 7-53. Unless otherwise noted, all cases use BOC kinetics. The results of the sensitivity studies indicate that peak primary pressure occurs when both trains of DHR inadvertently actuate (i.e., total loss of normal heat sink). The lowest-setpoint RSV operates to mitigate peak

pressurization. {{

}}^{2(a),(c)}

Table 7-53 Representative sensitivity studies – inadvertent decay heat removal system actuation

{{

}}^{2(a),(c)}

7.2.12 Feedwater System Pipe Break Inside or Outside Containment

The methodology used to simulate a postulated feedwater system pipe break for the NPM, and an evaluation of the resulting representative plant response against the acceptance criteria listed in Table 7-4, are presented below. Since both split breaks (relatively higher event frequency) and double-ended guillotine breaks (relatively lower event frequency) are analyzed, the more restrictive AOO criteria for system pressures, critical heat flux ratio, and fuel centerline melt applicable to breaks with higher event frequency are used in the evaluation.

A description of the event including biases and conservatisms, sensitivity studies, single active failure (SAF) and loss of power (LOP) scenarios, challenging case, and acceptance criteria evaluation are presented in the following sections.

7.2.12.1 General Event Description

A feedwater line break can occur inside or outside of containment, and can range in size from a small split crack to a double ended rupture. A feedwater line break inside containment results in a loss of containment vacuum and a high containment pressure MPS signal that actuates a reactor trip, isolates the secondary system and CVCS, and opens the DHRS valves. The steam generator, DHRS piping, and DHRS condenser on the affected side drain through the break. The non-affected steam generator system and DHRS loop provide cooling to the RCS via heat transfer to the reactor pool.

A feedwater line break outside containment causes a loss of feedwater flow to the steam generators and a heatup of the RCS. Larger breaks result in rapid heatup events that pressurize the RCS beyond the high PZR pressure analytical limit. Smaller breaks cause a more gradual heatup, loss of secondary pressure, and reactor trip and DHRS actuation on low steam pressure or high steam superheat. The DHRS provides cooling to the RCS via heat transfer to the reactor pool. Reactor trip and transition to stable DHRS flow terminates the transient with the NPM in a safe, stable condition.

{{

}}^{2(a),(c)}

Table 7-54 lists the relevant acceptance criteria, SAF, and LOP scenarios.

Breaks outside of containment result in higher system pressures compared to breaks inside containment because of the relatively rapid MPS signal on high containment pressure for breaks inside of containment. The limiting pressure responses occur for breaks outside of containment, when the event is initiated from full power conditions, and the initial conditions are biased in the conservative directions. A loss of normal AC power at the event initiation provides the most challenging peak primary pressure for this event.

Sensitivity studies on primary and secondary conditions, and break size/location are performed to identify the conditions that maximize peak primary and secondary pressures.

Table 7-54 Acceptance criteria, single active failure, loss of power scenarios – feedwater line break

Acceptance Criteria / Single Active Failure / Loss of Power Scenarios of Interest	Discussion
Primary pressure, secondary pressure	System pressures are challenged during this overheating event.
No single failure	The challenging cases occur when all equipment is operational.
Loss of AC power at transient initiation	Maximizes system pressures.

7.2.12.2 Acceptance Criteria

Evaluation of the most challenging case(s) relative to the acceptance criteria is presented in Table 7-55.

Table 7-55 Acceptance criteria – feedwater line break

Acceptance Criteria	Discussion
Primary pressure	Primary pressure quickly rises to the peak value, then drops as the lowest setpoint RSV lifts to reduce pressure.
Secondary pressure	Peak secondary pressurization is largely a function of DHRS actuation, in addition to the actual FWLB. The DHRS heat removal is limited by the DHR condenser so some pressurization is expected for every actuation of this system.
Critical heat flux ratio	This criterion is evaluated by downstream subchannel analysis.
Maximum fuel centerline temperature	This criterion is evaluated by downstream subchannel analysis.
Containment integrity	Containment integrity is evaluated by a separate analysis methodology.
Escalation to a more serious accident or consequential loss of functionality	This criterion is satisfied by demonstrating stable RCS flow rates and constant or downward trending RCS and DHRS pressures and temperatures exist at the end of the transient, all acceptance criteria evaluated in the transient analysis are met, and shutdown margin is maintained at the end of the transient. RCS conditions during extended DHRS cooling are addressed in a separate analysis.

The biases and conservatisms presented in Table 7-56 are considered in identifying the bounding transient simulation for primary and steam generator pressure.

Parameter	Bias / Conservatism	Basis
Initial reactor power	RTP biased upwards to account for measurement uncertainty.	$\{\{ \} \}^{2(a),(c)}$
Initial RCS average temperature	Varied.	$\{\{ \} \}^{2(a),(c)}$
Initial RCS flow rate	Biased to the low condition.	$\{\{ \} \}^{2(a),(c)}$
Initial PZR pressure	Varied.	$\{\{ \} \}^{2(a),(c)}$
Initial PZR level	Varied.	$\{\{ \} \}^{2(a),(c)}$
Initial feedwater temperature	Varied.	$\{\{ \} \}^{2(a),(c)}$
Initial fuel temperature	Biased to the high condition.	$\{\{ \} \}^{2(a),(c)}$
MTC	Consistent with BOC kinetics.	$\{\{ \} \}^{2(a),(c)}$
Kinetics	Biased to BOC conditions.	$\{\{ \} \}^{2(a),(c)}$
Decay heat	Biased to the high condition.	$\{\{ \} \}^{2(a),(c)}$
Initial SG pressure ⁽¹⁾	Varied.	$\{\{ \} \}^{2(a),(c)}$

© Copyright 2019 by NuScale Power, LLC

Parameter	Bias / Conservatism	Basis
Steam Pressure Control Turbine throttle valves	Enabled.	{{
Turbine bypass valves	Disabled.	}}
Feedwater and Turbine Load Control feedwater pump speed	Disabled.	{{
CNV Pressure Control CNV evacuation system	Enabled.	{{

Sensitivity studies are performed as needed to identify the limiting response(s) for the acceptance criteria parameter(s) challenged by the event (i.e., system pressures for overheating events, MCHFR for overcooling events). Consequently, sensitivity studies are performed to identify cases with the highest pressure responses for this overheating event. For example, a sensitivity study is performed to identify the highest primary and secondary side pressures, varying primary conditions, break size and location, steam generator heat transfer and pressure, etc. (other parameters are biased as indicated in Table 7-56).

Representative results of this sensitivity study are presented in Table 7-57. Unless otherwise noted, all breaks are located at the bioshield, all RCS flows are initialized at the minimum value, and losses of normal AC power occur at event initiation. The results of the sensitivity studies indicate that peak primary pressures occur during a break coincident with a loss of AC power; under these conditions the lowest setpoint RSV operates to mitigate peak pressurization and initial condition biasing contributions are secondary compared to the pressure response to the total loss of heat sink. With respect to maximum secondary side SG pressure, maximum SG pressure occurs during a 10 percent split break just outside of containment coincident with a loss of AC power when initial SG pressure is biased to the high condition and the nonsafety-related check valve fails to seat upon the onset of flow reversal (FWIVs subsequently close as expected).

Table 7-57 Representative sensitivity studies – feedwater line break

{{

}}^{2(a),(c)}

7.2.13 Uncontrolled Control Rod Assembly Bank Withdrawal from Subcritical or Low Power Startup Conditions

The methodology used to simulate a postulated uncontrolled CRA bank withdrawal from subcritical or low power startup conditions for the NPM, and an evaluation of the resulting representative plant response against the acceptance criteria listed for an AOO in Table 7-4, are presented below.

The range of initial power levels associated with low power startup conditions for the NPM is based on the low setting for the high power signal. When core power reaches 15 percent RTP, a hold point is established to alter the high power setting. Thus, low power startup conditions exist until reactor power reaches 15 percent RTP.

A description of the event including biases and conservatisms, sensitivity studies, single active failure (SAF) and loss of power (LOP) scenarios, challenging case, and acceptance criteria evaluation are presented in the following sections.

7.2.13.1 General Event Description and Methodology

The limiting event consequences to an uncontrolled CRA bank withdrawal from subcritical or low power startup conditions typically (for most PWR designs) occur for cases with very low initial power levels (~1 Watt). The primary reason for this behavior is the flux rate signals associated with the source range and intermediate range are typically either not safety related or not of sufficient quantity to adequately address single failures. The NPM, however, incorporates a safety related signal for each of these channels from each core quadrant into the MPS. Consequently, the limiting event consequences for the NPM occur for cases with higher initial power levels.

A spectrum of constant reactivity insertion rates is evaluated. These reactivity insertion rates encompass the credible range resulting from a single control bank withdrawal. If necessary, this range is supplemented to include the reactivity insertion rates associated with an inadvertent decrease in boron concentration event (Section 7.2.16).

Two event scenarios with different protection schemes are evaluated to determine which scenario produces the limiting event consequences. The first scenario arises when the high count rate signal is available because the intermediate range channel does not have an established signal. In this instance, the high power rate signal is not active (below 15 percent RTP), so core protection is provided by the high count rate signal and the startup rate (source range) signal. {{

}}^{2(a),(c)}

The second scenario arises when the high count rate signal is not available because the intermediate range channel has an established signal. In this instance, the high power rate signal is not active (below 15 percent RTP), thus core protection is provided by the high power signal and the startup rate (intermediate range) signal. The event scenario with the highest core power corresponds to the initial power level and reactivity insertion rate that cause the high power signal (low setting) and the startup rate (intermediate range) signal to occur at nearly the same time. This scenario is limiting because it represents the maximum rate of power change at the maximum core power. If the initial power is increased, the plant will trip on the high power signal but at a slower rate of power increase. Similarly, if the reactivity insertion rate is increased, the plant will trip on the startup rate but at a lower core power.

Before initiating an approach to critical, the reactor coolant is heated to a temperature greater than or equal to 420 degrees F, i.e., the minimum temperature for criticality. The heating of the reactor coolant is performed by the Module Heatup System (MHS) via the CVCS.

At least one feedwater pump is operating when the RCS temperature exceeds 300 degrees F. Since feedwater flow is provided to both SGs, it may continue to provide decay heat removal following an uncontrolled CRA bank withdrawal from subcritical or low power startup conditions. If normal feedwater flow is not available, then depending on the point at which the event occurs in the startup process, the flooded containment or the DHRS will provide decay heat removal. The peak power and duration of the power spike are not sufficient to cause a significant temperature or pressure increase. Hence, the maximum power and minimum CHF occur shortly after reactor trip while the RCS pressure and MS pressure do not challenge the relevant acceptance criteria.

Sensitivity studies are performed on a variety of parameters, as necessary, to identify the case(s) with a potentially limiting MCHFR or fuel centerline temperature. The NRELAP5 MCHFR pre-screening process is employed to identify the cases sent for a detailed subchannel evaluation.

Table 7-58 lists the relevant acceptance criteria, SAF, and LOP scenarios.

Table 7-58 Acceptance criteria, single active failure, loss of power scenarios – uncontrolled control rod bank withdrawal from subcritical or low power startup conditions

Acceptance Criteria / Single Active Failure / Loss of Power Scenarios of Interest	Discussion
MCHFR and maximum fuel centerline temperature.	MCHFR and maximum fuel centerline temperature are challenged during this reactivity anomaly event.
No single failure.	The challenging cases occur when all equipment is operational.
No loss of power.	The challenging cases occur when AC power is available for the event duration.

7.2.13.2 Acceptance Criteria

Evaluation of the most challenging case(s) relative to the acceptance criteria is presented in Table 7-59.

Table 7-59 Acceptance criteria – uncontrolled control rod bank withdrawal from subcritical or low power startup conditions

Acceptance Criteria	Discussion
Primary pressure	This criterion is not an acceptance criterion listed in Section 15.4.1 of the SRP (Reference 15). The analysis shows the NPM does not introduce more challenging conditions for primary pressure compared to other AOOs.
Secondary pressure	This criterion is not an acceptance criterion listed in Section 15.4.1 of the SRP (Reference 15). The analysis shows the NPM does not introduce more challenging conditions for secondary pressure compared to other AOOs.
Critical heat flux ratio	This criterion is evaluated by downstream subchannel analysis.
Maximum fuel centerline temperature	This criterion is evaluated by downstream subchannel analysis.
Containment integrity	Containment integrity is evaluated by a separate analysis methodology.
Escalation of an AOO to an accident	This criterion is satisfied by demonstrating stable RCS flow rates and constant or downward trending RCS and DHRS (if actuated) pressures and temperatures exist at the end of the transient, all acceptance criteria evaluated in the transient analysis are met, and shutdown margin is maintained at the end of the transient. RCS conditions during extended DHRS cooling are addressed in a separate analysis.

7.2.13.3 Biases, Conservatisms, and Sensitivity Studies

The biases and conservatisms presented in Table 7-60 are considered in order to identify the bounding transient simulation for MCHFR and maximum fuel centerline temperature.

Table 7-60 Initial conditions, biases, and conservatisms – uncontrolled control rod bank withdrawal from subcritical or low power startup conditions

Parameter	Bias / Conservatism	Basis
Initial reactor power	Varied.	{{ }} ^{2(a),(c)}
Initial RCS average temperature	Nominal.	{{ }} ^{2(a),(c)}
Initial RCS flow rate	Biased to the low condition.	{{ }} ^{2(a),(c)}
Initial PZR pressure	Nominal.	{{ }} ^{2(a),(c)}
Initial PZR level	Nominal.	{{ }} ^{2(a),(c)}
Initial feedwater temperature	Nominal.	{{ }} ^{2(a),(c)}
Initial fuel temperature	Nominal.	{{ }} ^{2(a),(c)}
MTC	Most positive	{{ }} ^{2(a),(c)}
Kinetics	Biased to BOC conditions.	{{ }} ^{2(a),(c)}
Decay heat	Biased to the high condition.	{{ }} ^{2(a),(c)}
Initial SG pressure ⁽¹⁾	Nominal.	{{ }} ^{2(a),(c)}
SG heat transfer	Nominal.	{{ }} ^{2(a),(c)}
RSV lift setpoint	Biased to the high condition.	{{ }} ^{2(a),(c)}
SG tube plugging	Biased to the low condition.	{{ }} ^{2(a),(c)}

Parameter	Bias / Conservatism	Basis
Reactivity insertion rate	Varied.	{ { } } ^{2(a),(c)}
	Maximum	
RCS Temperature Control Automatic rod control	N/A.	{ { } } ^{2(a),(c)}
Boron concentration	Not credited.	
PZR Pressure Control PZR spray (normal)	Disabled.	{ { } } ^{2(a),(c)}
(bypass)	Disabled.	
PZR heaters (non-prop.)	Disabled.	
(prop.)	Nominal.	
PZR Level Control Charging	Not credited.	{ { } } ^{2(a),(c)}
Letdown	Nominal.	
Steam Pressure Control Turbine throttle valves	N/A.	{ { } } ^{2(a),(c)}
Turbine bypass valves	Enabled.	

Parameter	Bias / Conservatism	Basis
Feedwater and Turbine Load Control feedwater pump speed	N/A.	{{ }} ^{2(a),(c)}
CNV Pressure Control CNV evacuation system	Enabled.	{{ }} ^{2(a),(c)}

1 {{
}}^{2(a),(c)}

Sensitivity studies are performed as needed to identify the limiting response(s) for the acceptance criteria parameter(s) challenged by the event. Consequently, a sensitivity study is generally performed to identify cases for lowest MCHFR and highest fuel centerline temperature for this reactivity event. As an example, the initial core power, reactivity insertion rate, and initial core inlet temperature were varied to achieve the results presented in Table 7-61.

These results demonstrate the lack of challenging MCHFR values predicted for this event by NRELAP5, which is further supported by the values predicted with the approved subchannel methodology. {{

}}^{2(a),(c)}

Table 7-61 Representative sensitivity studies – uncontrolled control rod bank withdrawal from subcritical or low power startup conditions

{{

}}^{2(a),(c)}

7.2.14 Uncontrolled Control Rod Assembly Bank Withdrawal at Power

The methodology used to simulate a postulated uncontrolled control rod assembly (CRA) bank withdrawal at power for the NPM, and an evaluation of the resulting representative plant response against the acceptance criteria for an AOO listed in Table 7-4, are presented below.

A description of the event including biases and conservatisms, sensitivity studies, single active failure (SAF) and loss of power (LOP) scenarios, challenging case, and acceptance criteria evaluation are presented in the following sections.

7.2.14.1 General Event Description and Methodology

As stated in Section 7.2.13, low power startup conditions exist for the NPM until reactor power reaches 15 percent RTP. Accordingly, the uncontrolled CRA bank withdrawal at power event extends from 15 percent RTP to HFP.

The withdrawal of the control bank causes a reactivity insertion that increases reactor power and leads to a rise in coolant temperature, pressurizer level, and RCS pressure. Feedback from the rising fuel temperature partially counteracts the reactivity insertion, slowing the power increase, which continues until the system trips on high power, high power rate, high pressurizer pressure, or high RCS riser temperature. The maximum power and minimum MCHFR occur just after the resulting scram, while the peak primary pressure occurs some time later, as the DHRS begins to function and remove heat through the steam generators. Finally, stable DHRS cooling is established at the end of the transient.

Following reactor trip and subsequent turbine trip, the turbine bypass to the condenser will open to control the RCS temperature. However, the actions of the turbine bypass system are not credited, so as to minimize heat removal by the secondary side. Although turbine load is an input to the feedwater controller, no changes are made to this controller because the RCS responses are not sufficient to affect feedwater control.

The limiting MCHFR occurs for a reactivity insertion rate that results in reactor trip on core power, pressurizer pressure, and RCS riser temperature signals at approximately the same time. These conditions arise for events initiated from partial power with lower reactivity insertion rates because higher reactivity insertion rates cause the MPS to trip much earlier on high power rate. The earlier reactor trip reduces the energy added to the reactor coolant, thereby producing a higher MCHFR. The range of reactivity insertion rates considered is sufficient to identify the point of transition to the high power rate signal. Sensitivity studies are performed on a variety of parameters, as necessary, to identify the case(s) with a potentially limiting MCHFR. The NRELAP5 MCHFR pre-screening process is employed to identify the cases sent for a detailed subchannel evaluation.

In contrast, the maximum fuel centerline temperature occurs when core power exceeds its analytical limit. This condition arises for events initiated from full power with the highest

reactivity insertion rate as determined from the resulting bank worth and control rod step speed.

A spectrum of constant reactivity insertion rates is evaluated. These reactivity insertion rates encompass the credible range resulting from a single control bank withdrawal. If necessary, this range is supplemented to cover the reactivity insertion rates associated with an inadvertent decrease in boron concentration event (Section 7.2.16).

Table 7-62 lists the relevant acceptance criteria, SAF, and LOP scenarios.

Table 7-62 Acceptance criteria, single active failure, loss of power scenarios – uncontrolled control rod bank withdrawal at power

Acceptance Criteria / Single Active Failure / Loss of Power Scenarios of Interest	Discussion
MCHFR and maximum fuel centerline temperature	MCHFR and maximum fuel centerline temperature are challenged during this reactivity anomaly event.
No single failure	The challenging cases occur when all equipment is operational.
No loss of power	The challenging cases occur when AC power is available for the event duration.

7.2.14.2 Acceptance Criteria

Evaluation of the most challenging case(s) relative to the acceptance criteria is presented in Table 7-63.

Table 7-63 Acceptance criteria – uncontrolled control rod bank withdrawal at power

Acceptance Criteria	Discussion
Primary pressure	This criterion is not an acceptance criterion listed in Section 15.4.2 of the SRP (Reference 15). The analysis shows the NPM does not introduce more challenging conditions for primary pressure compared to other AOOs.
Secondary pressure	This criterion is not an acceptance criterion listed in Section 15.4.2 of the SRP (Reference 15). The analysis shows the NPM does not introduce more challenging conditions for secondary pressure compared to other AOOs.
Critical heat flux ratio	This criterion is evaluated by downstream subchannel analysis.
Maximum fuel centerline temperature	This criterion is evaluated by downstream subchannel analysis.
Containment integrity	Containment integrity is evaluated by a separate analysis methodology.

Acceptance Criteria	Discussion
Escalation of an AOO to an accident	This criterion is satisfied by demonstrating stable RCS flow rates and constant or downward trending RCS and DHRS pressures and temperatures exist at the end of the transient, all acceptance criteria evaluated in the transient analysis are met, and shutdown margin is maintained at the end of the transient. RCS conditions during extended DHRS cooling are addressed in a separate analysis.

7.2.14.3 Biases, Conservatisms, and Sensitivity Studies

The biases and conservatisms presented in Table 7-64 are considered in order to identify the bounding transient simulation for MCHFTR and maximum fuel centerline temperature.

Table 7-64 Initial conditions, biases, and conservatisms – uncontrolled control rod bank withdrawal at power

Parameter	Bias / Conservatism	Basis
Initial reactor power	Varied. RTP biased upwards to account for measurement uncertainty.	{{ }} ^{2(a),(c)}
Initial RCS average temperature	Varied. Biased to the high condition.	{{ }} ^{2(a),(c)}
Initial RCS flow rate	Biased to the low condition.	{{ }} ^{2(a),(c)}
Initial PZR pressure	Varied.	{{ }} ^{2(a),(c)}
Initial PZR level	Varied.	{{ }} ^{2(a),(c)}

Parameter	Bias / Conservatism	Basis
Initial feedwater temperature	Nominal.	{{ }} ^{2(a),(c)}
Initial fuel temperature	Biased to the low condition.	{{ }} ^{2(a),(c)}
MTC	Most positive	{{ }} ^{2(a),(c)}
Kinetics	Biased to BOC conditions.	{{ }} ^{2(a),(c)}
Decay heat	Biased to the high condition.	{{ }} ^{2(a),(c)}
Initial SG pressure ⁽¹⁾	Nominal.	{{ }} ^{2(a),(c)}
SG heat transfer	Nominal.	{{ }} ^{2(a),(c)}
RSV lift setpoint	Biased to the high condition.	{{ }} ^{2(a),(c)}
SG tube plugging	Biased to the low condition.	{{ }} ^{2(a),(c)}
Reactivity insertion rate	Varied Maximum	{{ }} ^{2(a),(c)}
RCS Temperature Control Automatic rod control	N/A.	{{
Boron concentration	Not credited.	{{ }} ^{2(a),(c)}

Parameter	Bias / Conservatism	Basis
PZR Pressure Control PZR spray (normal)	Varied.	{
(bypass)	Nominal.	
PZR heaters (non-prop.)	Varied.	
(prop.)	Nominal.	
PZR Level Control Charging	Not credited.	{
Letdown	Varied.	
Steam Pressure Control Turbine throttle valves	Enabled.	{
Turbine bypass valves	Disabled.	
Feedwater and Turbine Load Control feedwater pump speed	Enabled.	{
CNV Pressure Control CNV evacuation system	Enabled.	{

1. {

}}^{2(a),(c)}

Sensitivity studies are performed as needed to identify the limiting response(s) for the acceptance criteria parameter(s) challenged by the event. Consequently, a sensitivity study is generally performed to identify cases for lowest MCHFR for this reactivity event. As an example, the initial core power, reactivity insertion rate, pressurizer pressure, pressurizer level, reactor coolant average temperature, pressurizer spray flow, pressurizer heater status, letdown status, and loss of power were varied to achieve the results presented in Table 7-65. These results demonstrate the MCHFR occurs at initial power levels of 75 percent RTP and above, with AC power available for the event duration, the RCS average temperature biased low, and the spray flow rate tuned to delay reactor trip on high pressurizer pressure.

Table 7-65 Representative sensitivity studies – uncontrolled control rod bank withdrawal at power

{{

}}^{2(a),(c)}

7.2.15 Control Rod Misoperation

The methodology used to simulate a postulated control rod misoperation for the NPM, and an evaluation of the resulting representative plant response against the acceptance criteria for an AOO listed in Table 7-4, are presented below.

A description of the event including biases and conservatisms, sensitivity studies, SAF and LOP scenarios, challenging case, and acceptance criteria evaluation are presented in the following sections.

7.2.15.1 General Event Description and Methodology

The rod control system is used to move (insert or withdraw) the control rod assemblies (CRAs) in response to an operator action or an automatic control. Since these transients are initiated by a malfunction in the rod control system, a variety of reactivity related conditions can result. Specific reactivity conditions for the NPM include: 1) withdrawing a single CRA; 2) dropping one or more CRAs; or, 3) leaving one or more CRAs behind when inserting or withdrawing a control bank. The consequences for each of these reactivity conditions are discussed below.

Table 7-66 lists the relevant acceptance criteria, single active failure, and loss of power scenarios.

Withdrawal of a Single CRA

The withdrawal of a single CRA causes a reactivity insertion that increases reactor power and leads to a rise in coolant temperature, pressurizer level, and RCS pressure. Feedback from the rising fuel temperature is not sufficient to counteract the reactivity insertion, so the power increases until the system trips on high power, high power rate, high pressurizer pressure, or high RCS riser temperature. The maximum power and minimum MCHFR occur just after the resulting scram, while the peak primary pressure occurs some time later, as the DHRS begins to function and remove heat through the steam generators. Finally, stable DHRS cooling is established at the end of the transient.

The limiting MCHFR occurs for a reactivity insertion rate that results in reactor trip on core power, pressurizer pressure, and RCS riser temperature signals at approximately the same time. These conditions arise for events initiated from partial power with lower reactivity insertion rates because higher reactivity insertion rates cause the MPS to trip much earlier on high power rate. The earlier reactor trip reduces the energy added to the reactor coolant, thereby producing a higher MCHFR. The asymmetry associated with the core power response causes the ex-core detectors to respond differently for each quadrant. Consequently, the range of reactivity insertion rates considered is sufficient to identify the point of transition to the high power rate signal (using the lowest reading ex-core detector based on the minimum after to before event initiation ratio of the radial peaking factors for the outer row of fuel assemblies). Sensitivity studies are performed on a variety of parameters, as necessary, to identify the case(s) with a potentially limiting

MCHFR. The NRELAP5 MCHFR pre-screening process is employed to identify the cases sent for a detailed subchannel evaluation.

In contrast to the uncontrolled CRA bank withdrawal at power event (Section 7.2.14), the highest reactivity insertion rate as determined from the resulting rod worth and control rod step speed is significantly lower for the withdrawal of a single CRA event. In this instance the highest reactivity insertion rate is less than half, so the magnitude of the power overshoot beyond the analytical limit is also lower. Consequently, the maximum fuel centerline temperature occurs at transient conditions nearer to those of the limiting MCHFR, i.e., at a much lower reactivity insertion rate.

Dropping One or More CRAs

Based on the minimum worth at any time during the cycle for a given core power, i.e., with the control bank positioned at the PDIL, dropping a single CRA causes a reactivity insertion that decreases reactor power. Feedback from the decreasing fuel temperature and the actions of the rod control system to restore power are generally not sufficient to counteract the reactivity insertion, so the power decreases until the system trips on high power rate. For event scenarios without a return to power, the maximum core power, peak primary pressure, and MCHFR occur at event initiation. The peak secondary system pressure occurs some time after the scram, as the DHRS begins to function and remove heat through the steam generators. Finally, stable DHRS cooling is established at the end of the transient.

The potential for a return to power exists only for events initiated from less than or equal to 50 percent RTP because the reduced worth of the dropped rod gives the rod control system time to act. The corresponding MCHFR for a dropped rod event with a return to power is considerably greater than the MCHFR for events initiated from HFP. Hence, the limiting MCHFR cases occur at HFP conditions.

Following reactor trip and subsequent turbine trip, the turbine bypass to the condenser will open to control the RCS temperature. However, the actions of the turbine bypass system are not credited, so as to minimize heat removal by the secondary side. Although turbine load is an input to the feedwater controller, no changes are made to this controller because the RCS responses are not sufficient to affect feedwater control.

The asymmetry associated with the core power response causes the ex-core detectors to respond differently for each quadrant. The power input to the high power rate signal uses the highest reading ex-core detector, multiplying the core average power by the maximum after drop to before drop ratio of the radial peaking factors for the outer row of fuel assemblies. Sensitivity studies are performed on a variety of parameters, as necessary, to identify the case(s) with a potentially limiting MCHFR. The NRELAP5 MCHFR pre-screening process is employed to identify the cases sent for a detailed subchannel evaluation.

The maximum fuel centerline temperature occurs at event initiation for those event scenarios with an immediate reactor trip. If the event scenario has a return to power, the maximum

fuel centerline temperature is bounded by the fuel centerline temperature at HFP because the associated power peak is substantially less than full power.

Misalignment of One or More CRAs

The misalignment of CRAs occurs as a result of one or more CRAs being left behind when inserting or withdrawing the control bank. These conditions are not evaluated with NRELAP5 as part of the non-LOCA event methodology because this event is not a transient. Instead, the MCHFR is determined as part of a detailed subchannel evaluation.

Table 7-66 Acceptance criteria, single active failure, loss of power scenarios – control rod misoperation

Acceptance Criteria / Single Active Failure / Loss of Power Scenarios of Interest	Discussion
MCHFR and maximum fuel centerline temperature	MCHFR and maximum fuel centerline temperature are challenged during this reactivity anomaly event.
Single failure of an ex-core flux detector	Delays time of reactor trip by requiring actuation based on responses of the least affected core quadrants.
No loss of power	A loss of AC power at event initiation is non-limiting (early reactor trip), while a loss of AC power coincident with reactor trip does not alter the MCHFR or fuel centerline temperature because the time of reactor trip is not changed.

7.2.15.2 Acceptance Criteria

Evaluation of the most challenging case(s) relative to the acceptance criteria is presented in Table 7-67.

Table 7-67 Acceptance criteria – control rod misoperation

Acceptance Criteria	Discussion
Primary pressure	This criterion is not an acceptance criterion listed in Section 15.4.3 of the SRP (Reference 15). The analysis shows the NPM does not introduce more challenging conditions for primary pressure compared to other AOOs.
Secondary pressure	This criterion is not an acceptance criterion listed in Section 15.4.3 of the SRP (Reference 15). The analysis shows the NPM does not introduce more challenging conditions for secondary pressure compared to other AOOs.
Critical heat flux ratio	This criterion is evaluated by downstream subchannel analysis.
Maximum fuel centerline temperature	This criterion is evaluated by downstream subchannel analysis.
Containment integrity	Containment integrity is evaluated by a separate analysis methodology.
Escalation of an AOO to an accident	This criterion is satisfied by demonstrating stable RCS flow rates, and constant or downward trending RCS and DHRS pressures and temperatures exist at the end of the transient, all acceptance criteria evaluated in the transient analysis are met, and shutdown margin is maintained at the end of the transient. RCS conditions during extended DHRS cooling are addressed in a separate analysis.

7.2.15.3 Biases, Conservatisms, and Sensitivity Studies

Withdrawal of a Single CRA

The biases and conservatisms presented in Table 7-68 are considered in order to identify the bounding transient simulation for MCHFTR and maximum fuel centerline temperature for the withdrawal of a single CRA event.

Table 7-68 Initial conditions, biases, and conservatisms – control rod misoperation, single control rod assembly withdrawal

Parameter	Bias / Conservatism	Basis
Initial reactor power	Varied. RTP biased upwards to account for measurement uncertainty.	{{ }} ^{2(a),(c)}
Initial RCS average temperature	Varied. Biased to the high condition.	{{ }} ^{2(a),(c)}
Initial RCS flow rate	Biased to the low condition.	{{ }} ^{2(a),(c)}
Initial PZR pressure	Varied.	{{ }} ^{2(a),(c)}
Initial PZR level	Varied.	{{ }} ^{2(a),(c)}
Initial feedwater temperature	Nominal.	{{ }} ^{2(a),(c)}
Initial fuel temperature	Biased to the low condition.	{{ }} ^{2(a),(c)}
MTC	Most positive	{{ }} ^{2(a),(c)}
Kinetics	Biased to BOC conditions.	{{ }} ^{2(a),(c)}
Decay heat	Biased to the high condition.	{{ }} ^{2(a),(c)}
Initial SG pressure ⁽¹⁾	Nominal.	{{ }} ^{2(a),(c)}

Parameter	Bias / Conservatism	Basis
SG heat transfer	Nominal.	{{ }} ^{2(a),(c)}
RSV lift setpoint	Biased to the high condition.	{{ }} ^{2(a),(c)}
SG tube plugging	Biased to the low condition.	{{ }} ^{2(a),(c)}
Reactivity insertion rate	Varied. Maximum	{{ }} ^{2(a),(c)}
RCS Temperature Control Automatic rod control	N/A.	{{ }} ^{2(a),(c)}
Boron concentration	Not credited.	
PZR Pressure Control PZR spray (normal)	Varied.	{{ }} ^{2(a),(c)}
(bypass)	Nominal.	
PZR heaters (non-prop.)	Varied.	
(prop.)	Varied.	

Parameter	Bias / Conservatism	Basis
PZR Level Control Charging	Not credited.	{
Letdown	Varied.	
		$\}}^{2(a),(c)}$
Steam Pressure Control Turbine throttle valves	Enabled.	{
Turbine bypass valves	Disabled.	
		$\}}^{2(a),(c)}$
Feedwater and Turbine Load Control feedwater pump speed	Enabled.	{
		$\}}^{2(a),(c)}$
CNV Pressure Control CNV evacuation system	Enabled.	{
		$\}}^{2(a),(c)}$

1. { $\}}^{2(a),(c)}$

Sensitivity studies are performed as needed to identify the limiting response(s) for the acceptance criteria parameter(s) challenged by the event. Consequently, a sensitivity study is generally performed to identify cases for lowest MCHFR for this reactivity event. As an example, the initial core power, reactivity insertion rate, pressurizer pressure, pressurizer level, reactor coolant average temperature, pressurizer spray flow, pressurizer heater status, letdown status, and loss of power were varied to achieve the results presented in Table 7-69 for the withdrawal of a single CRA event. These results demonstrate the MCHFR occurs at an initial power level of 75 percent RTP, with AC power available for the event duration, the RCS average temperature biased low, the pressurizer pressure biased low, the pressurizer level biased low, and the spray flow rate tuned to delay reactor trip on high pressurizer pressure.

Table 7-69 Representative sensitivity studies – control rod misoperation, single control rod assembly withdrawal

{{

}}^{2(a),(c)}

{{

}}^{2(a),(c)}

Dropping One or More CRAs

The biases and conservatisms presented in Table 7-70 are considered in order to identify the bounding transient simulation for MCHFTR and maximum fuel centerline temperature for the dropped CRA(s) event.

Table 7-70 Initial conditions, biases, and conservatisms – control rod misoperation, dropped control rod assemblies

Parameter	Bias / Conservatism	Basis
Initial reactor power	RTP biased upwards to account for measurement uncertainty.	{{ }} ^{2(a),(c)}
Initial RCS average temperature	Biased to the high condition.	{{ }} ^{2(a),(c)}
Initial RCS flow rate	Biased to the low condition.	{{ }} ^{2(a),(c)}
Initial PZR pressure	Biased to the high condition.	{{ }} ^{2(a),(c)}
Initial PZR level	Nominal.	{{ }} ^{2(a),(c)}
Initial feedwater temperature	Nominal.	{{ }} ^{2(a),(c)}
Initial fuel temperature	Nominal.	{{ }} ^{2(a),(c)}

© Copyright 2019 by NuScale Power, LLC

Sensitivity studies are performed as needed to identify the limiting response(s) for the acceptance criteria parameter(s) challenged by the event. Consequently, a sensitivity study is generally performed to identify cases for lowest MCHFR for this reactivity event. As an example, the initial core power, dropped CRA worth, and core time-in-life were varied to achieve the results presented in Table 7-71 for the dropped CRA(s) event. These results demonstrate the MCHFR occurs at full power conditions.

Table 7-71 Representative sensitivity studies – control rod misoperation, dropped control rod assemblies

{{

}}^{2(a),(c)}

7.2.16 Inadvertent Decrease in Boron Concentration

The methodology used to simulate an inadvertent decrease in boron concentration for the NPM, and an evaluation of the resulting representative plant response against the acceptance criteria for an AOO listed in Table 7-4, are presented below.

A description of the event including biases and conservatisms, sensitivity studies, single active failure (SAF) and loss of power (LOP) scenarios, challenging case, and acceptance criteria evaluation are presented in the following sections.

7.2.16.1 General Event Description and Methodology

The boric acid blend system incorporated into the NuScale plant design permits the operator to control the boron concentration of the reactor coolant via the charging fluid chemistry. While the NuScale plant design incorporates both automatic and manual controls, strict administrative procedures govern the process for adjusting the boron concentration of the reactor coolant. These administrative procedures establish limits on the rate and duration of the dilution.

The primary means of causing an inadvertent decrease in boron concentration is failure of the blend system, either by controller or mechanical failure, or operator error. The event is terminated by isolating the source for the diluted water, i.e., by closing the demineralized water system (DWS) isolation valves.

For Mode 1 plant operating conditions, the perfect mixing model and the wave front model are both evaluated. The perfect mixing model is evaluated for Mode 1 operating conditions because it provides a slower reactivity insertion rate, delaying detection, potentially allowing further loss of shutdown margin. The wave front model is physically conservative because it assumes the maximum amount of reactivity as the diluted slug of water sweeps through the core. This model does not assume any axial blending to ensure that this reactivity insertion rate is maximized. For all other operating modes where boron dilution

is allowed and limited mixing exists, a wave front model is used. These mixing models are generally performed as a hand calculation, but may be automated via a spreadsheet or other process.

The following mathematical expression is used to determine the time required to erode the shutdown margin with the perfect mixing model. Equation 7-1 shows that the reactivity insertion rate depends on the dilution rate and the total RCS mass.

$$t_{dil} = -\frac{1}{K} \ln \left(\frac{C_i}{C_f} \right) \quad \text{Eq. 7-1}$$

where:

t_{dil}	=	time required to dilute from the initial boron concentration to the final boron concentration, s
K	=	$(Q_{in} \rho_{in}) / (60 V_r \rho_r)$
Q_{in}	=	dilution flow rate of unborated water, gpm
ρ_{in}	=	dilution water density, lbm/ft ³
V_r	=	effective water volume of the RCS, gal
ρ_r	=	density of the water in the RCS, lbm/ft ³
C_i	=	initial boron concentration (maximum critical boron concentration including uncertainties), ppm
C_f	=	final boron concentration (boron concentration at which shutdown margin is lost), ppm

The following mathematical expressions are used to determine the number of wave fronts and the time required to erode the shutdown margin with the wave front model. In this model, the boron concentration of the RCS is reduced in discrete steps at each time, t , corresponding to the time the wave front passes through the core. The reactivity insertion rate is determined from the reactivity step change calculated as the product of the change in boron concentration and boron worth, divided by the core transport time. The core transport time is calculated as the total mass in the core divided by the RCS flow rate. As shown in Equation 7-2, the change in boron concentration is also inversely proportional to the RCS flow rate, therefore the ratio of total reactivity step change and core transport time makes the initial reactivity insertion rate independent of the RCS flow rate.

$$C_N = C_i \left[\frac{W_{NC}}{(W_D + W_{NC})} \right]^N \quad \text{Eq. 7-2}$$

$$t = \frac{M_{RCSI}}{(W_D + W_{NC})} + (N - 1) \frac{M_{RCS}}{(W_D + W_{NC})} \quad \text{Eq. 7-3}$$

where:

- C_N = the N^{th} front boron concentration, ppm
- C_i = initial boron concentration, ppm
- W_D = dilution mass flow rate, lbm/s
- W_{NC} = natural circulation mass flow rate, lbm/s
- M_{RCS} = RCS fluid mass minus the pressurizer, lbm
- M_{RCSI} = initial pass RCS fluid mass (mass between the CVCS injection point to core inlet), lbm
- N = number of times the wave front passes through the core

Mode 1 (Operations) HFP

In this mode of plant operation, an inadvertent decrease in boron concentration causes a reactivity insertion that increases reactor power, which leads to a rise in coolant temperature, pressurizer level, and RCS pressure. A loss of shutdown margin would occur quickest for the highest reactivity insertion rate, i.e., the maximum dilution flow rate of 50 gpm (2 CVCS pumps) with unborated water. The reactivity insertion rate associated with this configuration is determined using both the perfect mixing model (Equation 7-1) and the wave front model (Equation 7-2 and Equation 7-3). The time of reactor trip and isolation of the dilution source via closure of the DWS isolation valves is obtained from the results for the uncontrolled control rod bank withdrawal at power event (Section 7.2.14) for the case with the same initial power, the same (or lower) reactivity insertion rate, and the longest time to reactor trip. The calculations performed with the mixing model are also used to determine the shutdown margin available after isolation of the DWS, and the time at which the shutdown margin would be lost if the dilution source was not terminated. The system responses for all other acceptance criteria are comparable to the uncontrolled control rod bank withdrawal at power event.

Mode 1 (Operations) 25 percent RTP

In this mode of plant operation, an inadvertent decrease in boron concentration causes a reactivity insertion that increases reactor power, which leads to a rise in coolant temperature, pressurizer level, and RCS pressure. A loss of shutdown margin would occur quickest for the highest reactivity insertion rate, i.e., the maximum dilution flow rate of 25 gpm (1 CVCS pump) with unborated water. The reactivity insertion rate associated with this configuration is determined using both the perfect mixing model (Equation 7-1) and the wave front model (Equation 7-2 and Equation 7-3). Since the results of the rod withdrawal at power analysis have demonstrated that the consequences of the reactivity insertion events initiated from partial powers are bounded by the events initiated from full power initial condition with respect to MCHF and peak RCS pressure, the calculated reactivity insertion rates based on the perfect mixing assumption and the integrated reactivity steps based on the wave front model were compared to the reactivity insertion rates for dilutions initiated from HFP and HZP initial conditions respectively to confirm the non-limiting nature of the dilution events that are initiated from partial power conditions.

Mode 1 (Operations) HZP

In this mode of plant operation, an inadvertent decrease in boron concentration causes a reactivity insertion that increases reactor power, but does not lead to a rise in coolant temperature, pressurizer level, or RCS pressure. A loss of shutdown margin would occur quickest for the highest reactivity insertion rate, i.e., the maximum dilution flow rate of 25 gpm (1 CVCS pump) with unborated water. The reactivity insertion rate associated with this configuration is determined using both the perfect mixing model (Equation 7-1) and the wave front model (Equation 7-2 and Equation 7-3). The time of reactor trip and isolation of the dilution source via closure of DWS isolation valves is obtained from the results for the uncontrolled CRA bank withdrawal from subcritical or low power startup conditions event (Section 7.2.13) for the case with the same (or lower) initial power, the same (or lower) reactivity insertion rate, and the longest time to reactor trip. The calculations also determine the shutdown margin available after isolation of the DWS, and the time at which the shutdown margin would be lost if the dilution source was not terminated. The system responses for all other acceptance criteria are comparable to the uncontrolled CRA bank withdrawal from subcritical or low power startup conditions event.

Mode 2 (Hot Shutdown)

In this mode of plant operation, the MPS protection logic ensures the DWS is isolated when the RCS flow rate is less than 1.7 ft³/s (763 gpm). This protection scheme precludes any possibility for an inadvertent decrease in boron concentration.

When the RCS flow rate is greater than or equal to 1.7 ft³/s (763 gpm), the reactivity insertion from the maximum dilution flow rate of 25 gpm (1 CVCS pump) with unborated water causes an increase in reactor power (neutron population). The increase in neutron flux is detected by the MPS count rate protection signal and used to close the DWS isolation valves. The calculations performed with the wave front model (Equation 7-2 and Equation 7-3) determine the shutdown margin available after isolation of the DWS, and

the time at which the shutdown margin would be lost if the dilution source was not terminated.

Mode 3 (Safe Shutdown)

Similar to plant operation in Mode 2 (Hot Shutdown), the MPS protection logic ensures the DWS is isolated in this mode of plant operation when the RCS flow rate is less than 1.7 ft³/s. Thus, isolation of the DWS precludes any possibility for an inadvertent decrease in boron concentration.

When the RCS flow rate is greater than or equal to 1.7 ft³/s, the reactivity insertion from the maximum dilution flow rate of 25 gpm (1 pump) with unborated water causes an increase in reactor power (neutron population). The increase in neutron flux is detected by the MPS count rate protection signal and used to close the DWS isolation valves. The calculations performed with the wave front model (Equation 7-2 and Equation 7-3) determine the shutdown margin available after isolation of the DWS, and the time at which the shutdown margin would be lost if the dilution source was not terminated.

Mode 4 (Transition)

In this mode of plant operation, all CVCS connections to the NPM are disconnected, isolated, or locked out. Thus, the possibility of a design-basis inadvertent decrease in boron concentration is precluded.

Mode 5 (Refueling)

In this mode of plant operation, the Technical Specifications require the pool boron concentration to be sufficient to have appropriate shutdown margin. Surveillance of the boron concentration of the refueling pool will be performed at appropriate intervals to prevent any significant inadvertent dilution from flow paths to the reactor pool, or proximate water sources such as fire mains or feedwater piping.

The relevant acceptance criteria, SAF, and LOP scenarios are listed in Table 7-72.

Table 7-72 Acceptance criteria, single active failure, loss of power scenarios – inadvertent decrease in boron concentration

Acceptance Criteria / Single Active Failure / Loss of Power Scenarios of Interest	Discussion
MCHFR	MCHFR is challenged during this reactivity anomaly event. (Reactivity insertion rates are insufficient to challenge fuel centerline temperature.)
No single failure	The challenging cases occur when all equipment is operational.
No loss of power	The challenging cases occur when AC power is available to the CVCS equipment for the event duration.

7.2.16.2 Acceptance Criteria

Evaluation of the most challenging case(s) relative to the acceptance criteria is presented in Table 7-73.

Table 7-73 Acceptance criteria – inadvertent decrease in boron concentration

Acceptance Criteria	Discussion
Primary pressure	This criterion is not evaluated because the NPM does not introduce more challenging conditions for primary pressure compared to other AOOs.
Secondary pressure	This criterion is not evaluated because the NPM does not introduce more challenging conditions for secondary pressure compared to other AOOs.
Critical heat flux ratio	This criterion is evaluated by downstream subchannel analysis; or by demonstrating that a loss of shutdown margin does not occur.
Maximum fuel centerline temperature	This criterion is not evaluated because the reactivity insertion rates are insufficient to challenge the temperature limit.
Containment integrity	Containment integrity is evaluated by a separate analysis methodology.
Escalation of an AOO to an accident	This criterion is satisfied by demonstrating stable RCS flow rates and constant or downward trending RCS and DHRS (if actuated) pressures and temperatures exist at the end of the transient, all acceptance criteria evaluated in the transient analysis are met, and shutdown margin is maintained at the end of the transient. RCS conditions during extended DHRS cooling are addressed in a separate analysis.

7.2.16.3 Biases, Conservatisms, and Sensitivity Studies

The biases and conservatisms presented in Table 7-74 are considered in order to identify the bounding conditions for MCHFR, which coincide with the quickest loss of shutdown margin.

Table 7-74 Initial conditions, biases, and conservatisms – inadvertent decrease in boron concentration

Parameter	Bias / Conservatism	Basis
Initial reactor power	Excluded.	Not part of mixing model.
Initial RCS average temperature	Biased to the high condition.	{{ }} ^{2(a),(c)}

Parameter	Bias / Conservatism	Basis
Initial RCS flow rate	Biased to the low condition.	{{ }} ^{2(a),(c)}
Initial PZR pressure	Nominal.	{{ }} ^{2(a),(c)}
Initial PZR level	Excluded.	Not part of mixing model.
Initial feedwater temperature	Excluded.	Not part of mixing model.
Initial fuel temperature	Excluded.	Not part of mixing model.
MTC	Excluded.	Not part of mixing model.
Kinetics	Biased to BOC conditions.	{{ }} ^{2(a),(c)}
Decay heat	Excluded.	Not part of mixing model.
Initial SG pressure ⁽¹⁾	Excluded.	Not part of mixing model.
SG heat transfer	Excluded.	Not part of mixing model.
RSV lift setpoint	Excluded.	Not part of mixing model.
SG tube plugging	Excluded.	Does not alter active RCS volume.
Shutdown margin	Biased to the low condition.	{{ }} ^{2(a),(c)}
Initial boron concentration	Biased to the high condition	{{ }} ^{2(a),(c)}
Boron worth	Biased to the high condition.	{{ }} ^{2(a),(c)}
Active RCS volume	Biased to the low condition.	{{ }} ^{2(a),(c)}
Makeup flow rate	Biased to the high condition.	{{ }} ^{2(a),(c)}
Makeup temperature	Biased to the low condition.	{{ }} ^{2(a),(c)}
RCS Temperature Control Automatic rod control	Excluded.	Not part of mixing model.
Boron concentration	Not credited.	{{ }} ^{2(a),(c)}
PZR Pressure Control PZR spray (normal)	Excluded.	Not part of mixing model.
(bypass)	Excluded.	Not part of mixing model.
PZR heaters (non-prop.)	Excluded.	Not part of mixing model.
(prop.)	Excluded.	Not part of mixing model.

Parameter	Bias / Conservatism	Basis
PZR Level Control Charging	Enabled.	{
Letdown	Enabled.	
Steam Pressure Control Turbine throttle valves	Excluded.	}} ^{2(a),(c)}
Turbine bypass valves	Excluded.	
Feedwater and Turbine Load Control feedwater pump speed	Excluded.	Not part of mixing model.
CNV Pressure Control CNV evacuation system	Excluded.	Not part of mixing model.

{

}}^{2(a),(c)}

Table 7-75 Representative results – inadvertent decrease in boron concentration in Mode 1 at hot full power with the Perfect Mixing Model

Mode 1 (HFP)	1 CVCS Pump	2 CVCS Pumps
Dilution Flow Rate (gpm)	25	50
Initial boron concentration (ppm)	1400	1400
Final boron concentration (ppm)	1196	1196
Perfect mixing reactivity insertion rate (pcm/s)	0.50	1.00
Reactor trip / DWS isolation time (s)	161	78
DWS isolation valves closed (s)	166	83
Shutdown margin at time of isolation (pcm)	Greater than 1944	Greater than 1912
Shutdown margin lost assuming no isolation (s)	4092 (68.2 min)	2046 (34.1 min)

Table 7-76 Representative results – inadvertent decrease in boron concentration in Mode 1 at 25 percent rated thermal power

Mode 1 (25 percent RTP)	1 CVCS Pump
Dilution flow rate (gpm)	25
Initial boron concentration (ppm)	1800
Final boron concentration (ppm)	1596
Perfect mixing reactivity insertion rate (pcm/s)	0.65
Wave front reactivity insertion rate (pcm/s)	19.1
Wave front initial reactivity step (pcm)	91
Shutdown margin lost assuming no isolation (s)	3120 (52 min)

Table 7-77 Representative results – inadvertent decrease in boron concentration in Mode 1 at hot zero power with the Wave Front Model

Mode 1 (HZIP, 1 MWt)	1 CVCS Pump
Dilution Flow Rate (gpm)	25
Initial boron concentration (ppm)	1800
Final boron concentration (ppm)	1596
Initial reactivity step (pcm)	685
Wave front reactivity insertion rate (pcm/s)	17.3
Duration of reactivity insertion rate for each wave (s)	39.5
Initial wave front reaches core inlet	900
Initial wave front reaches core exit	939.5
Reactor trip / DWS isolation time ⁽¹⁾ (s) (wave front at core exit + UCRWS trip time)	Approximately 2028
DWS isolation valves closed (s)	Approximately 2033
Shutdown margin at time of isolation (pcm)	Greater than 697
Shutdown margin lost assuming no isolation (s) (critical wave at core inlet)	4200 (70 min)

1. Conservatively estimated to occur upon arrival of the subsequent wave

Table 7-78 Representative results – inadvertent decrease in boron concentration in Mode 2

Mode 2 (Coolant Flow ≥ 1.7 ft³/s))	1 CVCS Pump
Dilution Flow Rate (gpm)	25
Initial boron concentration (ppm)	785.5
Final boron concentration (ppm)	600
Initial reactivity step (pcm)	329
Wave front reactivity insertion rate (pcm/s)	8.32
Duration of reactivity insertion rate for each wave (s)	39.5
Reactor trip/DWS isolation wave at core inlet (s)	5280 (88 min)
DWS isolation valves closed (s)	5475
Shutdown margin at time of isolation (pcm)	Greater than 517
Shutdown margin lost assuming no isolation (s) (critical wave at core inlet)	7440 (124 min)

Table 7-79 Representative results – inadvertent decrease in boron concentration in Mode 3

Mode 3 (Coolant Flow ≥ 1.7 ft³/s))	1 CVCS Pump
Dilution flow rate (gpm)	25
Initial boron concentration (ppm)	813
Final boron concentration (ppm)	650
Initial reactivity step (pcm)	378
Wave front reactivity insertion rate (pcm/s)	9.55
Duration of reactivity insertion rate for each wave (s)	39.6
Reactor trip / DWS isolation wave at core inlet (s)	4200 (70 min)
DWS isolation valves closed (s)	4395
Shutdown margin at time of isolation (pcm)	Greater than 613
Shutdown margin lost assuming no isolation (s) (critical wave at core inlet)	6360 (106 min)

7.2.17 Chemical and Volume Control System Malfunction that Increases Reactor Coolant System Inventory

The methodology used to simulate a postulated CVCS malfunction that increases RCS inventory for the NPM, and an evaluation of the resulting representative plant response against the acceptance criteria for an AOO listed in Table 7-4, are presented below.

A description of the event including biases and conservatisms, sensitivity studies, single active failure (SAF) and loss of power (LOP) scenarios, challenging case, and acceptance criteria evaluation are presented in the following sections.

7.2.17.1 General Event Description

The NuScale reactor does not have a pumped ECCS, therefore, the unplanned increase in RCS inventory event is caused by a malfunction of the CVCS makeup pumps or pressurizer level control system. If borated water at the same concentration of the primary system is added to the RCS, the addition of large amounts of water to the primary system will generate a reactor trip on high pressurizer (PZR) water level or high PZR pressure. Table 7-80 lists the relevant acceptance criteria, SAF, and LOP scenarios.

The malfunction is assumed to isolate letdown and actuate both makeup pumps (each flowing at their maximum capacity), causing an unplanned increase in RCS inventory. The limiting pressure response occurs when the event is initiated from full power conditions, and the initial conditions are biased in the conservative directions. The increase in RCS inventory event is terminated by CVCS isolation on high PZR level or low- low RCS flow. (The CVCS containment isolation valves are dual safety related valves.)

Sensitivity studies to identify the challenging conditions are performed, as necessary, to identify the case(s) with the potentially limiting system pressures. Cases that include the effects of CVCS recirculation, which increases the flow into the RCS, are also analyzed.

Table 7-80 Acceptance criteria, single active failure, loss of power scenarios – reactor coolant system inventory increase

Acceptance Criteria / Single Active Failure / Loss of Power Scenarios of Interest	Discussion
Primary pressure, secondary pressure	System pressures are challenged during this mass addition event.
No single failure	The CVCS is isolated via dual safety-related isolation valves. If one of the isolation valves were to fail, the secondary CVCS isolation valve would provide system isolation.
No loss of power	Continued operation of the CVCS maximizes system pressures.

7.2.17.2 Acceptance Criteria

Evaluation of the most challenging case(s) relative to the acceptance criteria is presented in Table 7-81.

Table 7-81 Acceptance criteria – reactor coolant system inventory increase

Acceptance Criteria	Discussion
Primary pressure	Primary pressure rises to the peak value, then drops as the lowest setpoint RSV lifts to reduce pressure.
Secondary pressure	Secondary pressure increases rapidly to the peak value upon turbine trip, then decreases as the plant cools down via DHR.
Critical heat flux ratio	This criterion is evaluated by downstream subchannel analysis.
Maximum fuel centerline temperature	This criterion is evaluated by downstream subchannel analysis.
Containment integrity	Containment integrity is evaluated by a separate analysis methodology.
Escalation of an AOO to an accident	This criterion is satisfied by demonstrating stable RCS flow rates and constant or downward trending RCS and DHRS pressures and temperatures exist at the end of the transient, all acceptance criteria evaluated in the transient analysis are met, and shutdown margin is maintained at the end of the transient. RCS conditions during extended DHRS cooling are addressed in a separate analysis.

7.2.17.3 Biases, Conservatisms, and Sensitivity Studies

The biases and conservatisms presented in Table 7-82 are considered in identifying the bounding transient simulation for primary pressure.

Table 7-82 Initial conditions, biases, and conservatisms – reactor coolant system inventory increase

Parameter	Bias / Conservatism	Basis
Initial reactor power	RTP biased upwards to account for measurement uncertainty.	{{ }} ^{2(a),(c)}
Initial RCS average temperature	Varied.	{{ }} ^{2(a),(c)}

Parameter	Bias / Conservatism	Basis
Initial RCS flow rate	Varied.	{{ }} ^{2(a),(c)}
Initial PZR pressure	Varied.	{{ }} ^{2(a),(c)}
Initial PZR level	Varied.	{{ }} ^{2(a),(c)}
Initial feedwater temperature	Nominal.	{{ }} ^{2(a),(c)}
Initial fuel temperature	Biased to the low condition	{{ }} ^{2(a),(c)}
MTC	Consistent with EOC kinetics.	{{ }} ^{2(a),(c)}
Kinetics	Biased to EOC conditions.	{{ }} ^{2(a),(c)}
Decay heat	Biased to the high condition.	{{ }} ^{2(a),(c)}
Initial SG pressure ⁽¹⁾	Nominal.	{{ }} ^{2(a),(c)}
Steam generator heat transfer	Nominal.	{{ }} ^{2(a),(c)}
RSV lift setpoint	Biased to the high condition.	{{ }} ^{2(a),(c)}
SG tube plugging	Biased to the low condition.	{{ }} ^{2(a),(c)}
Makeup temperature	Varied	{{ }} ^{2(a),(c)}

$\}^{2(a),(c)}$

Parameter	Bias / Conservatism	Basis
Feedwater and Turbine Load Control Feedwater pump speed	Enabled.	{{ }} ^{2(a),(c)}
CNV Pressure Control CNV evacuation system	Enabled.	{{ }} ^{2(a),(c)}

1. {{

}}^{2(a),(c)}
2. These inputs, in conjunction with least negative Doppler temperature coefficient, are selected to maximize the power response (if any) induced by the addition of colder CVCS water. However, since this event is driven by mass addition, reactivity effects prior to RTS actuation (if any) are small when compared to the pressurization associated with the increase in primary inventory.

Sensitivity studies are performed as needed to identify the limiting response(s) for the acceptance criteria parameter(s) challenged by the event, including cases with the highest pressure responses for this inventory increase event. For example, a sensitivity study is performed to identify the highest primary and secondary side pressures, varying primary conditions, makeup temperature, spray availability (other parameters are biased as indicated in Table 7-82).

Representative results of this sensitivity study are presented in Table 7-83. The results of the sensitivity studies indicate that peak primary pressure occurs when initial primary temperature and pressure are biased to the low condition, and makeup temperature is biased to the high condition as the RTS actuates on high PZR pressure and the lowest-setpoint RSV operates to mitigate peak pressurization. With respect to maximum secondary side SG pressure, maximum SG pressure occurs when nonsafety-related spray is used to delay the RTS actuation until high PZR level is reached.

Table 7-83 Representative sensitivity studies – reactor coolant system inventory increase

{{

}}^{2(a),(c)}

7.2.18 Failure of Small Lines Outside Containment

The methodology used to simulate a postulated failure of a small line connected to the primary coolant system outside of containment for the NPM, and an evaluation of the resulting representative plant response against the acceptance criteria for an infrequent event listed in Table 7-4, are presented below.

A postulated break in a small line carrying primary coolant is typically evaluated for radiological consequences. Neither the plant design nor the use of natural circulation flow for the NPM introduces a more challenging condition for other acceptance criteria. Consequently, this event is evaluated only for radiological consequences. Evaluation of postulated small line breaks within the context of a 10 CFR 50 Appendix K regulatory LOCA analysis is covered separately in the LOCA-EM topical report.

7.2.18.1 General Event Description and Methodology

The event is initiated by a break in a line connected to the primary coolant system outside containment that causes a decrease in pressurizer pressure and level. The rate of decrease for both parameters depends on the break location and size. The subsequent decrease in RCS pressure provides little core reactivity from moderator feedback, so the reactor power remains relatively constant until reactor trip. In the absence of a loss of power at event initiation, the decreasing pressurizer pressure and level causes RTS actuation on the low pressurizer pressure signal or the low pressurizer level signal.

If the RTS low pressurizer level signal is reached first, the reactor is tripped and the pressurizer heaters are deactivated. Regardless of the presence of a reactor trip, the sustained loss of reactor coolant from the break causes a continuous decrease in pressurizer pressure and level. Eventually an MPS low pressurizer pressure signal is generated. This MPS signal leads to a reactor trip (if not previously generated), DHRS actuation, and CVCS isolation. Closure of the FWIVs and MSIVs following DHRS actuation isolates the steam generators, while CVCS isolation terminates the loss of reactor coolant through the break (assumed to be in the CVCS system since this is the only primary coolant system pipe line that penetrates the containment). Core decay heat drives natural circulation, which transfers thermal energy from the RCS to the reactor pool via the DHRS. Passive DHRS cooling is established and the transient terminates with the NPM in a safe, stable condition.

Several lines within the CVCS qualify as candidates for evaluation. These lines include makeup lines; letdown lines; pressurizer spray lines; and, the degassing (high point vent) line. However, the degassing line is eliminated from evaluation based on similarity with the spray lines: 1) the spray lines and degassing line are the same size; 2) both line types connect to the top of the pressurizer; and, 3) both line types penetrate the containment head. From a system response perspective, the plant response to a break in a spray line will be nearly the same as the plant response to a break in the degassing line. Thus, a break in the degassing line is not explicitly modeled.

When determining the magnitude of mass released for a break in a CVCS line outside containment the timing of CVCS isolation is critical, as CVCS isolation stops the release of mass from the RPV into the reactor building. Maximizing the mass released from the RPV and the duration of the iodine spike maximizes the radiological consequences.

The nature of a spray line break differs from that for a break in either the makeup line or letdown line because vapor is expelled from the break instead of liquid. As a result, steam production in the pressurizer is a key phenomenon for a spray line break, but much less important for makeup or letdown line breaks. A brief description of each break location is presented below.

Spray Line Breaks

Calculations were performed to assess the plant responses to a spectrum of spray line break sizes. Specifically, each break was modelled as either a double-ended guillotine

rupture, or a smaller size break, of the spray line piping. {{

}}^{2(a),(c)}

A break with an area of 100 percent of the spray line causes a rapid depressurization that quickly trips the reactor and isolates the CVCS. As such, a break of this size is not limiting. While the rate of depressurization declines proportionally as the break area is reduced, a break area within the steam production capability of the pressurizer heaters allows the pressurizer pressure to be maintained until the reactor trips on a low pressurizer level signal. After reactor trip, the rate of decrease for both the pressurizer pressure and level is nearly independent of break flow, and any reduction in pressure reduces the mass released through the break. Regardless of the break size, a break in a spray line is less limiting from a dose perspective than a break in either a makeup line or a letdown line because vapor is released instead of liquid, with no significant difference in event duration or iodine spiking time, thus the total mass released is smaller. Thus, breaks in a spray line are not evaluated as part of the non-LOCA transient analyses.

Makeup and Letdown Line Breaks

The evaluation of the makeup and letdown line breaks is divided into two phases:

1. Before Reactor Trip

This phase lasts until the reactor trips. During this phase, the total break mass release depends primarily on the liquid density at the location of the break. The break is modelled as either a double-ended guillotine rupture, or a smaller size break, of the line piping. {{

}}^{2(a),(c)}

2. After Reactor Trip

This phase lasts from the time of reactor trip until isolation of the CVCS. During this phase, the pressurizer level decreases independently of the break flow due to the mismatch between heat generation in the core and heat removal via the steam generators. Since the rate of decrease for both the pressurizer pressure and level is nearly independent of break flow, and any reduction in pressure reduces the mass released through the break, the mass released is maximized by increasing the break area to include both lines prior to CVCS isolation. In contrast, the spiking time is maximized when the break is restricted to a single location.

Table 7-84 lists the relevant acceptance criteria, single active failure, and loss of power scenarios.

Table 7-84 Acceptance criteria, single active failure, loss of power scenarios – breaks in small lines carrying primary coolant outside containment

Acceptance Criteria / Single Active Failure / Loss of Power Scenarios of Interest	Discussion
Radiological consequences	A postulated break in a small line carrying primary coolant is evaluated for radiological consequences.
No single failure	The isolation valves on the makeup, letdown, and spray lines are safety grade and redundant. Therefore, failure of a single valve does not prevent isolation or significantly increase the radiological consequences.
Loss of AC at event initiation	The loss of heat transfer to the secondary system associated with a loss of AC power at event initiation results in the most challenging integrated mass release and spiking time.

7.2.18.2 Acceptance Criteria

Evaluation of the most challenging case relative to the acceptance criteria is presented in Table 7-85.

Table 7-85 Acceptance criteria – breaks in small lines carrying primary coolant outside containment

Acceptance Criteria	Discussion
Primary pressure	Due to the depressurizing nature of the small line breaks carrying primary coolant event, sensitivities that maximize primary pressure are not analyzed. The peak primary pressure experienced during this event does not vary significantly from the pressure at event initiation. In all instances, the peak primary pressure remains below the design pressure, thereby providing margin to the acceptance criterion.
Secondary pressure	Secondary pressure increases rapidly post-DHRS actuation. However, due to the depressurizing nature of this event, sensitivities that maximize peak secondary pressure are not analyzed. In all instances the peak secondary pressure experienced during this event remains below the design pressure, thereby providing margin to the acceptance criterion.
Fuel cladding integrity	Fuel failure directly relates to dose by dictating the isotopic concentration of the reactor coolant being released. Consequently, the MCHFR and fuel centerline temperature criteria are relevant to determining the appropriate source term for the downstream radiological analysis. The depressurization following a break in a small line carrying primary coolant is slow enough to preclude an increase in core power or significant reduction in core flow prior to reactor trip. After considering the NuScale CHF trend with pressure, and the ranges bounded by the steady-state subchannel analysis, the CHFR is not challenged during the transient prior to reactor trip. Therefore, the fuel cladding integrity acceptance criteria are not challenged and event-specific follow-on MCHFR and fuel centerline temperature evaluations are not necessary.
Containment integrity	Containment integrity is evaluated in a separate analysis methodology.

Acceptance Criteria	Discussion
Consequential loss of system functionality	This criterion is satisfied by demonstrating stable RCS flow rates and constant or downward trending RCS and DHRS pressures and temperatures exist at the end of the transient, the water level in the RPV remains above the top of the core throughout the transient, all acceptance criteria evaluated in the transient analysis are met, and shutdown margin is maintained at the end of the transient.
Radiological consequences	The radiological consequences acceptance criteria are evaluated by downstream radiological analysis using the mass release calculated in the non-LOCA transient analysis.

7.2.18.3 Biases, Conservatisms, and Sensitivity Studies

The biases and conservatisms indicated in Table 7-86 are considered in identifying a bounding transient simulation for dose.

Table 7-86 Initial conditions, biases, and conservatisms – breaks in small lines carrying primary coolant outside containment

Parameter	Bias / Conservatism	Basis
Initial reactor power	Varied.	{{ }} ^{2(a),(c)}
Initial RCS average temperature	Biased to the high condition.	{{ }} ^{2(a),(c)}
Initial RCS flow rate	Biased to the low condition.	{{ }} ^{2(a),(c)}
Initial PZR pressure	Biased to the high condition	{{ }} ^{2(a),(c)}
Initial PZR level	Biased to the high condition.	{{ }} ^{2(a),(c)}
Initial feedwater temperature	Varied.	{{ }} ^{2(a),(c)}
Initial fuel temperature	Nominal.	{{ }} ^{2(a),(c)}

© Copyright 2019 by NuScale Power, LLC

© Copyright 2019 by NuScale Power, LLC

$$1. \{ \{ \quad \} \}^{2(a),(c)}$$

A sensitivity study is performed as needed to identify the most challenging break location and break size for small line breaks with respect to iodine spiking time. Representative results for this study are presented in Table 7-88. These results indicate the iodine spiking duration (elapsed time from reactor trip to CVCS isolation) is maximized with a break in the makeup line, AC power lost at event initiation, RCS average temperature biased high, and no break in the letdown line coincident with reactor trip.

Table 7-87 Representative break, time in life, power, flow, and temperature sensitivity study for mass release - breaks in small lines carrying primary coolant outside containment

{{

}}^{2(a),(c)}

Table 7-88 Representative break, time in life, power, flow, and temperature sensitivity study for iodine spiking time - breaks in small lines carrying primary coolant outside containment

{{

}}^{2(a),(c)}

7.2.19 Steam Generator Tube Failure

The methodology used to simulate a postulated failure of a steam generator tube for the NPM, and an evaluation of the resulting representative plant response against the acceptance criteria for an accident listed in Table 7-4, are presented below.

A postulated failure of a steam generator tube is typically evaluated for radiological consequences. Neither the design of the steam generator nor the use of natural circulation flow for the NPM introduce a more challenging condition for other acceptance criteria. Consequently, this event is evaluated only for radiological consequences.

7.2.19.1 General Event Description and Methodology

The event is initiated by the failure of a steam generator tube that causes a decrease in pressurizer pressure and level. The rate of decrease for both parameters depends on the break location and size. The subsequent decrease in RCS pressure provides little core reactivity from moderator feedback, so the reactor power remains relatively constant until reactor trip. In the absence of a loss of power at event initiation, the decreasing pressurizer pressure and level causes RTS actuation on the low pressurizer pressure signal or the low pressurizer level signal.

If the RTS low pressurizer level signal is reached first, the reactor is tripped and the pressurizer heaters are deactivated; otherwise, reactor trip is delayed until the RTS low pressurizer pressure signal is reached. Regardless of the presence of a reactor trip, the sustained loss of reactor coolant from the failed tube causes a continuous decrease in pressurizer pressure and level. Eventually an MPS low pressurizer pressure signal or low low pressurizer level signal is generated and DHRS is actuated. Closure of the FWIVs and MSIVs following DHRS actuation isolates the steam generator, which also terminates the loss of reactor coolant from the failed tube to the environment. Core decay heat drives natural circulation, which transfers thermal energy from the RCS to the reactor pool via the DHRS. Passive DHRS cooling is established and the transient ends with the NPM in a safe, stable condition.

When determining the magnitude of mass released for a steam generator tube failure (SGTF) event the timing of SG isolation is critical, since SG isolation terminates the release of mass from the RPV to other plant areas. Maximizing the mass released to the environment and the duration of the iodine spike (elapsed time from reactor trip to steam generator isolation) maximizes the radiological consequences.

Calculations were performed to assess the plant responses to a spectrum of break sizes. Specifically, each break was modelled as either a double-ended guillotine rupture, or a smaller size break, of the steam generator tube. {{

}}^{2(a),(c)} The results of sensitivity studies on break type and location indicate a rupture of the steam generator tube at the top of the steam generator provides the greatest integrated mass released and the longest spiking time. While the rate of depressurization declines proportionally as the break area

is reduced, the rate of decrease after reactor trip for both the pressurizer pressure and level is nearly independent of break flow, and any reduction in pressure reduces the mass released through the break.

An SGTF event initiated from HFP leads to a higher break flow, and thus a higher integrated mass released, because the pressure difference between the primary and secondary system is larger. Similarly, an SGTF event initiated from HFP leads to a longer spiking time because the stored energy of the core is greater.

Table 7-89 lists the relevant acceptance criteria, single active failure, and loss of power scenarios.

Table 7-89 Acceptance criteria, single active failure, loss of power scenarios – steam generator tube failure

Acceptance Criteria / Single Active Failure / Loss of Power Scenarios of Interest	Discussion
Radiological consequences	A postulated failure of a steam generator tube is evaluated for radiological consequences.
Failure of primary MSIV to close on affected SG	The primary MSIV is assumed to fail to isolate to maximize the radiological consequences. Delaying isolation until closure of the secondary MSIV leads to additional mass released to the environment and a longer iodine spike duration.
No loss of power	A loss of AC power at event initiation or coincident with turbine trip results in less integrated mass released and a shorter iodine spiking duration.

7.2.19.2 Acceptance Criteria

Evaluation of the most challenging case relative to the acceptance criteria is presented in Table 7-90.

Table 7-90 Acceptance criteria – steam generator tube failure

Acceptance Criteria	Discussion
Primary pressure	Due to the depressurizing nature of the steam generator tube failure event, sensitivities that maximize primary pressure are not analyzed. However, sensitivities were performed to demonstrate that, with the exception of those cases that involve a loss of power at event initiation, the peak primary pressure experienced during this event does not vary significantly from the pressure at event initiation. In all instances, i.e. with and without a loss of AC power at event initiation, the peak primary pressure remains below the design pressure, thereby providing margin to the acceptance criterion.
Secondary pressure	Pressure in the portion of the secondary system between the FWIVs and MSIVs increases rapidly post-DHRS actuation for both SGs, and the failed SG tube allows the pressure in the affected SG to approach RCS pressure conditions. Sensitivities were performed to demonstrate that the peak secondary system pressure remains at least 200 psia below the peak RCS pressure. In all instances, i.e., with and without a loss of AC power at event initiation, the peak secondary system pressure remains below the design pressure, thereby providing margin to the acceptance criterion.

Acceptance Criteria	Discussion
Fuel cladding integrity	Fuel failure directly relates to dose by dictating the isotopic concentration of the reactor coolant being released. Consequently, the MCHFR and fuel centerline temperature criteria are relevant to determining the appropriate source term for the downstream radiological analysis. The SGTF is a slow depressurization event that does not result in an increased core power or significantly reduced core flow prior to reactor trip. After considering the NuScale CHF trend with pressure and the ranges bounded by steady-state subchannel analysis, the CHF is not challenged during the transient prior to reactor trip. Therefore, the fuel cladding integrity acceptance criteria are not challenged and event-specific follow-on MCHFR and fuel centerline temperature evaluations are not necessary.
Containment integrity	Containment integrity is evaluated in a separate analysis methodology.
Consequential loss of system functionality	This criterion is satisfied by demonstrating stable RCS flow rates and constant or downward trending RCS and DHRS pressures and temperatures exist at the end of the transient, the water level in the RPV remains above the top of the core throughout the transient, all acceptance criteria evaluated in the transient analysis are met, and shutdown margin is maintained at the end of the transient.
Radiological consequences	The radiological consequences acceptance criteria are evaluated by downstream radiological analysis.

7.2.19.3 Biases, Conservatisms, and Sensitivity Studies

The biases and conservatisms indicated in Table 7-91 are considered in identifying a bounding transient simulation for dose.

Table 7-91 Initial conditions, biases, and conservatisms – steam generator tube failure

Parameter	Bias / Conservatism	Basis
Initial reactor power	RTP biased to the high condition.	{{ }} ^{2(a),(c)}
Initial RCS average temperature	Varied.	{{ }} ^{2(a),(c)}
Initial RCS flow rate	Biased to the low condition.	{{ }} ^{2(a),(c)}
Initial PZR pressure	Biased to the high condition	{{ }} ^{2(a),(c)}
Initial PZR level	Biased to the high condition.	{{ }} ^{2(a),(c)}
Initial feedwater temperature	Varied.	{{ }} ^{2(a),(c)}
Initial fuel temperature	Biased to the high condition.	{{ }} ^{2(a),(c)}
MTC	Varied.	{{ }} ^{2(a),(c)}
Kinetics	Varied.	{{ }} ^{2(a),(c)}
Decay heat	Biased to the high condition.	{{ }} ^{2(a),(c)}

$$\}}^{2(a),(c)}$$

$$1. \{ \{ \dots \}^{2(a),(c)}$$

© Copyright 2019 by NuScale Power, LLC

Table 7-92 Representative break characteristics, initial conditions, loss of power, and single active failure sensitivity study - steam generator tube failure

{{

}}^{2(a),(c)}

8.0 Representative Calculations

The methodology of Chapter 7 is utilized in conjunction with the NRELAP5 model of Chapter 6 to provide representative transient results. The transients noted below were selected to demonstrate the application of the NuScale Non-LOCA methodology for analysis of the plant responses to a wide range of postulated equipment failures and malfunctions.

1. Cooldown and/or Depressurization of the RCS (Section 8.1)
2. Heatup and/or Pressurization of the RCS (Section 8.2)
3. Reactivity Anomaly (Section 8.3)
4. Increase in RCS Inventory (Section 8.4)
5. Decrease in RCS Inventory (Section 8.5)

The information included for each representative transient includes: an event description; the results for the acceptance criteria of interest; and, conclusions regarding the acceptance criteria of interest. These results are presented to demonstrate the application of the non-LOCA methodology to the NPM. Fuel rod and core physics parameter inputs for the representative transients were developed using COPERNIC (Reference 22) and SIMULATE5 (Reference 23) respectively.

8.1 Cooldown and/or Depressurization of the Reactor Coolant System

8.1.1 Decrease in Feedwater Temperature

The purpose of this section is to present the thermal-hydraulic response of the NPM for a decrease in feedwater temperature event. This event is evaluated for MCHFR.

8.1.1.1 Event Description

The general decrease in feedwater temperature (DFWT) event description can be found in Section 7.2.1.1. Based on Section 7.2.1.1, MCHFR is the only acceptance criterion that may be potentially challenged during the DFWT event. No single failure is applied since the challenging cases occur when all equipment operates as designed. No loss of power is applied since all loss of power scenarios terminate feedwater or trip the reactor, thus reducing the overcooling event. Chosen from a series of MCHFR sensitivity cases, the representative DFWT case presented here represents a case that could challenge MCHFR, based on the NRELAP5 MCHFR pre-screening. This case features the following conditions:

- Conservative initial condition biasing (as shown in Table 7-7) is applied in order to maximize the consequences of the overcooling event in terms of MCHFR. This representative case is initialized at 102 percent reactor power. RCS average temperature is biased at high condition (555 degrees F). RCS flow rated is biased to

the low condition (535 kg/s). Pressurizer pressure is biased to the high condition (1920 psia). Pressurizer level is biased to the high condition (53 percent). Initial feedwater temperature is biased to the high condition (307.5 degrees F).

- Transient feedwater temperature decreases linearly from 307.5 degrees F at the rate of 1.18 degrees F per second which minimize the MCHFR based on the MCHFR pre-screening process.
- Feedwater flow is maintained at a constant volumetric flow rate. This prevents the controller from reducing feedwater flow in response to decreasing feedwater temperature which maximizes RCS overcooling.
- Turbine trip on reactor trip and subsequent operation of the turbine bypass system is not credited in this case, rather the turbine boundary is conservatively held constant at the pre-reactor trip condition in order to maximize the overcooling of the RCS.
- EOC reactivity coefficients are applied which maximizes the reactor power response.
- A low fuel temperature bias (applied by increasing gap conductance) is applied in this case although a nominal temperature is acceptable.
- No operator action was credited in the representative case. Normal control system such as PZR spray, heater, letdown controls and automatic rod control are modeled based on the control status shown in Table 7-7.

8.1.1.2 Analysis Results

The following describes the event sequence of the representative DFWT event. Table 8-1 summarizes the sequence of events. Figure 8-1 through Figure 8-9 show some key parameters during the representative DFWT event.

The DFWT event begins at time zero. The hydraulic feedwater source boundary condition is linearly changed from a constant temperature at 307.5 degrees F at a rate of 1.18 degrees F per second (Figure 8-1). Since the feedwater flow control is held at a constant volumetric pump rate, decreasing feedwater temperature means feedwater density and mass flow rate increases. The RCS response to the overcooling event begins once the cold feedwater front propagates through the secondary system piping and reaches the SG.

As heat removal from the RCS through the SG increases above its steady state value, downcomer temperature begins to decrease. The drop in average RCS temperature prompts the control rod controller to begin pulling the regulating bank out of the core at ~28 seconds. The addition of positive reactivity causes reactor power to increase. This increase in power is significant enough that moderator feedback stays slightly negative in response to the core heatup. Power and RCS riser temperature continue to rise until the high RCS riser temperature analytical limit (610 degrees F) is reached at ~139 seconds (Figure 8-2 and Figure 8-3). Because there is a total 8 second delay between the high RCS riser temperature signal and reactor scram, power continues to rise until reaching the high power limit (125 percent RTP) at ~145 seconds; there is a 2 second delay between the high power signal and reactor scram. Both the high power signal and the high

RCS riser temperature signal initiate reactor scram at ~147 seconds, which terminates the power excursion. Power peaks at 200.6 MWth before reactor scram.

The high RCS riser temperature signal also initiates DHRS actuation at the same time as reactor scrams. This closes the FWIVs and MSIVs, which isolate the SG from the remaining secondary system and ends the overcooling transient. Steam generator pressure increase resulting from main steam isolation is expected and is not a direct consequence of the decrease in feedwater temperature event itself. SG pressure starts to decrease once the DHRS cooling is established (Figure 8-4). RCS pressure and level have an overall decreasing trend as inventory shrinks due to increased heat removal during the overcooling transient. Once the PZR level is lower than the low PZR level analytical limit (35 percent) at ~725 seconds, PZR heaters are disabled and RCS pressure continues to decrease after that (Figure 8-5 and Figure 8-6).

After reactor trip and actuation of DHRS, RCS flow decreases rapidly and becomes stagnant and slightly reversed at ~180 seconds (Figure 8-7). Following that, oscillations are observed due to temperature and density differences between the riser and downcomer (as discussed in Section 7.2 and shown in Figure 8-3, Figure 8-7, and Figure 8-8); therefore the calculation is continued to verify that the module transitions into passive and stable DHRS cooling. At ~30 minutes, RCS flow has stabilized, and the RCS temperature and pressure are steadily decreasing as the DHRS transfers decay heat from the RPV to the reactor pool (Figure 8-3, Figure 8-5, Figure 8-7, and Figure 8-8). It is concluded that by 30 minutes the overcooling transient has been terminated and that stable DHRS cooling has been achieved. Subcritical margin is verified as net reactivity remains less than 0.0 dollars at the time stable DHRS cooling has been achieved (Figure 8-9). No operator action was credited to mitigate this event.

Table 8-1 Decrease in feedwater temperature sequence of events

Event	Time (sec)
Malfunction that initiates the decrease in feedwater temperature event. Feedwater temperature is linearly decreased from 307.5°F at a rate of 1.18°F per second.	0
Cold water front reaches core inlet. Regulating bank begins to withdraw in response to a decrease in average RCS temperature. Reactor power begins to rise.	28
High RCS riser temperature limit is reached (610°F). Control rod insertion begins after 8 second delay.	139
Peak RPV pressure is reached (1951 psia).	145
High reactor power limit is reached (125% RTP). Control rod insertion begins after 2 second delay.	145
Peak reactor power is reached (200.6 MW).	147
RTS actuation on both high power and high RCS riser temperature signals, control rods begin to insert into the core.	147
DHRS actuation on the high RCS riser temperature signal. DHRS actuation valves open immediately.	147
Limiting MCHFR is reached (2.591 as calculated by NRELAP5).	148
FWIVs and MSIVs are fully closed. Feedwater flow stops.	152
RCS flow is stagnant and slightly reversed	~ 180
Peak SG pressure is reached (1463 psia).	193
Low PZR level limit is reached (35%). PZR heaters are disabled after 3 second delay.	725
Low low PZR level is reached (20%). Containment and CVCS isolation begins after 3 second delay.	1767
Establishment of stable RCS flow. Pressure and temperature are steadily decreasing.	1800
End of calculation. Stable DHRS cooling has been established. Net reactivity remains < \$0.0.	2700

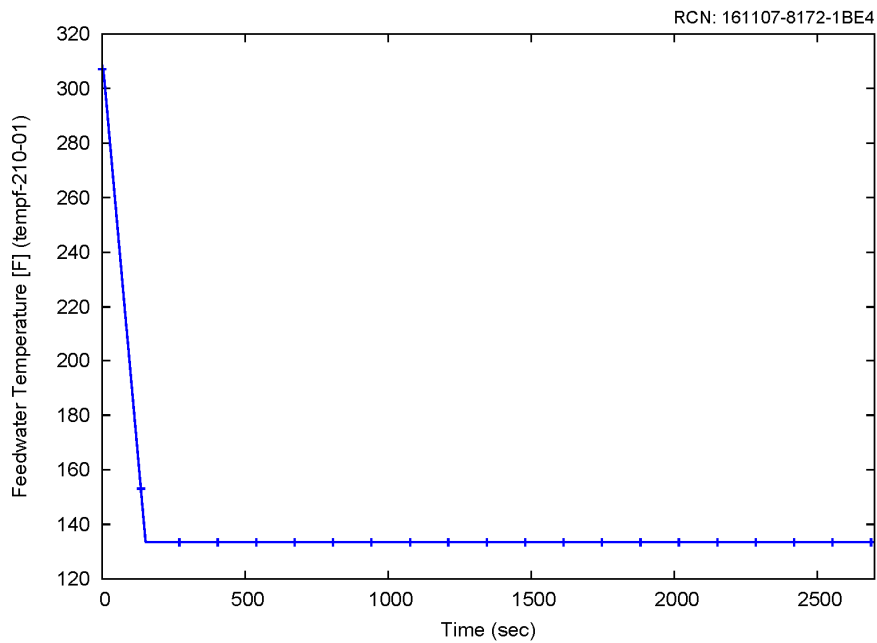


Figure 8-1 Temperature of feedwater during the representative decrease in feedwater temperature event

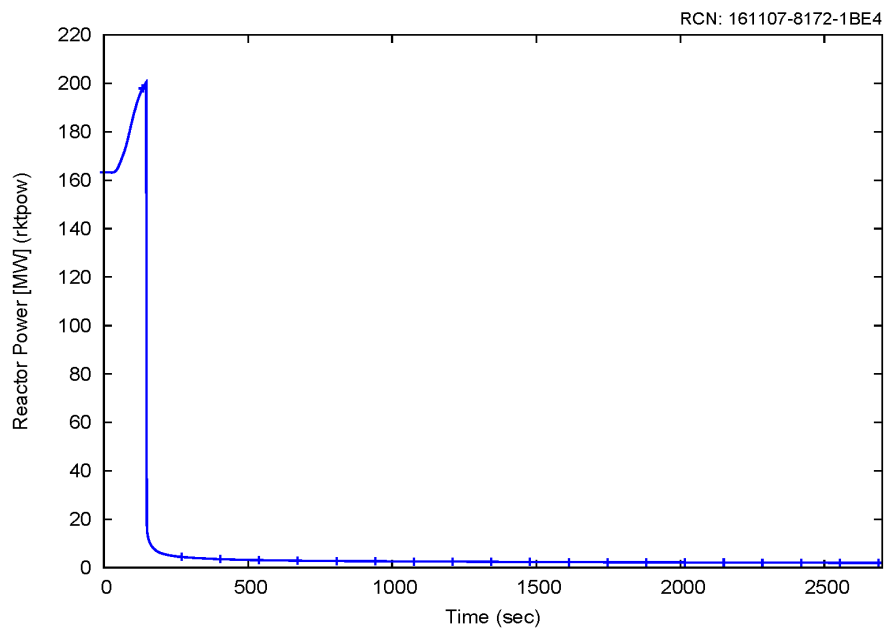


Figure 8-2 Power response for the representative decrease in feedwater temperature event

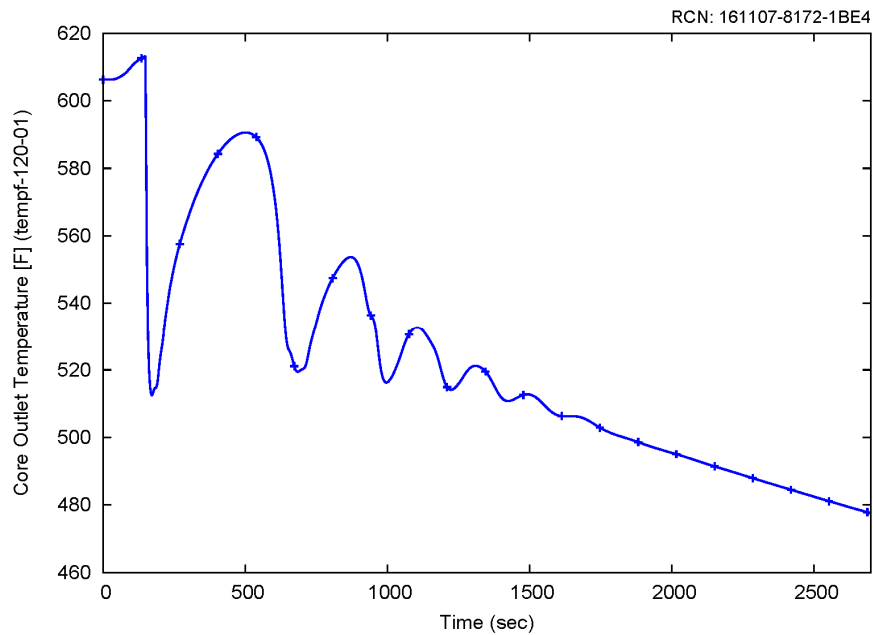


Figure 8-3 Core outlet temperature for the representative decrease in feedwater temperature event

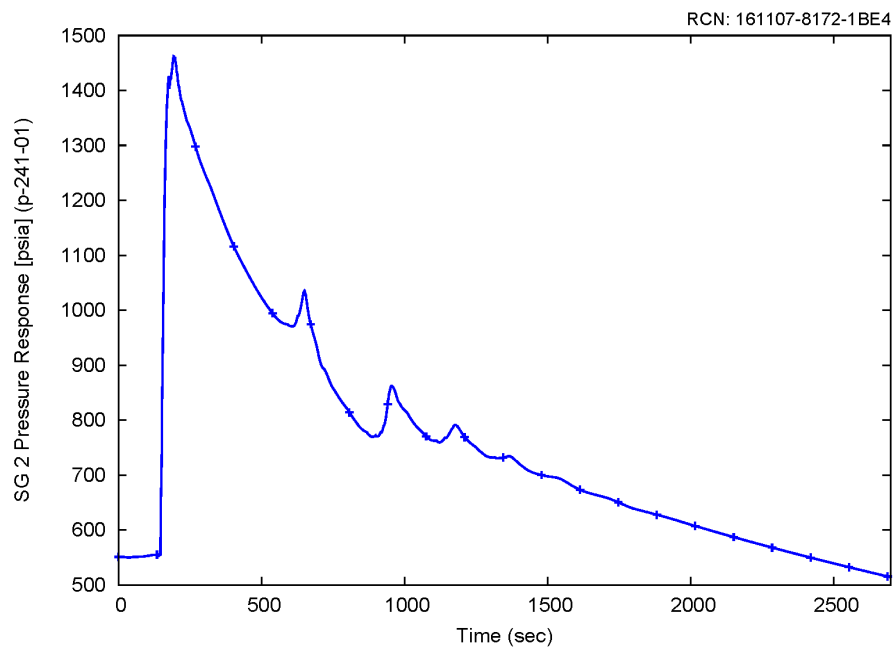


Figure 8-4 Steam generator 2 pressure response for the representative decrease in feedwater temperature event

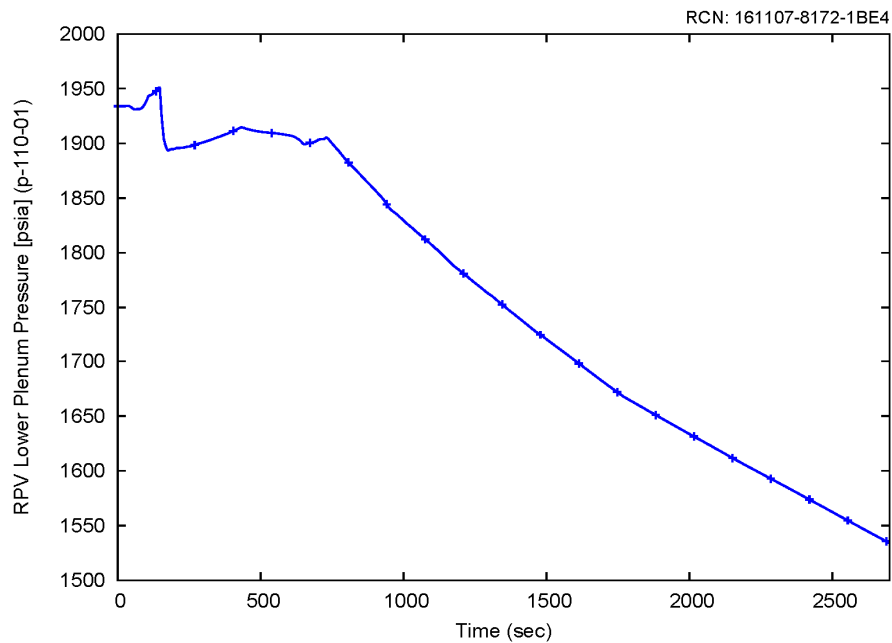


Figure 8-5 Reactor pressure vessel pressure response for the representative decrease in feedwater temperature event

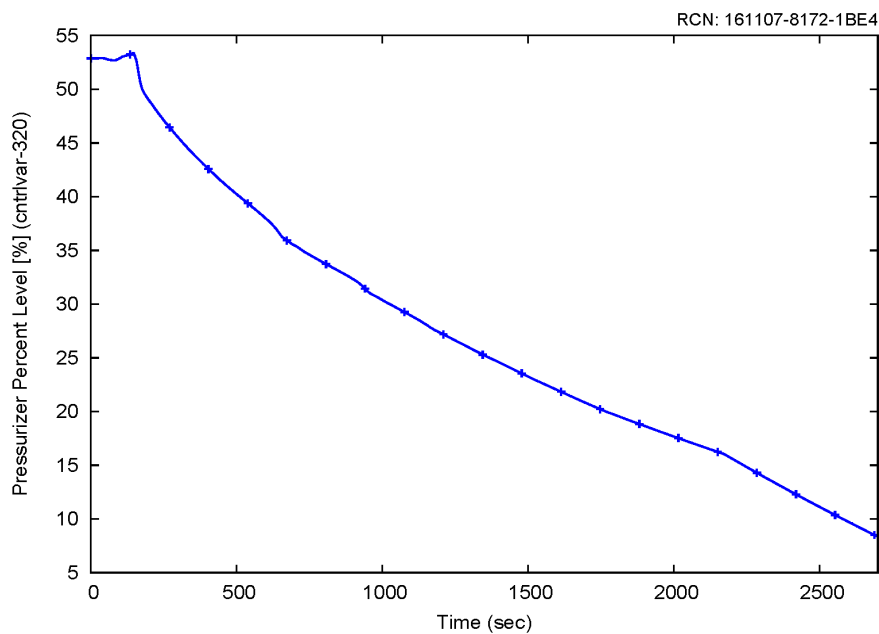


Figure 8-6 Pressurizer level for the representative decrease in feedwater temperature event

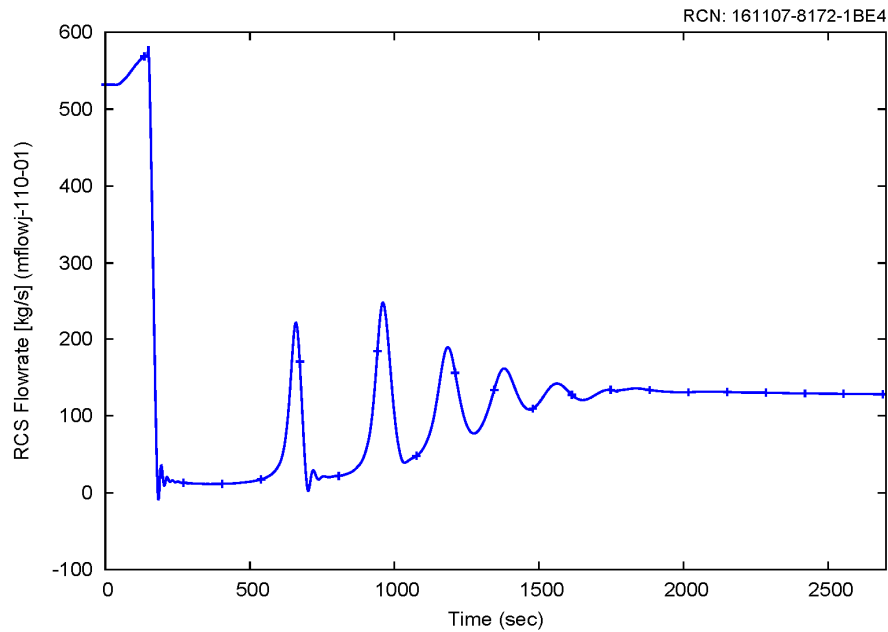


Figure 8-7 Reactor coolant system flow rate for the representative decrease in feedwater temperature event

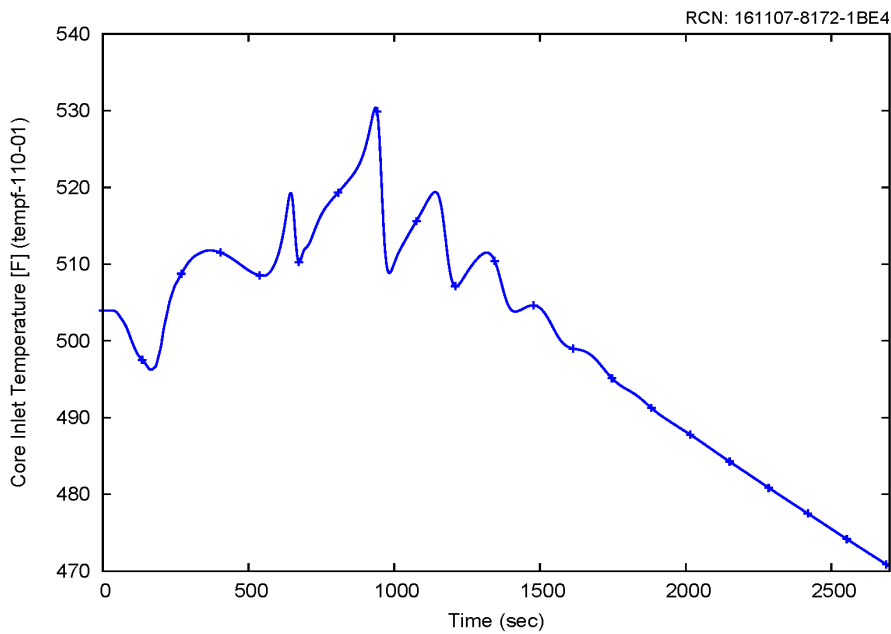


Figure 8-8 Core inlet temperature for the representative decrease in feedwater temperature event

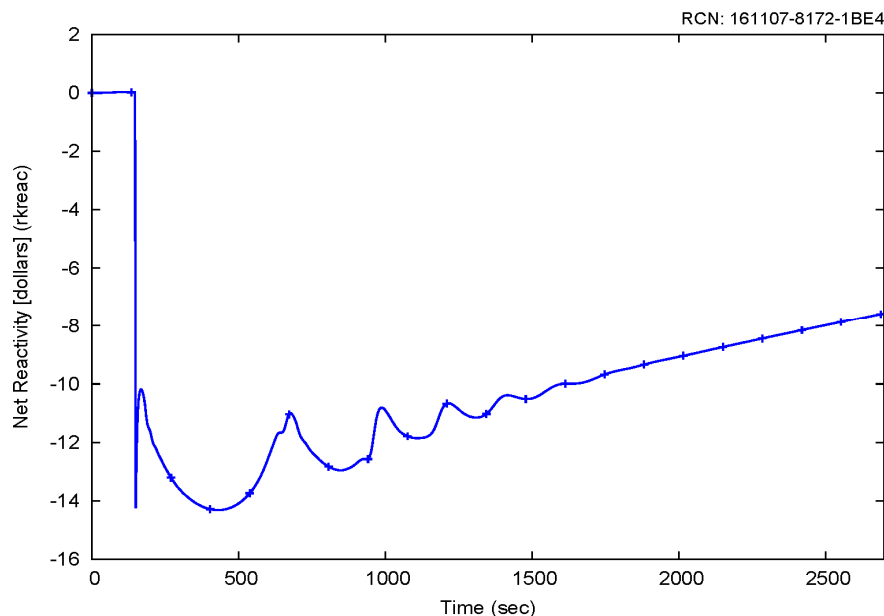


Figure 8-9 Net reactivity for the representative decrease in feedwater temperature event

8.1.1.3 Conclusion

A representative case that could challenge MCHFR was identified for a decrease in feedwater temperature event. The results of this case, as presented in Section 8.1.1.2, are subsequently used as input to an MCHFR evaluation using the NuScale subchannel analysis methodology.

8.1.2 Increase in Steam Flow

The purpose of this section is to present the thermal-hydraulic response of the NPM for an increase in steam flow event. This event is evaluated for MCHFR.

8.1.2.1 Event Description

The general increase in steam flow event description can be found from Section 7.2.3.1. Based on Section 7.2.3.1, MCHFR is the only acceptance criterion that may be potentially challenged during the increase in steam flow event. No single failure is applied since the challenging cases occur when all equipment operates as designed. No loss of power is applied since all loss of power scenarios terminate feedwater or trip the reactor, thus reducing the overcooling event. Chosen from a series of MCHFR sensitivity cases, the representative increase in steam flow case presented here represents a case that could challenge MCHFR, based on the NRELAP5 MCHFR pre-screening. This case features the following conditions:

- Conservative initial condition biasing (as shown in Table 7-19) is applied in order to maximize the consequences of the overcooling event in terms of MCHFR. This representative case is initialized at 102 percent reactor power. RCS average temperature is biased at high condition (555 degrees F). RCS flow rate is biased to the low condition (535 kg/s). Pressurizer pressure is biased to the high condition (1920 psia). Pressurizer level is biased to the high condition (53 percent).
- SG heat transfer is decreased 30 percent by applying a heat transfer coefficient multiplier of 0.7 in the steady state initialization model. As identified in Section 7.2.3.3, this biasing has insignificant impact on the overall limiting MCHFR conditions for the transient.
- Steam flow is increased 14.45 percent instantly at the beginning of the event. A time-dependent junction that controls steam mass flow rate is used to model the turbine.
- During the increase in steam flow event, the feedwater pump speed remains constant and the pump curve allows a 1.0 lbm/s increase in feedwater flow for every 1 psi decrease in SG pressure. This maximizes the overcooling event by increasing the available source of secondary coolant.
- EOC reactivity coefficients are applied which maximizes the reactor power response.
- A low fuel temperature bias (applied by increasing gap conductance) is applied in this case although a nominal temperature is acceptable.
- No operator action was credited in the representative case. Normal control system such as PZR spray, heater, letdown controls and automatic rod control are modeled based on the control status shown in Table 7-19.

8.1.2.2 Analysis Results

The following describes the event sequence of the representative increase in steam flow event. Table 8-2 summarizes the sequence of events. Figure 8-10 through Figure 8-19 show some key parameters during the representative increase in steam flow event.

The increase in steam flow event begins at time zero, as can be seen in Figure 8-10. The main steam flow rate at the secondary system hydraulic exit boundary is increased by 14.45 percent. Figure 8-11 shows that decreasing pressure in the secondary system also causes an increase in feedwater pump flow due to the pump curve, as shown in Figure 8-12. The RCS response to the overcooling event begins once steam flow through the steam generators starts to increase.

As heat removal from the RCS through the SG increases above its steady state value, downcomer temperature begins to decrease (Figure 8-13). The drop in average RCS temperature prompts the CR controller to pull the regulating bank out of the core at ~5 seconds. The addition of positive reactivity causes reactor power to increase, as seen in Figure 8-14. Power continues to rise until peaking at ~57 seconds. Peak power is calculated to be 199.97 MW, which is slightly lower than the high power analytical limit (200 MW or 125 percent RTP - increased from the analytical limit of 120 percent to conservatively account for the decalibration of the excore neutron detectors as

downcomer density increases in response to an overcooling event). Therefore the representative increase in steam flow event is not tripped on high power. Soon after, the limiting MCHFR is reached at ~62 seconds. Figure 8-15 shows the RCS riser temperature, which continues to rise until the high RCS riser temperature limit (610 degrees F) is reached at ~68 seconds. There is a total of 8 second delay between the high RCS riser temperature signal and RTS/DHRS actuation. Once RTS and DHRS actuate, the subsequent reactor scram and steam generator isolation terminate the overcooling event at ~76 seconds.

DHRS actuation closes the FWIVs and MSIVs, which isolate the SG from the remaining secondary system and ends the overcooling transient. Steam generator pressure increase resulting from MS isolation is expected and is not a direct consequence of the increase in steam flow event itself. SG pressure starts to decrease once the DHRS cooling is established (Figure 8-11). RCS pressure and level have an overall decreasing trend as inventory shrinks due to increased heat removal during the overcooling transient. Once the PZR level is lower than the low PZR level analytical limit (35 percent) at ~670 seconds, PZR heaters are disabled and RCS pressure continues to decrease after that (Figure 8-16 and Figure 8-17).

After reactor trip and actuation of DHRS, RCS flow decreases rapidly and becomes stagnant and slightly reversed at ~112 seconds (Figure 8-18). Following that, oscillations are observed due to temperature and density differences between the riser and downcomer (as discussed in Section 7.2 and shown in Figure 8-13, Figure 8-15, and Figure 8-18); therefore the calculation is continued to verify that the module transitions into passive and stable DHRS cooling. By 40 minutes, RCS flow has stabilized, and the RCS temperature and pressure are steadily decreasing as the DHRS transfers decay heat from the RCS to the reactor pool (Figure 8-13, Figure 8-15, Figure 8-16 and Figure 8-18). It is concluded that by 40 minutes the transient has been terminated and that stable DHRS cooling has been achieved. Subcritical margin is verified as net reactivity remains less than 0.0 dollars at the time stable DHRS cooling has been achieved (Figure 8-19). No operator action was credited to mitigate this event.

Table 8-2 Increase in steam flow sequence of events

Event	Time (sec)
An instant increase of 14.45% is applied to the steam flow to model the spurious opening of the turbine bypass valve or the main steam safety valve	0
Cold water front reaches core inlet. Regulating bank begins to withdraw in response to a decrease in average RCS temperature. Reactor power begins to rise.	5
Peak reactor power is reached (199.97 MW).	58
Limiting MCHFR is reached (3.570 as calculated by NRELAP5).	62
High RCS riser temperature limit is reached (610°F).	68
Actuation of the RTS. Control rods begin to insert into the core.	76
Actuation of the DHRS. The DHRS actuation valves open immediately. The FWIVs and MSIVs begin closing.	76
Peak RPV pressure is reached (1991 psia).	77
FWIVs and MSIVs are fully closed. Steam generator isolation from the remaining secondary system terminates the overcooling transient.	81
RCS flow is stagnant and slightly reversed.	112
Peak steam generator pressure is reached (1248 psia).	128
Low PZR level limit is reached (35%). PZR heaters are disabled after 3 second delay.	670
Low low PZR level is reached (20%). Containment and CVCS isolation begins after a 5 second delay.	1620
End of calculation. Stable DHRS cooling has been established. Net reactivity remains < \$0.0.	2400

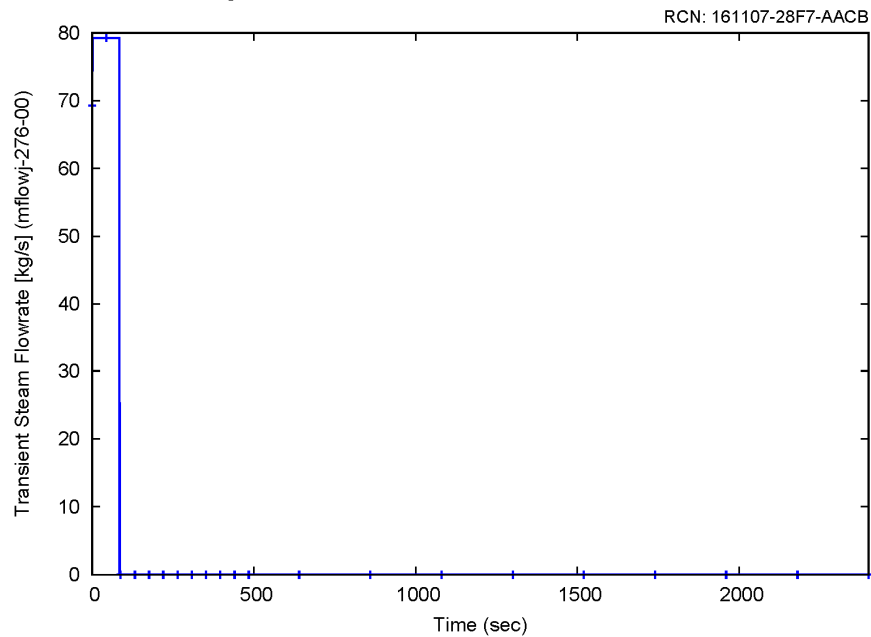


Figure 8-10 Main steam transient flow rate during the representative increase in steam flow event

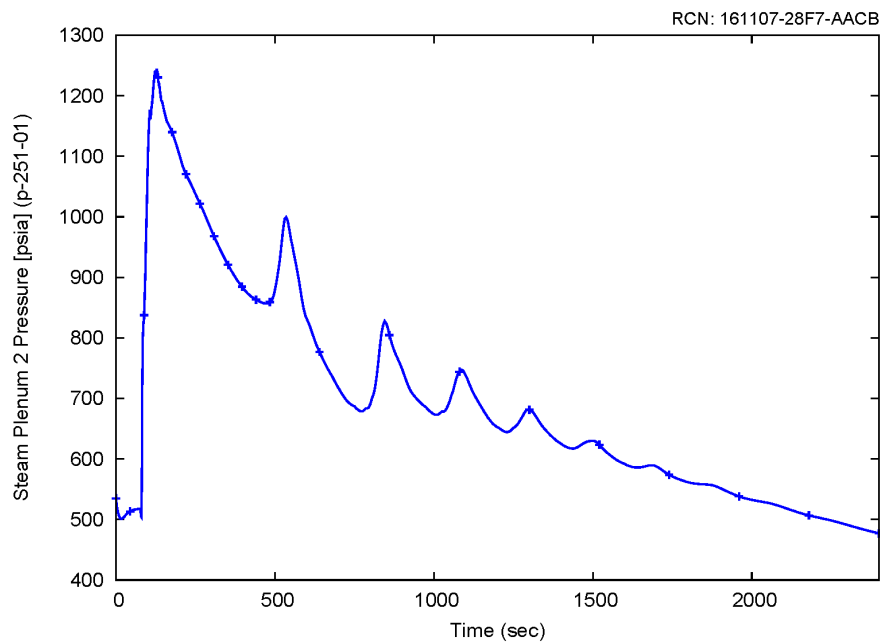


Figure 8-11 Steam generator 2 pressure response for the representative increase in steam flow event

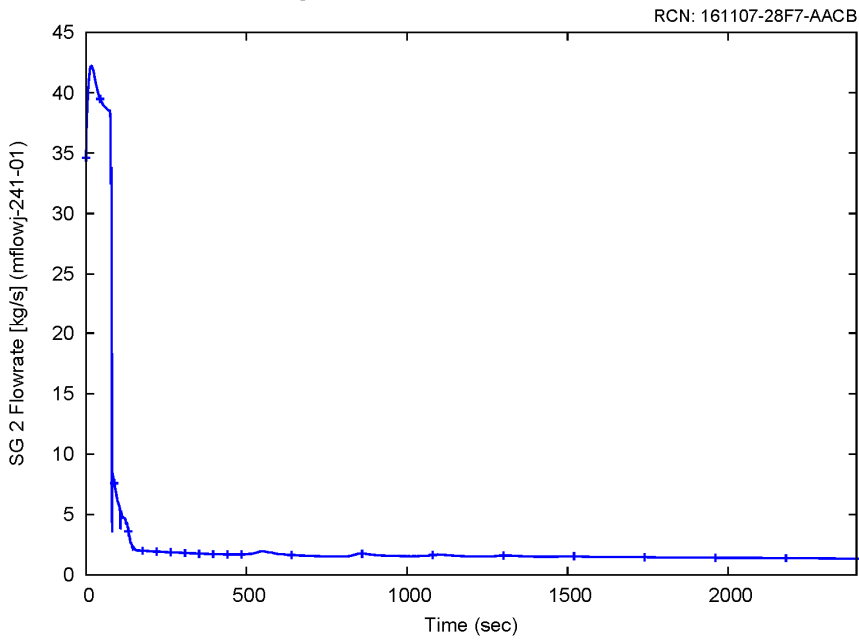


Figure 8-12 Steam generator 2 secondary side flow for the representative increase in steam flow event

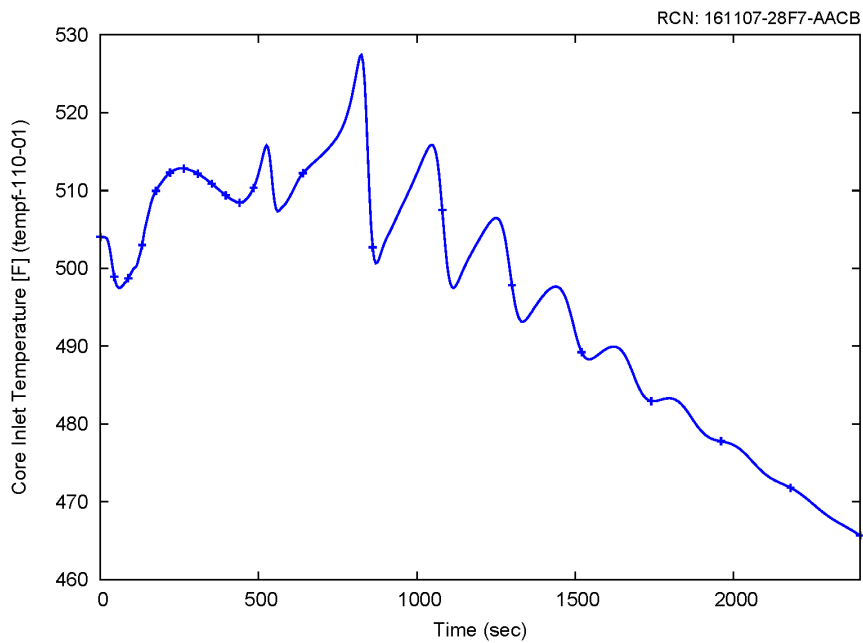


Figure 8-13 Core inlet temperature for the representative increase in steam flow event

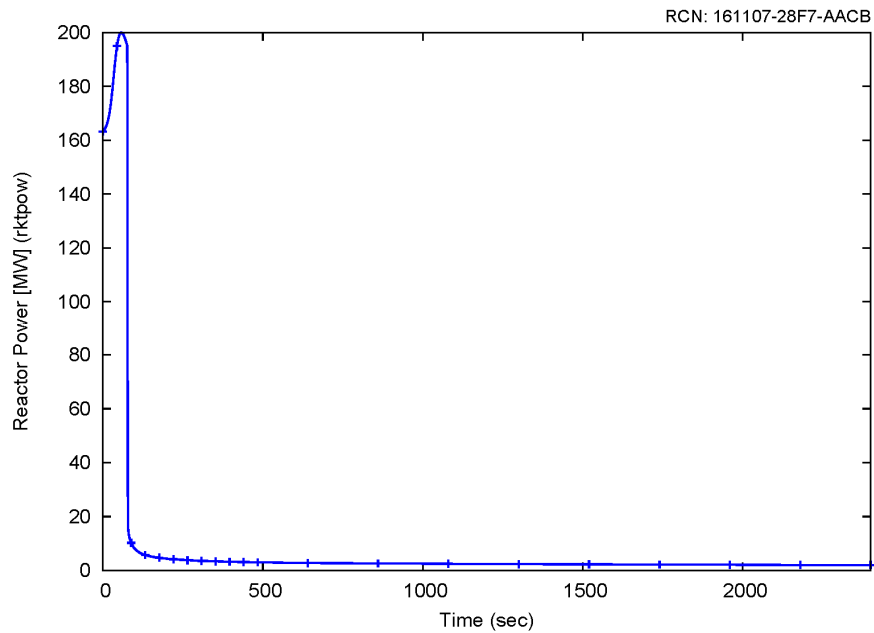


Figure 8-14 Power response for the representative increase in steam flow event

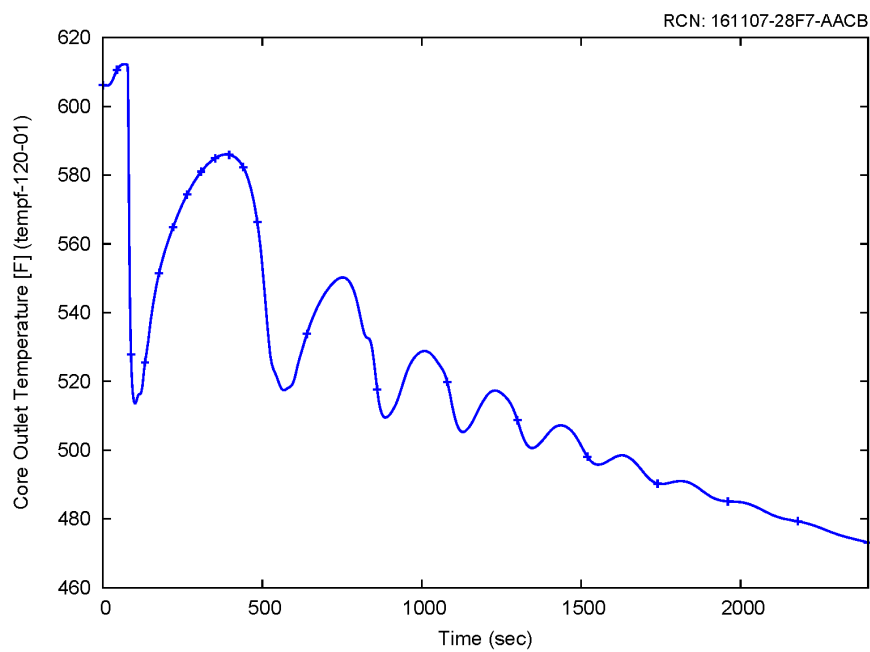


Figure 8-15 Core outlet temperature for the representative increase in steam flow event

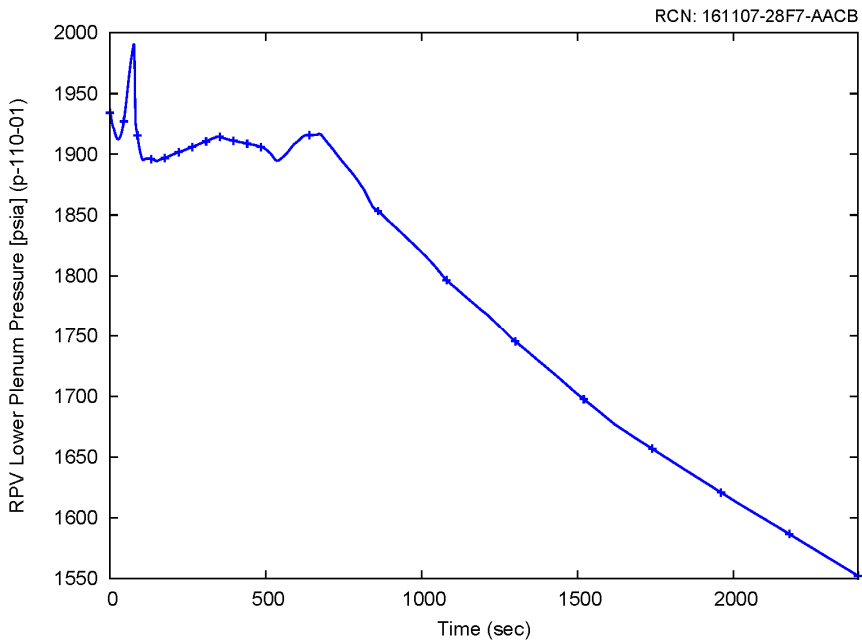


Figure 8-16 Reactor pressure vessel pressure response for the representative increase in steam flow event

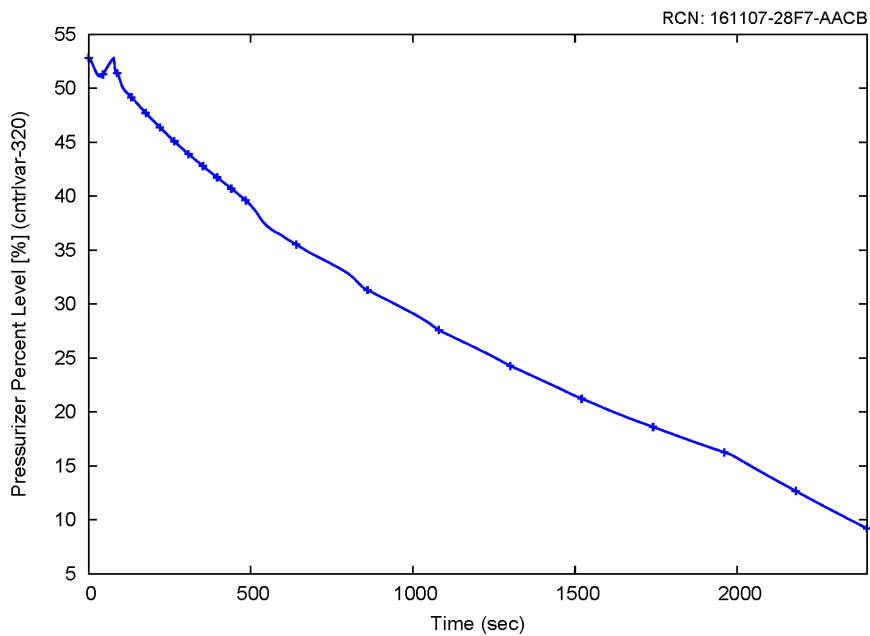


Figure 8-17 Pressurizer level for the representative increase in steam flow event

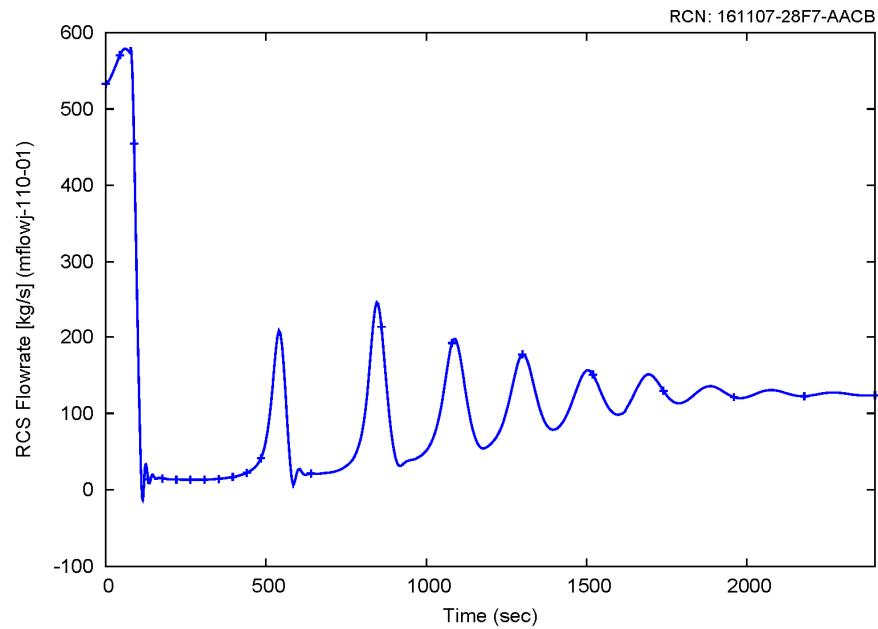


Figure 8-18 Reactor coolant system flow rate for the representative increase in steam flow event

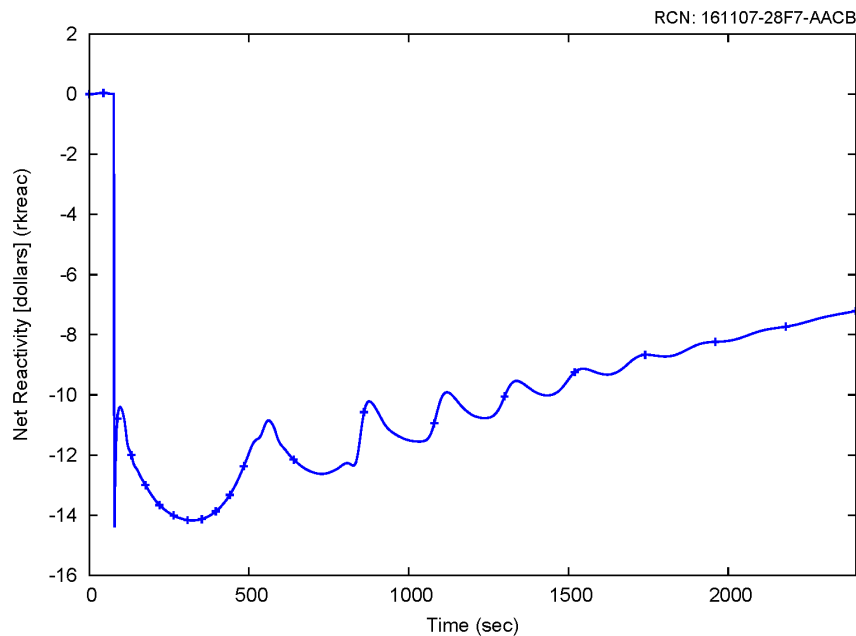


Figure 8-19 Net reactivity for the representative increase in steam flow event

8.1.2.3 Conclusion

A representative case that could challenge MCHFR was identified for an increase in steam flow event. The results of this case, as presented in Section 8.1.2.2, are subsequently used as input to an MCHFR evaluation using the NuScale subchannel analysis methodology.

8.1.3 Main Steam Line Break

The purpose of this section is to present the thermal-hydraulic response of the NPM for a main steam line break event. This event is evaluated for MCHFR, and mass releases are determined for input to downstream accident radiological dose analysis. A representative case evaluated for MCHFR is presented.

8.1.3.1 Event Description

The general description for main steam line break event can be found from Section 7.2.4.1. Based on Section 7.2.4.1, MCHFR is the only acceptance criterion that may be potentially challenged during the main steam line break event. The MCHFR case assumes a failed MSIV on the affected SG train; however, the timing of MCHFR is well before the MSIV would have closed so it is concluded there is no limiting failure for the MCHFR case. No loss of power is applied since all loss of power scenarios terminate feedwater or trip the reactor, thus reducing the overcooling event. Chosen from a series of MCHFR sensitivity cases, the representative main steam line break case presented here represents a case that could challenge MCHFR, based on the NRELAP5 MCHFR pre-screening. This case features the following conditions:

- Conservative initial condition biasing (as shown in Table 7-24) is applied in order to maximize the consequences of the overcooling event in terms of MCHFR. The case is initialized at 102 percent reactor power with conservatively high RCS temperature and pressure. RCS average temperature is biased at high condition (555 degrees F). RCS flow rate is biased to the low condition (535 kg/s). Pressurizer pressure is biased to the high condition (1920 psia). Pressurizer level is biased to the high condition (58 percent). Feedwater temperature is biased to the high condition (310 degrees F). Minimum RCS design flow is assumed.
- SG heat transfer is increased 30 percent by applying a heat transfer coefficient multiplier of 1.3 in the steady state initialization model. As identified in Section 7.2.4.3, this biasing has insignificant impact on the overall limiting MCHFR conditions, spiking time or mass released. There is no tube plugging in the SGs for this representative calculation.
- The feedwater controller is based on FW pressure error rather than turbine load demand. This allows for the implementation of the feedwater pump flow response to the pressure loss events. In the steam line piping failure transient, the details of how the pumps speed controller will respond are ignored and bounded by a conservative pump curve to maximize the flow response due to the drop in FW pressure.

- Steam pressure control is a flow based controller rather than a back pressure control. This is a better physical representation of the turbine response to a drop in steam pressure. During the transients the turbine is treated as a constant steam flow sink without automated runback.
- A low fuel temperature bias (applied via increase gap conductance) is applied which minimizes negative Doppler feedback following an increase in power.
- EOC reactivity coefficients are applied which maximizes the reactor power response.
- No operator action was credited in the representative case. Normal control system such as PZR spray, heater, letdown controls and automatic rod control are modeled based on the control status shown in Table 7-24.

8.1.3.2 Analysis Results –MCHFR Case

As discussed in Section 7.2.4.1, in the NPM design the smaller breaks can result in a delayed detection time compared to larger breaks and be more challenging for MCHFR. The MCHFR case is identified as a small (3.3 percent of the pipe cross section area) split break in the MS piping just outside of containment.

The following describes the event sequence of the MCHFR case for the steam line break event. Table 8-3 summarizes the sequence of events. Figure 8-20 through Figure 8-28 show some key parameters during the event.

The main steam line break event begins at time zero. Steam flow increases following the initiation of the break, as seen in Figure 8-20. As heat removal from the RCS through the SG increases above its steady state value, RCS temperature begins to decrease (Figure 8-21). The drop in average RCS temperature prompts the CR controller to pull the regulating bank out of the core. The addition of positive reactivity causes reactor power to increase (Figure 8-22). At ~47 seconds, the high power analytical limit (200 MWth or 125 percent RTP) is reached (Figure 8-23). At ~49 seconds, power is peaked at 202.8 MWth when reactor starts to scram. Approximately at the same time, the limiting MCHFR calculated by NRELAP5 is reached.

SG pressure decreases during the initial phase of the transient due to the break. As reactor power increases the SG pressure starts to increase and reaches the analytical limit of 800 psia at ~59 seconds (Figure 8-24). This is the time when DHRS is actuated. DHRS actuation closes the FWIVs and MSIVs, which isolate the SGs and the break from the remaining secondary system and ends the overcooling transient. Steam generator pressure increase resulting from MS isolation is expected. SG pressure starts to decrease once the DHRS cooling is established. Because of the single failure of the MSIV on the affected SG (failure to close), the affected SG and the associated DHRS train are depleted through the break after DHRS actuation. The unaffected SG and the associated DHRS train remove the decay heat (Figure 8-20 and Figure 8-24).

RCS level has an overall decreasing trend as inventory shrinks due to increased heat removal due to steam line break (Figure 8-25). The PZR level is still above the low PZR

level analytical limit (35 percent) by the end of the transient so the PZR heaters can still function.

The RCS pressure initially drops as inventory shrinks due to increased heat removal. As reactor power increases and as the PZR heaters respond, an increase in RPV pressure to ~1997 psia is observed. When the reactor is tripped, the RCS pressure has a sudden drop and then gradually returns to its setpoint, using pressurizer heaters (Figure 8-26).

After reactor trip and actuation of DHRS, RCS flow decreases rapidly and becomes stagnant and slightly reversed at ~85 seconds (Figure 8-27). Following that, oscillations are observed due to temperature and density differences between the riser and downcomer (as discussed in Section 7.2 and shown in Figure 8-20, Figure 8-21, Figure 8-27, and Figure 8-28); therefore the calculation is continued to verify that the module transitions into passive and stable DHRS cooling. By 30 minutes, RCS flow has stabilized, and the RCS temperature and pressure are steadily decreasing as the DHRS transfers decay heat from the RCS to the reactor pool (Figure 8-21, Figure 8-26, Figure 8-27, and Figure 8-28). It is concluded that by 30 minutes the transient has been terminated and that stable DHRS cooling has been achieved. Subcritical margin is verified as net reactivity remains less than 0.0 dollars at the time stable DHRS cooling has been achieved (Figure 8-22). No operator action was credited to mitigate this event.

Table 8-3 Main steam line break sequence of events

Event	Time (sec)
Initiation of a split main steam line break (3.3% of the pipe cross sectional area) on SG 2	0
High power (125% RTP) analytical limit is reached.	47
RTS is actuated and control rods begin to insert into the core.	49
Peak power is 202.8 MW.	49
MCHFR is reached (3.682 as calculated by NRELAP5)	49
Control rods fully inserted.	51
Peak RCS pressure is reached (~1997 psia).	52
High SG pressure analytical limit (800 psia) is reached. DHRS is actuated. ⁽¹⁾	59
RCS flow is stagnant and slightly reversed.	~85
Peak main steam system pressure (~1207 psia) is reached.	133
End of calculation. Stable DHRS cooling has been established. Net reactivity remains < \$0.0.	1800

- (1) In this example transient calculation the pressurizer heater trip on high SG pressure was not modeled. The calculation shows the heaters maintain the RCS pressure. The overall event progression is not affected because reactor trip and DHRS actuation have occurred.

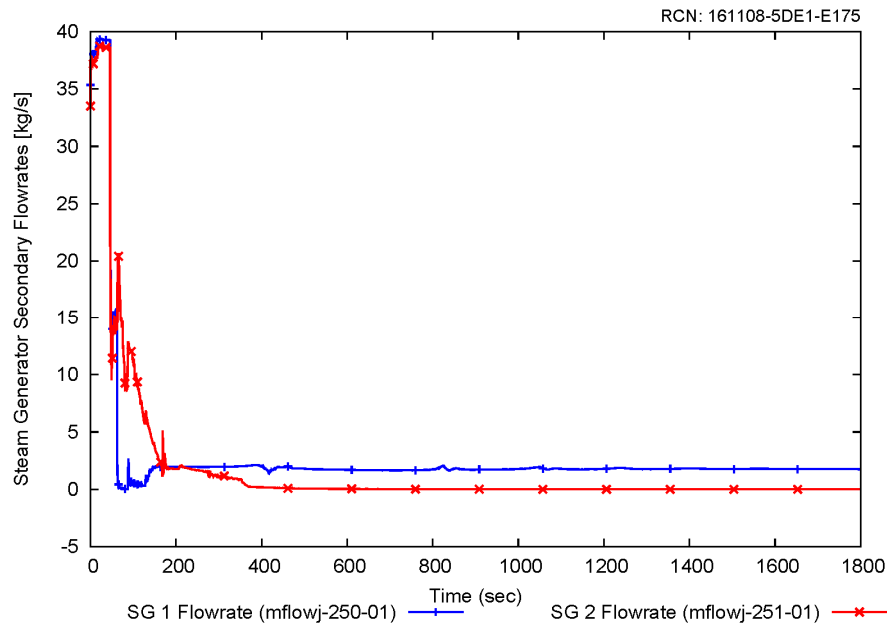


Figure 8-20 Steam generators 1 (unaffected) and 2 (affected) secondary flow rates for the representative main steam line break event

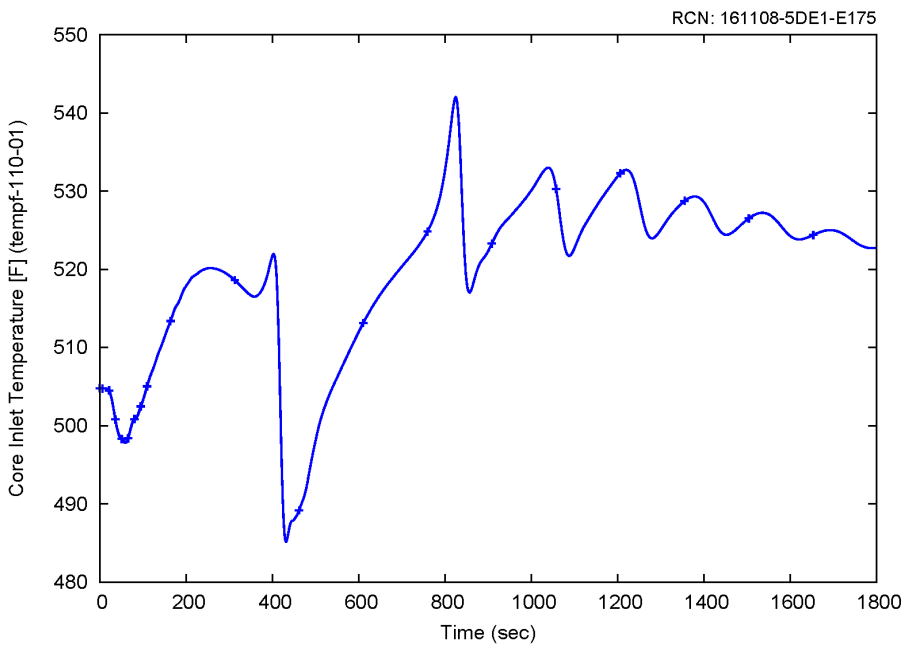


Figure 8-21 Core inlet temperature for the representative main steam line break event

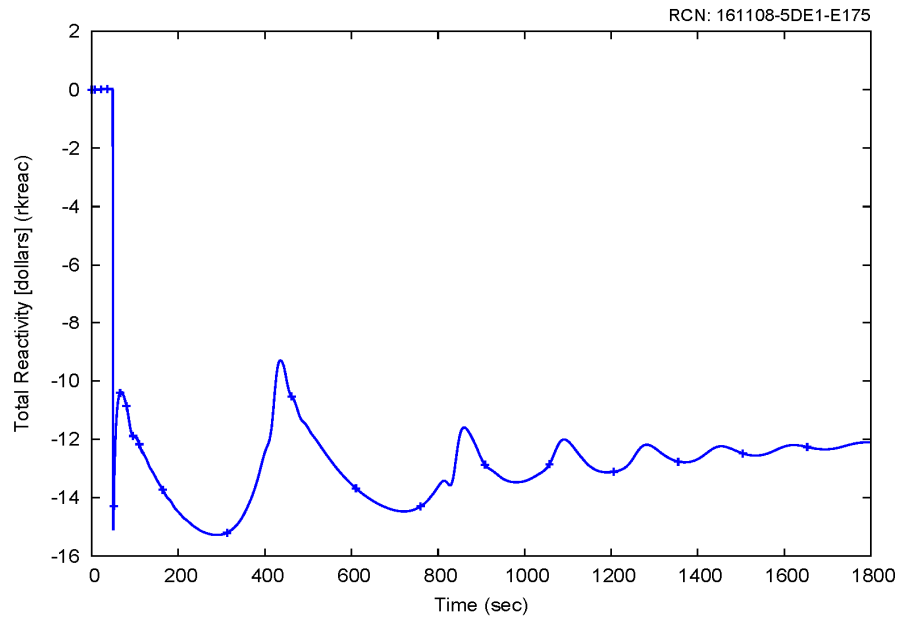


Figure 8-22 Net reactivity for the representative main steam line break event

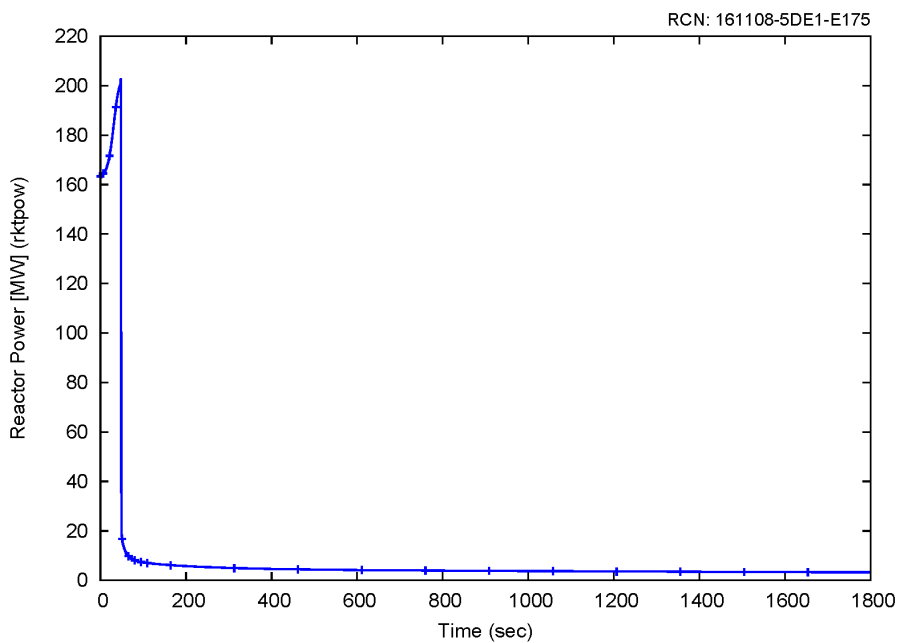


Figure 8-23 Power response for the representative main steam line break event

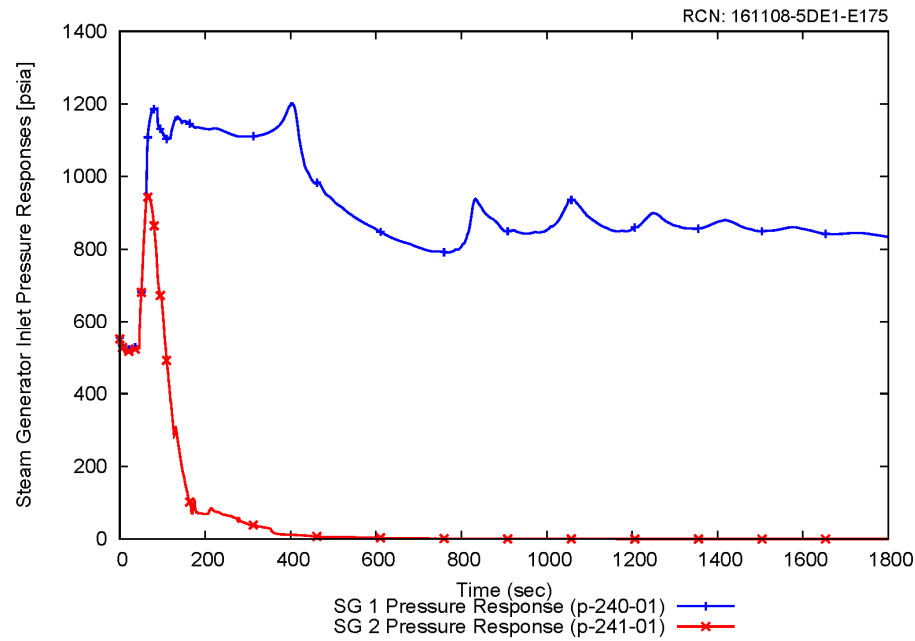


Figure 8-24 Steam generators 1 (unaffected) and 2 (affected) pressure response for the representative main steam line break event

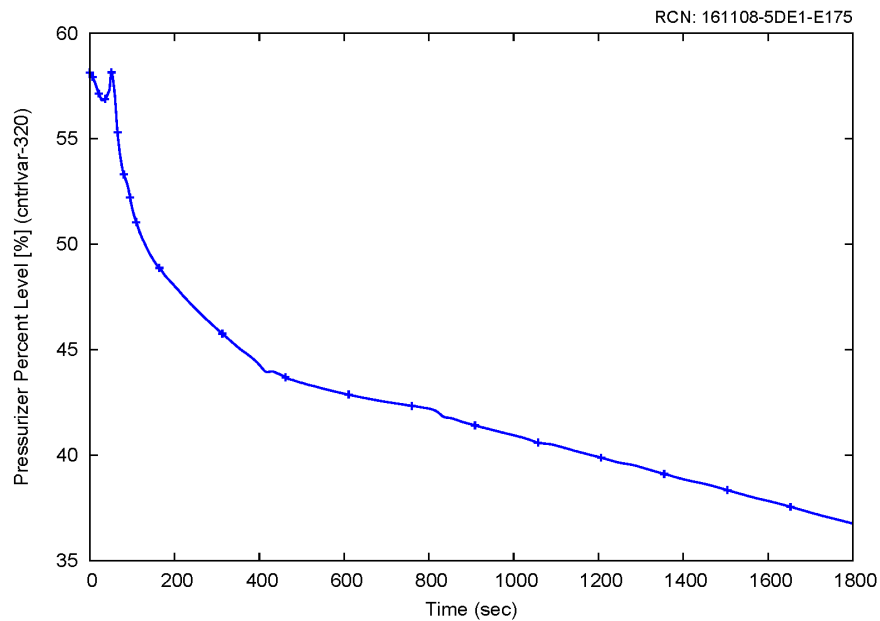


Figure 8-25 Pressurizer level for the representative main steam line break event

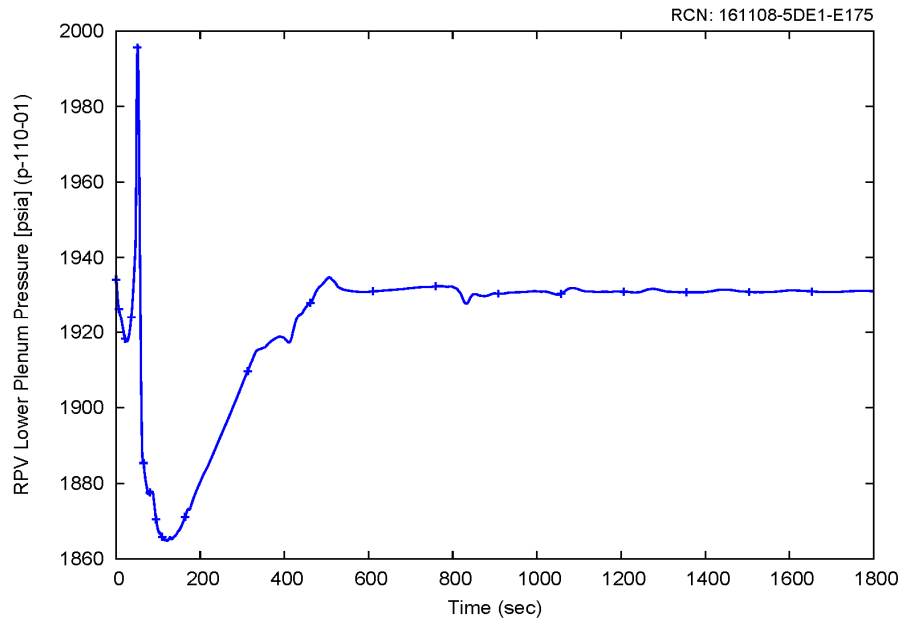


Figure 8-26 Reactor pressure vessel pressure response for the representative main steam line break event

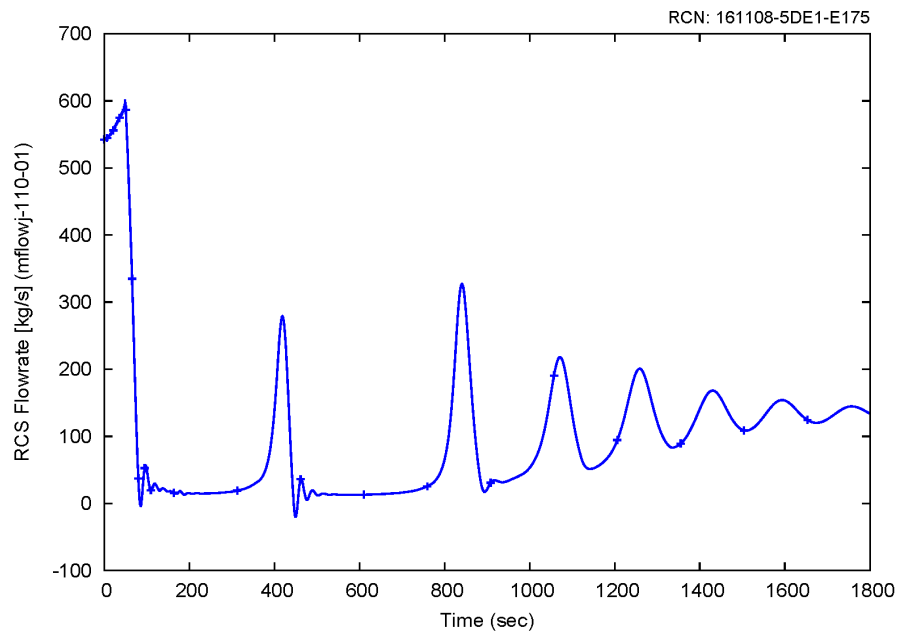


Figure 8-27 Reactor coolant system flow rate for the representative main steam line break event

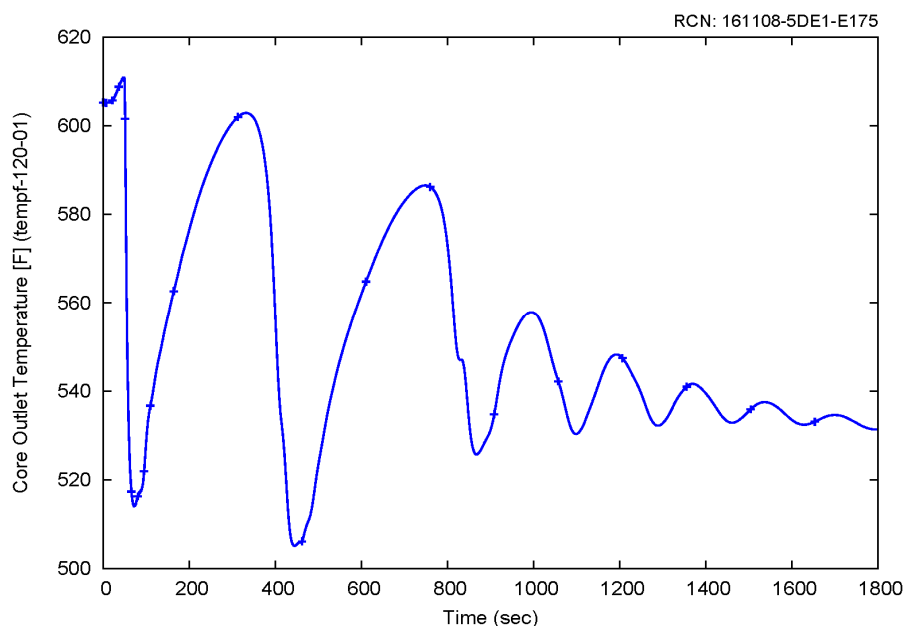


Figure 8-28 Core outlet temperature for the representative main steam line break event

8.1.3.3 Conclusion

A representative case that could challenge MCHFR was identified for a main steam line break event. The results of this case, as presented in Section 8.1.3.2, are subsequently used as input to an MCHFR evaluation using the NuScale subchannel analysis methodology.

8.2 Heatup and/or Pressurization of the Reactor Coolant System

8.2.1 Loss of Normal Feedwater Flow

The purpose of this section is to present the thermal-hydraulic response of the NPM for loss of normal feedwater flow. This event is evaluated for primary pressure and secondary pressure. Different initial condition biases and conservatisms are used for the RCS pressure case and the secondary pressure case.

8.2.1.1 Event Description –Reactor Coolant System Pressure Case

The general loss of normal feedwater flow event description can be found in Section 7.2.10. Chosen from a series of RCS pressure sensitivity cases, the sample loss of normal feedwater flow case here represents a case that could challenge the RCS pressure acceptance criterion. No single failure is applied since the challenging cases occur when

all equipment operates as designed. Normal AC power is lost at turbine trip since this maximizes the system pressure responses. This case features the following conditions:

- The initial power is 102 percent. RCS average temperature is biased at high condition (555 degrees F). RCS flow rated is biased to the low condition (535 kg/s). Pressurizer pressure is biased to the low condition (1780 psia). Pressurizer level is biased to the high condition (58 percent). Initial feedwater temperature is biased to the high condition (312.5 degrees F). Initial SG pressure is biased to the high condition (535 psia).
- SG heat transfer is increased 30 percent by applying a heat transfer coefficient multiplier of 1.3 on both the primary and secondary sides of the steam generator tubes in the steady state initialization model. As identified in Section 7.2.10.3, this biasing does not significantly affect margin to the RCS pressure acceptance criteria. There is no SG tube plugging for this representative calculation.
- BOC reactivity coefficients are used since they are bounding for overheating events.
- No operator action was credited in the representative case. Normal control system such as PZR spray, heater, letdown controls and automatic rod control are modeled based on the control status shown in Table 7-48.

8.2.1.2 Analysis Results –RCS Pressure Case

The following describes the event sequence of a representative case for the loss of normal feedwater flow event that could challenge the primary pressure. Table 8-4 summarizes the sequence of events. Figure 8-29 through Figure 8-37 show some key parameters during the representative loss of normal feedwater flow event.

The feedwater flow is completely lost at time zero of the transient. Due to the overheating after loss of feedwater, pressurizer pressure and level start to increase (Figure 8-29 and Figure 8-30). At 17.6 seconds after transient initiation, the pressurizer pressure reaches the reactor trip analytical limit (Figure 8-29). At 18.6 seconds, the turbine trips (on the reactor trip signal), normal power is lost—causing MSIV closure—and steam generator pressures begin to increase (Figure 8-31). At 19.6 seconds, scram rod insertion begins, which causes the reactor power to decrease (Figure 8-32), resulting in a RCS flow decrease (Figure 8-33). After reaching high pressurizer pressure analytical limit, the DHRS is also actuated at 19.6 seconds, but conservative modeling of the DHRS actuation valve opening delays initiation of flow in the DHRS until 49.3 seconds.

At 20.0 seconds, minimum MCHFR is reached (4.37 as calculated by NRELAP5).

At 24.2 seconds, the pressurizer dome pressure reaches the 2137.3 psia Reactor Safety Valve 1 biased setpoint, Reactor Safety Valve 1 begins to stroke open. At 24.6 seconds, the pressure at the bottom of the reactor vessel reaches a maximum value of 2156.1 psia and begins to decrease (Figure 8-29). That maximum RCS pressure value is well below 110 percent of the RCS design pressure (2310 psia). At 33.1 seconds, Reactor Safety Valve 1 closes. For the remainder of the transient, pressurizer pressure and level continue to decrease (Figure 8-29 and Figure 8-30).

At 49.3 seconds, flows through the DHRS actuation valves and into the steam generator inlet plena begin. The steam generator pressure starts to increase. At ~322 seconds, steam generator pressure reaches the maximum of 1243.4 psia and begins to decrease (Figure 8-31).

After reactor trip and actuation of DHRS, RCS flow decreases rapidly and becomes almost stagnant at ~50 seconds (Figure 8-33). Following that, oscillations are observed due to temperature and density differences between the riser and downcomer (as discussed in Section 7.2). The oscillations gradually diminish as the stable natural circulation flow is established in the RCS (Figure 8-31, Figure 8-33, and Figure 8-34).

By 2500 seconds, DHRS operation and RCS flow are stable (Figure 8-33, Figure 8-34, and Figure 8-37); RCS pressure, temperatures, and steam generator pressure are trending downward (Figure 8-29, Figure 8-31, Figure 8-34 and Figure 8-35); the subcritical margin remains large at the end of the transient calculation (Figure 8-36).

Table 8-4 Loss of normal feedwater flow sequence of events – reactor coolant system pressure case

Event	Time (sec)
Total loss of feedwater	0.0 s
Pressurizer pressure analytical limit (2000 psia) is reached.	17.6 s
Turbine trips, normal AC power is assumed to be lost	18.6 s
Scram rod insertion begins, and DHRS is actuated	19.6 s
MCHFR is reached (4.37 as calculated by NRELAP5)	20.0 s
Peak RCS pressure is reached (2156.1 psia)	24.6 s
RCS flow is stagnant	~50 s
SG pressures reach maximum (1243.4 psia) and begin to decrease	322.2 s
End of calculation. Stable DHRS cooling has been established. Net reactivity remains < \$0.0.	2500.0 s

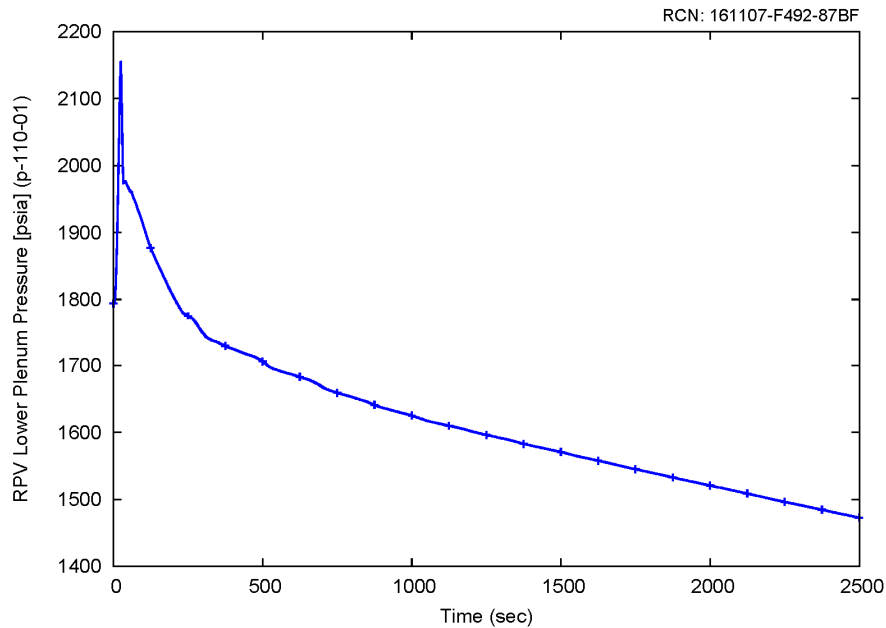


Figure 8-29 Reactor pressure vessel pressure response for the representative loss of normal feedwater flow event – reactor coolant system pressure case

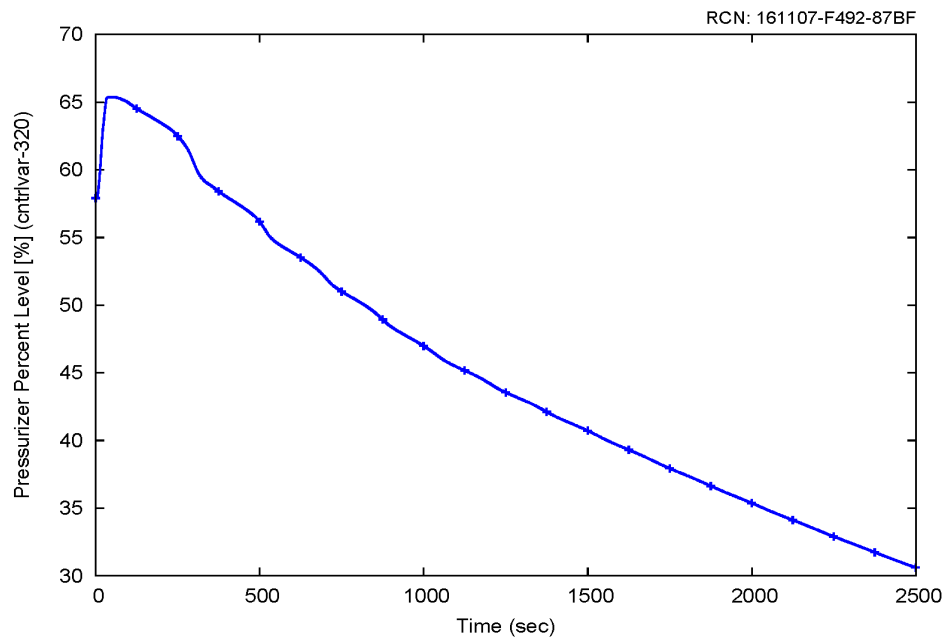


Figure 8-30 Pressurizer level for the representative loss of normal feedwater flow event – reactor coolant system pressure case

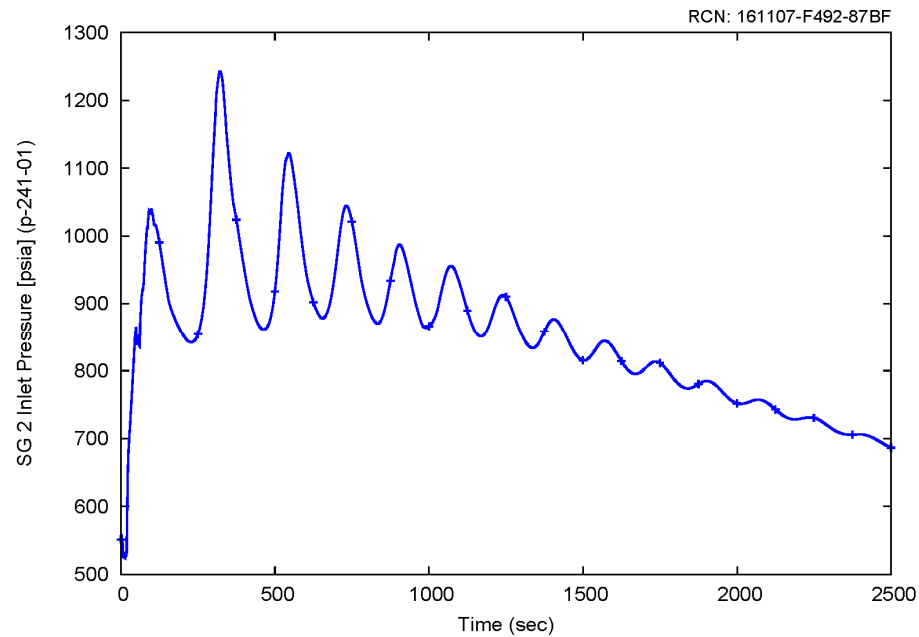


Figure 8-31 Steam generator 2 pressure response for the representative loss of normal feedwater flow event – reactor coolant system pressure case

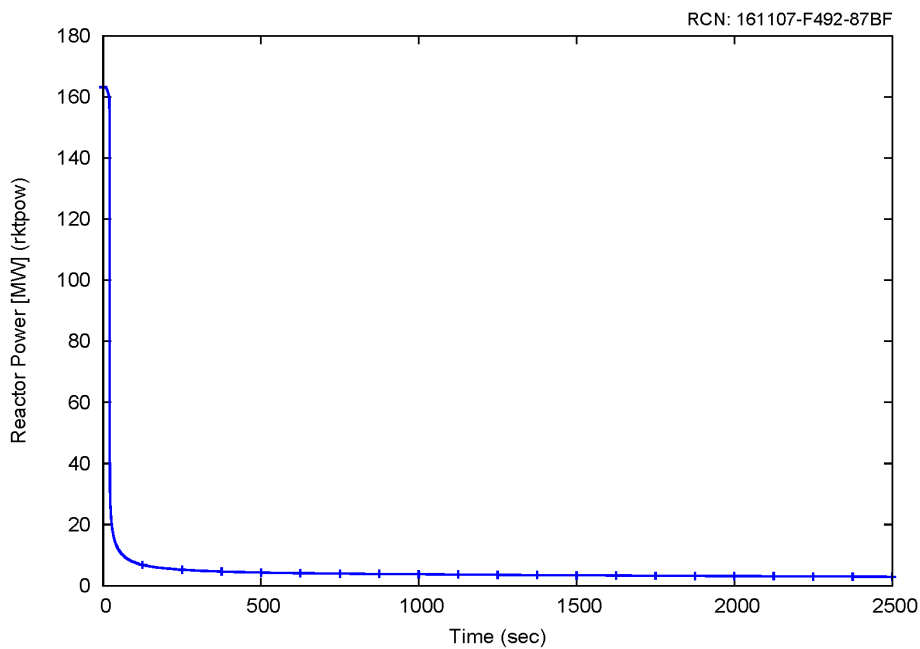


Figure 8-32 Power response for the representative loss of normal feedwater flow event – reactor coolant system pressure case

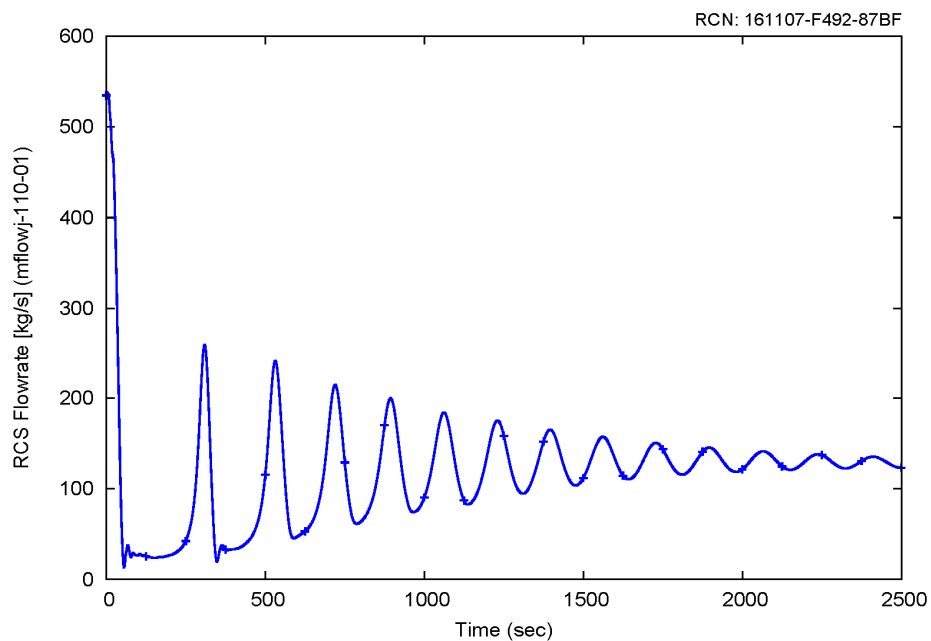


Figure 8-33 Reactor coolant system flow rate for the representative loss of normal feedwater flow event – reactor coolant system pressure case

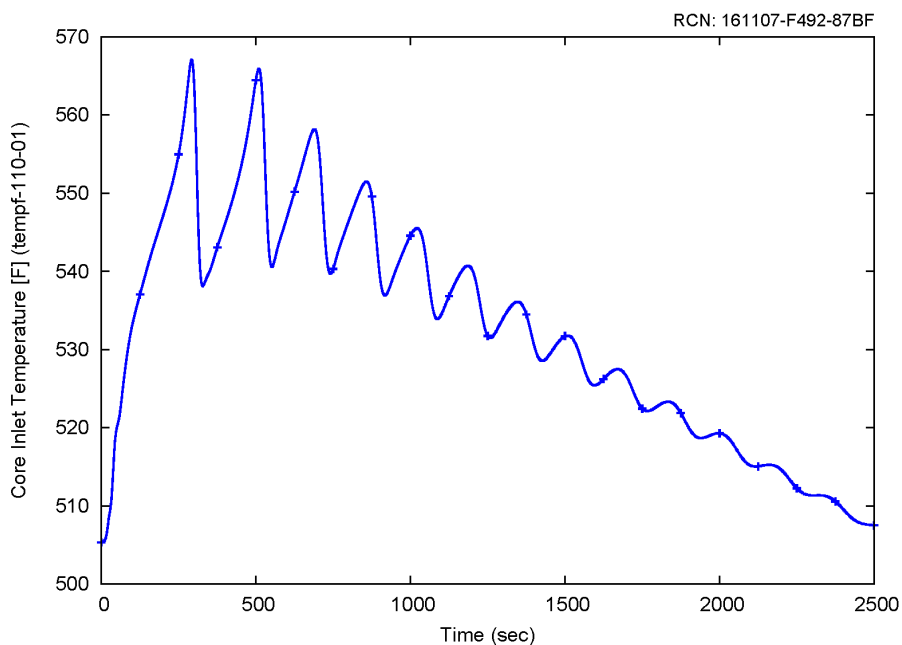


Figure 8-34 Core inlet temperature for the representative loss of normal feedwater flow event – reactor coolant system pressure case

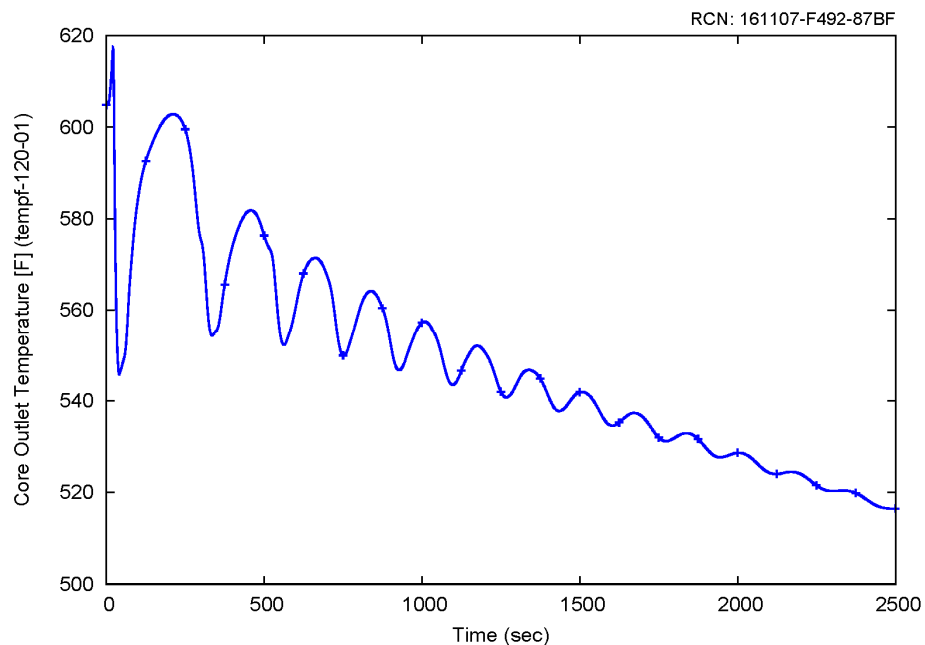


Figure 8-35 Core outlet temperature for the representative loss of normal feedwater flow event – reactor coolant system pressure case

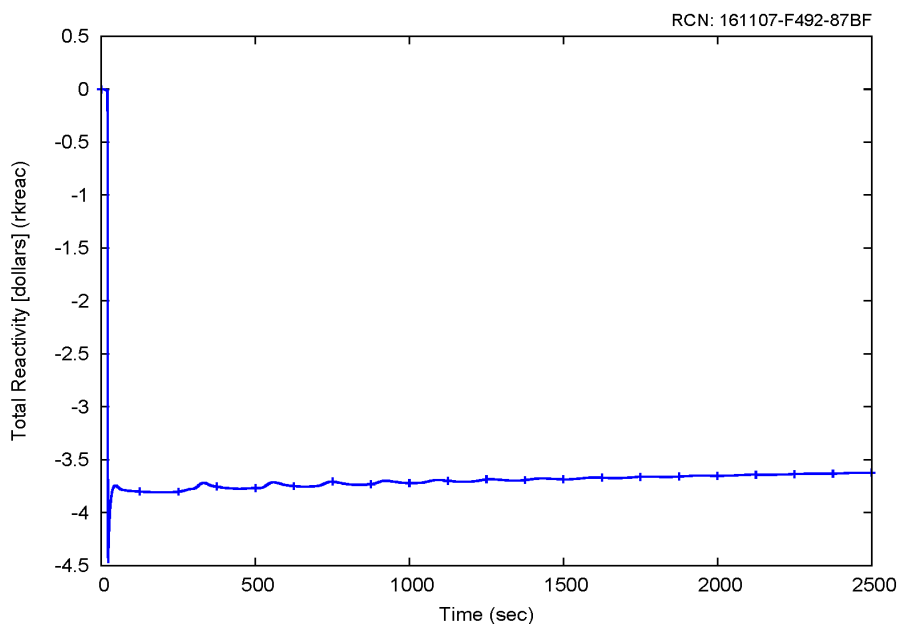


Figure 8-36 Net reactivity for the representative loss of normal feedwater flow event – reactor coolant system pressure case

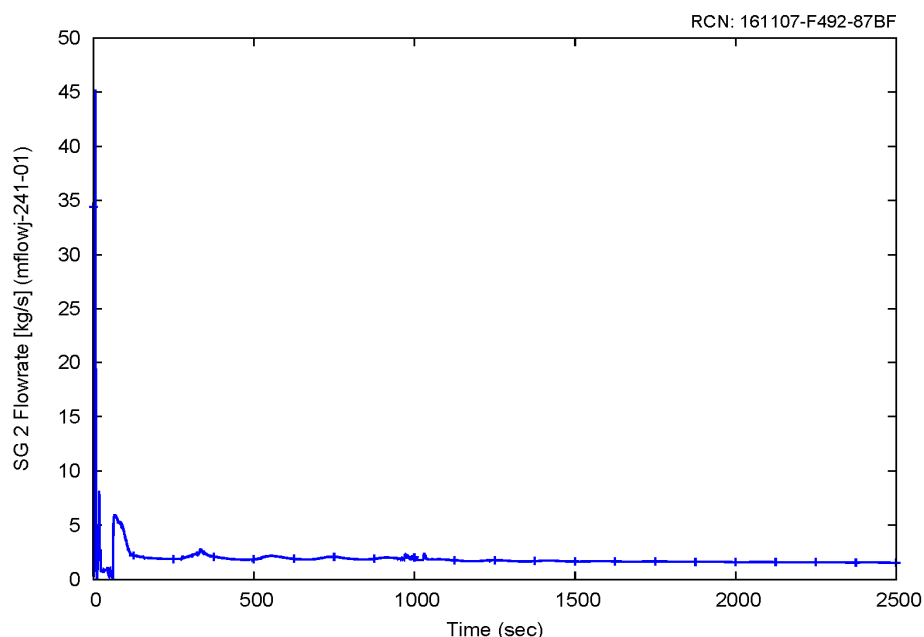


Figure 8-37 Steam generator 2 secondary flow for the representative loss of normal feedwater flow event – reactor coolant system pressure case

8.2.1.3 Conclusion –RCS Pressure Case

A representative case that could challenge the RCS pressure acceptance criterion was identified. The results of this case, as presented in Section 8.2.1.2, demonstrate the RCS pressure acceptance criterion is met.

8.2.1.4 Event Description –Secondary Pressure Case

The general loss of normal feedwater flow event description can be found in Section 7.2.10. Chosen from a series of secondary pressure sensitivity cases, the sample loss of normal feedwater flow case here represents a case that could challenge the secondary pressure acceptance criterion. No single failure is applied since the challenging cases occur when all equipment operates as designed. Normal AC power is lost at turbine trip since this maximizes the system pressure responses. This case features the same conditions as for the RCS pressure case (shown in Section 8.2.1.1), except that the feedwater flow is not totally lost at the beginning of the event. Instead, only a partial feedwater flow is lost (2.3 percent).

8.2.1.5 Analysis Results –Secondary Pressure Case

The following describes the event sequence of a representative case for the loss of normal feedwater flow event that could challenge the secondary pressure. Table 8-5 summarizes the sequence of events. Figure 8-38 through Figure 8-46 show some key parameters during the representative loss of normal feedwater flow event.

The transient for this case is initiated by a fault that is postulated to result in a partial (2.3 percent) loss of feedwater flow. Automatic rod control is conservatively disabled and therefore control rods are not modeled to insert to reduce power. The RCS heats up slowly (Figure 8-38 and Figure 8-39), and the RCS pressure and pressurizer level start to increase (Figure 8-40 and Figure 8-41).

At 638.3 seconds after transient initiation, the RCS riser leg temperature reaches the reactor trip analytical limit. At 645.3 seconds, it is assumed that the turbine trips (on the reactor trip signal) and normal power AC power is lost. The loss of AC power causes MSIV closure, and the steam generator pressures and RCS pressure begin to increase (Figure 8-40 and Figure 8-42). At 646.3 seconds, scram rod insertion begins, which causes the reactor power to decrease (Figure 8-43), resulting in a RCS flow decrease (Figure 8-44). After reaching the high RCS riser leg temperature analytical limit, the DHRS is also actuated at 646.3 seconds, but conservative modeling of the DHRS actuation valve opening delays initiation of DHRS flow until 676.0 seconds.

At 658.9 seconds, the RCS pressure reaches a maximum (1939.4 psia) and begins to decrease (Figure 8-40); the maximum value in this case is less than that for the RCS pressure case and the RSV do not open. For the remainder of the transient, the RCS pressure and pressurizer level continue to decrease (Figure 8-40 and Figure 8-41).

At 676.0 seconds, flow through the DHRS actuation valves and into the steam generator inlet plena begins (Figure 8-46). The steam generator pressure starts to increase. At ~716.3 seconds, steam generator pressure reaches the maximum of 1421.6 psia and begins to decrease (Figure 8-42).

After reactor trip and actuation of DHRS, RCS flow decreases rapidly and briefly becomes almost stagnant at ~700 seconds (Figure 8-44). Following that, oscillations are observed due to temperature and density differences between the riser and downcomer (as discussed in Section 7.2). The oscillations gradually diminish as the stable natural circulation flow is established in the RCS (Figure 8-38 and Figure 8-42 through Figure 8-44).

By 2500 seconds, DHRS operation and RCS flow are stable (Figure 8-38 through Figure 8-44); RCS pressure, temperatures, and steam generator pressure are trending downward (Figure 8-38, Figure 8-39, Figure 8-40, and Figure 8-42); the subcritical margin remains large (Figure 8-45).

Table 8-5 Loss of normal feedwater flow sequence of events – secondary pressure case

Event	Time (sec)
Feedwater flow begins 0.1 s rampdown to 97.7% of initial value	0.0 s
RCS riser leg temperature analytical limit (610°F) is reached	638.3 s
Turbine trips, normal AC power is assumed to be lost	645.3 s
Scram rod insertion begins, and DHRS is actuated	646.3 s
Peak RCS pressure is reached (1939.4 psia)	658.9 s
RCS flow briefly becomes almost stagnant	~700 s
SG pressures reach maximum (1421.6 psia) and begin to decrease	716.3 s
End of calculation. Stable DHRS cooling has been established. Net reactivity remains < \$0.0.	2500.0 s

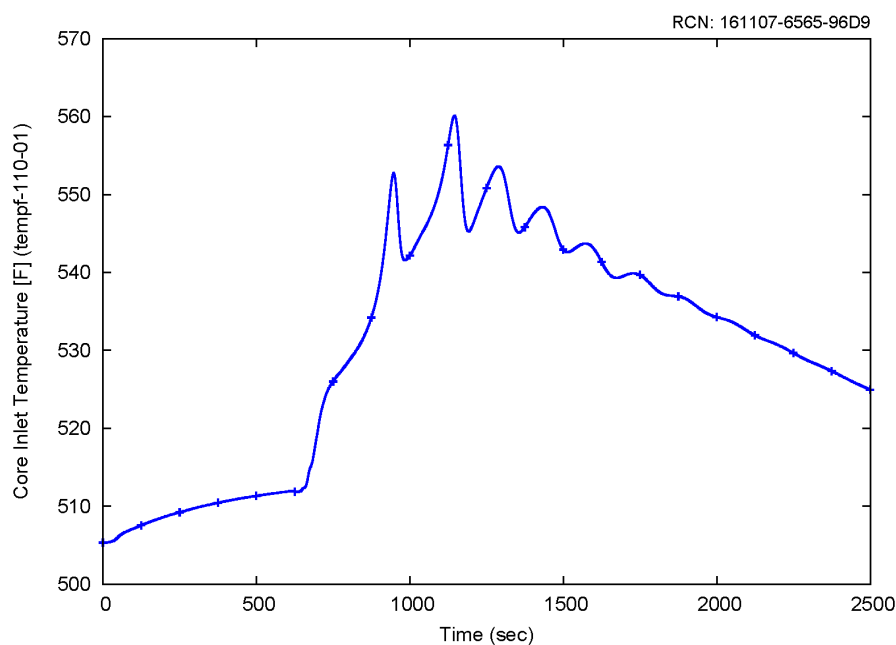


Figure 8-38 Core inlet temperature for the representative loss of normal feedwater flow event – secondary pressure case

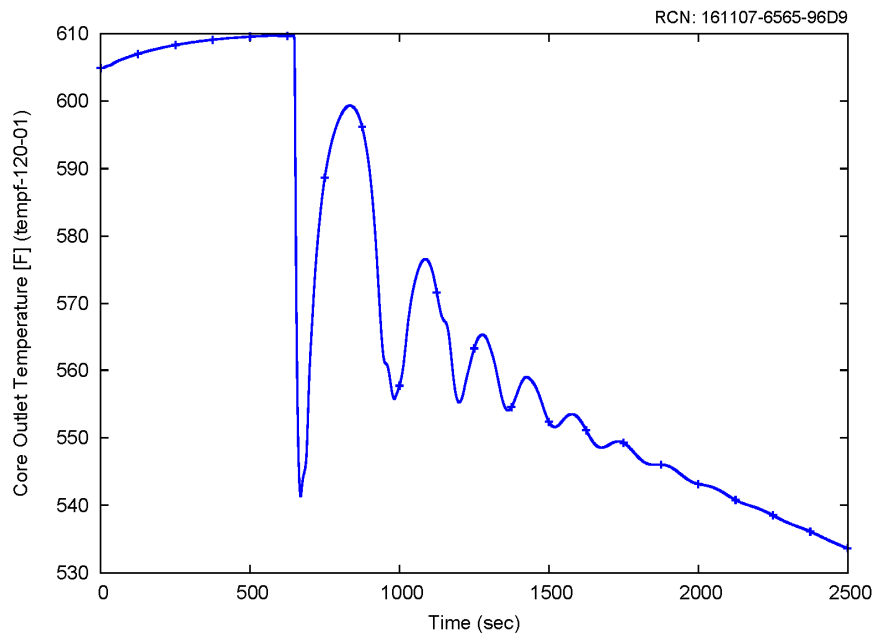


Figure 8-39 Core outlet temperature for the representative loss of normal feedwater flow event – secondary pressure case

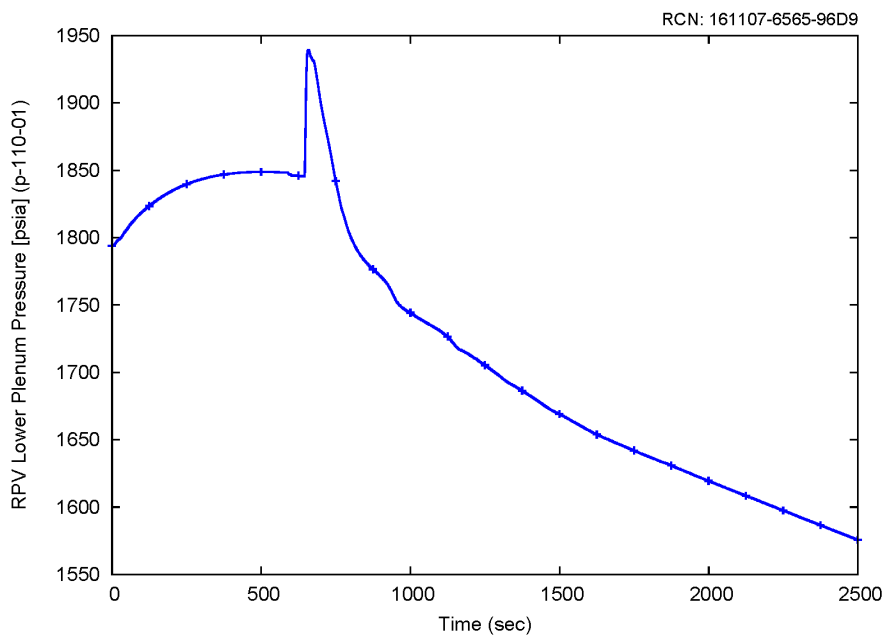


Figure 8-40 Reactor pressure vessel pressure response for the representative loss of normal feedwater flow event – secondary pressure case

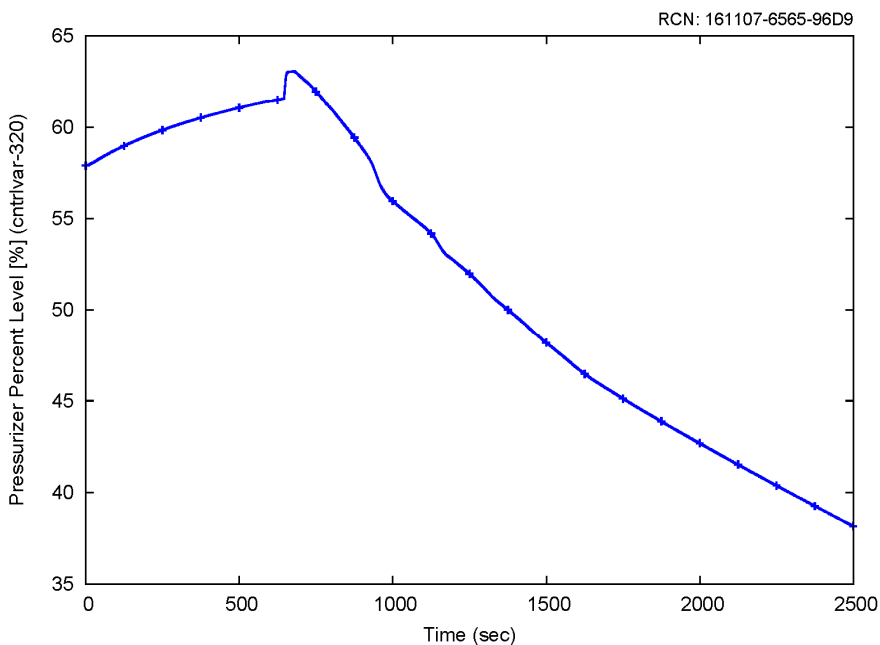


Figure 8-41 Pressurizer level for the representative loss of normal feedwater flow event – secondary pressure case

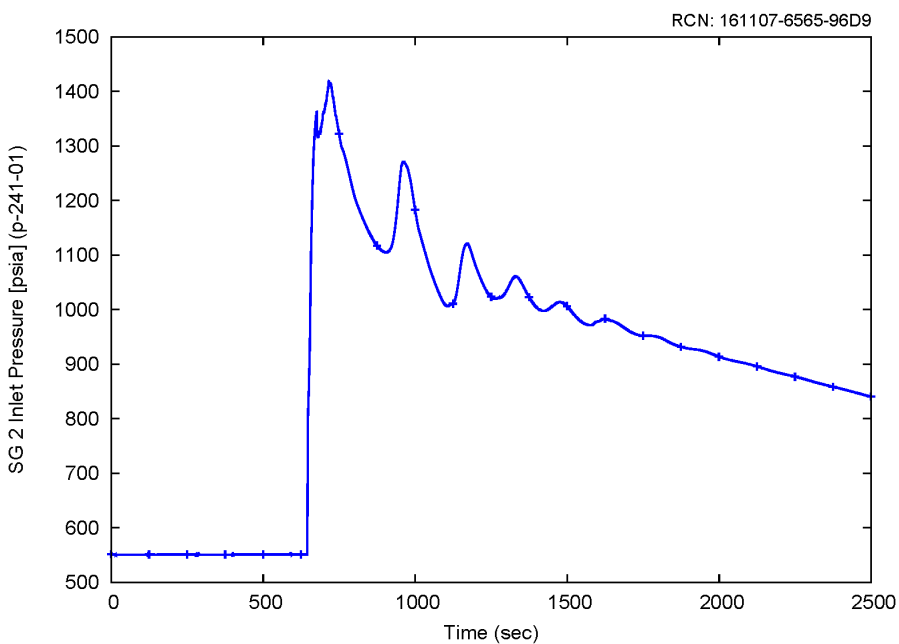


Figure 8-42 Steam generator 2 pressure response for the representative loss of normal feedwater flow event – secondary pressure case

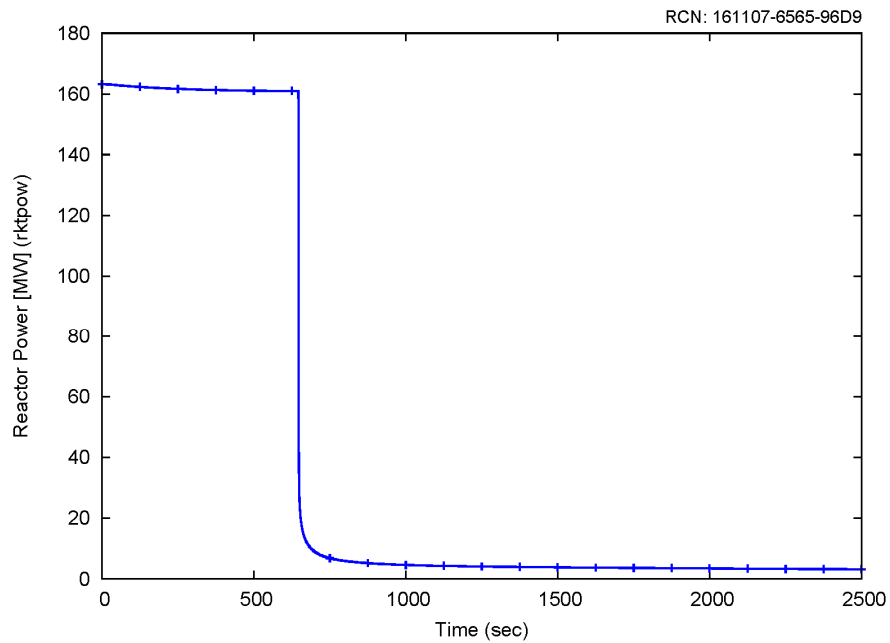


Figure 8-43 Power response for the representative loss of normal feedwater flow event – secondary pressure case

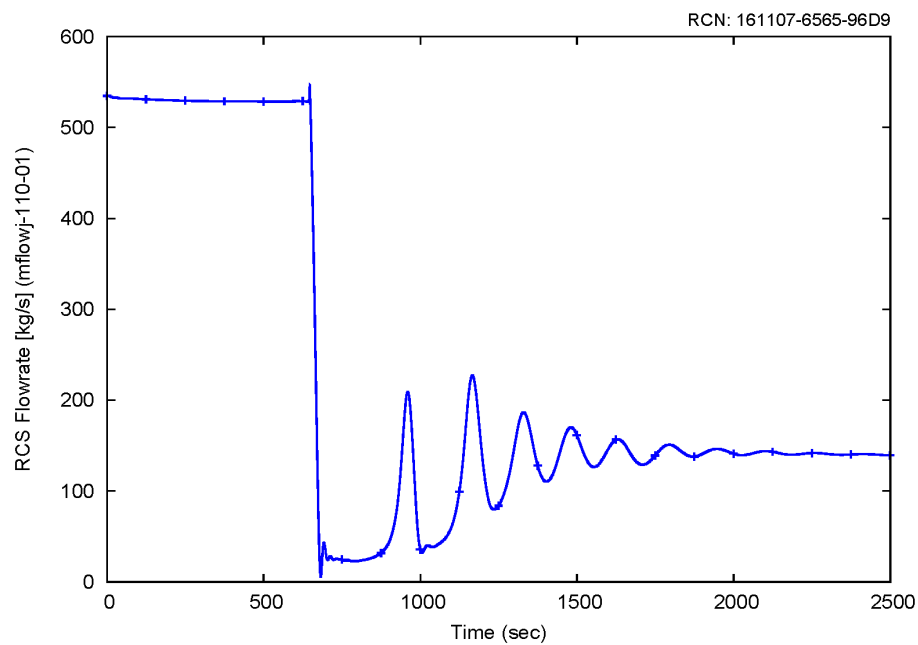


Figure 8-44 Reactor coolant system flow rate for the representative loss of normal feedwater flow event – secondary pressure case

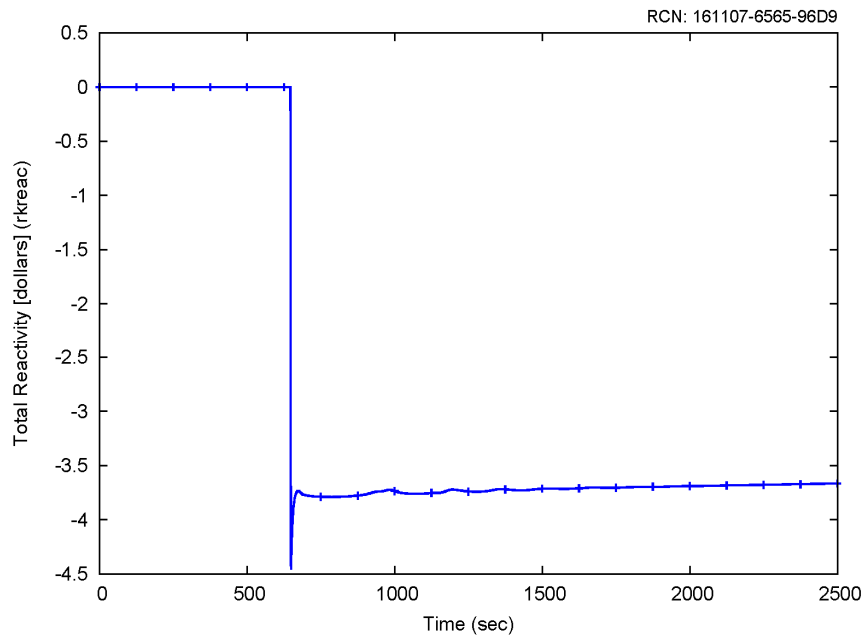


Figure 8-45 Net reactivity for the representative loss of normal feedwater flow event – secondary pressure case

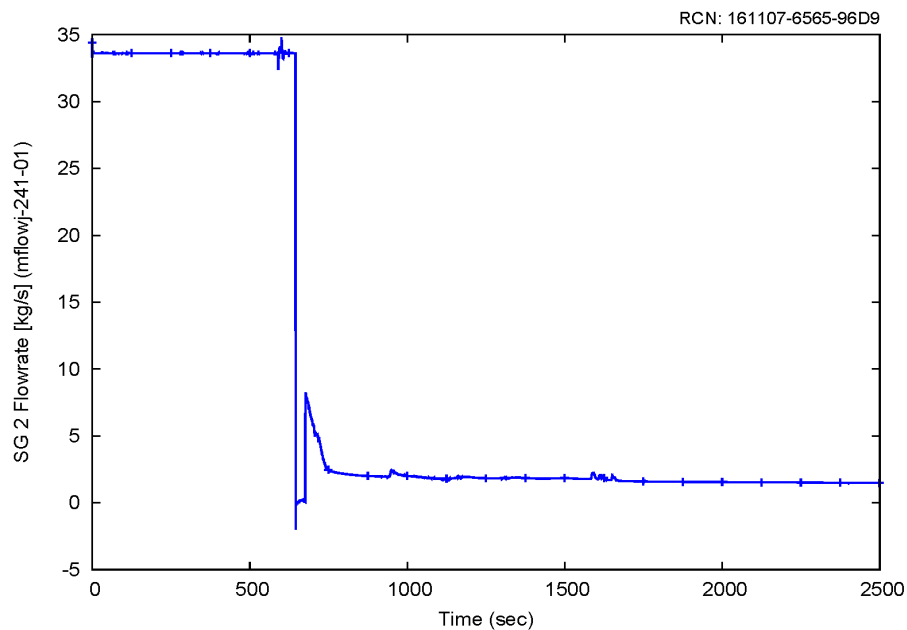


Figure 8-46 Steam generator 2 secondary flow for the representative loss of normal feedwater flow event – secondary pressure case

8.2.1.6 Conclusion – Secondary Pressure Case

A representative case that could challenge secondary pressure acceptance criteria was identified. The results of this case, as presented in Section 8.2.1.5 demonstrate the secondary pressure acceptance criterion is met.

8.2.2 Loss of Normal AC Power

The purpose of this section is to present the thermal-hydraulic response of the NPM for loss of normal AC power. This event is evaluated for primary pressure and secondary pressure. A representative case evaluated for primary pressure is presented.

8.2.2.1 Event Description

The general event description for a loss of normal AC power is found in Section 7.2.9.1. Based on Section 7.2.9.1, the acceptance criterion for primary pressure is potentially challenged by the loss of normal AC power. The challenging case occurs when all equipment is operational.

The representative case presented here represents a case that could challenge the primary pressure response (as shown in Table 7-44). Case features include the following conditions:

- Conservative initial condition biasing is applied in order to maximize the consequences of this event. This representative case is initialized at 102 percent reactor power.
- The RSV set pressure is biased to the high condition (2137.25 psia, which includes a 3 percent drift allowance) to maximize primary pressure response.
- The reactor pool temperature is biased to the maximum bounding value (200 degrees F) to provide a bounding high temperature for events/cases that require heat removal using the DHRS.
- The initial pressurizer pressure is biased to the maximum value (1920 psia) for the primary side pressurization case.
- The initial pressurizer level is biased to the maximum value (58 percent) to maximize the primary side pressure response.
- BOC reactivity coefficients are applied to maximize the primary side pressurization.

8.2.2.2 Analysis Results

The following describes the event sequence of the loss of normal AC power event. Table 8-6 summarizes the sequence of events. Figure 8-47 through Figure 8-53 show some key parameters during the loss of normal AC power event.

The loss of normal AC power occurs at zero seconds, which causes an immediate turbine trip. In this case, it is assumed that the highly reliable DC power system (EDSS) batteries are available. The control rods do not immediately insert on loss of AC power. Rather, a

delay to reactor trip, DHRS actuation, and containment isolation are assumed to maximize RCS pressure. During this delay period, primary and secondary pressure increase due to the turbine trip. Primary temperatures (Figure 8-47) and system pressures (Figure 8-48, curves for SG1 and SG2 overlap) initially increase due to the mismatch between primary side heat production and secondary side heat sink. The analytical limit for high pressurizer pressure is reached at approximately 6 seconds, actuating reactor trip (Figure 8-49). DHRS valves begin to open at approximately 8 seconds (Figure 8-50). At approximately 12 seconds one of the two RSVs lifts (Figure 8-51). A peak pressure of 2155 psia is reached in the RPV.

Subsequent to reactor trip and RSV lift, system pressures and temperatures decrease, and system shrinkage reduces the PZR level (Figure 8-53).

After reactor trip and actuation of DHRS, oscillations are observed due to temperature and density differences between the riser and downcomer (as discussed in Section 7.2); therefore the calculation is continued to verify that the module transitions into passive and stable DHRS cooling. Figure 8-47, Figure 8-50, and Figure 8-52 show that at ~15 minutes, RCS flow has stabilized, and the RCS temperatures are steadily decreasing as the DHRS is transferring decay heat from the RPV to the reactor pool. It is concluded that by 30 minutes the transient has been terminated and that stable DHRS cooling has been achieved. No operator action was credited to mitigate this event.

Table 8-6 Sequence of events for loss of AC power

Event	Time (sec)
Loss of AC power occurs	0.0
Turbine trip occurs	0.0
CVCS isolation occurs	0.0
High PZR pressure analytical limit is reached (2000 psia).	6
RTS actuation on high pressurizer pressure signal.	8
DHRS actuation on the high pressurizer pressure signal. DHRS actuation valves begin to open. FWIVs and MSIVs begin to close.	8
RSV1 opens	12
Peak RPV pressure is reached (2155 psia)	12
MSIVs are fully closed.	13
FWIVs are fully closed.	13
DHRS actuation valves are fully open.	38
Peak steam generator pressure is reached (1250 psia).	80
Establishment of stable RCS flow. Pressure and temperature are steadily decreasing.	1500
End of calculation. Stable DHRS cooling has been established.	1800

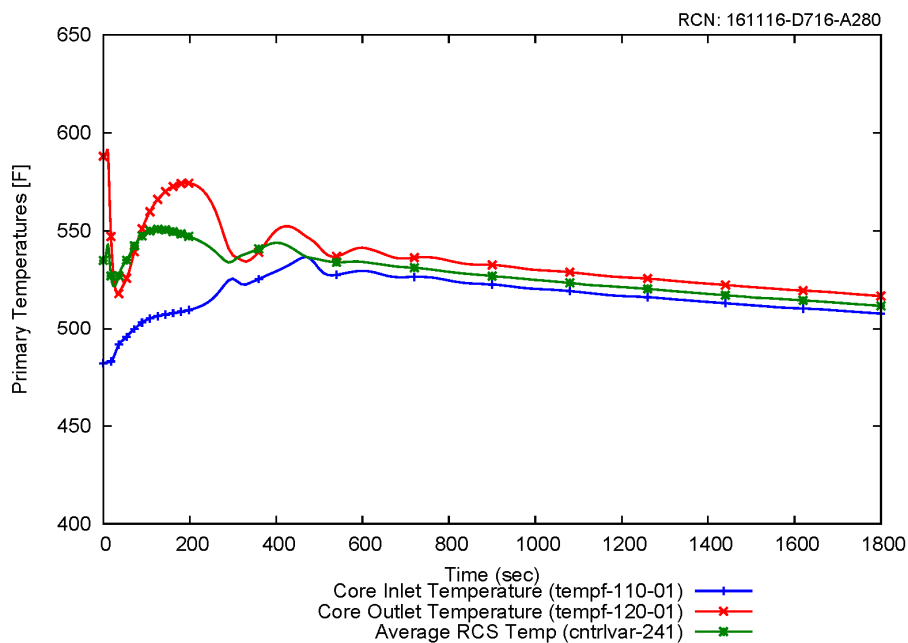


Figure 8-47 Primary temperature response for the representative loss of AC power event

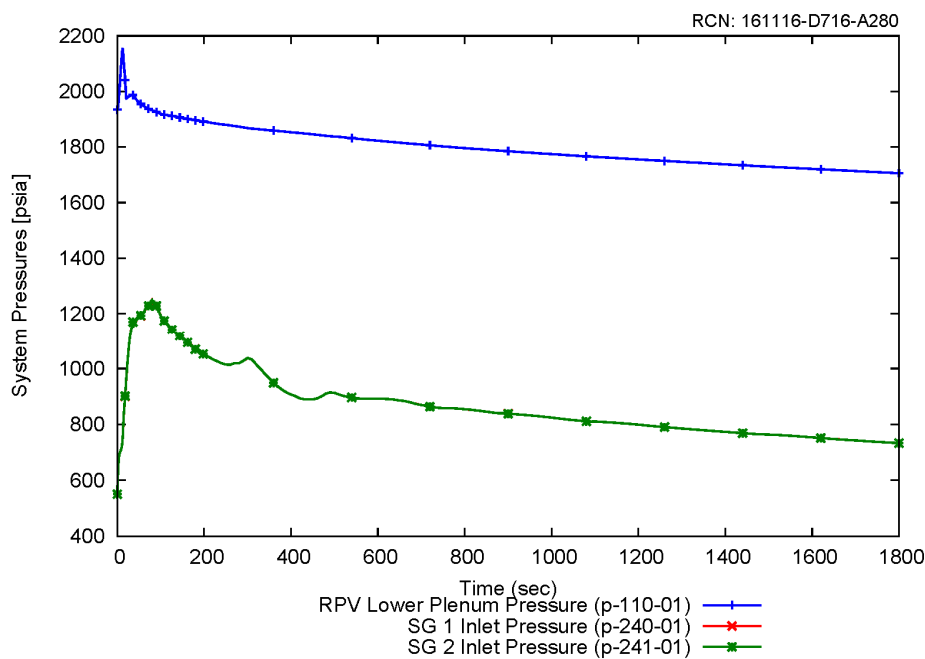


Figure 8-48 System pressure response for the representative loss of AC power event

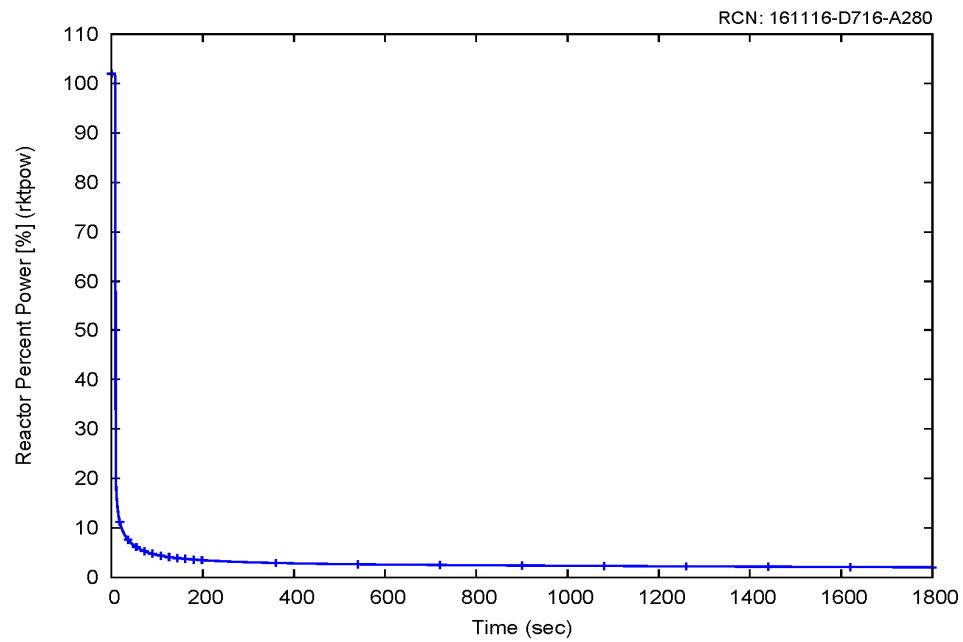


Figure 8-49 Reactor pressure vessel core power response for the representative loss of AC power event

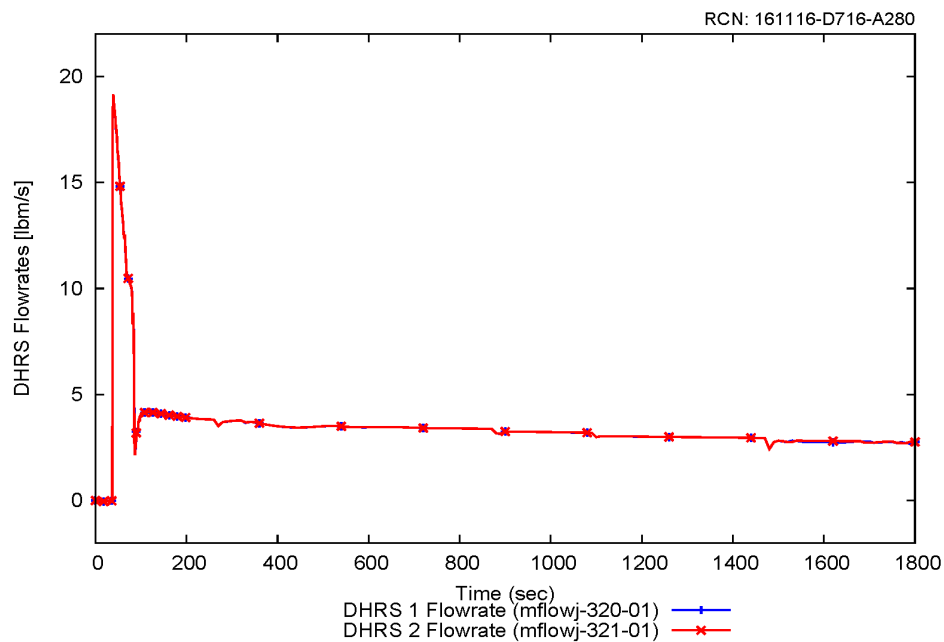


Figure 8-50 Decay heat removal system response for the representative loss of AC power event

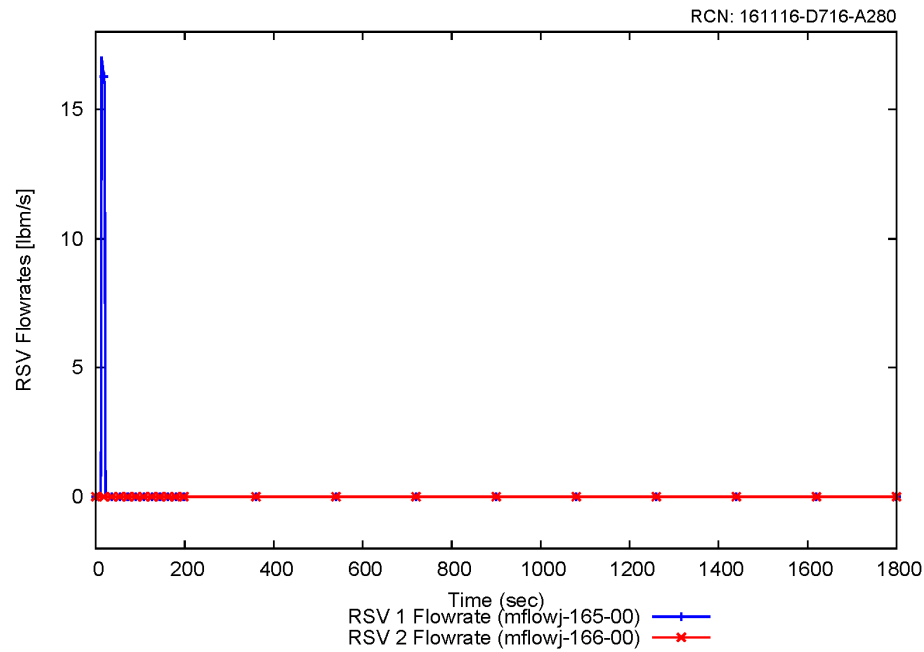


Figure 8-51 RSV flow response for the representative loss of AC power event

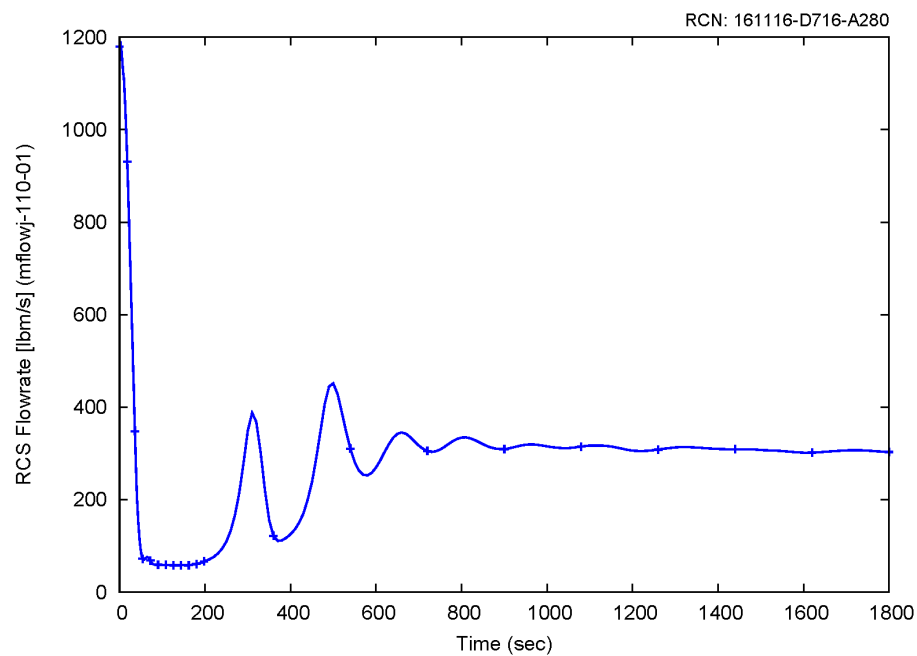


Figure 8-52 Reactor coolant system flow response for the representative loss of AC power event

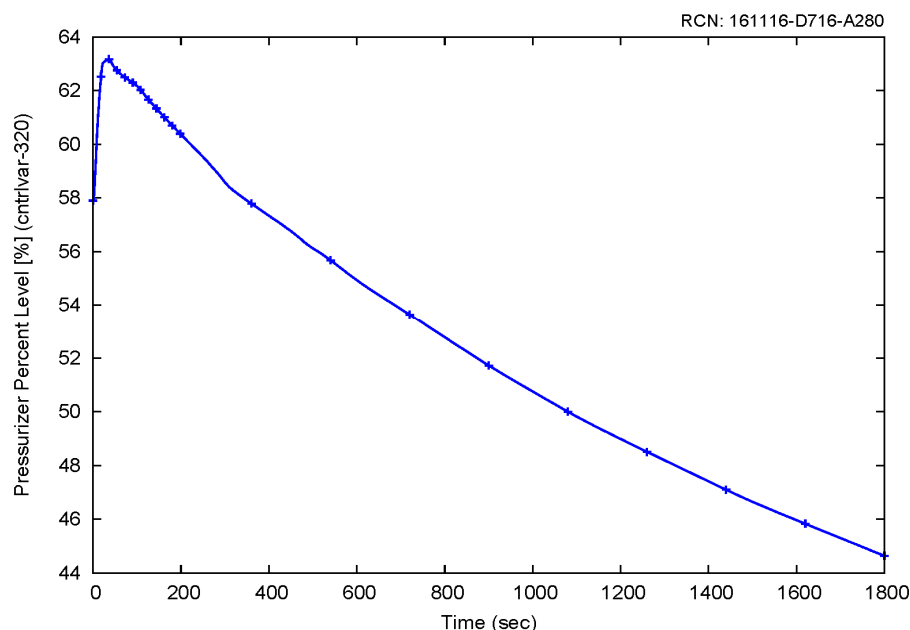


Figure 8-53 Pressurizer level response for the representative loss of AC power event

8.2.2.3 Conclusion

A representative case that could challenge primary pressure acceptance criterion was identified. The results of this case, as presented in Section 8.2.2.2, demonstrate that the primary pressure acceptance criterion is met.

8.2.3 Feedwater Line Break

The purpose of this section is to present the thermal-hydraulic response of the NPM to a feedwater system piping failure. The challenging case occurs when AC power is lost at event initiation and all equipment is operational. This event is evaluated for primary pressure and secondary pressure. A representative case evaluated for primary pressure is presented.

8.2.3.1 Event Description

The general event description for a feedwater system piping failure is found in Section 7.2.12.1. Based on Section 7.2.12.1, the acceptance criterion for primary pressure is potentially challenged by the feedwater system piping failure.

The representative case presented here represents a case that could challenge the primary pressure response (as shown in Table 7-56). Case features include the following conditions:

- Conservative initial condition biasing is applied in order to maximize the consequences of this event. This representative case is initialized at 102 percent reactor power.
- The initial primary temperatures are biased to the maximum value (~545 degrees F) to produce a (slightly) higher energy system.
- The RSV set pressure is biased to the high condition (2137.25 psia, which includes a 3 percent drift allowance) to maximize primary pressure response.
- The initial feedwater temperature is biased to the maximum value (~305 degrees F) to produce a (slightly) higher energy system.
- The reactor pool temperature is biased to the maximum bounding value (~200 degrees F) to provide a bounding high temperature for events/cases that require heat removal using the DHRS.
- The initial pressurizer pressure is biased to the maximum value (1920 psia) for the primary side pressurization case.
- The initial pressurizer level is biased to the maximum value (58 percent) to maximize the primary side pressure response.
- BOC reactivity coefficients are applied to maximize the primary side pressurization.
- Automatic rod control is disabled.

8.2.3.2 Analysis Results

The following describes the event sequence of the feedwater line break event. Table 8-7 summarizes the sequence of events. Figure 8-54 through Figure 8-61 show some key parameters during the feedwater line break event.

A feedwater line break outside of containment occurs at zero seconds coincident with a loss of AC power, causing an immediate turbine trip and feedwater pump trip (Figure 8-54). In this case, it is assumed that the highly reliable DC power system (EDSS) batteries are available. To maximize RCS pressure, in this case it is assumed that after normal AC power is lost and MPS senses the loss of power to the EDSS battery chargers, there is a delay before MPS actuates reactor trip, DHRS and containment isolation. Since the reactor does not immediately trip, primary temperatures (Figure 8-55, curves for inlet temperature and RCS temperature overlap) and system pressures (Figure 8-56, curves for SG1 and SG2 overlap) initially increase due to the mismatch between primary side heat production and secondary side heat sink. The analytical limit for PZR pressure is reached at approximately 6 seconds. RTS actuation (Figure 8-57) occurs at approximately 8 seconds and RSV lift (Figure 8-58) occurs at approximately 11 seconds. A peak pressure of 2158 psia is reached in the RPV. The DHRS valves are fully open at approximately 36 seconds (Figure 8-59, curves for DHRS 1 and DHRS 2 overlap).

Subsequent to reactor trip and RSV lift, system pressures and temperatures decrease, and system shrinkage reduces the PZR level (Figure 8-60).

After reactor trip and actuation of DHRS, oscillations are observed due to temperature and density differences between the riser and downcomer (as discussed in Section 7.2); therefore the calculation is continued to verify that the module transitions into passive and stable DHRS cooling. Figure 8-55, Figure 8-59, and Figure 8-61 show that at ~30 minutes, RCS flow has stabilized, and the RCS temperatures are steadily decreasing as the DHRS is transferring decay heat from the RPV to the reactor pool. It is concluded that by ~40 minutes the transient has been terminated and that stable DHRS cooling has been achieved. In this case, the EDSS batteries hold the ECCS valves closed for the duration of the transient calculation. No operator action was credited to mitigate this event.

Table 8-7 Sequence of events for feedwater line break outside containment

Event	Time (sec)
A double ended guillotine break in the SG 2 feedwater line occurs under the bioshield (just outside of containment).	0
AC power is lost resulting in turbine trip and FW pump trip	0
High PZR pressure analytical limit is reached (2000 psia)	6
RTS and DHRS ESFAS actuated	8
MSIVs close	8
Control rods fully inserted	10
RSV lift point is reached (2137 psia)	11
Peak RCS pressure reached (2158 psia)	12
FWIVs close (check valves already seated)	15
RSV reseats	22
DHRS actuation valves open	36
Peak pressure reached in SG 1 (1299 psia)	77
End of calculation. Stable DHRS cooling has been established.	3600

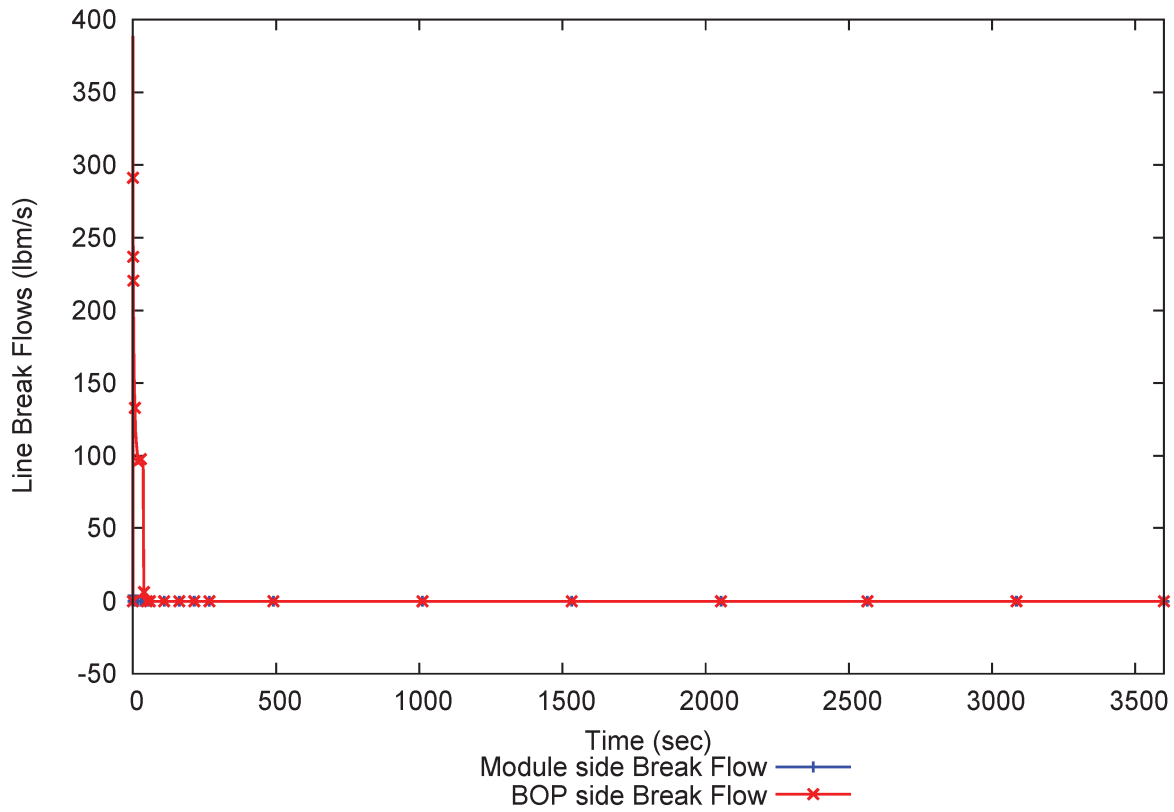


Figure 8-54 Feedwater line break flow response for the representative feedwater line break event

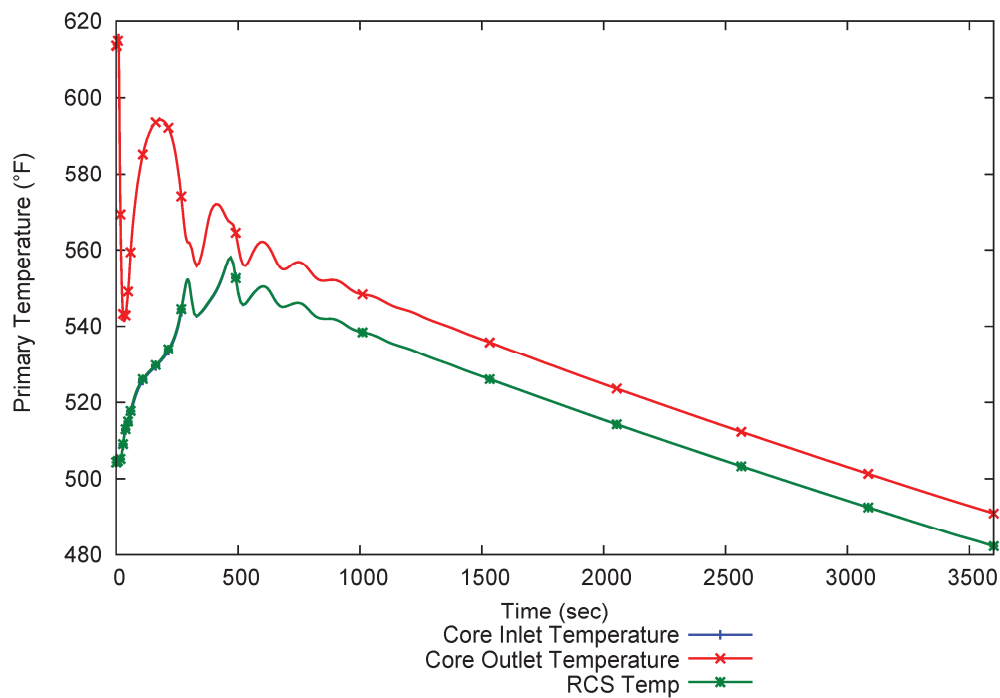


Figure 8-55 Primary temperature response for the representative feedwater line break event

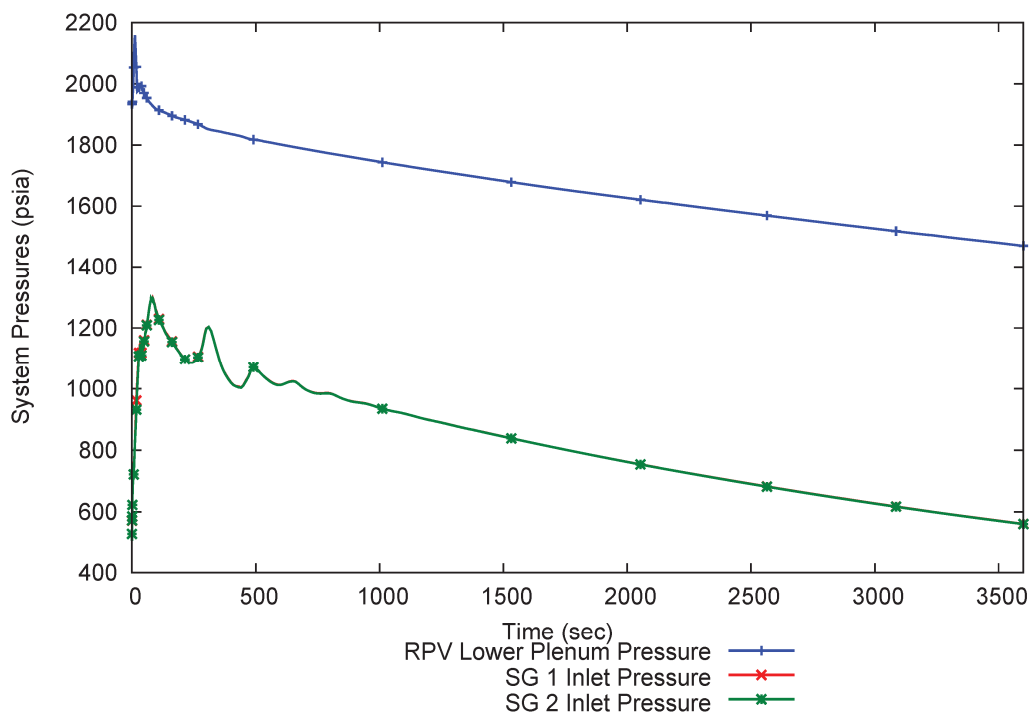


Figure 8-56 System pressure response for the representative feedwater line break event

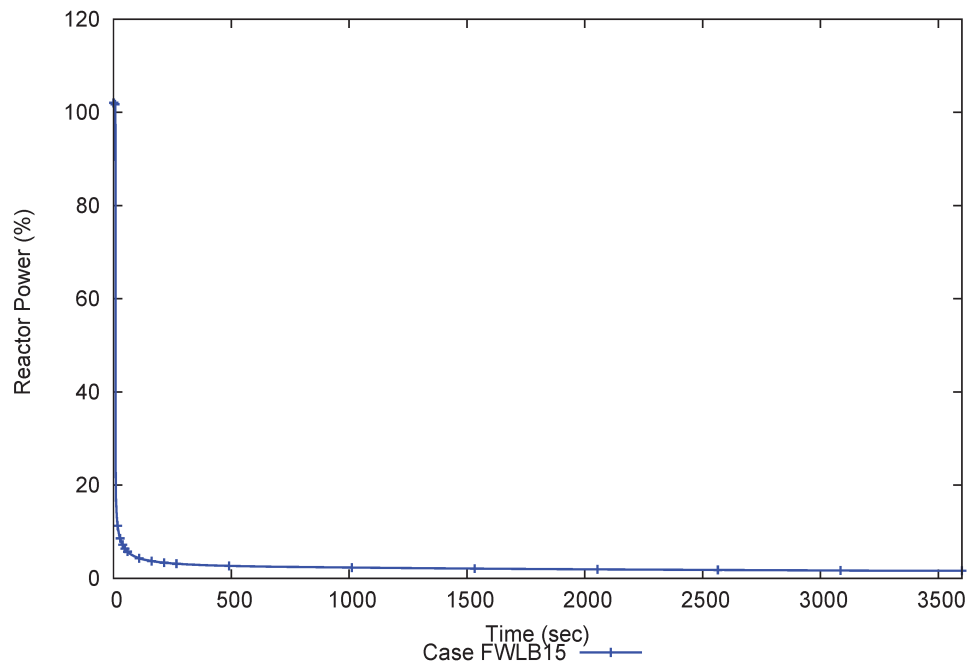


Figure 8-57 Reactor pressure vessel core power response for the representative feedwater line break event

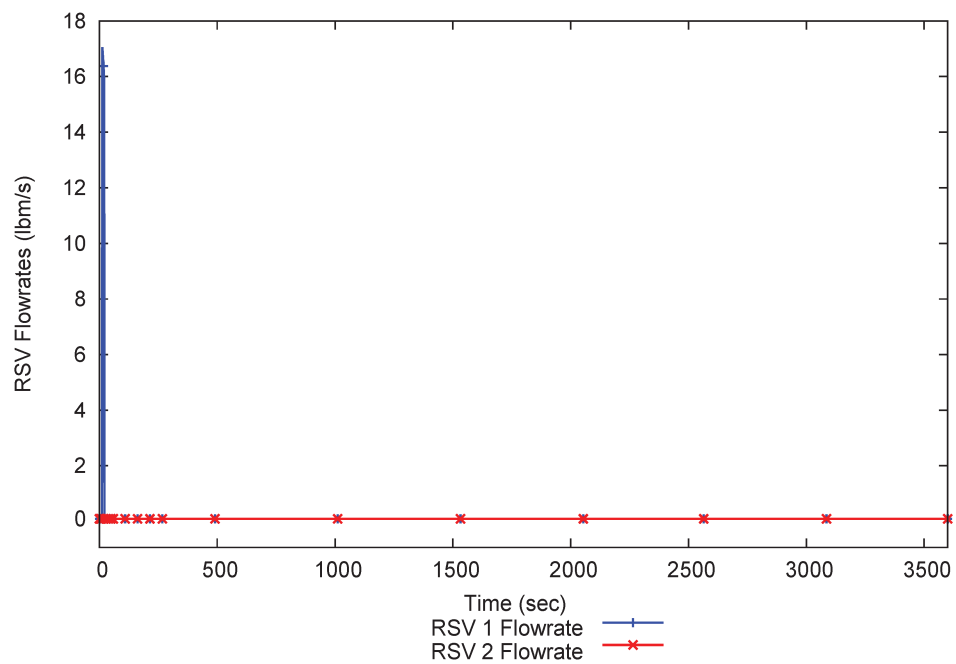


Figure 8-58 Reactor safety valve flow response for the representative feedwater line break event

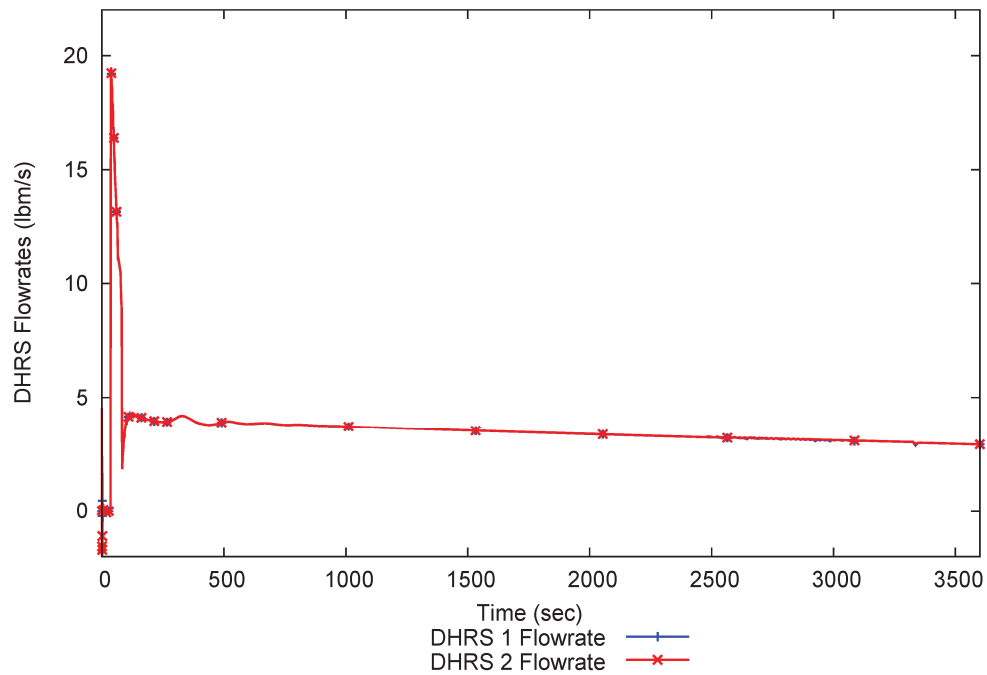


Figure 8-59 Decay heat removal system response for the representative feedwater line break event

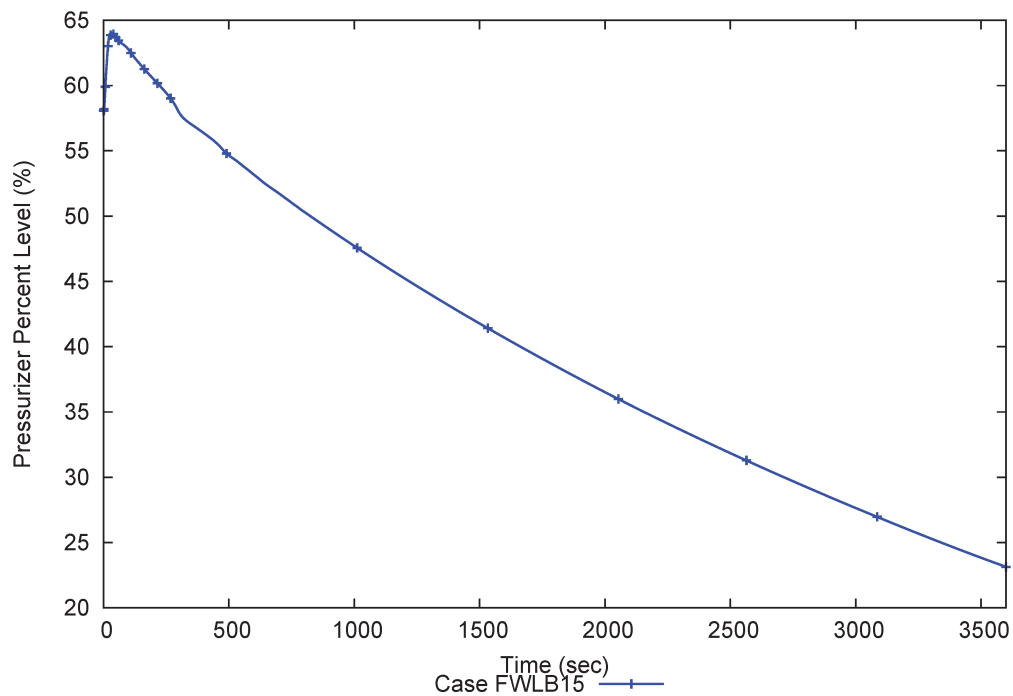


Figure 8-60 Pressurizer level response for the representative feedwater line break event

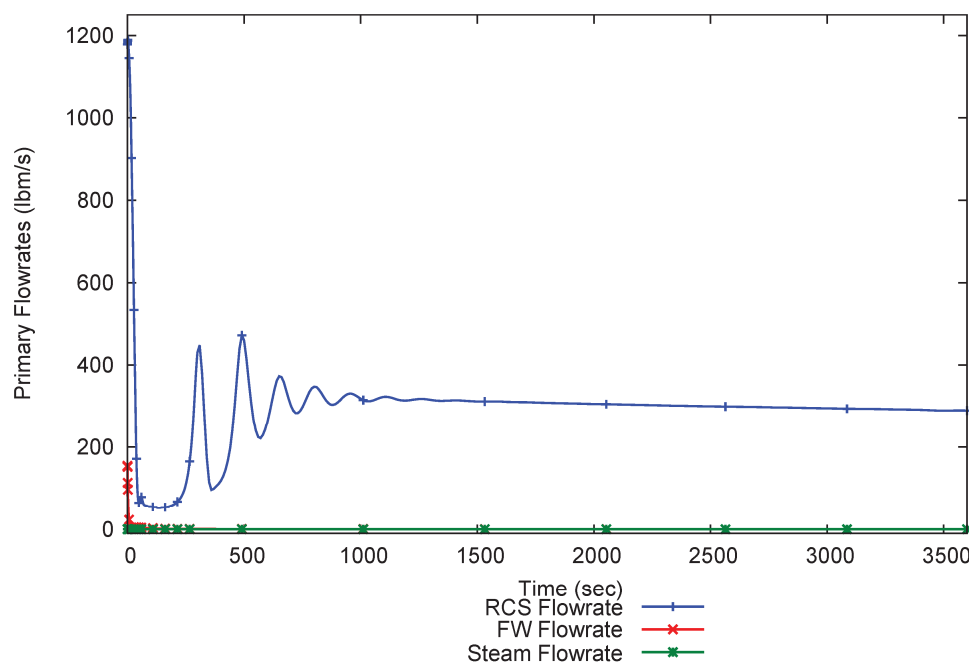


Figure 8-61 Reactor coolant system flow response for the representative feedwater line break event

8.2.3.3 Conclusion

A representative case that could challenge the RCS pressure acceptance criteria was identified. The results of this case, as presented in Section 8.2.3.2, demonstrate the RCS pressure acceptance criterion is met.

8.3 Reactivity Anomaly

8.3.1 Uncontrolled Control Rod Assembly Bank Withdrawal from Subcritical or Low Power Startup Conditions

The purpose of this section is to present the thermal-hydraulic and core neutronic responses of the NPM for an uncontrolled control rod assembly bank withdrawal from subcritical or low power startup conditions event. This event is evaluated for both MCHFR and maximum fuel centerline temperature.

8.3.1.1 Event Description

The event description for a bank withdrawal from low power startup conditions can be found in Section 7.2.13. Based on Section 7.2.13, the acceptance criteria for MCHFR and maximum fuel centerline temperature are potentially challenged. For the NPM, the results of the sensitivity studies indicate the event scenario with the lowest MCHFR may differ

from the event scenario with the highest fuel centerline temperature; but a single active failure cannot make the event consequences worse.

The representative case presented here corresponds to one of the more limiting peak power cases, and therefore a case that may challenge MCHFR. This case features the following conditions for a bank withdrawal from low power startup conditions:

- The initial core power is 15 percent RTP, which is the maximum power level for this event classification.
- The high count rate signal is inactive.
- The RCS core inlet temperature is the minimum allowed for criticality (420 degrees F).
- Heat removal is through the steam generators with coolant provided by the operating feedwater pump.
- The reactivity insertion rate is 35 pcm/s.
- No loss of normal AC power.
- No operator action was credited in the representative case.

8.3.1.2 Analysis Results

The following describes the event sequence of the withdrawal of a control rod assembly bank from a low power startup condition. Table 8-8 summarizes the sequence of events. Figure 8-62 through Figure 8-69 show some key parameters for this case.

The bank withdrawal occurs at time zero. The addition of positive reactivity (Figure 8-69) causes reactor power to increase (Figure 8-64). Since the high power rate signal is not active (below 15 percent RTP), core protection is provided by the high power signal and the startup rate (intermediate range) signal. In this instance, the analytical limit for the startup rate (intermediate range) is reached (3 DPM (decades per minute)) at 4 seconds. The control rods are free to fall after two seconds (Figure 8-69), while the DWS isolation valves begin to close. This latter action occurs as a precaution to the reactivity addition being caused by a dilution of the reactor coolant boron concentration. The peak core power (42.0 percent RTP) occurs at 7 seconds.

The quick action of the MPS to trip the reactor precludes the addition of significant energy into the reactor coolant. For instance, the pressurizer pressure increases by less than 10 psia (Figure 8-62), while the increase in SG pressures is comparable (Figure 8-63). The delay between energy production in the fuel and heat addition to the reactor coolant causes the core outlet temperature (Figure 8-67) and RCS flow rate (Figure 8-68) to remain relatively constant until increasing shortly before reactor trip. Both parameters peak at ~10 seconds before decreasing rapidly as the core heat flux reduces. The core inlet temperature (Figure 8-65) and density (Figure 8-66) remain relatively constant because the transient is terminated prior to completion of one loop transit. The MCHFR predicted by NRELAP5 (greater than 25) occurs at 7 seconds.

At high initial power levels, the calculation would normally be continued to verify that the module transitions into passive and stable DHRS cooling. However, the system responses at this operating condition are negligible compared to the heat removal capability of the plant (normal feedwater, containment flooding, etc.). Since there is little additional energy to remove, core cooling is ensured and the evaluation can be quickly terminated. As noted above, the RCS flow peaked and is starting to decrease (Figure 8-68), while the core outlet temperature (Figure 8-67) and pressurizer pressure (Figure 8-62) are steady or decreasing. No operator action was credited to mitigate this event.

Table 8-8 Withdrawal of a control rod assembly bank from a low power startup condition sequence of events

Event	Time (sec)
Malfunction that initiates the withdrawal of a CRA bank	0
High startup rate (intermediate range) analytical limit (3 DPM) reached	4
RTS actuation (control rods are free to fall)	6
DWS isolation (valves begin to close)	6
Maximum core power occurs (42.0% RTP)	7
Lowest MCHFR occurs (> 25 as calculated by NRELAP5)	7
Maximum RCS pressure occurs (1873 psia)	9
DWS isolation valves closed	11
Transient terminated	20

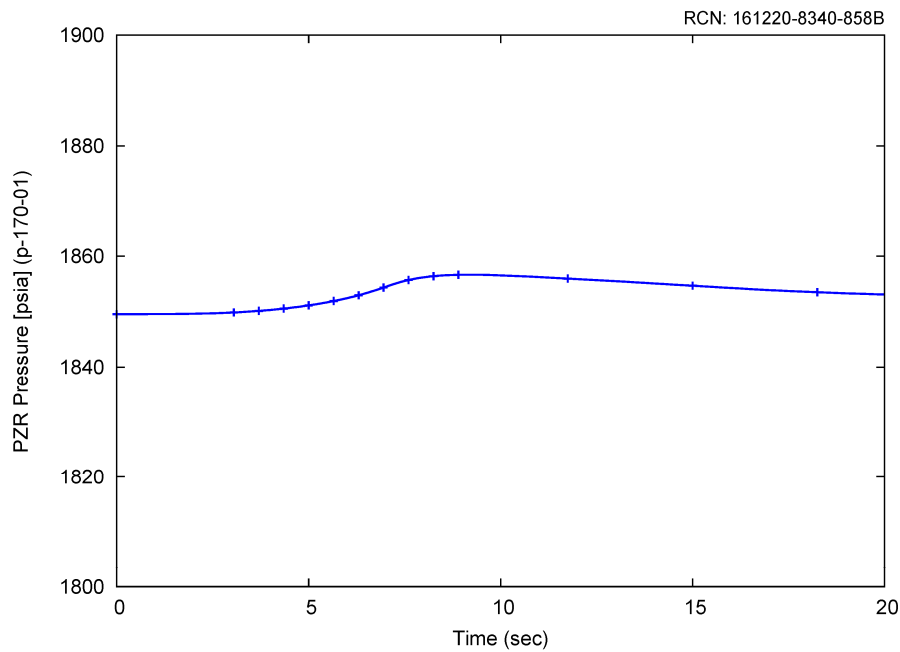


Figure 8-62 Pressurizer pressure response for the bank withdrawal from a low power startup condition

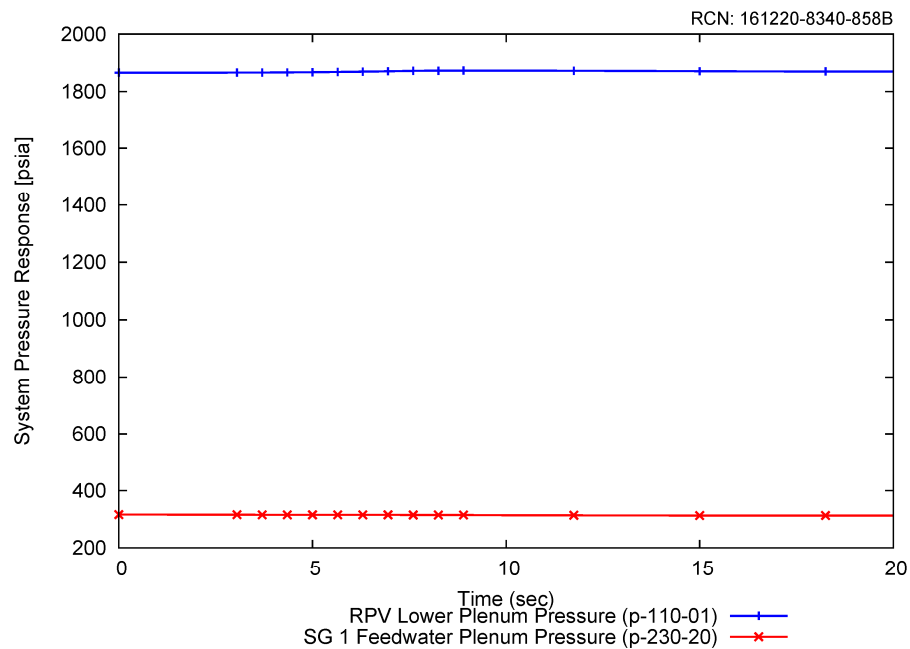


Figure 8-63 Reactor pressure vessel and steam generator pressure responses for the bank withdrawal from a low power startup condition

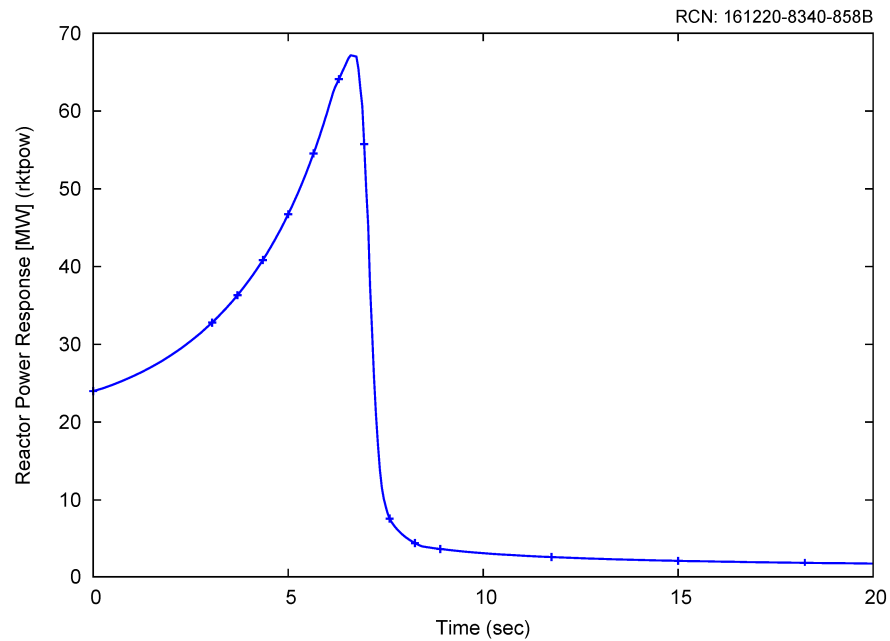


Figure 8-64 Power response for the bank withdrawal from a low power startup condition

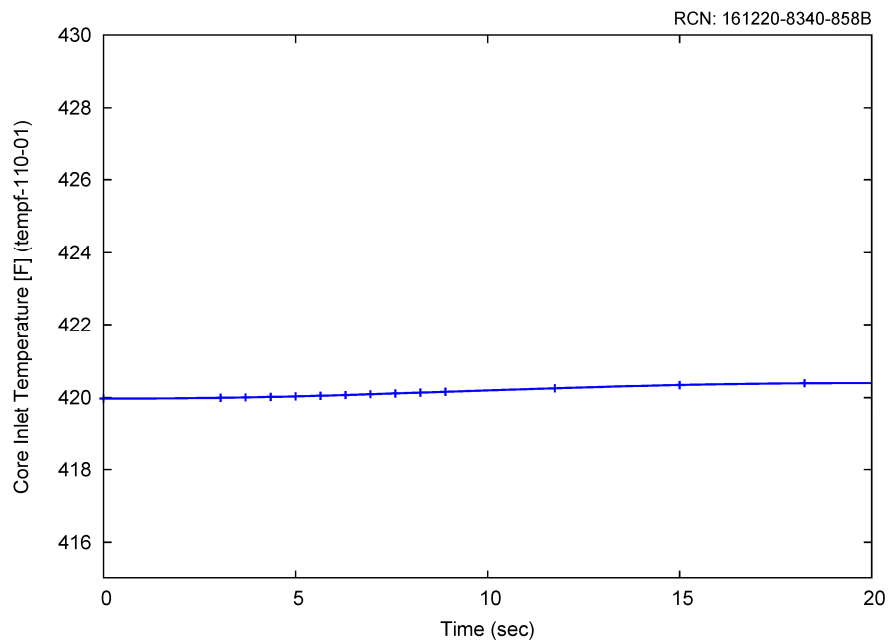


Figure 8-65 Core inlet temperature for the bank withdrawal from a low power startup condition

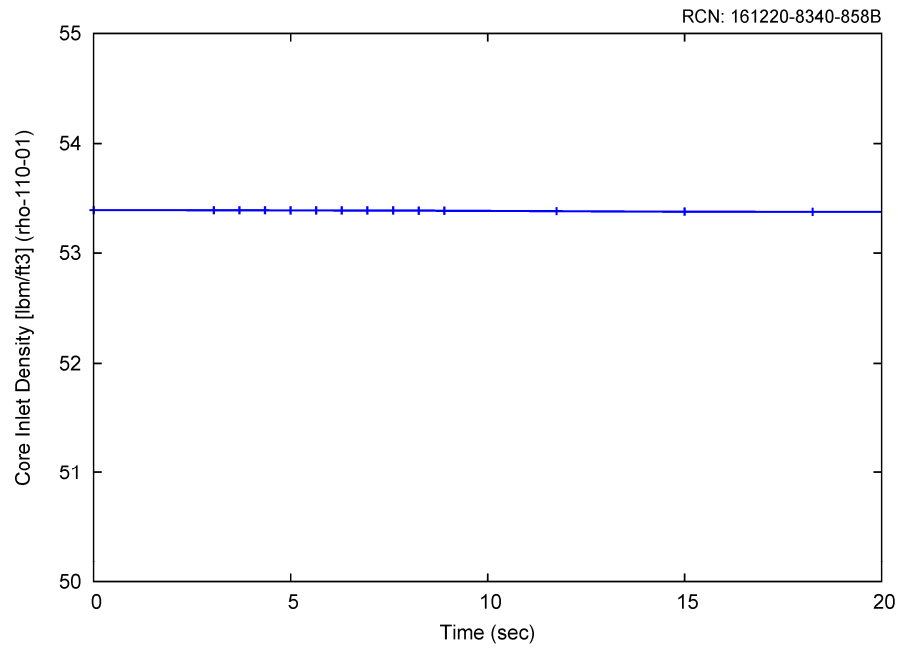


Figure 8-66 Core inlet density for the bank withdrawal from a low power startup condition

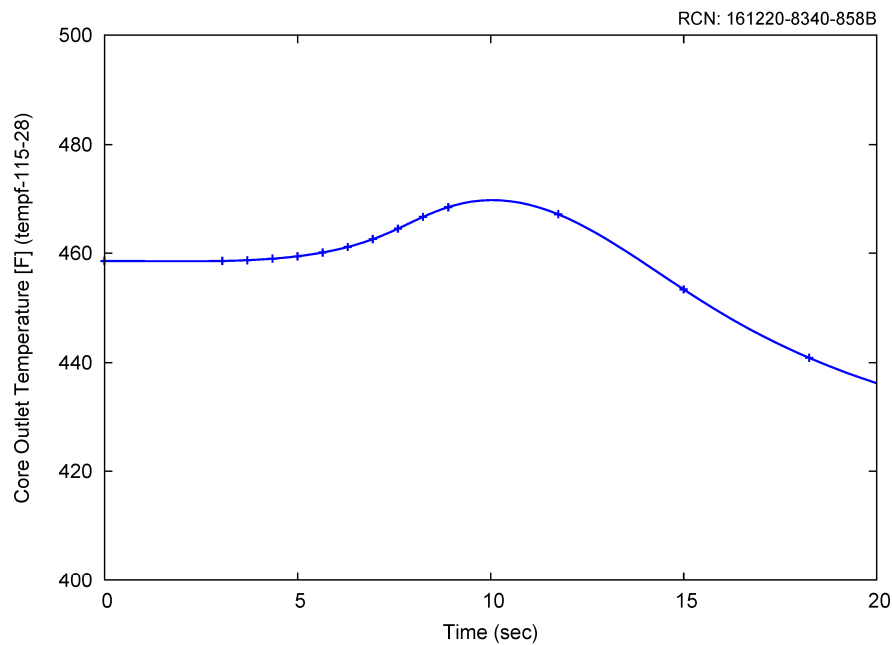


Figure 8-67 Core outlet temperature for the bank withdrawal from a low power startup condition

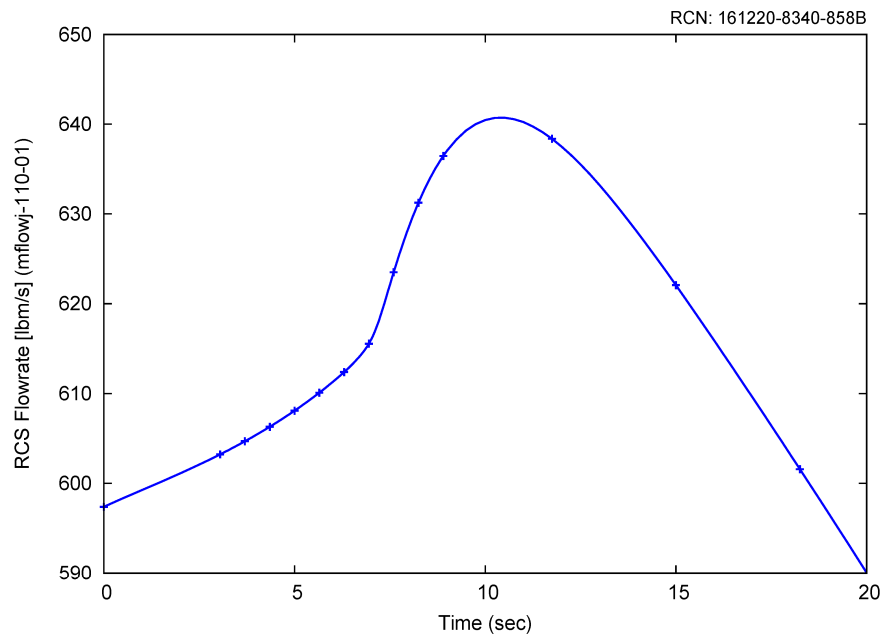


Figure 8-68 Reactor coolant system flow rate for the bank withdrawal from a low power startup condition

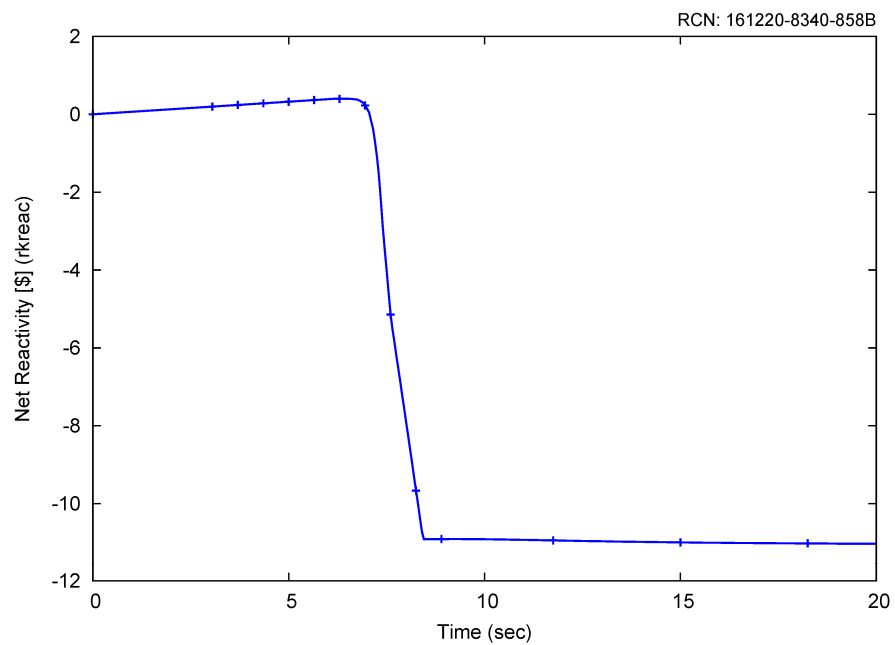


Figure 8-69 Net reactivity for the bank withdrawal from a low power startup condition

8.3.1.3 Conclusion

A representative challenging case regarding MCHFR was identified for a bank withdrawal from a low power startup condition. The results of this case, as presented in Section 8.3.1.2, are subsequently used as input to an MCHFR evaluation using the NuScale subchannel analysis methodology.

8.3.2 Control Rod Misoperation

The purpose of this section is to present the thermal-hydraulic and core neutronic responses of the NPM for control rod misoperation events. Based on Section 7.2.15.1, the control rod misoperation analysis consists of two major transients: single rod withdrawal and rod drop. A representative single rod withdrawal transient is presented in this section. For the single rod withdrawal transient, MCHFR is the acceptance criterion that may be potentially challenged during the transient.

8.3.2.1 Single Rod Withdrawal MCHFR Case - Event Description

The general description for the control rod misoperation event can be found from Section 7.2.15.1. Chosen from a series of MCHFR sensitivity cases, the representative single rod withdrawal case presented here represents a case that could challenge MCHFR, based on the NRELAP5 MCHFR pre-screening. No single failure is applied since the challenging cases occur when all equipment operates as designed. No loss of power is applied since loss of power scenarios trips the reactor and does not make the MCHFR worse. This case features the following conditions:

- The initial power is 75 percent.
- Conservative initial condition biasing (as shown in Table 7-68) is applied in order to maximize the consequences of the single rod withdrawal event in terms of MCHFR. RCS flow rate is biased at low conditions for MCHFR. Average RCS temperature is biased at low condition (535 degrees F) for maximum delay to the high RCS riser temperature trip.
- To maximize the RCS pressure at time of trip without causing an earlier trip on pressurizer pressure, letdown is active, the pressurizer heater is off, and the spray flow is set to 97.6 percent of the CVCS recirculation flow. Additionally, the pressurizer pressure and level were given biases of -70 psi and -3 percent, respectively.
- The reactivity insertion rate is 2.3 pcm/s, which is the maximum that does not result in an earlier trip on high power rate.
- Automatic rod control is disabled since it will counteract the reactivity insertion due to the rod withdrawal at the beginning of the event.
- BOC reactivity coefficients are applied, which is conservative for overpower events.

8.3.2.2 Single Rod Withdrawal MCHFR Case - Analysis Results

The following describes the event sequence of the single rod withdrawal MCHFR case. Table 8-9 summarizes the sequence of events. Figure 8-70 through Figure 8-78 show some key parameters for the single rod withdrawal MCHFR case.

The single rod withdrawal event begins at time zero. The addition of positive reactivity causes reactor power, pressurizer pressure and level to increase (Figure 8-70, Figure 8-71, and Figure 8-72). To bound the limiting single failure of an ex-core flux detector, the lowest reading ex-core detector is used to determine if the high power trip analytical limit of 120 percent is reached. Therefore the actual reactor power reaches a maximum of ~198 MWth, slightly exceeding the 120 percent limit, at ~147 s; this power level is not sufficient for the lowest reading ex-core detector to indicate that the 120 percent analytical limit is reached. As the power increases, the RCS riser temperature increases; in this case, the high RCS riser temperature limit of 610 degrees F is reached at ~139 seconds (Figure 8-73). There is a total 8 second delay between the high RCS riser temperature signal and RTS/DHRS actuation. RTS and DHRS are actuated at ~147 seconds. The limiting MCHFR is also reached at ~147 seconds.

DHRS actuation closes the FWIVs and MSIVs. Steam generator pressure increases as a result of the MS isolation. SG pressure starts to decrease once the DHRS cooling is established (Figure 8-74, SG2 shown but SG1 response is identical). Pressurizer pressure reaches its peak value, less than 2100 psia, around 157 seconds and starts to decrease. Pressurizer level has a similar transient response (Figure 8-71 and Figure 8-72).

After reactor trip and actuation of DHRS, RCS flow decreases rapidly and becomes stagnant and slightly reversed at ~184 seconds (Figure 8-75). Following that, flow oscillations are observed due to temperature and density differences between the riser and downcomer (as discussed in Section 7.2 and shown by Figure 8-73, Figure 8-75, and Figure 8-77). By 40 minutes, RCS flow and DHRS flow have stabilized (Figure 8-75 and Figure 8-76), and RCS temperature and pressure are steadily decreasing as the DHRS transfers decay heat from the RCS to the reactor pool (Figure 8-71, Figure 8-73, and Figure 8-77). It is concluded that by 40 minutes the transient has been terminated and that stable DHRS cooling has been achieved. Subcritical margin is verified as net reactivity remains less than 0.0 dollars at the time stable DHRS cooling has been achieved (Figure 8-78). No operator action was credited to mitigate this event.

Table 8-9 Single rod withdrawal sequence of events – MCHFR case

Event	Time (sec)
Malfunction that initiates the withdrawal of a single CRA.	0
High RCS riser temperature analytical limit (610°F) is reached	139
High pressurizer pressure analytical limit (2000 psia) is reached	145
RTS is actuated and control rod insertion begins	147
DHRS is actuated. The DHRS actuation valves begin opening. The FWIVs and MSIVs begin closing.	147
Lowest MCHFR is reached (3.107 as calculated by NRELAP5)	147
RCS flow is stagnant and slightly reversed.	~184
End of calculation. Stable DHRS cooling has been established. Net reactivity remains < \$0.0.	2400

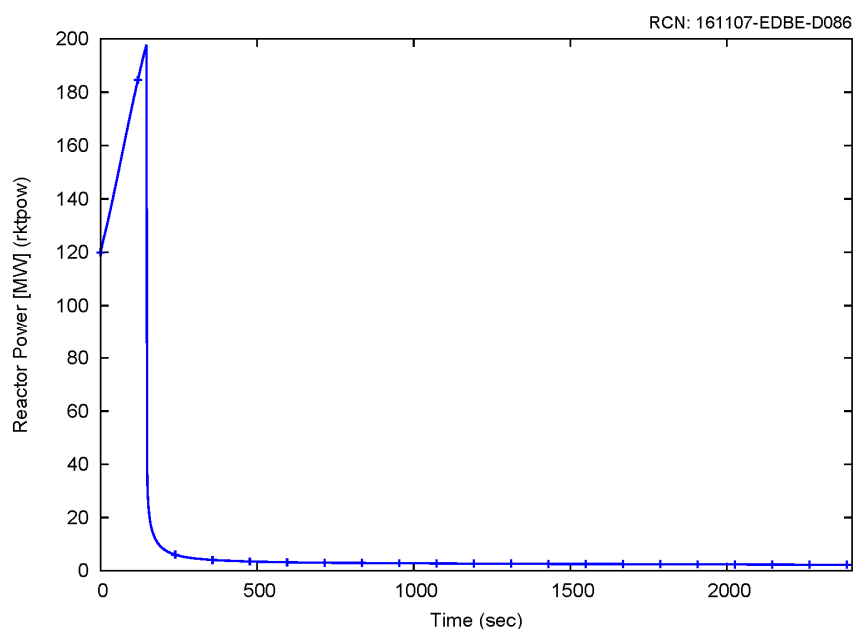


Figure 8-70 Power response for the representative single rod withdrawal MCHFR case

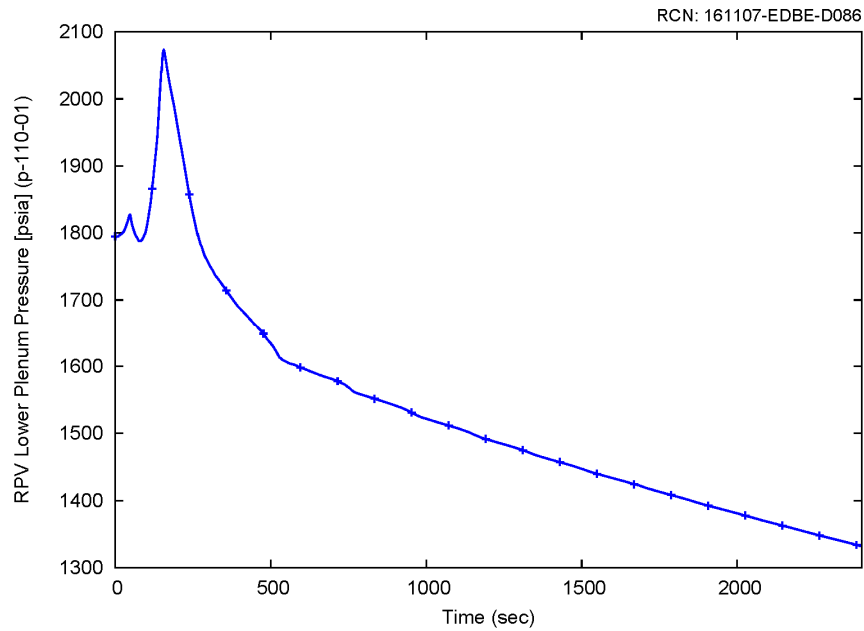


Figure 8-71 Reactor pressure vessel pressure response for the representative single rod withdrawal MCHFR case

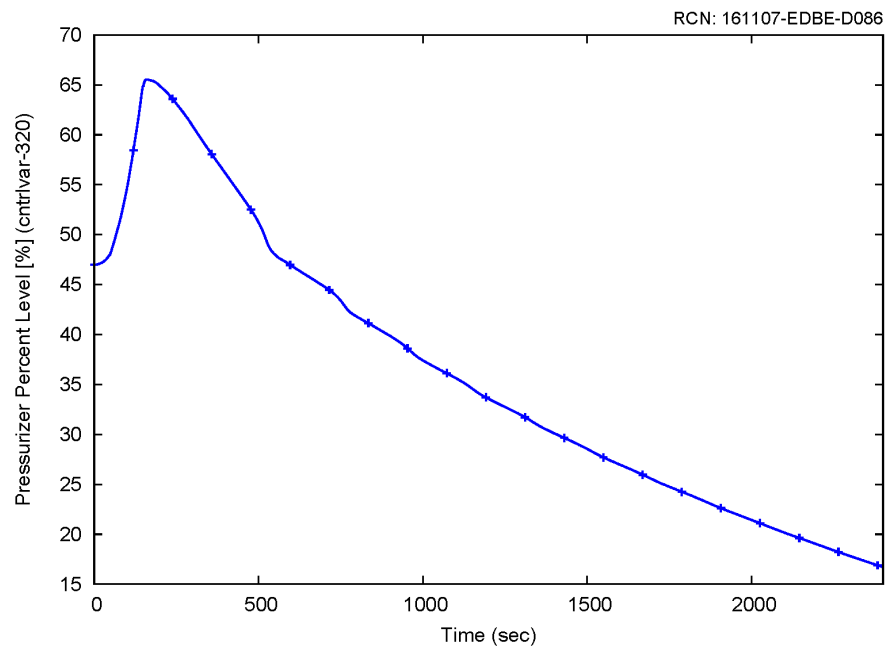


Figure 8-72 Pressurizer level for the representative single rod withdrawal MCHFR case

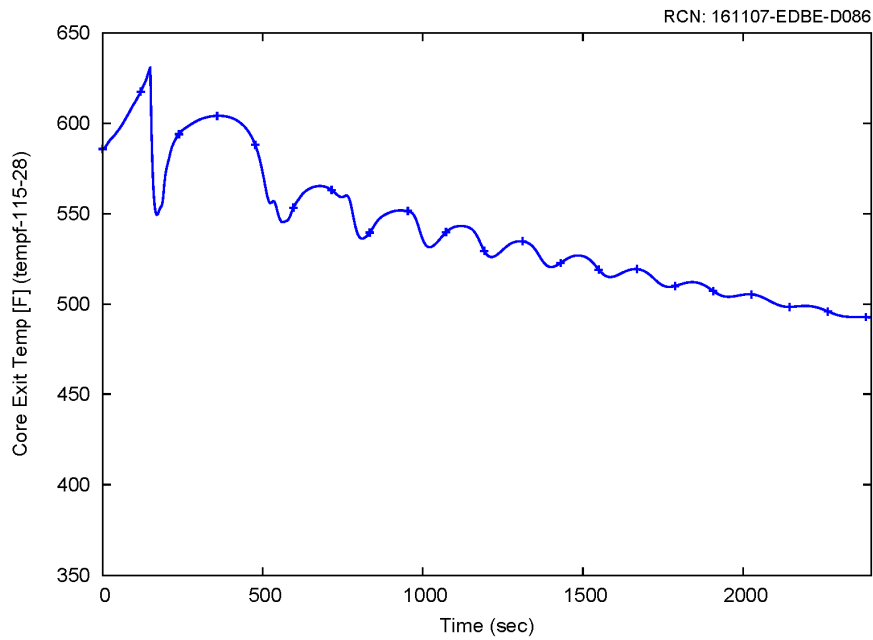


Figure 8-73 Core outlet temperature for the representative single rod withdrawal MCHFR case

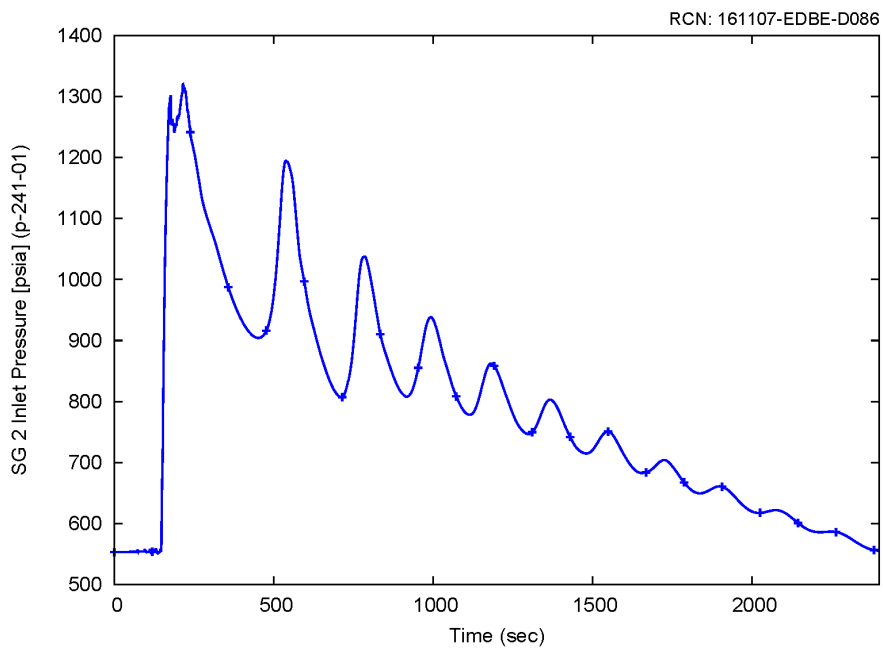


Figure 8-74 Steam generator 2 pressure response for the representative single rod withdrawal MCHFR case

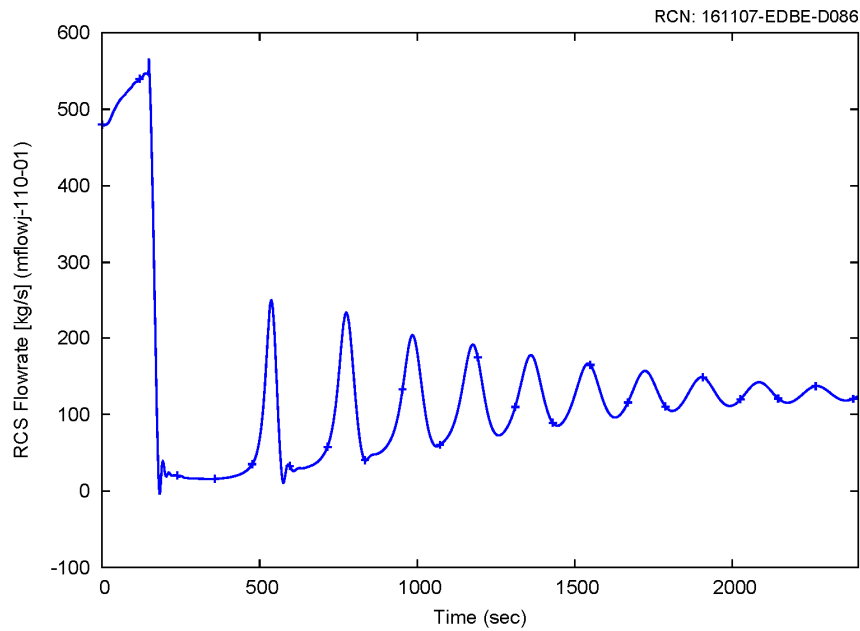


Figure 8-75 Reactor coolant system flow rate for the representative single rod withdrawal MCHFR case

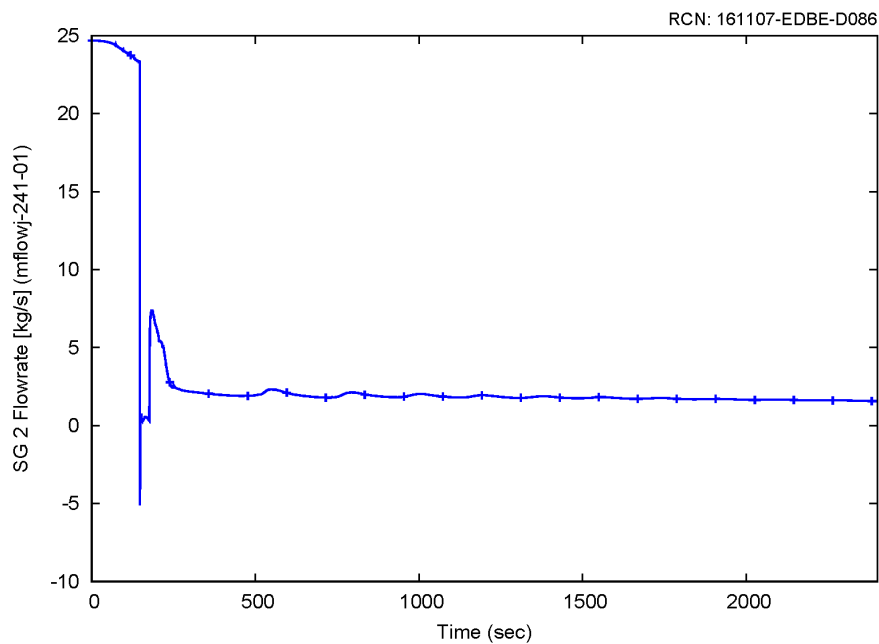


Figure 8-76 Steam generator 2 secondary flow for the representative single rod withdrawal MCHFR case

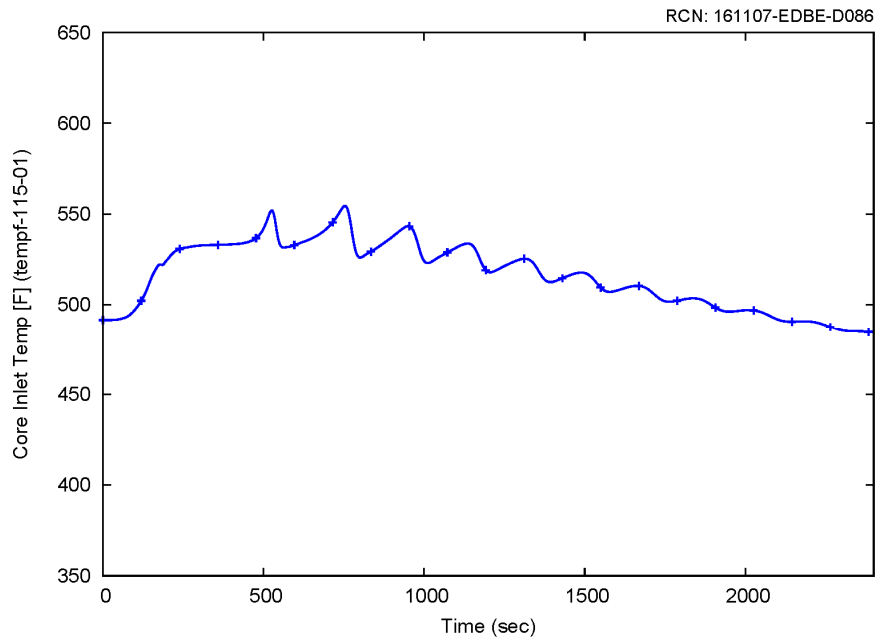


Figure 8-77 Core inlet temperature for the representative single rod withdrawal MCHFR case

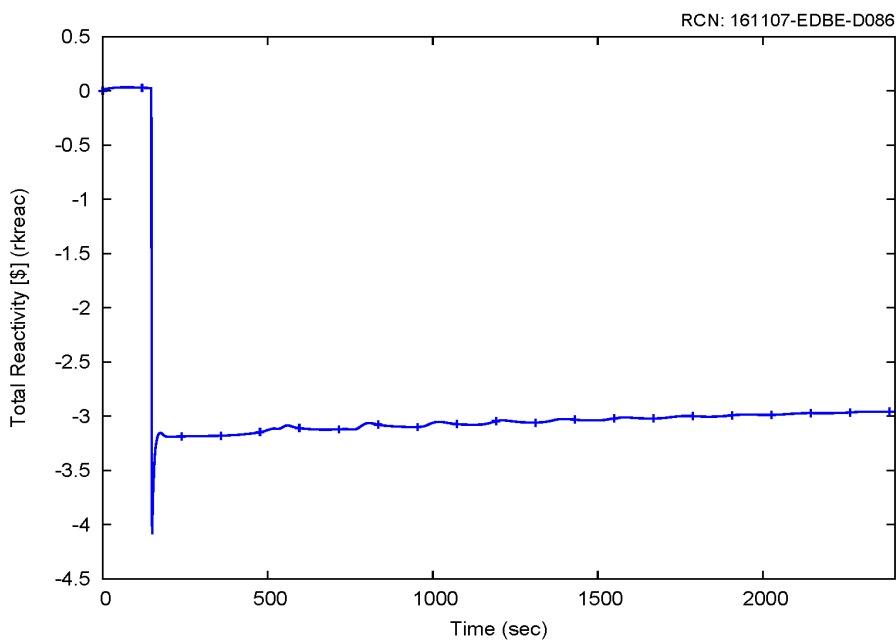


Figure 8-78 Net reactivity for the representative single rod withdrawal MCHFR case

8.3.2.3 Single Rod Withdrawal MCHFRC Case - Conclusion

A representative case that could challenge MCHFRC was identified for the single rod withdrawal event. The results of this case, as presented in Section 8.3.2.2, are subsequently used as input to an MCHFRC evaluation using the NuScale subchannel analysis methodology.

8.4 Increase in Reactor Coolant System Inventory

8.4.1 Chemical and Volume Control System Malfunction that Increases Reactor Coolant System Inventory

The purpose of this section is to present the thermal-hydraulic response of the NPM for a CVCS malfunction that increases the RCS inventory. This event is evaluated for primary and secondary pressure. A representative case evaluated for primary pressure is presented.

8.4.1.1 Event Description

The general event description associated with a malfunction of the CVCS that increases RCS inventory is provided in Section 7.2.17. Based on Section 7.2.17, the RCS primary pressure is the acceptance criterion that may be challenged during the CVCS malfunction event. A representative case that could challenge the RCS primary pressure is presented here. This case features the following conditions:

- Conservative initial condition biasing is applied to maximize the consequences of the RCS inventory increase event. This case is initialized at 102 percent reactor power, low pressurizer pressure and high pressurizer level. Minimum RCS design flow is assumed. Low RCS average temperature is assumed.
- Net CVCS mass flow rate of 5.4 lbm/s (40 gpm) into the RPV (this includes CVCS recirculation flow rate into and out of the RPV)
- High CVCS makeup temperature of 150 degrees F
- Pressurizer spray and letdown assumed unavailable

8.4.1.2 Analysis Results

The following describes the event sequence of the representative CVCS malfunction that increases RCS inventory event. Table 8-10 summarizes the sequence of events. Figure 8-79 through Figure 8-91 show some key parameters during the representative increase in RCS inventory event.

For this event, constant makeup flow is injected into the RCS until the CVCS is isolated (Figure 8-79). The CVCS also recirculates flow (Figure 8-80); no letdown flow is modeled (Figure 8-81). Therefore, there is a net increase of flow into the RCS (Figure 8-82 and Figure 8-83).

Upon initiation of makeup, pressurizer level and RCS pressure were observed to rise. Pressurizer pressure and level are shown in Figure 8-84 and Figure 8-85, respectively.

RCS pressure reached the high pressurizer pressure analytical limit, actuating reactor trip (Figure 8-86) and DHRS (Figure 8-88 and Figure 8-89, curves for SG1 and SG2 overlap). In this case, the normal control system is assumed to trip the turbine on reactor trip, which reduced secondary side heat removal, increasing the rate of RCS pressurization. The inventory addition continued following reactor trip because RCS flow remained above 0 lbm/s (Figure 8-87) and therefore CVCS remained un-isolated.

After reactor trip and actuation of DHRS, RCS flow oscillations were observed due to temperature and density differences between the riser and downcomer (as discussed in Section 7.2). Oscillations can be seen in Figure 8-87, Figure 8-90 and Figure 8-91.

After reactor trip, the pressurizer pressure and level began to decrease for a short period of time but the makeup flow continued and the pressurizer level and primary pressure eventually began to increase again. Once the RSV 1 lift pressure was reached, RCS pressure was reduced as vapor from the pressurizer was vented into the containment vessel. A peak pressure of 2155 psia was reached in the RPV. Inventory increase continued for approximately 100 seconds further before the high pressurizer level analytical limit was reached. After reaching the high pressurizer level of 80 percent, CVCS was isolated and the event ended. Pressurizer level never exceeds 80 percent, thus ensuring a steam bubble in the pressurizer throughout this transient.

The calculation is continued to verify that the module transitions into passive and stable DHRS cooling. Figure 8-84, Figure 8-87, Figure 8-88, Figure 8-89, and Figure 8-90 show that at ~ 1 hour, RCS and DHRS flows have stabilized, primary and secondary pressures are decreasing, and the RCS temperatures are steadily decreasing as the DHRS is transferring decay heat from the RPV to the reactor pool. Shutdown margin is maintained at the end of the transient calculation (Figure 8-91). It is concluded that by ~ 1 hour the transient has been terminated and that stable DHRS cooling has been achieved.

Table 8-10 Increase in reactor coolant system inventory sequence of events

Event	Time (sec)
CVCS malfunction initiates an excess CVCS mass flow rate of 5.4 lbm/s into the RPV	0.0
Analytical limit for high pressurizer pressure (2000 psia) is reached	510.9
Turbine stop valve closed	511.8
RTS* and DHRS actuation on high pressurizer pressure analytical limit	512.9
Primary MSIVs fully closed	518.8
RSV 1 actuates	3370.9
Peak RCS pressure is reached (2155 psia)	3371.0
Analytical limit for high pressurizer level (80%) is reached	3465.9
CVCS isolation actuation on high pressurizer level analytical limit	3468.9
CVCS isolation valves closed on high pressurizer level analytical limit	3473.9
End of calculation. Stable DHRS cooling has been established.	4000

* Control rods are assumed to be fully inserted 2.278 seconds following RTS actuation.

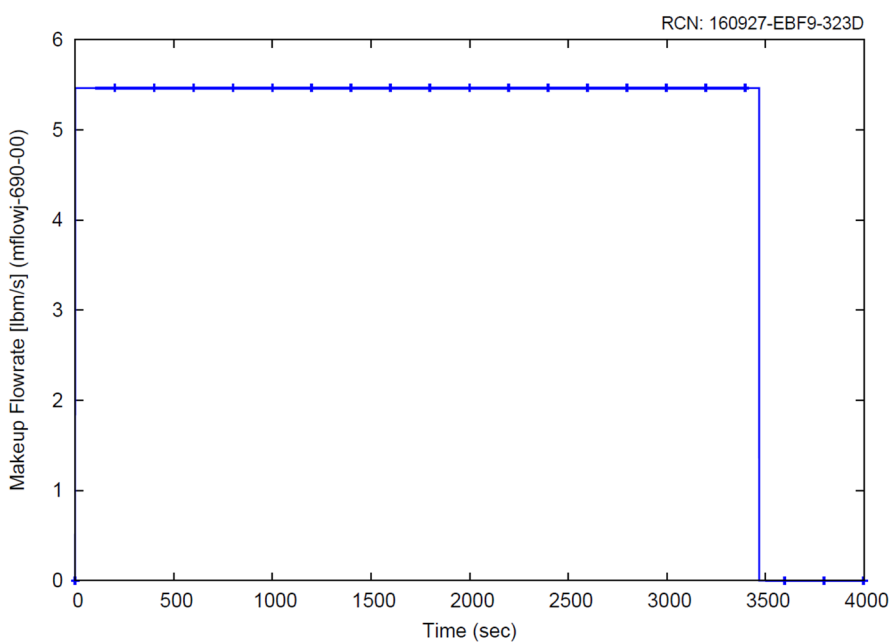


Figure 8-79 Makeup flow for increase in reactor coolant system inventory

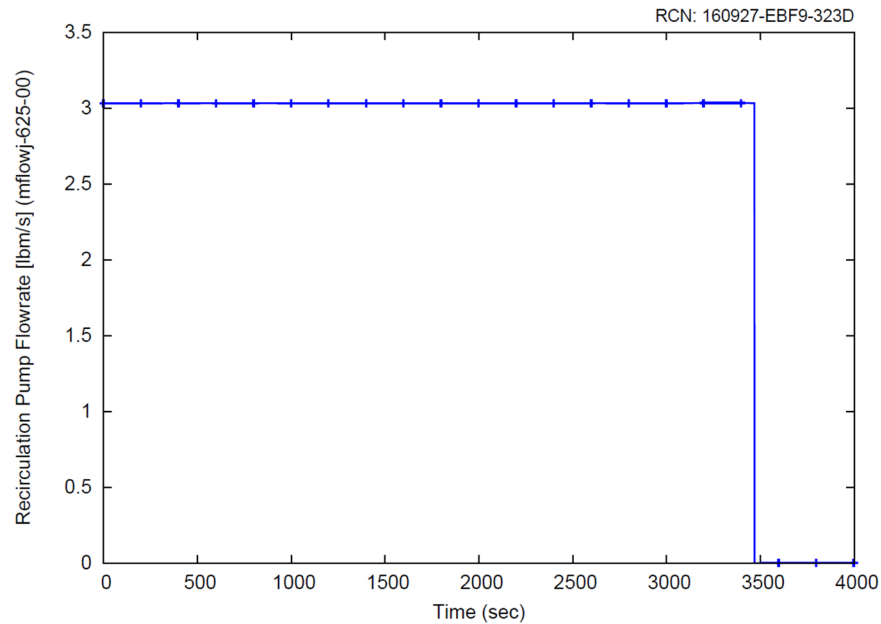


Figure 8-80 Recirculation pump flow for increase in reactor coolant system inventory

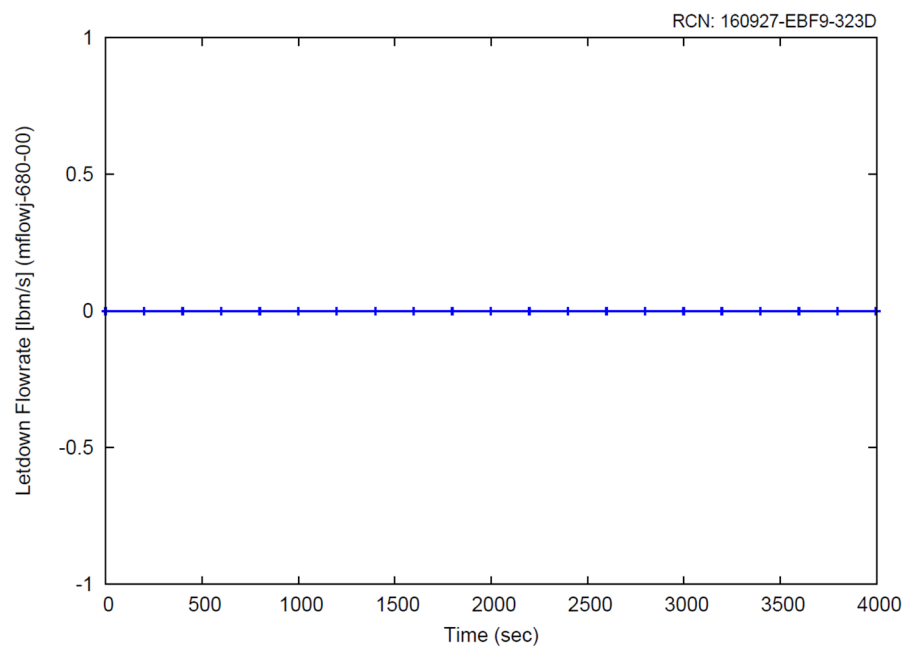


Figure 8-81 Letdown flow for increase in reactor coolant system inventory

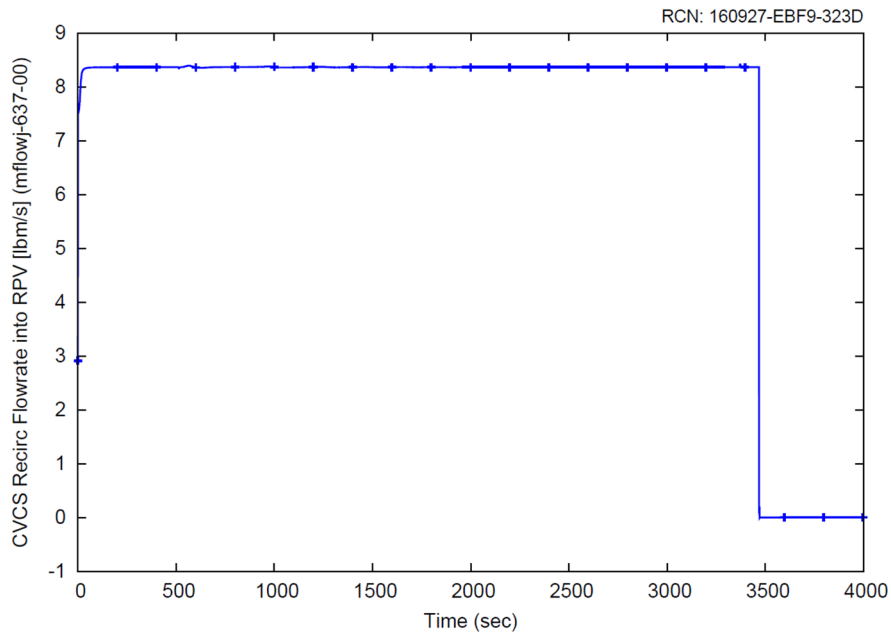


Figure 8-82 CVCS recirculation flow rate into the reactor pressure vessel for increase in reactor coolant system inventory

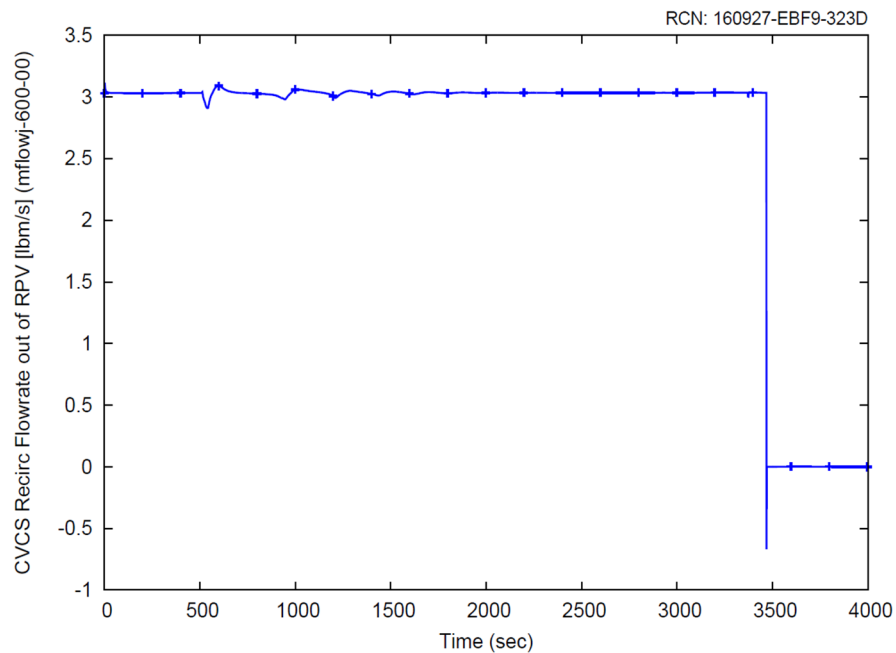


Figure 8-83 CVCS recirculation flow rate out of the reactor pressure vessel for increase in reactor coolant system inventory

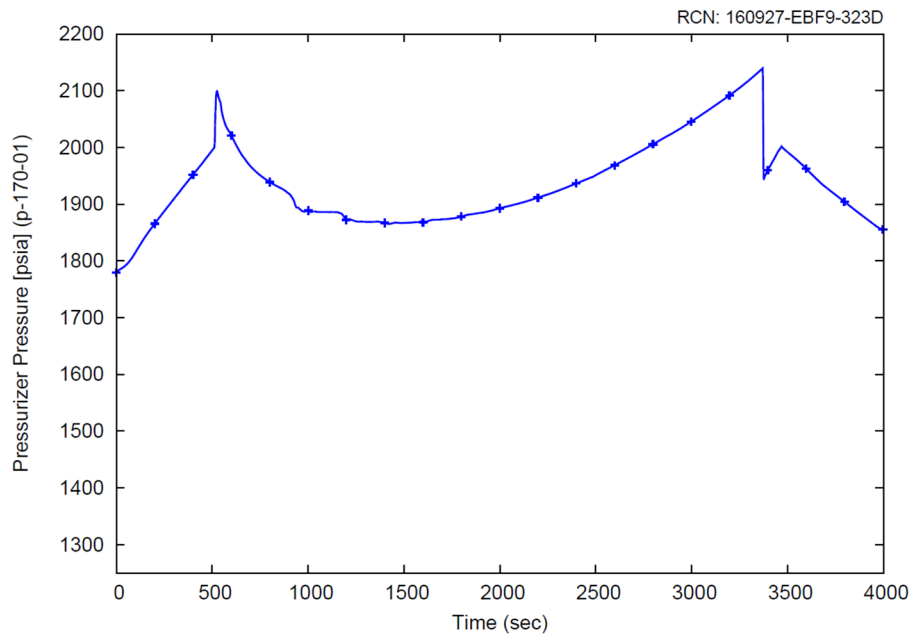


Figure 8-84 Pressure at the bottom of the pressurizer for increase in reactor coolant system inventory

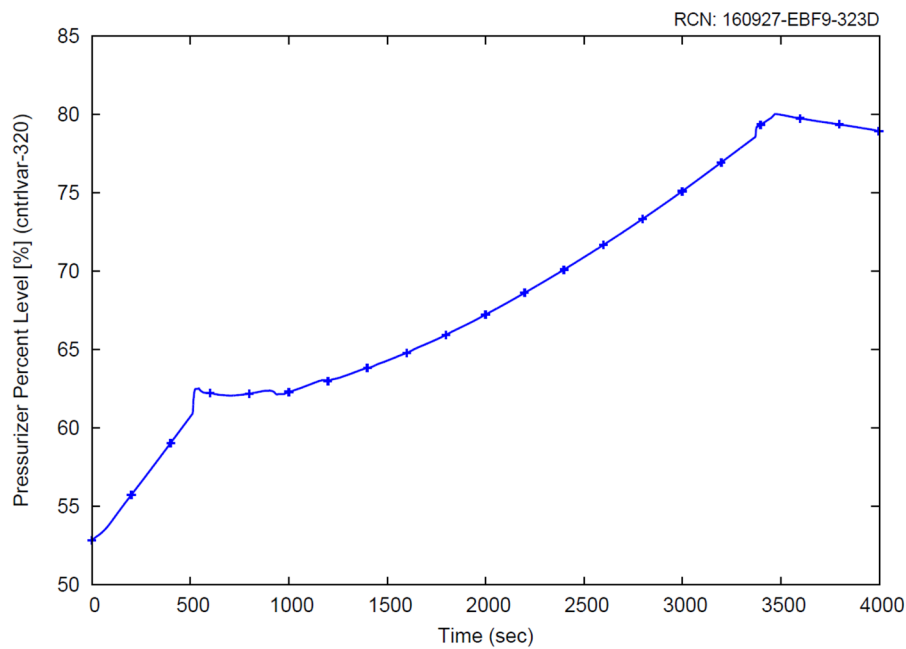


Figure 8-85 Pressurizer level for increase in reactor coolant system inventory

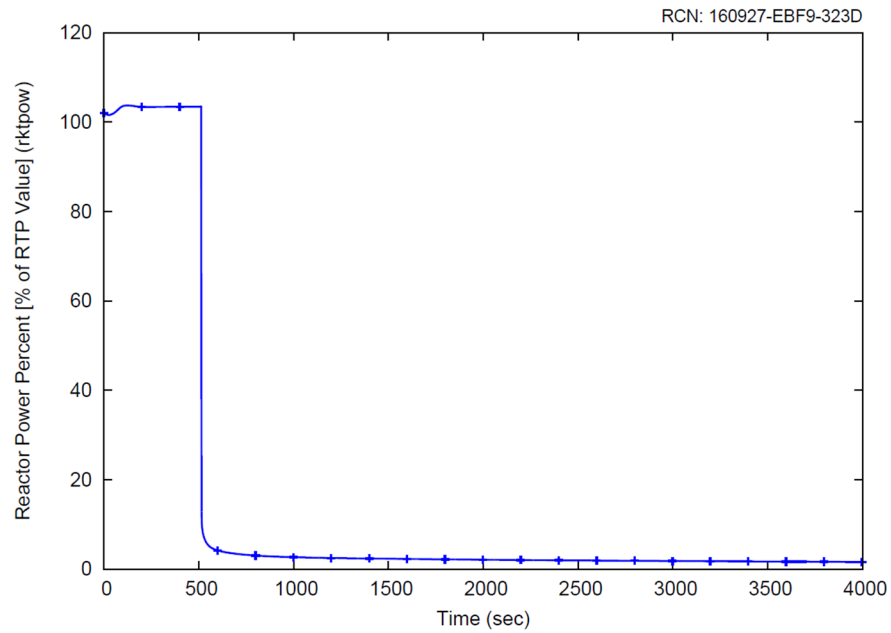


Figure 8-86 Reactor power for increase in reactor coolant system inventory

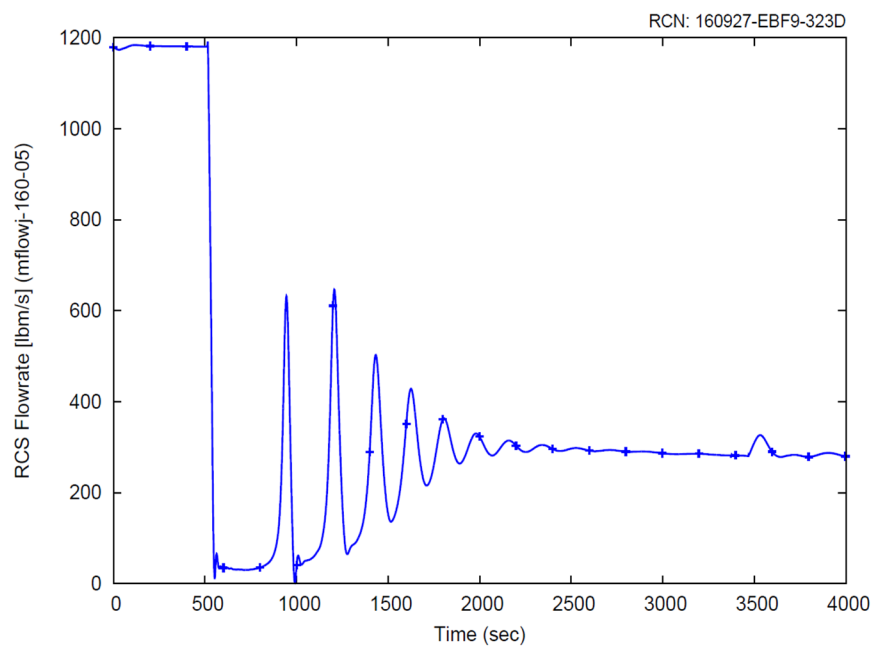


Figure 8-87 Reactor coolant system flow for increase in reactor coolant system inventory

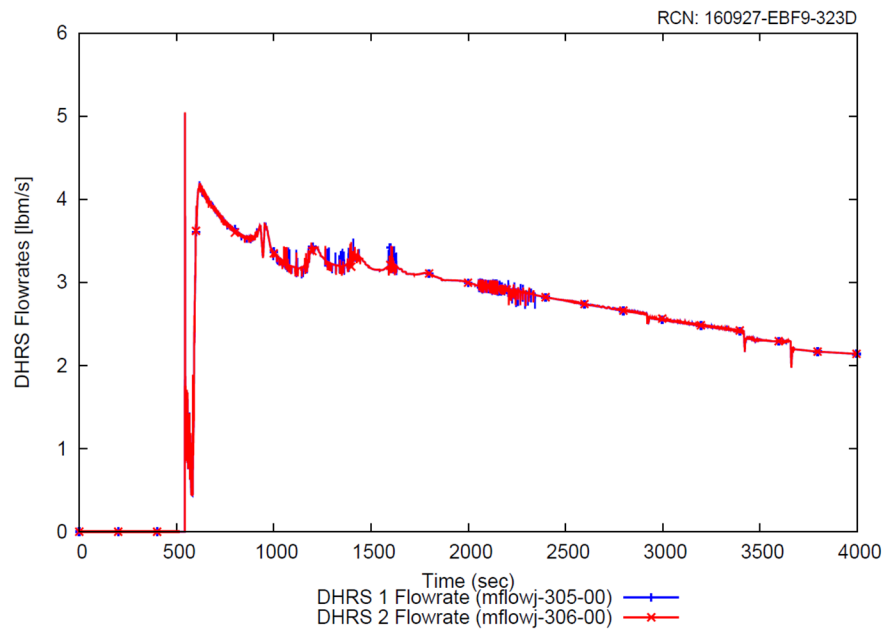


Figure 8-88 Decay heat removal system flow rate for increase in reactor coolant system inventory

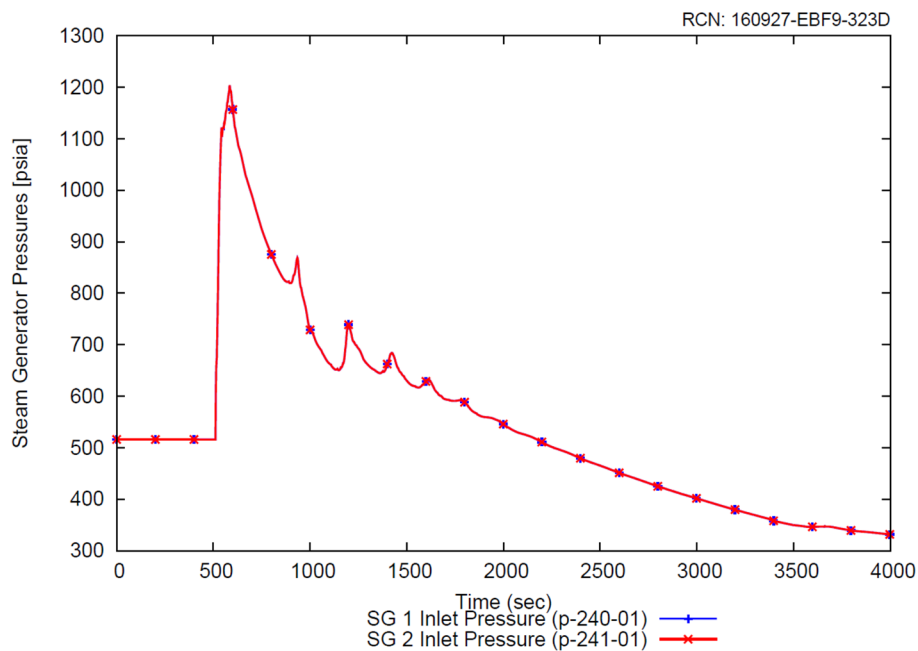


Figure 8-89 Steam generator pressure for increase in reactor coolant system inventory

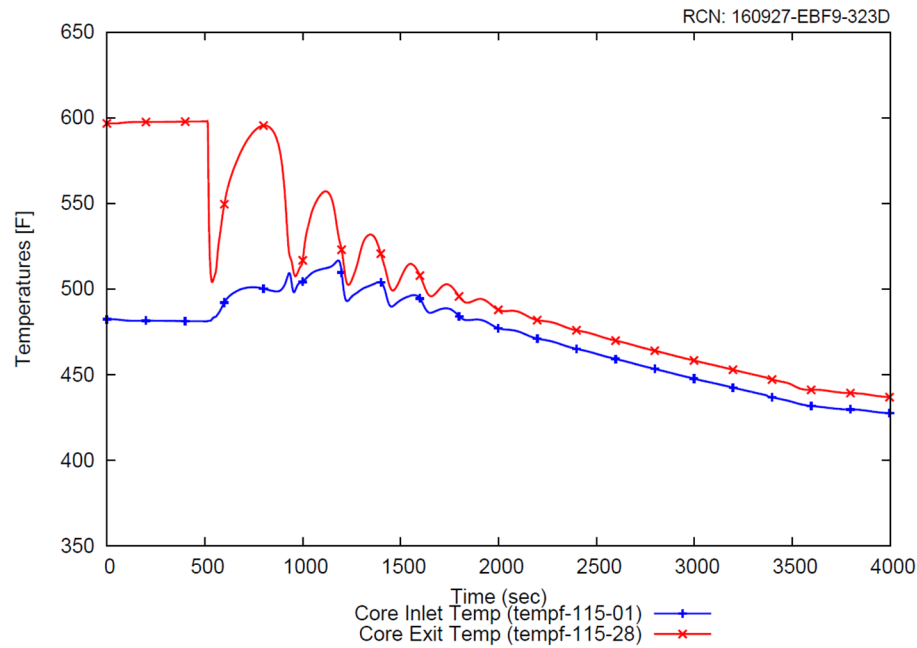


Figure 8-90 Core inlet and exit coolant liquid temperature for increase in reactor coolant system inventory

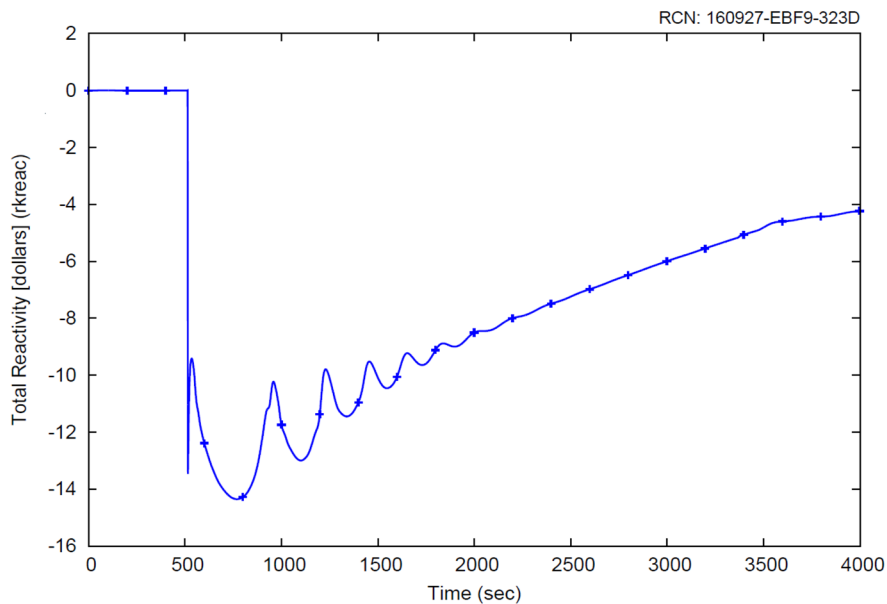


Figure 8-91 Total reactivity for increase in reactor coolant system inventory

8.4.1.3 Conclusion

A representative case that could challenge the RCS pressure acceptance criterion was identified. The results of this case, as presented in Section 8.4.1.2, demonstrate the RCS pressure acceptance criterion is met.

8.5 Decrease in Reactor Coolant System Inventory

8.5.1 Small Line Break Outside of Containment

The purpose of this section is to present the thermal-hydraulic and core neutronic responses of the NPM for a postulated break in a small line carrying primary coolant. For the reasons discussed in Section 7.2.18, the lines evaluated are the CVCS charging lines, the CVCS letdown lines, and the CVCS pressurizer spray lines. This event is evaluated for offsite and onsite radiological dose consequences. The transient analysis results are input to downstream radiological consequences evaluations and downstream subchannel evaluations. This analysis is not intended to be used for 10 CFR 50 Appendix K compliance for a LOCA as the separate LOCA-EM topical report encompasses this subject.

8.5.1.1 Event Description

The event description for a break in a small line carrying reactor coolant can be found in from Section 7.2.18. Based on Section 7.2.18, the acceptance criteria for radiological consequences are potentially challenged by the break in a small line carrying reactor coolant event; but a single active failure cannot make the event consequences worse.

Radiological Consequences

The representative case presented here corresponds to one of the more limiting integrated mass released cases, and therefore a case with higher dose consequences. This case features the following conditions for a DEG break of 100 percent area in the letdown line:

- Conservative initial condition biasing (as shown in Table 7-86) is applied in order to maximize the consequences of this event. This representative case is initialized at 102 percent reactor power.
- The initial RCS average temperature is biased to the maximum value (555 degrees F) to maximize the mass released through the break.
- The initial feedwater temperature is biased to the minimum value (~290 degrees F) in this case.
- The initial pressurizer pressure is biased to the maximum value (1920 psia) to delay actuation of the low pressurizer pressure RTS and ESFAS protection signals.
- The initial pressurizer level is biased to the maximum value (68 percent) to delay actuation of the low pressurizer level RTS and ESFAS protection signals.

- EOC reactivity coefficients are applied to obtain the mass released through the break associated with a specific time in core life.
- A loss of normal AC Power at event initiation is utilized, consistent with Table 7-87, to maximize the mass released through the break.
- No operator action was credited in the representative case.

8.5.1.2 Analysis Results

The following describes the event sequence of the representative small break outside CNV event. Table 8-11 summarizes the sequence of events. Figure 8-92 through Figure 8-102 show some key parameters during the representative small break outside CNV event.

A letdown line break of 100 percent area occurs at time zero with a coincident loss of AC power. Critical flow conditions are quickly established at the break location causing the break flow rate to stabilize (Figure 8-92). The reactor coolant lost through the break causes an immediate decrease in pressurizer level (Figure 8-93) and RPV pressure (Figure 8-94). In contrast, the SG pressure immediately increases (Figure 8-95) as a result of the turbine trip induced by the loss of AC power. The reduced secondary heat sink associated with tripping the feedwater pumps on loss of AC power is sufficient to cause the pressurizer level and RPV pressure to begin to increase. The exit pressures of the SGs reach the analytical limit for high steam line pressure (800 psia) at 11.7 seconds. Another two seconds is needed before the control rods are free to fall (Figure 8-96). Coincident with reactor trip at 13.7 seconds, the DHRS valves begin to open; the FWIVs begin to close; the MSIVs begin to close; and, the makeup line break opens fully (Figure 8-92). Opening the break in the makeup line causes the total break flow rate to increase sharply (Figure 8-92), then decrease and stabilize as critical flow conditions are established through the makeup line. Closing the FWIVs and MSIVs isolates the SGs from the remaining secondary system.

The system shrinkage associated with the reactor trip works in conjunction with the increased break flow to cause the pressurizer level and RPV pressure to decrease. The analytical limit for low pressurizer level (35 percent) is reached at 86.3 seconds, and the pressurizer heaters are de-energized two seconds later. The pressurizer pressure continues to decrease until the analytical limit for low pressurizer pressure (1600 psia) is reached at 89.9 seconds. Containment isolation is initiated after a delay of 2 seconds. Closing the CVCS isolation valves terminates the break flow (Figure 8-92). The maximum integrated break flow of 12,940 lbm is reached at 97 seconds (Figure 8-97).

After reactor trip and actuation of DHRS, oscillations are observed due to temperature and density differences between the riser and downcomer (as discussed in Section 7.2); therefore the calculation is continued to verify that the module transitions into passive and stable DHRS cooling. At ~25 minutes, RCS flow (Figure 8-98) has stabilized, and the RCS temperature (Figure 8-99) and pressure (Figure 8-100) are steadily decreasing as the DHRS transfers decay heat from the RPV to the reactor pool. The net reactivity (Figure 8-101) becomes negative shortly after reactor trip and remains negative during the

transition to stable DHRS cooling. Lastly, the RPV level (Figure 8-102) remains well above the top of the core throughout this transient. It is concluded that, by 25 minutes, the transient has been terminated and that stable DHRS cooling has been achieved. No operator action was credited to mitigate this event.

Table 8-11 Sequence of events for small line breaks carrying primary coolant outside containment

Event	Time (sec)
Letdown line break (DEG, 100% area) occurs with coincident loss of normal AC power; TSVs begin to close.	0
Peak reactor power is reached (163.6 MW).	0
TSVs are fully closed.	0.1
Limiting MCHFR is reached (5.009 as calculated by NRELAP5).	1.0
High steam line 1 pressure limit is reached (800 psia).	11.7
High steam line 2 pressure limit is reached (800 psia).	11.7
RTS actuation on high steam line 1 pressure signal, control rods are inserted into the core.	13.7
CVCS makeup line break (DEG, 100% area) occurs.	13.7
DHRS actuation on the high steam line 1 pressure signal. DHRS actuation valves begin to open. FWIVs and MSIVs begin to close.	13.7
Peak RPV pressure is reached (1983 psia).	13.9
FWIVs and MSIVs are fully closed.	18.7
DHRS actuation valves are fully open.	43.7
Low PZR level limit is reached (35%). PZR heaters are disabled after 2 second delay.	86.3
Low PZR pressure is reached (1600 psia). Containment and CVCS isolation begins after 2 second delay.	89.9
CVCS isolation valves are fully closed.	96.9
Maximum integrated RCS break flow (11,940 lbm) occurs.	97
Establishment of stable RCS flow. Pressure and temperature are steadily decreasing.	1500
End of calculation. Stable DHRS cooling has been established.	3000

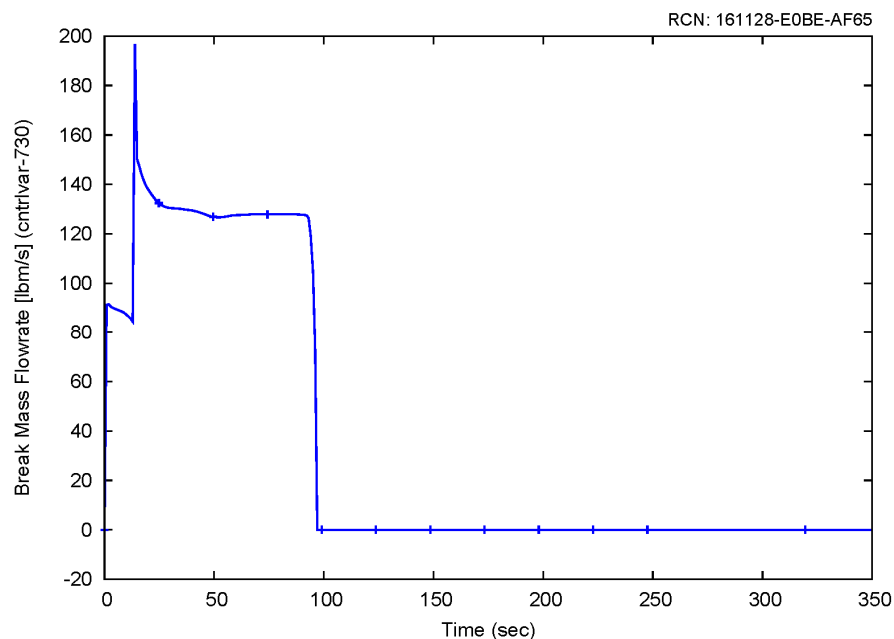


Figure 8-92 Instantaneous break flow response (0 to 350 sec) for the representative small break outside containment event

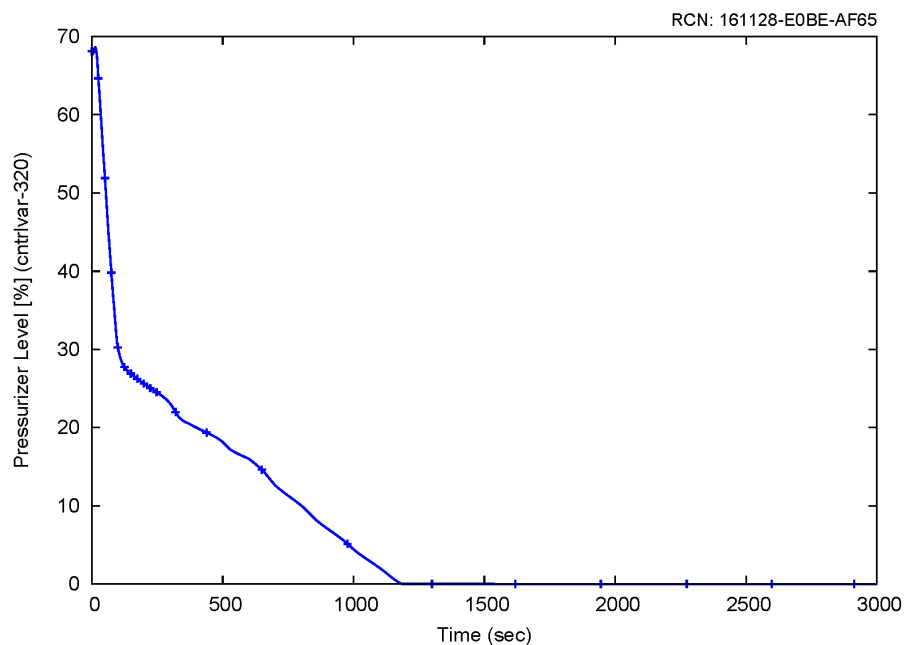


Figure 8-93 Pressurizer level response for the representative small break outside containment event

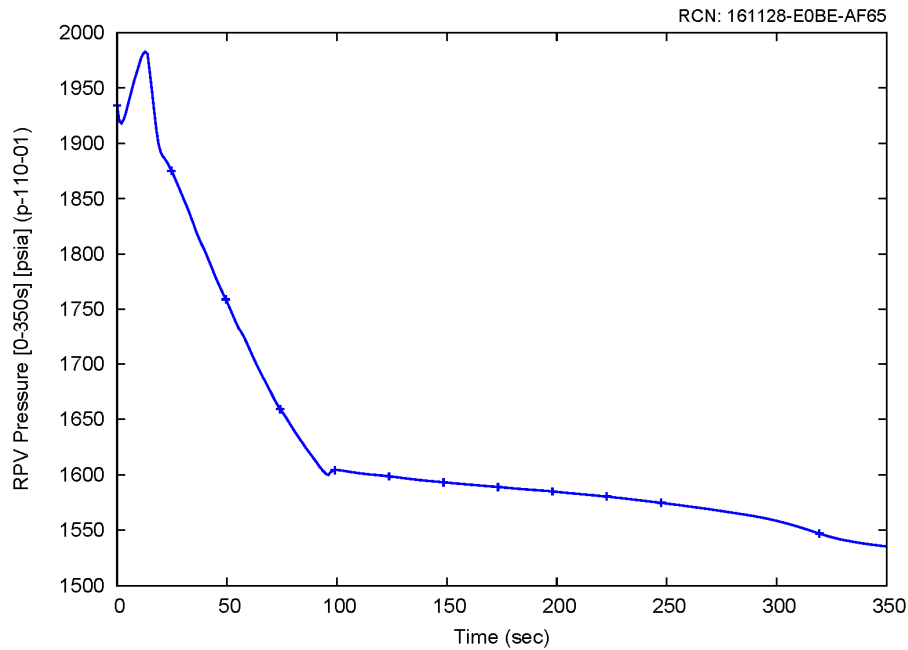


Figure 8-94 Reactor pressure vessel pressure response (0 to 350 sec) for the representative small break outside containment event

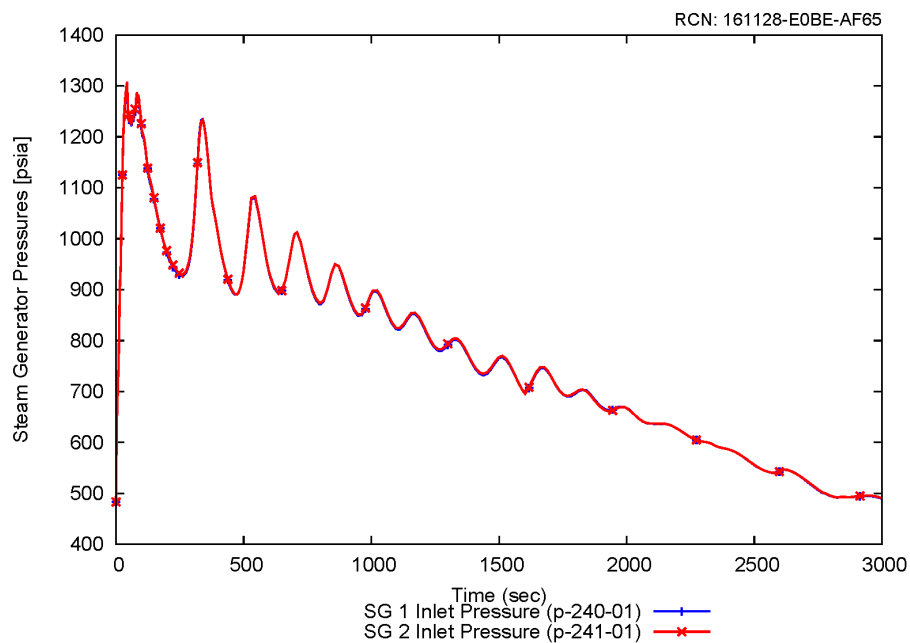


Figure 8-95 Steam generator pressure responses for the representative small break outside containment event

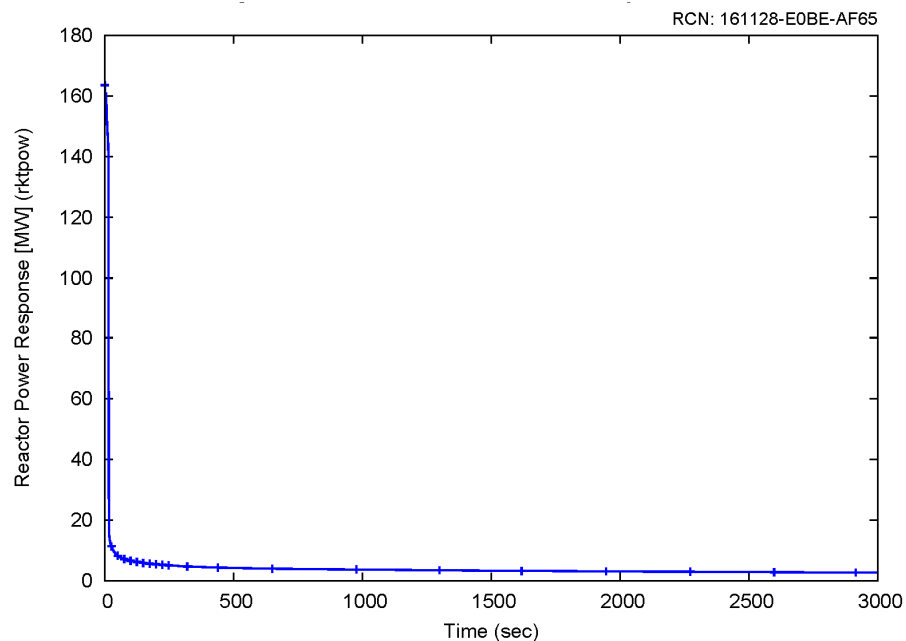


Figure 8-96 Core power response for the representative small break outside containment event

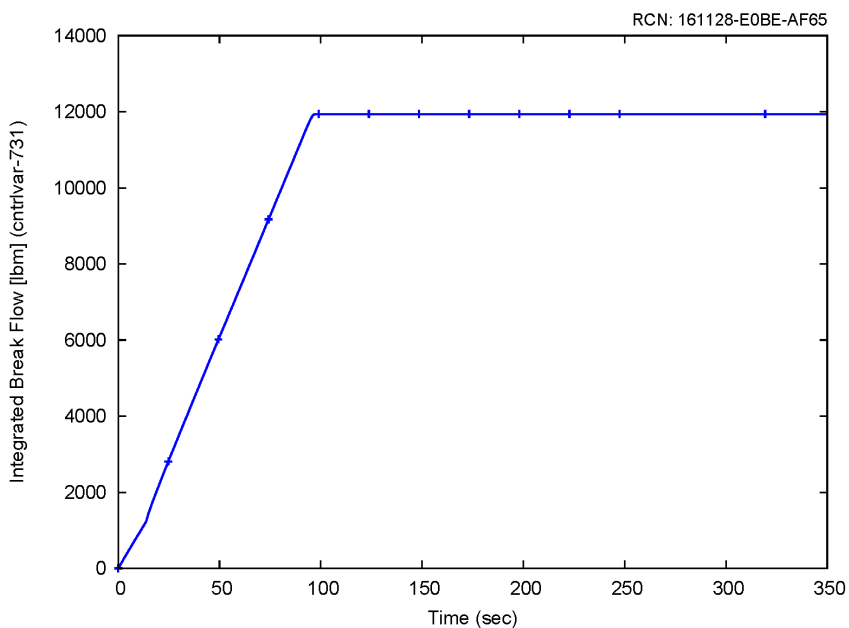


Figure 8-97 Integrated break flow response (0 to 350 sec) for the representative small break outside containment event

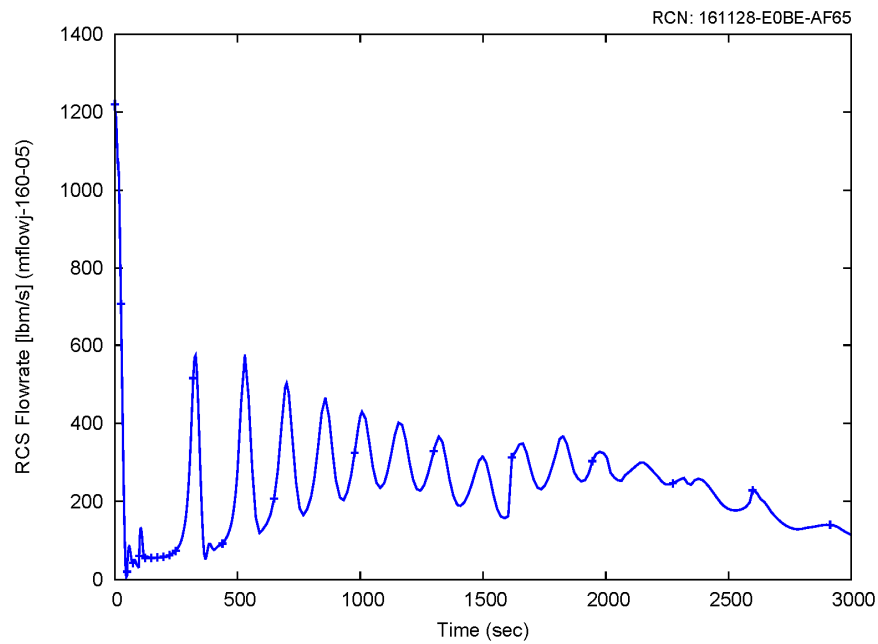


Figure 8-98 Reactor coolant system flow rate response for the representative small break outside containment event

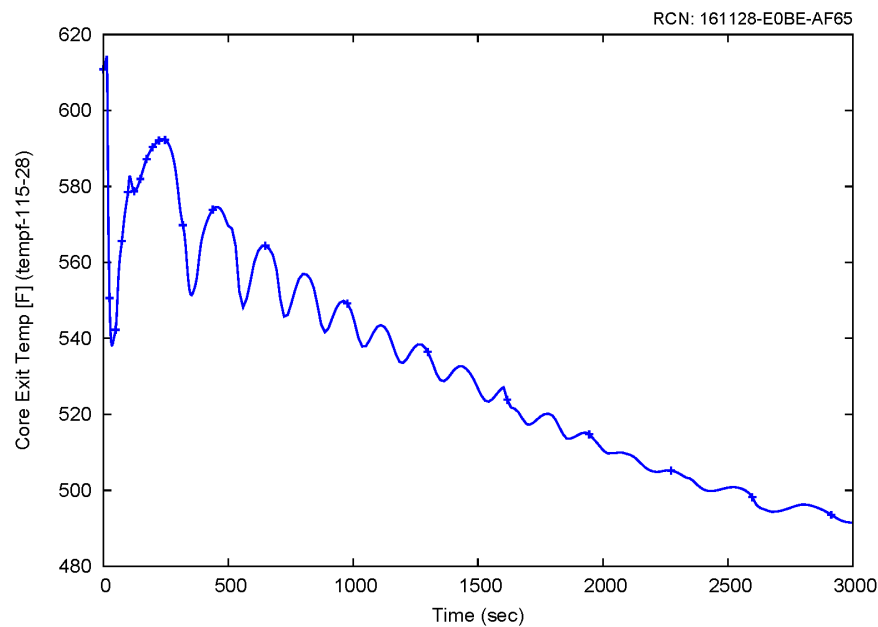


Figure 8-99 Core outlet temperature response for the representative small break outside containment event

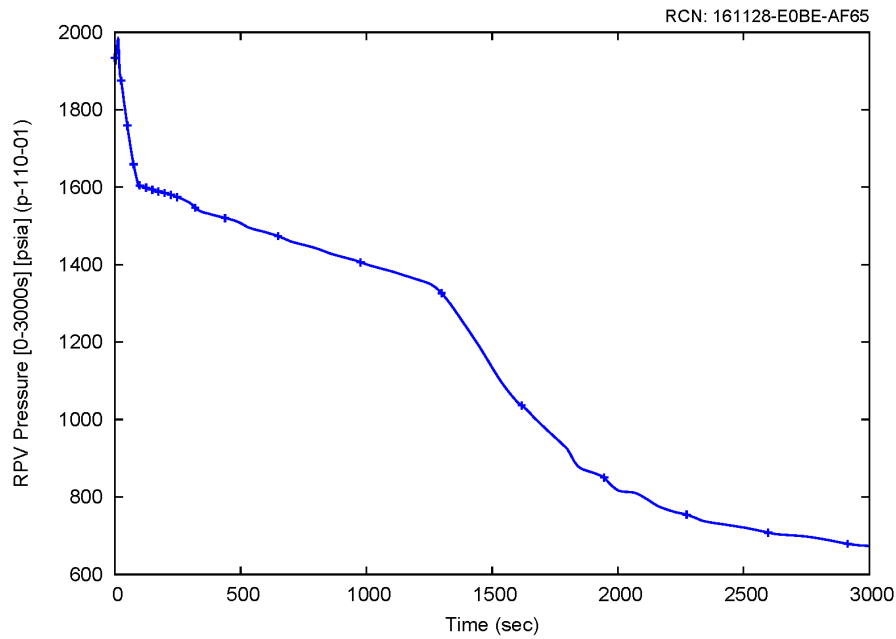


Figure 8-100 Reactor pressure vessel pressure response (0 to 3000 sec) for the representative small break outside containment event

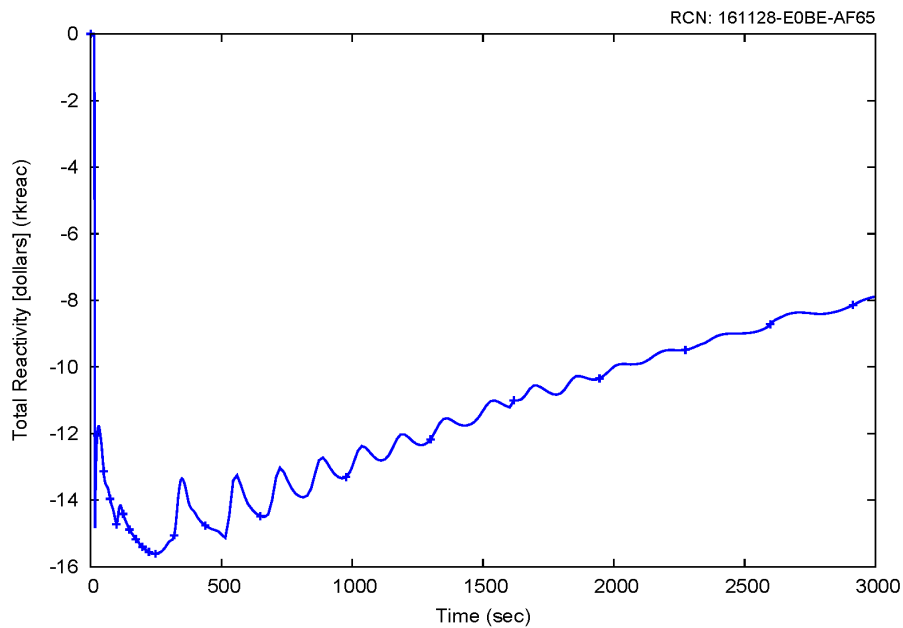


Figure 8-101 Net reactivity response for the representative small break outside containment event

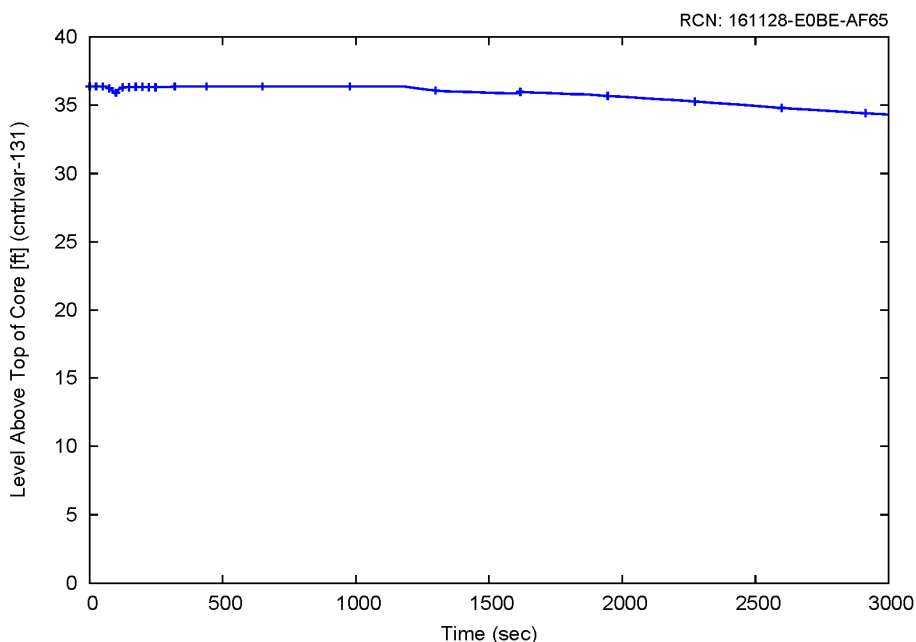


Figure 8-102 Level above top of core response for the representative small break outside containment event

8.5.1.3 Conclusion

A representative challenging case regarding integrated mass released was identified for a break in a small line carrying reactor coolant. The results of this case, as presented in Section 8.5.1.2, are subsequently used as input to a dose evaluation using the NuScale radiological consequences methodology to demonstrate the respective acceptance criteria are met.

8.5.2 Steam Generator Tube Failure

The purpose of this section is to present the thermal-hydraulic and core neutronic responses of the NPM for a steam generator tube failure event. This event is evaluated for offsite and onsite doses, which includes an assessment of the fuel cladding integrity. Thus, the transient analysis results are provided for input to downstream radiological consequences evaluations.

8.5.2.1 Event Description

The event description for a failure of the steam generator tube can be found in Section 7.2.19. Based on Section 7.2.19, the acceptance criteria for radiological consequences are potentially challenged by a steam generator tube failure event. For the NPM, the results of the sensitivity studies indicate the event scenario with the highest integrated

mass released to the environment may differ from the event scenario with the longest iodine spiking duration. The limiting radiological dose consequences are associated with the event scenario having the highest integrated mass released to the environment.

Radiological Consequences – Mass Released

The representative case presented here corresponds to one of the more limiting integrated mass released to the environment cases, i.e., a case with higher dose consequences. This case features the following conditions for the failure of a steam generator tube:

- Conservative initial condition biasing (as shown in Table 7-91) is applied in order to maximize the consequences of this event. This representative case is initialized at 102 percent reactor power.
- Double-ended guillotine break of 100 percent area at top of a single steam generator tube.
- Single active failure of primary MSIV to close on affected SG.
- No loss of normal AC Power.
- No operator action was credited in the representative case.

8.5.2.2 Analysis Results

The following describes the event sequence of the representative steam generator tube failure event. Table 8-12 summarizes the sequence of events. Figure 8-103 through Figure 8-113 show some key parameters during the representative steam generator tube failure event.

The tube failure occurs at time zero. The reactor coolant lost through the break causes an immediate decrease in pressurizer level (Figure 8-103) and RPV pressure (Figure 8-104). In contrast, the SG pressure remains constant (Figure 8-104) as the flow from the tube failure is carried to the turbine. The pressurizer heater power increases in an attempt to compensate for the pressure reduction. The flow through the failed tube causes the pressurizer level to reach the analytical limit for low pressurizer level (35 percent) at 146.0 seconds. The pressurizer heaters are de-energized one second later, while the control rods are free to fall after two seconds (Figure 8-105). The system shrinkage associated with the reactor trip works in conjunction with the break flow to increase the rate of RPV depressurization. The pressurizer pressure continues to decrease until the analytical limit for low pressurizer pressure (1600 psia) is reached at 168.4 seconds. Two seconds later the DHRS valves begin to open; the FWIVs begin to close; and the MSIVs begin to close. The SGs are isolated from the remaining secondary system when the FWIVs and MSIVs close five seconds later. However, the SAF of the primary MSIV on the affected SG to close delays isolation of that SG until the secondary MSIV closes 30 seconds after the DHRS actuation. Isolating the SGs terminates the releases to the environment, but does not terminate flow from the failed tube (Figure 8-106). Following isolation of the SGs, the water level for the affected SG increases and ultimately goes off-scale high, while the level for the intact SG is maintained at the nominal post-trip level (Figure 8-107). The maximum

integrated break flow to the environment (8477 lbm) is reached at 200.5 seconds (Figure 8-108).

After reactor trip and actuation of DHRS, oscillations are observed due to temperature and density differences between the riser and downcomer (as discussed in Section 7.2); therefore the calculation is continued to verify that the module transitions into passive and stable DHRS cooling. At 30 minutes, RCS flow (Figure 8-109) has stabilized, and the primary system temperature (Figure 8-110) and pressure (Figure 8-111) are steadily decreasing as the DHRS transfers decay heat from the RPV to the reactor pool. The net reactivity (Figure 8-112) becomes negative shortly after reactor trip and remains negative during the transition to stable DHRS cooling. The RPV level (Figure 8-113) remains well above the top of the core for the entire transient. Since stable DHRS cooling has been achieved and minimal flow exists through the failed tube, the transient is terminated at 60 minutes. No operator action was credited to mitigate this event.

Table 8-12 Sequence of events for steam generator tube failure

Event	Time (sec)
Steam generator tube fails in SG1.	0
Peak RPV pressure is reached (1931 psia).	0.5
Peak reactor power is reached (165.4 MW).	3.5
Limiting MCHFR is reached (5.297 as calculated by NRELAP5).	21.0
Low PZR level limit is reached (35%). PZR heaters are disabled after 1 second delay.	146.0
RTS actuation on low PZR level signal, control rods are inserted into the core.	148.0
Low PZR pressure is reached (1600 psia). Containment isolation and DHRS actuation begins after 2 seconds delay.	168.4
DHRS actuation on the low PZR pressure signal. DHRS actuation valves begin to open. FWIVs and MSIVs begin to close. Primary MSIV for faulted SG remains open.	170.4
FWIVs and MSIV (intact SG) are fully closed.	175.4
DHRS actuation valves are fully open.	200.4
Secondary MSIV (faulted SG) is fully closed.	200.5
Maximum integrated break flow to SG (8477 lbm) occurs.	200.5
Peak steam generator pressure is reached (1382 psia).	305.5
Establishment of stable RCS flow. Pressure and temperature are steadily decreasing.	1800
End of calculation. Stable DHRS cooling has been established and pressure difference across failed tube minimized.	6000

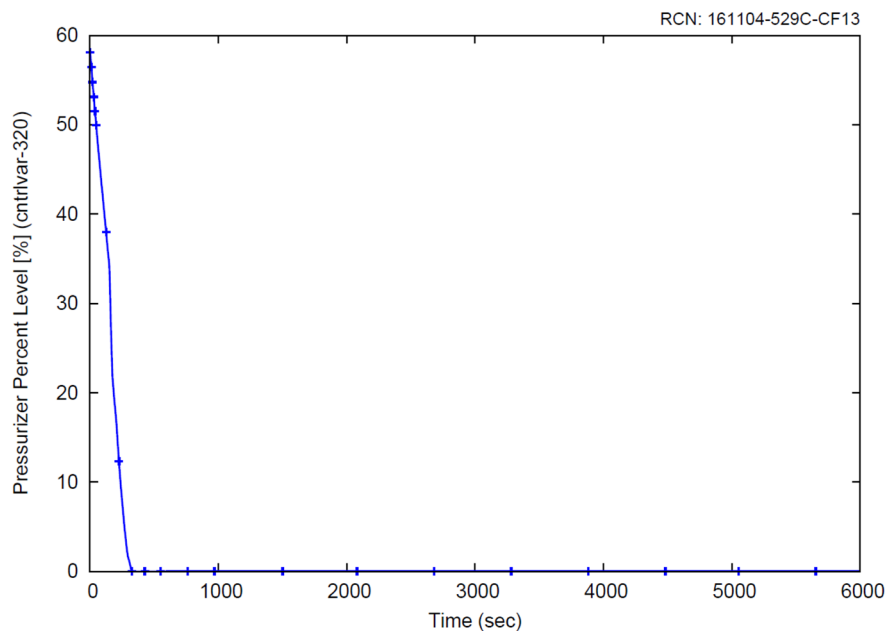


Figure 8-103 Pressurizer level response for the representative steam generator tube failure event

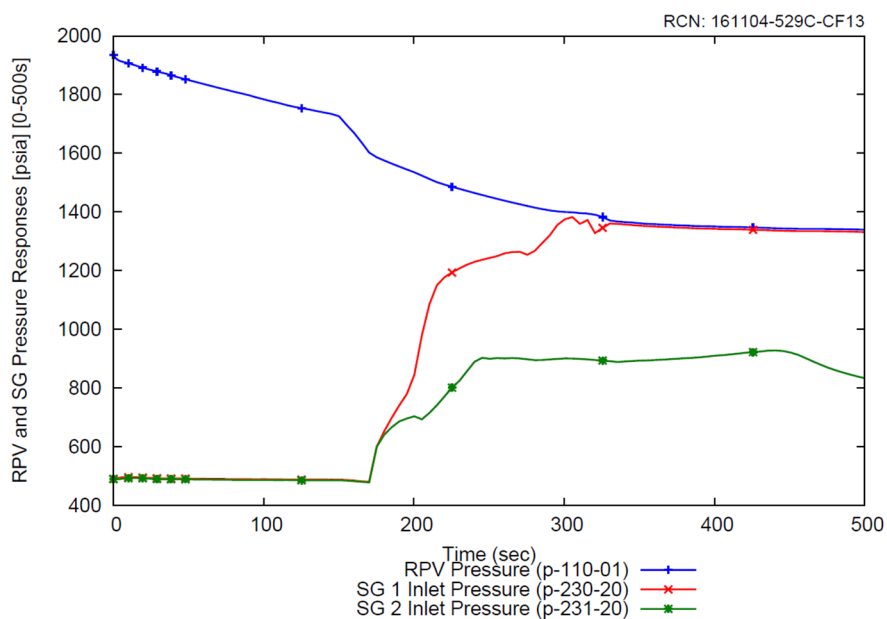


Figure 8-104 Reactor pressure vessel and steam generator pressure responses (0 to 500 sec) for the representative steam generator tube failure event (tube failure occurs in SG1)

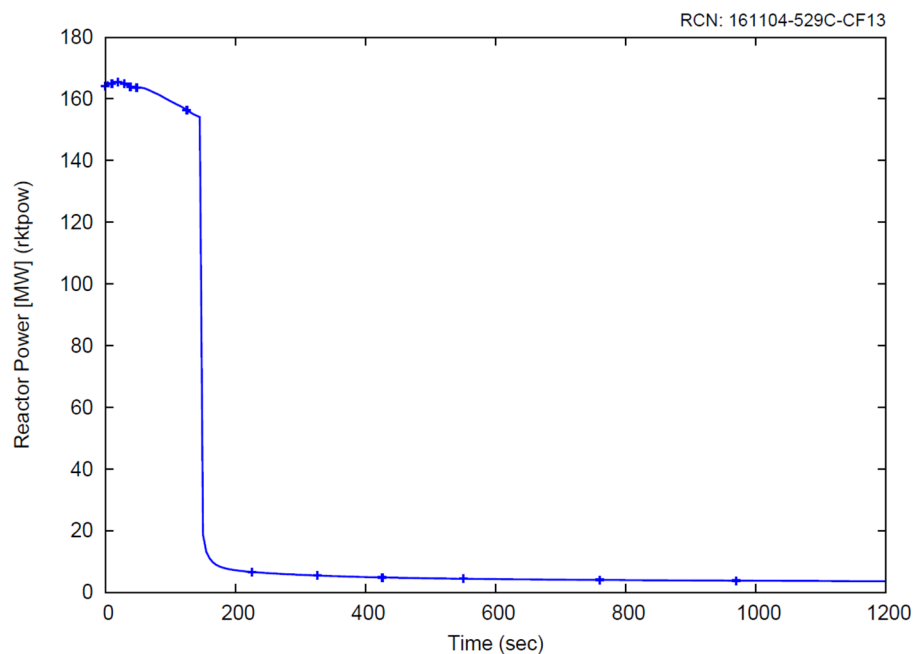


Figure 8-105 Core power response for the representative steam generator tube failure event

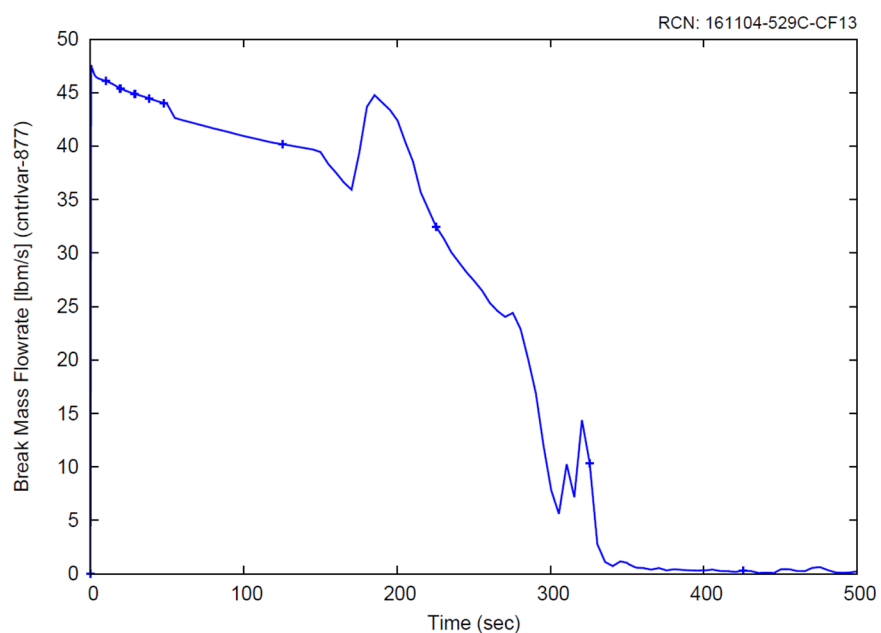


Figure 8-106 Instantaneous break flow response for the representative steam generator tube failure event

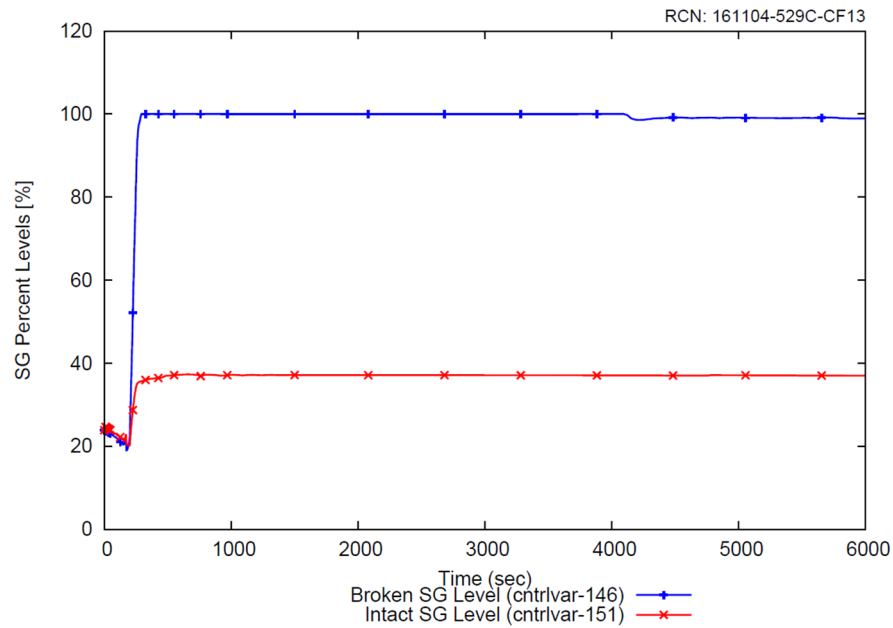


Figure 8-107 Steam generator level response for the representative steam generator tube failure event

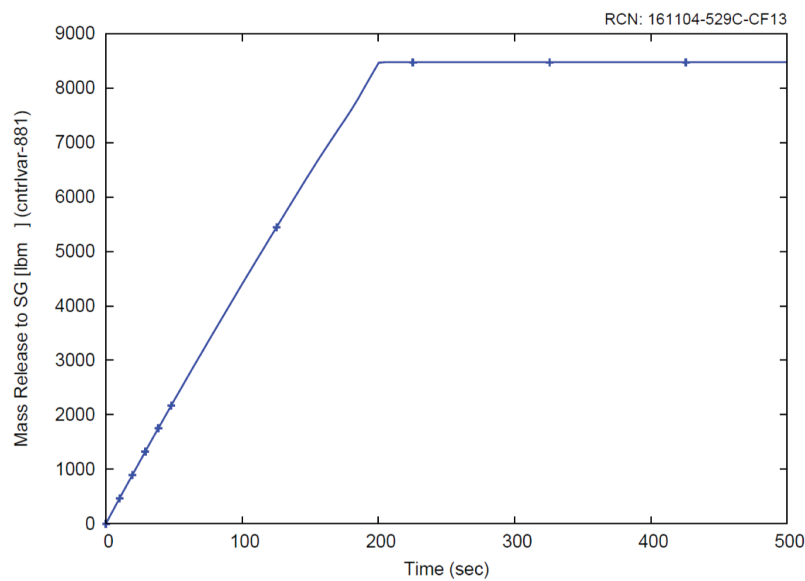


Figure 8-108 Integrated break mass release to steam generator before isolation (0 to 500 sec) for the representative steam generator tube failure event

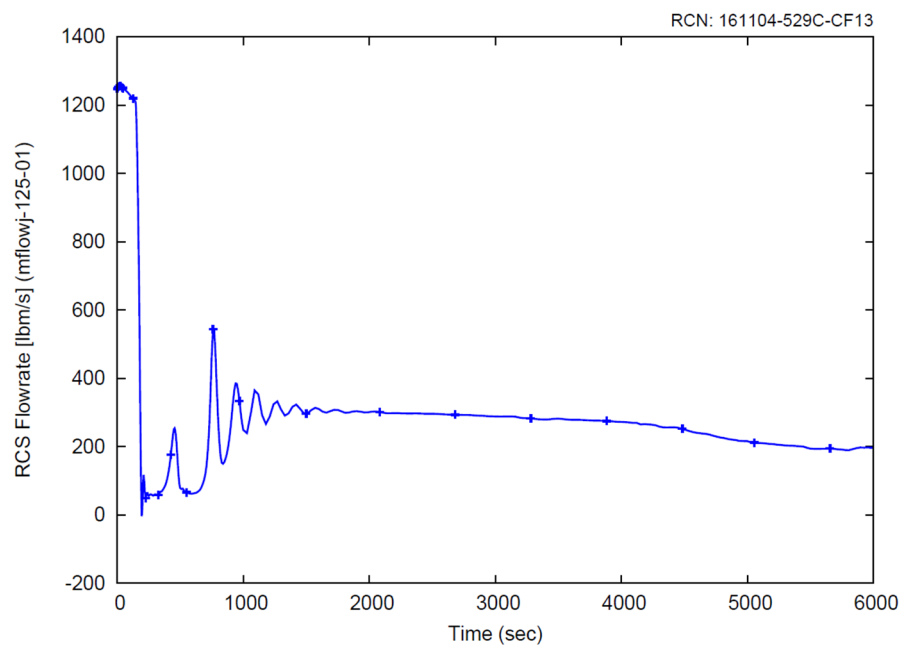


Figure 8-109 Reactor coolant system flow rate response for the representative steam generator tube failure event

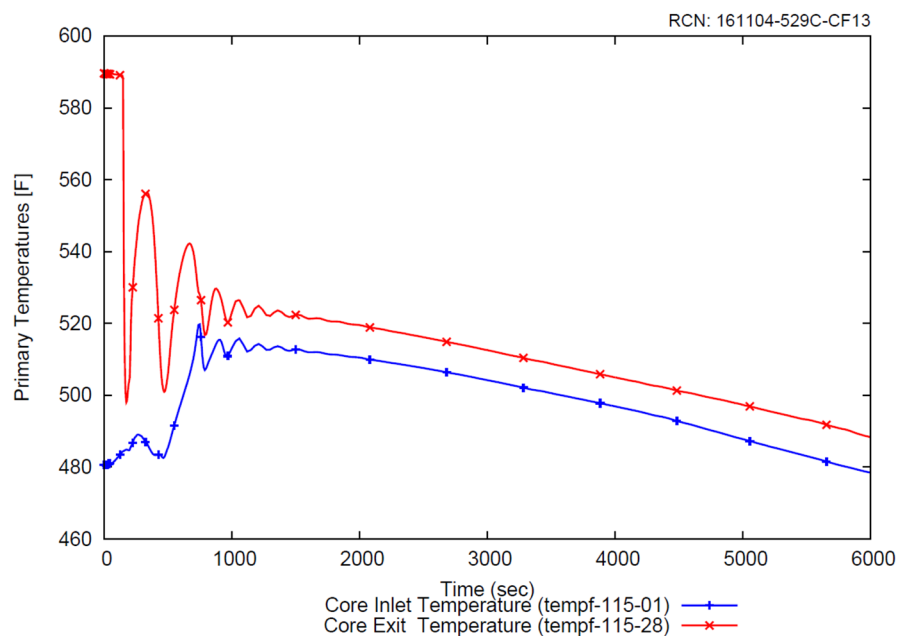


Figure 8-110 Core inlet and exit temperature responses for the representative steam generator tube failure event

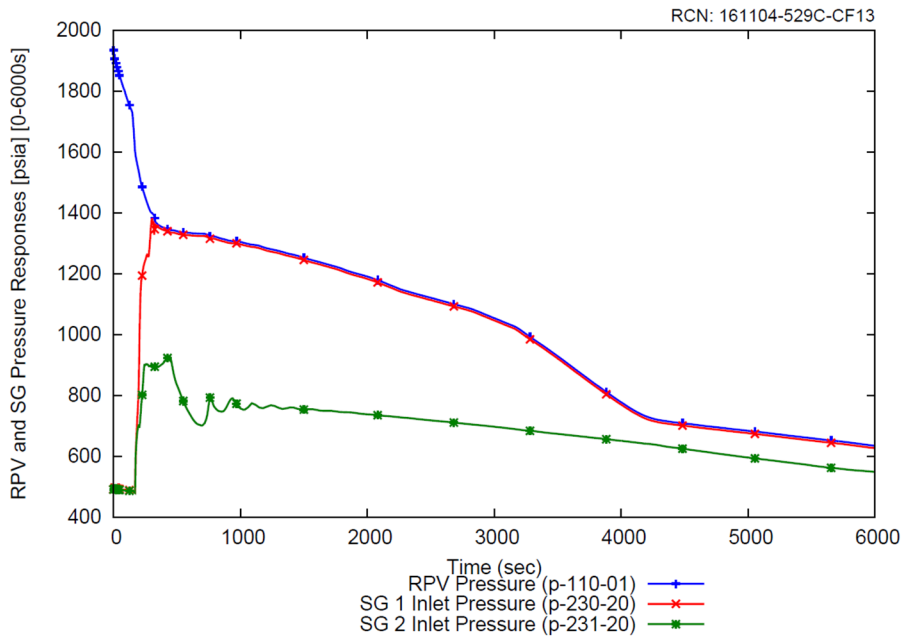


Figure 8-111 Reactor pressure vessel and steam generator responses (0 to 6000 sec) for the representative steam generator tube failure event

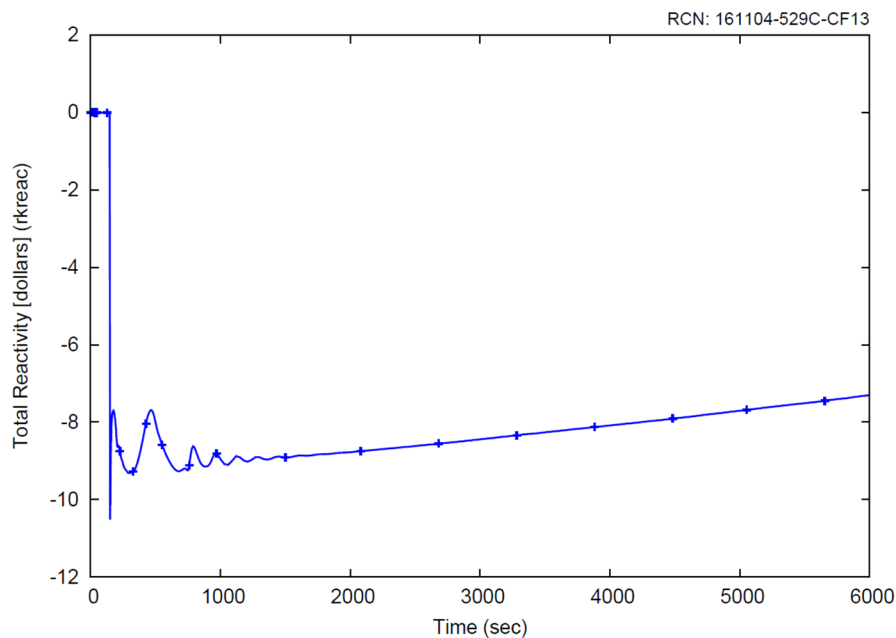


Figure 8-112 Net reactivity response for the representative steam generator tube failure event

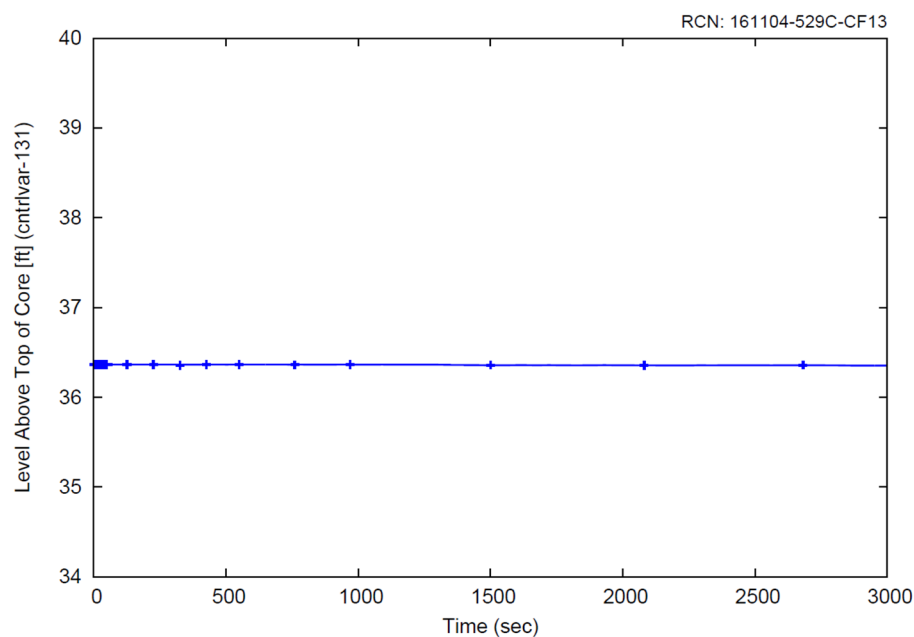


Figure 8-113 Level above top of core response for the representative steam generator tube failure event

8.5.2.3 Conclusion

A representative challenging case regarding integrated mass released was identified for the failure of a steam generator tube. The results of this case, as presented in Section 8.5.2.2, are subsequently used as input to a dose evaluation using the NuScale radiological consequences methodology demonstrate the acceptance criteria are met.

9.0 Quality Assurance

The NuScale Topical Report: Quality Assurance Program Description for the NuScale Power Plant, NP-TR-1010-859-NP-A (Reference 3), complies with the requirements of 10 CFR 50 Appendix B (Reference 19) and Quality Assurance Requirements for Nuclear Facility Applications, ASME NQA-1 2008 and NQA-1a-2009 Addenda (Reference 20).

As described in Reference 2, the NRELAP5 code has been developed following the requirements of NuScale's QAP.

The non-LOCA system transient analysis is performed and documented in accordance with NuScale's QAP.

10.0 Summary and Conclusions

The NuScale evaluation model used to evaluate the NPM system short term transient thermal-hydraulic response to non-LOCA events has been presented in this report. The non-LOCA system transient evaluation model was developed following a graded approach in accordance with the guidance provided in RG 1.203.

The NPM plant design for which this evaluation model is applicable is described in this report. The NPM is a natural circulation pressurized water reactor (PWR) with a reactor core, two helical coil SGs, and a pressurizer integral to the reactor vessel. Many of the events analyzed for operating PWRs and in recent design certification applications are applicable to the NuScale design. NuScale-specific events reflect unique aspects of the NuScale design such as the DHRS and normal operation of the containment at vacuum conditions. The NPM design was evaluated in detail to assure that a sufficiently broad spectrum of transients, accidents, and initiating events have been included in the scope of design basis analyses presented in DCD Chapter 15. The design-basis events were categorized by type and expected frequency of occurrence so that limiting cases in each group may be quantitatively analyzed and specific acceptance criteria applicable to each postulated initiating event are applied. The NPM design basis events for which the non-LOCA evaluation model is applicable were identified.

NRELAP5 is NuScale's system thermal-hydraulics code used to simulate the NPM system response during both the non-LOCA and LOCA short-term transient event progression. The NRELAP5 code is described in the separate NuScale LOCA evaluation model topical report. Applicability of the NRELAP5 code for non-LOCA system transient analysis is presented in this report. The NRELAP5 code is applicable for calculation of the NPM thermal-hydraulic system response for the non-LOCA short-term transient event progression as part of this EM. This conclusion is based on the high-ranked phenomena identified from the non-LOCA and LOCA PIRT processes, separate effects and integral effects testing, code to code benchmarking, and appropriately conservative input for initial and boundary conditions.

The non-LOCA transient analysis process is described in this report. The methodology for conservatively biasing initial and boundary conditions for event analysis is presented. Then, each initiating event is considered to identify the acceptance criteria that may be challenged during the event. For each non-LOCA event, a description of the event is provided including biases and conservatisms applied, sensitivity studies performed, single active failures and loss of power scenarios that challenge the event acceptance criteria. For each transient event, the acceptance criteria where margin to the limit may be challenged are identified. For these acceptance criteria, sensitivity calculations are performed as appropriate to confirm that suitably conservative inputs are specified and to determine conditions that result in minimum margin. For other acceptance criteria where margin to the limit is not challenged, representative results from the overall scope of sensitivity calculations performed demonstrate that margin to the acceptance criterion is maintained. For non-LOCA initiating events that actuate the decay heat removal system, the EM is applicable for the short-term transient progression; during this time frame the

mixture level remains above the top of the riser and primary side natural circulation is maintained.

For selected non-LOCA events, representative system transient results are provided to demonstrate application of the evaluation model for the NPM. System transient calculations are executed for sufficient duration to demonstrate that the initiating event is mitigated and stable cooling is established. Results of representative calculations show that the maximum primary system and secondary system pressure acceptance criteria are not challenged in the NPM design. The representative results indicate that the primary system pressure is limited by the reactor safety valve and peak values are less than 2200 psia, compared to acceptance criteria of 2310 psia or 2520 psia, depending on the event classification; in the representative results the maximum secondary side pressure is less than 1600 psia, compared to acceptance criteria of 2310 psia or 2520 psia, depending on the event classification. Margin to other quantitative acceptance criteria for MCHFR, fuel centerline temperature, and radiological dose limits applicable for the non-LOCA events are demonstrated as part of separate downstream subchannel or accident radiological analyses, presented in separate reports, which are not part of the scope of this topical report.

11.0 References

1. U.S. Nuclear Regulatory Commission, "Transient and Accident Analysis Methods," Regulatory Guide 1.203, December 2005.
2. NuScale Power, LLC, "LOCA Evaluation Model," TR-0516-49422-P, Revision 1.
3. NuScale Power, LLC, "NuScale Topical Report: Quality Assurance Program Description for the NuScale Power Plant," NP-TR-1010-859-NP-A, Revision 4.
4. *U.S. Code of Federal Regulations*, "General Design Criteria for Nuclear Power Plants," Appendix A, Part 50 Chapter I, Title 10, "Energy," (10 CFR 50 Appendix A).
5. *U.S. Code of Federal Regulations*, "Contents of applications; technical information," Section 52.47, Part 52 Chapter I, Title 10, "Energy," (10 CFR 52.47).
6. NuScale Power, LLC, "Subchannel Analysis Methodology," TR-0915-17564-P-A, Revision 2.
7. NuScale Power, LLC, "NuScale Power Critical Heat Flux Correlations," TR-0116-21012-P-A, Revision 1.
8. NuScale Power, LLC, "Accident Source Term Methodology," TR-0915-17565-P, Revision 3.
9. U.S. Nuclear Regulatory Commission, "Standard Review Plan, Radiological Consequences of the Failure of Small Lines Carrying Primary Coolant Outside Containment," NUREG-0800, Chapter 15, Section 15.6.2, Rev. 2, July 1981.
10. NuScale Power, LLC, "Steady State Core Thermal-Hydraulics and Primary System Stability," TR-0516-49417-P, Revision 1.
11. S.M. Modro et al., "Multi-Application Small Light Water Reactor Final Report," Idaho National Engineering and Environmental Laboratory, INEEL/EXT-04-01626, December 2003.
12. Electric Power Research Institute, "RETRAN-3D — A Program for Transient Thermal-Hydraulic Analysis of Complex Fluid Flow Systems," Volumes 1 -5, EPRI NP-7450-A, Revision 10, September 2014.
13. Moghanaki, S. K. and Rahgoshay, M., "Pressurizer Modeling: Using Different Thermodynamic Models and Comparing Results with RELAP Code Results," Applied Mechanics and Materials (Volumes 423-426), pp. 1444-1448, 2013.
14. U.S. Nuclear Regulatory Commission, "Combined License Applications for Nuclear Power Plants," Regulatory Guide 1.206, June 2007.

15. U.S. Nuclear Regulatory Commission, "Standard Review Plan, Transient and Accident Analyses," NUREG-0800, Chapter 15, Revision 3, March 2007 and various Chapter 15 subsections.
16. *U.S. Code of Federal Regulations*, "Definitions," Section 50.2, Part 50 Chapter I, Title 10, "Energy," (10 CFR 50.2).
17. American National Standards Institute / American Nuclear Society, "Single Failure Criteria for Light Water Reactor Safety-Related Fluid Systems," ANSI/ANS-58.9-2002 R2015.
18. U.S. Nuclear Regulatory Commission, "Policy and Technical Issues Associated with the Regulatory Treatment of Non-Safety Systems in Passive Plant Designs," SECY-94-084, March 1994.
19. *U.S. Code of Federal Regulations*, "Quality Assurance Criteria for Nuclear Power Plants and Fuel Reprocessing Plants," Appendix B, Part 50 Chapter I, Title 10, "Energy," (10 CFR 50 Appendix B).
20. American Society of Mechanical Engineers, *Quality Assurance Program Requirements for Nuclear Facility Applications*, ASME NQA-1-2008, NQA-1a-2009 Addenda.
21. NuScale Power, LLC, "Rod Ejection Accident Methodology," TR-0716-50350-P, Revision 1.
22. NuScale Power, LLC, "Applicability of AREVA Methodology for the NuScale Design," TR-0116-20825-P-A, Revision 1.
23. NuScale Power, LLC, "Nuclear Analysis Codes and Methods Qualification," TR-0616-48793-P-A, Revision 1.
24. Kim, S.J., "Turbulent film condensation of high pressure steam in a vertical tube of passive secondary condensation system," PhD thesis, Korea Advanced Institute of Science and Technology, 2000.
25. SwUM-0304-17023, Revision 8, NRELAP5 Version 1.4 Theory Manual.

Enclosure 3:

Affidavit of Zackary W. Rad, AF-1119-67901

NuScale Power, LLC

AFFIDAVIT of Zackary W. Rad

I, Zackary W. Rad, state as follows:

- (1) I am the Director of Regulatory Affairs of NuScale Power, LLC (NuScale), and as such, I have been specifically delegated the function of reviewing the information described in this Affidavit that NuScale seeks to have withheld from public disclosure, and am authorized to apply for its withholding on behalf of NuScale.
- (2) I am knowledgeable of the criteria and procedures used by NuScale in designating information as a trade secret, privileged, or as confidential commercial or financial information. This request to withhold information from public disclosure is driven by one or more of the following:
 - (a) The information requested to be withheld reveals distinguishing aspects of a process (or component, structure, tool, method, etc.) whose use by NuScale competitors, without a license from NuScale, would constitute a competitive economic disadvantage to NuScale.
 - (b) The information requested to be withheld consists of supporting data, including test data, relative to a process (or component, structure, tool, method, etc.), and the application of the data secures a competitive economic advantage, as described more fully in paragraph 3 of this Affidavit.
 - (c) Use by a competitor of the information requested to be withheld would reduce the competitor's expenditure of resources, or improve its competitive position, in the design, manufacture, shipment, installation, assurance of quality, or licensing of a similar product.
 - (d) The information requested to be withheld reveals cost or price information, production capabilities, budget levels, or commercial strategies of NuScale.
 - (e) The information requested to be withheld consists of patentable ideas.
- (3) Public disclosure of the information sought to be withheld is likely to cause substantial harm to NuScale's competitive position and foreclose or reduce the availability of profit-making opportunities. The accompanying topical report reveals distinguishing aspects about the method by which NuScale develops its non-loss-of-coolant accident analysis.

NuScale has performed significant research and evaluation to develop a basis for this method and has invested significant resources, including the expenditure of a considerable sum of money.

The precise financial value of the information is difficult to quantify, but it is a key element of the design basis for a NuScale plant and, therefore, has substantial value to NuScale.

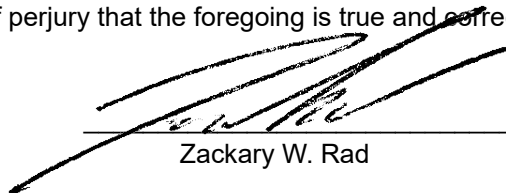
If the information were disclosed to the public, NuScale's competitors would have access to the information without purchasing the right to use it or having been required to undertake a similar expenditure of resources. Such disclosure would constitute a misappropriation of NuScale's intellectual property, and would deprive NuScale of the opportunity to exercise its competitive advantage to seek an adequate return on its investment.

- (4) The information sought to be withheld is in the enclosed topical report titled "Non-Loss-of-Coolant Accident Analysis Methodology," TR-0516-49416, Revision 2. The enclosure contains the designation "Proprietary" at the top of each page containing proprietary information. The information considered by NuScale to be proprietary is identified within double braces, "{{ }}" in the document.
- (5) The basis for proposing that the information be withheld is that NuScale treats the information as a trade secret, privileged, or as confidential commercial or financial information. NuScale relies upon

the exemption from disclosure set forth in the Freedom of Information Act ("FOIA"), 5 USC § 552(b)(4), as well as exemptions applicable to the NRC under 10 CFR § 2.390(a)(4) and 9.17(a)(4).

- (6) Pursuant to the provisions set forth in 10 CFR § 2.390(b)(4), the following is provided for consideration by the Commission in determining whether the information sought to be withheld from public disclosure should be withheld:
- (a) The information sought to be withheld is owned and has been held in confidence by NuScale.
 - (b) The information is of a sort customarily held in confidence by NuScale and, to the best of my knowledge and belief, consistently has been held in confidence by NuScale. The procedure for approval of external release of such information typically requires review by the staff manager, project manager, chief technology officer or other equivalent authority, or the manager of the cognizant marketing function (or his delegate), for technical content, competitive effect, and determination of the accuracy of the proprietary designation. Disclosures outside NuScale are limited to regulatory bodies, customers and potential customers and their agents, suppliers, licensees, and others with a legitimate need for the information, and then only in accordance with appropriate regulatory provisions or contractual agreements to maintain confidentiality.
 - (c) The information is being transmitted to and received by the NRC in confidence.
 - (d) No public disclosure of the information has been made, and it is not available in public sources. All disclosures to third parties, including any required transmittals to NRC, have been made, or must be made, pursuant to regulatory provisions or contractual agreements that provide for maintenance of the information in confidence.
 - (e) Public disclosure of the information is likely to cause substantial harm to the competitive position of NuScale, taking into account the value of the information to NuScale, the amount of effort and money expended by NuScale in developing the information, and the difficulty others would have in acquiring or duplicating the information. The information sought to be withheld is part of NuScale's technology that provides NuScale with a competitive advantage over other firms in the industry. NuScale has invested significant human and financial capital in developing this technology and NuScale believes it would be difficult for others to duplicate the technology without access to the information sought to be withheld.

I declare under penalty of perjury that the foregoing is true and correct. Executed on November 26, 2019.



Zackary W. Rad